UCGE Reports
Number 20203

Department of Geomatics Engineering

Development of Two Novel Carrier Phase-Based Methods for Multiple Reference Station Positioning

(URL: http://www.geomatics.ucalgary.ca/links/GradTheses.html)

by

Paulo R. S. Alves

Dec 2004

Abstract

Two methods for network-based carrier phase real-time kinematic positioning are proposed and evaluated in this thesis. These two methods are a correction-based, and a tightly coupled, approach. Novel algorithm enhancements are proposed for the correction-based approach, while the tightly coupled approach, which integrates reference station and user data in a single solution, is an innovative extension of a method previously developed.

Each stage of the correction-based approach requires coherent information. The covariance function provides the stochastic basis of the estimation process and is used in each stage of this approach. A novel method for implementing an adaptive covariance function that is used subsequently is proposed. The adaptive qualities are shown to effectively track changing temporal and spatial error conditions, especially atmospheric conditions, throughout the data sets.

The derivation of a least-squares prediction based approach, more specifically a least-squares collocation approach, is performed. This includes the value and variance-covariance of the estimated corrections. Further derivation shows the effect of these elements on the reduced rover measurements. This approach reduces the differential measurement errors and improves position accuracy relative to the single baseline approach.

The tightly coupled approach is an extension of a multiple mobile user positioning approach, whereby inter-receiver position differences are connected to all reference stations and user(s) in the same estimation filter. This could also be considered an extension of the correction-based approach where the position of one or more of the

reference stations is uncertain or unknown. This approach is also shown to improve position accuracy relative to the single baseline and correction-based approach.

These two methods are compared and analysed. In general, both methods perform better than the single reference station approach however, the tightly coupled approach performs slightly better than the correction-based approach in terms of position accuracy, based on the data sets used for the evaluation of the two methods.

Acknowledgements

This thesis would not have been possible in its current form without the assistance of the following people:

- My wonderful wife, Karla. You have been by me for all of the good times and the more frustrating times. Thank you for your patience and understanding from the beginning to the end.

- My parents, Paul and Heloisa. You have supported all of my education and choices. I appreciate your love and friendship. My family and extended family, Sylvia, Leslie, and Jennie, have also been the best support I could have asked for. I would not have made it this far without you.

- My supervisors, Gérard Lachapelle and Elizabeth Cannon. Thank you for giving me so many opportunities over the years. I have grown in the shadow of your leadership and experience.

- My graduate student peers, and friends. Without the support of my fellow graduate students this process would have been much more difficult. From clarifying minor points, challenging my ideas, and just being there to talk to when things were getting tough, I thank you for everything you have done. Special thanks to Mark Petovello, Sandra Kennedy, Kyle O'Keefe, Natalya Nicholson, Victoria Hoyle, Glenn MacGougan, Junjie Liu, Luiz Fortes, and Sam Ryan.

- My out of school friends, Eirik, Donna, Brad, Ira, Mellisa, Robb, Todd, Maurey, and Joseph Papparelli. You gave me a distraction when I needed it and the

encouragement to get back to it.

- The Natural Sciences and Engineering Research Council of Canada (NSERC), the Alberta Informatics Circle of Research Excellence(iCORE) and other scholarship sponsors for providing financial support for this dissertation.

- I would like to thank TUBITAK Marmara Continuous GPS Network (MAGNET) for the use of their data.

Table of Contents

List of Tables

List of Figures

Notation

Symbols

$\bullet_{z_c}$	Quantity $\bullet$ refered to the zenith correlated error
$\bullet_u$	Quantity $\bullet$ refered to the uncorrelated errors
$\bullet_k$	Quantity $\bullet$ at the k^{th} epoch
$\bullet^\circ$	A-priori estimate of quantity $\bullet$
$\bullet^*$	Quantity $\bullet$ of the predicted control point
$\bullet_g$	Quantity $\bullet$ used specifically for prediction
$\dot{\bullet}$	Time derivative of quantity $\bullet$
$\hat{\bullet}$	Estimated quantity $\bullet$
$\check{\bullet}$	Fixed quantity $\bullet$
$f(\bullet)$	Function of $\bullet$
A	Design matrix
A'	Linear transformation matrix
A_{pos}	Design matrix of the position parameters
B	Observation transformation matrix
B'	Alternate observation matrrix
B_{sd}	Single difference observation matrix
C_{ab}	Covariance matrix of a and b
$\mathrm{E}\{\bullet\}$	Expected value operator
F	Dynamics matrix
G	Shaping matrix

H	Linear transformation matrix
$I_\bullet$	Ionosphere error at the frequency $\bullet$
$I(\bullet)$	Ionosphere as a function of frequency $\bullet$
I	Identity matrix
M	Matrix of $BC_{ll}B^T$
N	Carrier phase ambiguity
	Electron density of the ionosphere
$N(a, b)$	Ambiguity as a function of the L1 and L2 measurement coefficients
P	Pseudo-range observation
P_0	Location of the network reference point
$\mathrm{P}_\bullet$	Location of $\bullet$
Q	Process noise matrix
T	Troposphere error
a	Vector of ambiguities
a, b, m	Function coefficients
c_1, c_2	Function coefficients
d	Distance
	Distance between reference stations
d_I	Distance between ionosphere pierce points
$d\rho$	Satellite position error
l	Vector of measurements
$l_\circ$	Vector of deterministic observation biases
l_n	Observation noise vector

l_s	Observation signal vector
q	Spectral density
r	Vector of residuals
s	Vector of signals
t	Time
x	Vector of parameters
x_a, y_a, z_a	Station a position components
w	White noise error
	Vector of misclosures
y	Measurement process
$\Delta\nabla l_{ab}^{12}$	Double difference measurements
Φ	Trnasition matrix
α	Angle between measurements
β	One over the correlation measure
δ	Vector of parameter corrections (update)
ε	Unmodelled measurement errors
$\varepsilon_{\hat{s}}$	Vector of estimated signal errors
λ	Carrier phase wavelength
$\mu(\varepsilon)$	Elevation mapping function
ϕ	Carrier phase observation
$\phi_{a,b}$	Linear combination of carrier phase measurements
ρ	Receiver-satellite range
$\sigma_{a,b}$	Covariance between quantities a and b

$\sigma^2_\bullet$	Variance of the quantity $\bullet$
τ	Correlation measure

Abbreviations and Acronyms

BIM	Broadcast ionosphere model
CODE	Centre for orbit determination in Europe
FASF	Fast ambiguity search filter
FKP	(*German*) *Flächen Korrektur Parameter*, area correction parameter
GF	Geometry free
GIM	Global ionosphere model
GPS	Global Positioning System
IF	Ionosphere free
IGS	International GPS Service
LAMBDA	Least squares ambiguity decorrelation adjustment
MAGNET	TUBITAK Maramara Continuous GPS Network
NMEA	National marine electronics association
ppm	Parts per million
RMS	Root mean squared
RTCM	Radio technical commission for maritime services
RTK	Real time kinematic, implies carrier phase based
SAN	Southern Alberta Network
UTC	Coordinated universal time
VRS	Virtual reference station

Chapter 1

Introduction

This thesis presents two novel real-time capable, approaches to multiple reference station carrier phase-based positioning. This chapter first identifies limitations of previous research that are overcome by this contribution. It then outlines research objectives and the significant original contribution of this work. Finally, a thesis overview is given.

1.1 Limitations of Previous Work

The study of many topics are required to develop a real-time capable multiple reference station system. This study requires an understanding of parameter estimation using code and carrier phase observations, ionosphere modelling, ambiguity resolution, covariance functions and stochastic processes, least squares collocation for prediction, and practical aspects of carrier phase positioning. Throughout the development of a cohesive system many advancements have been made. The background for these advancements is described in this section.

1.1.1 Multiple Reference Station Approach: Overview

This research focuses on collocation-based methods for multiple reference station positioning. This approach was first introduced by Raquet (1998). The collocation-based approach has been shown to provide a significant level of improvement over the

single reference station approach for a variety of networks around the world mainly in post mission (Cannon et al., 2001a,b; Fortes et al., 2000a,b, 2001; Raquet et al., 1998; Raquet, 1998) but also in real-time (Alves et al., 2001; Cannon et al., 2001a). Landau et al. (2002) discusses the ability to perform collocation-based multiple reference station positioning but does not show results with this approach. Zhang (1999) and Zhang and Lachapelle (2001) show an extension of this approach whereby the network of reference stations predict the tropospheric effect on a particular satellite pair.

An alternative to the collocation-based approach uses a simple linear two dimensional plane model using three surrounding reference stations (Wanninger, 1999; Vollath et al., 2000a,b, 2002; Wübbena et al., 2001a; Euler et al., 2001).

For either approach to interpolation and prediction, multiple reference station positioning is usually characterized as a three step process (Odijk, 2002):

1. Estimate and resolve the network ambiguities,

2. Calculate the corrections (error model) for the region, and

3. Transmit the corrections in a receiver-acceptable format.

Estimation and resolution of the network ambiguities is usually neglected in multiple reference station research because it can be performed using traditional single reference station methods. There are a few publications referring to the modelling of network errors to resolve the ambiguities in the network: Wübbena et al. (2001a,b) discuss the state space model for estimating the ambiguities. This model estimates a multitude of parameters including satellite clock, signal delay, satellite orbit, ionospheric delay, tropospheric delay, receiver clock offset, signal delay, multipath, measurement noise and carrier phase ambiguities. The network ambiguity estimation and resolution performance with this model is not discussed.

In previous research, there is no discussion of the integration of the stages of multiple reference station positioning. Network ambiguity estimation and resolution is discussed as an independent process from prediction of the corrections. This is a limitation of the previous approaches because without integrating the information from the network ambiguity estimation into the prediction it is very difficult to produce reasonable estimated accuracies of the corrections. Calculating and using accuracy estimates of the corrections will be discussed further in Section 1.1.2.

1.1.2 Collocation-Based Multiple Reference Station Positioning

Collocation-based multiple reference station positioning began with the NetAdjust method (Raquet, 1998). This method used fixed ambiguities and station coordinates to first measure the errors at the reference station locations and then predict those errors for the location of a roving receiver.

Covariance Function: $\mathbf{P}_0$

The covariance function models the statistical correlation characteristics of a process (Moritz, 1980). The covariance function is an important element of collocation-based prediction, however least squares prediciton is insensitive to the choice of covariance function (Fortes, 2002). The following discuss properties of previous covariance functions that could be improved.

The covariance function used by Raquet (1998) is a function of the elevations of the satellites, the coordinates of the stations and the location of the reference point, P_0. The reference point is an arbitrary location where the corrections are constrained to zero. The reference point constraint is used to resolve the datum deficiency caused by calculating single observation predictions from double differenced measured errors. However, the least squares collocation equations inherently resolve

this datum deficiency without the need for a reference point. Consequently, the use of P_0 in previous work was unnecessary to resolve the datum deficiency in the least squares prediction.

The elimination of the reference point simplifies the covariance function because the covariance function does not need to follow the form (Raquet, 1998)

$$f_{z_c}(P_a, P_b, P_0) = \frac{\sigma^2_{c_z}(P_a, P_0) + \sigma^2_{c_z}(P_b, P_0) - \sigma^2_{c_z}(P_a, P_b)}{2} \tag{1.1}$$

where c_z represents the zenith correlated errors, and P is the location of the stations a, b and the reference point, P_0. The variances of all of the measurements at the P_0 location are zero, which limits the variety of covariance function parameters. For example, the variances of all of the satellites at P_0 are zero, which means that the variance is not a function of elevation at this location. Elimination of the P_0 point allows for a wider variety of covariance functions.

Covariance Function: Form

The general form of the covariance function used by Raquet (1998), which models the variance and covariance of undifferenced observations, is

$$\sigma_{l_a^x, l_b^y} = \begin{cases} \mu^2(\varepsilon)\left[\frac{\sigma^2_{c_z}(p_a,p_0)+\sigma^2_{c_z}(p_b,p_0)-\sigma^2_{c_z}(p_a,p_b)}{2} + \sigma^2_{u_z}\right] & \text{if } a = b \text{ and } x = y, \\ \mu^2(\varepsilon)\left[\frac{\sigma^2_{c_z}(p_a,p_0)+\sigma^2_{c_z}(p_b,p_0)-\sigma^2_{c_z}(p_a,p_b)}{2}\right] & \text{if } a \neq b \text{ and } x = y, \\ 0 & \text{otherwise} \end{cases} \tag{1.2}$$

where l is an observation from stations a and b to satellites x and y, respectively, $\mu^2(\varepsilon)$ is the elevation mapping function, $\sigma^2_{c_z}(p_a, p_0)$ is a distance dependant function, and $\sigma^2_{u_z}$ is the variance of the uncorrelated errors.

The dependance on the P_0 point is evident in this equation. The distance dependent function, $\sigma^2_{c_z}(p_a, p_0)$ is a positive function that increases with distance. Variations

of this function are shown in Fortes (2002). The original function shown in Raquet (1998) is $c_1 d + c_2 d^2$, where d is the distance between the two station arguments, and c_1 and c_2 are precalculated coefficients.

In general, the observations are transformed to the zenith using a mapping function and then the covariance is determined using the distance-dependent function. The limitation of this covariance function is that correlation is mainly a function of distance. As a result, two measurements that are observed at the same station are deemed to be almost perfectly correlated. To avoid this correlation problem, this covariance function assumes that observations of different satellites are uncorrelated. Alternately, only the same satellites observed at different stations are correlated. In actuality, the correlation of two satellites measured by the same station would depend on the similarity of their signal paths through the atmosphere. In other words, this covariance function only models distance dependent errors between common satellites observed at different stations.

By limiting the correlation, the variance-covariance matrix of the observations will be less representative of the true measurement error properties. In addition, this covariance function cannot be used to predict the errors for a satellite that is not already observed by the network.

Covariance Function: Variability

The distance component of the covariance function proposed by Raquet (1998) is modelled by a second order polynomial. The parameters of this function, which are the coefficients of the second order polynomial, change from day to day (Townsend et al., 1999; Fortes et al., 1999, 2001), and day to night (Raquet et al., 2001), depending on the environmental conditions, and are network dependant (Fortes et al.,

2001). Fortes (2002) shows that up to an additional 14 percent improvement can be obtained using a covariance function that is calibrated using the same network's data. A covariance function calibration can only be performed in post-mission; however, the covariance function coefficients provide similar performance from one day to the next.

If the covariance function coefficients can be calibrated in conjunction with the network positioning service, then the coefficients can be tuned for changing environmental conditions.

Using the Corrections

The use of multiple reference station corrections in real-time is an area of study independent of the determination of the correction values. At the current time, receiver manufacturers are beginning to accommodate a standard format of network-based corrections. Network corrections must be transmitted to the roving receiver in a receiver-acceptable format. To do this, the multiple reference station corrections must be disguised as single reference station data so that the receiver will understand and use the corrections properly. However, the rover receiver will decide how to use the corrections based on the expected accuracy of its corrected measurements. The accuracy of these measurements is determined by the rover, based on the distance between itself and the reference station from which the corrections are sent.

It has been shown that the multiple reference station approach can reduce measurement errors relative to the single reference station approach using the closest reference station to the rover (Cannon et al., 2001a,b; Fortes et al., 2000a,b, 2001; Raquet et al., 1998; Raquet, 1998; Wanninger, 1999; Vollath et al., 2000a,b, 2002; Wübbena et al., 2001a; Euler et al., 2001). The rover receiver assumes a level of differential measurement error based on the distance between itself and the reference

station. In the multiple reference station case, the rover's differential measurement errors are less than in the single reference station approach. Consequently, the reference station position that is sent to the rover should be closer to the rover than the nearest reference station so that the rover assumes a more appropriate level of error.

The virtual reference station (VRS) method geometrically transforms the corrected measurements of a reference station to a new location to trick receivers into using a different baseline length dependent processing scheme (Townsend et al., 2000).

The formal accuracy of the corrections has been an area of concern but has not been rigorously investigated. Fortes (2002) investigated a method of improving the accuracy of the corrections over time through Kalman filtering. In this approach the corrections are time filtered independently from the correction generation. This was shown to be effective, especially at the beginning and end of a satellite pass, when the correction is determined by a limited number of reference stations. Although, this approach improves correction accuracy, it does not produce an estimated accuracy of the corrections.

1.2 Objectives

The overall objective of this research is to develop a beginning-to-end processing method for multiple reference station positioning. To this end, this thesis discusses two novel beginning-to-end multiple reference station approaches.

Specific sub-objectives of this contribution are to:

1. Develop a covariance function that improves on the covariance function developed by Raquet (1998) in terms of the covariance function properties. More specifically, a covariance function without the dependence on a P_0 point and

that can determine correlations between any satellite and station combination. This covariance function will produce a fully populated variance-covariance matrix that can be used to weight the observations for both stages of the multiple reference station approach, i.e. ambiguity estimation and error prediction. The coefficients of this covariance function are observable in real-time, which removes the need for post-mission calibration. This adaptive covariance function will affect all stages of the multiple reference station approach and will result in better modelling of the covariance of the observations allows for better estimation and resolution of network ambiguities (first stage) and improved prediction of the network errors through collocation (second stage).

2. Develop the least squares collocation equations for prediction using estimated parameters (i.e. ambiguities with float values). This includes equations for prediction of the errors as well as the equations to calculate the estimated variance-covariance of the corrections. In addition, the rigorous use of these corrections is explored mathematically, including the effect of the estimated variance-covariance of the corrections on the rover's estimated precision. This will improve the prediction of the errors at the rover location (second stage). It also allows for the calculation of the variance-covariance matrix of the corrections, which can be used to correctly apply the corrections in the final stage of the multiple reference station approach.

3. Develop and test a tightly integrated method for multiple reference station positioning. This approach integrates as much information as possible into obtaining the precise position of one or many roving receivers in the region of the network. This approach combines all three multiple reference station stages

into an integrated approach.

1.3 Original Contribution

Many topics related to the multiple reference station approach have been significantly advanced by this research. The development of two multiple reference station positioning methods are discussed. The first of which is an extension of the approach introduced by Raquet (1998).

The original work by Raquet (1998) assumes that the carrier phase ambiguities are known, which is not a reasonable assumption for real-time positioning. Removing this assumption requires considerable redevelopment of the problem. This is one major original contribution of this thesis. The first stage of this advancement was to reevaluate the least squares collocation equations, including variance-covariance information for unresolved estimated parameters. This includes the calculation of the variance-covariance matrix of the corrections, which is an important quality of the corrections that had not yet been considered. This solution was expanded to include ambiguity resolution using conditional decorrelation of the parameters and ionosphere modelling. Ionosphere modelling requires special considerations because the pseudo-ionosphere observations and ionosphere estimated parameters should not be used in the prediction of the corrections. The collocation-based equations using ionosphere modelling can be simplified by applying conditional decorrelation, which is traditionally applied to ambiguities, on the ionosphere parameters. This approach has not been shown in previous research.

This thesis discusses the use of the variance-covariance matrix of the corrections, which has not been considered in previous research. Consequently the use of this

information is unique to this thesis.

One of the requirements of this approach is that the covariance information for the parameter estimation and prediction stages is coherent. The development of covariance functions applied to GPS errors in post-mission is discussed in Raquet (1998), Radovanovic et al. (2001) and Kennedy (2002). The estimation of the covariance function parameters in real-time is an original contribution of this thesis. This allows for variations in error conditions to be modelled by the covariance function without the need for calibration.

The second multiple reference station positioning method discussed in this work is a tightly coupled approach. Although developed independently, this approach is similar to the precise relative positioning of multiple moving platforms shown in Luo (2001). However, the approach shown in Luo (2001) mainly concerns the datum problem of differential positioning without any reference stations and the optimal use of constraints. Luo (2001) also assumes that there is no correlation between the observations of different baselines. The tightly coupled approach shown in this research is significantly different from the approach shown in Luo (2001) in terms of its implementation and development.

1.4 Data sets

Two data set are used to compare the various approaches introduced in this work.

1.4.1 MAGNET Network (Turkey)

Data from the TUBITAK Marmara Continuous GPS Network (MAGNET) was collected from October 26 to 28, 2001. The baseline lengths range from 25 to 75 km. Figure 1.1 shows a map of the TUBITAK Marmara Continuous GPS Network (MAG-

NET).

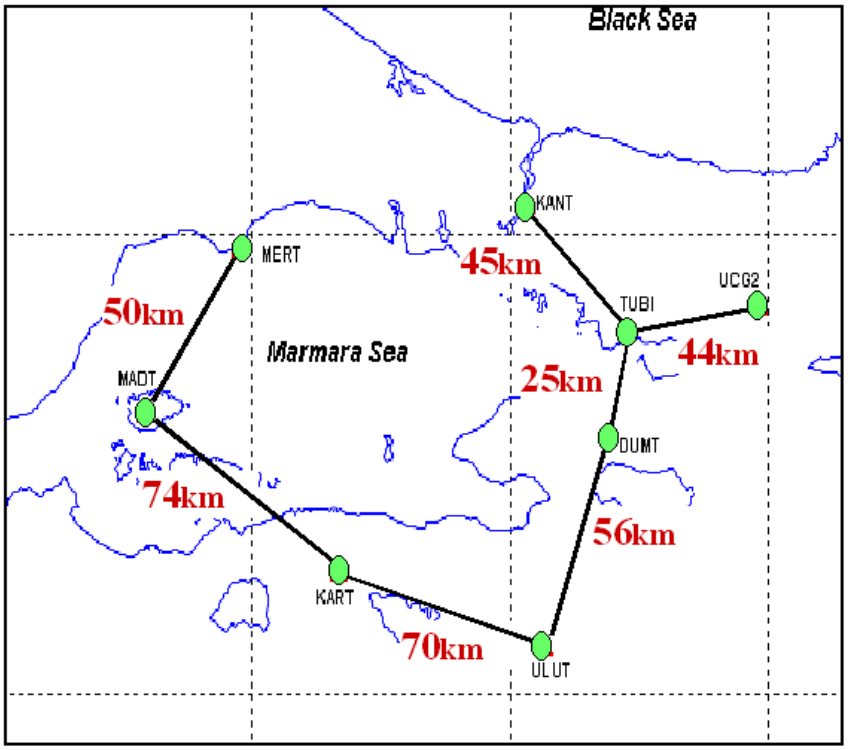

Figure 1.1: TUBITAK Marmara Continuous GPS Network (MAGNET)

The atmospheric effects for October 26 to 28 are shown in Table 1.1, residual troposphere and orbit error is 0.1 ppm for all the days and the ionosphere error ranges from 1.4 to 2.1 ppm. These errors can be considered average in magnitude.

Table 1.1: RMS error of the L1 ionosphere and residual troposphere and orbit errors for October 26, 27 and 28, 2001

	L1 Ionosphere	Residual Troposphere and Orbit
October 26	1.4 ppm	0.1 ppm
October 27	1.4 ppm	0.1 ppm
October 28	2.1 ppm	0.1 ppm

1.4.2 SAN Network (Canada)

Data from the Southern Alberta Network (SAN) was collected on June 8 and 14, 2004. The baseline lengths of this network range from 24 to 49 km. Figure 1.2 shows the SAN network.

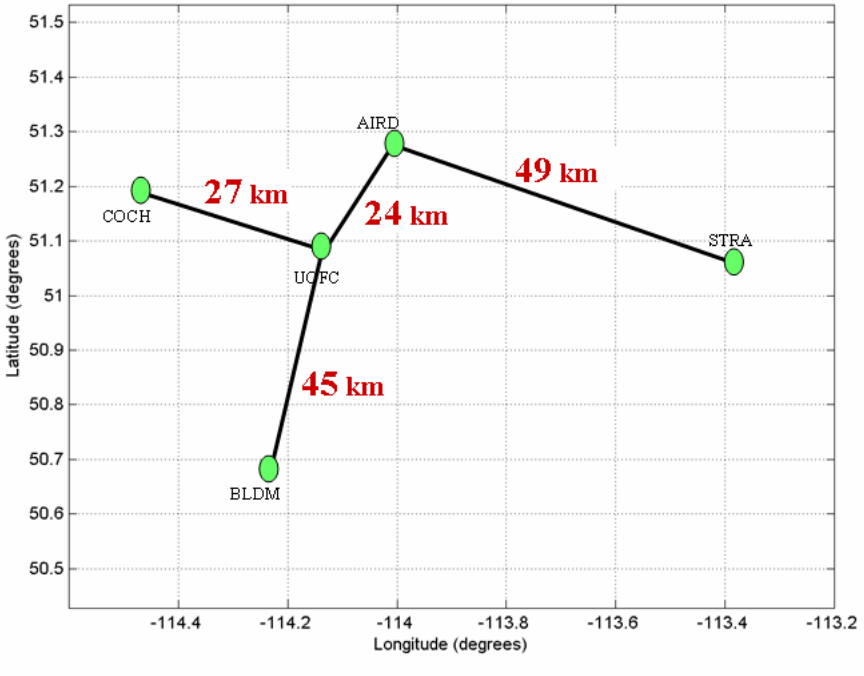

Figure 1.2: Subset of the Southern Alberta Network (SAN) Used for Data Collection

The RMS ionosphere, and troposphere and orbit errors for the SAN network on these days range from 0.8 to 0.9 ppm for the ionosphere error and 0.2 ppm for the residual troposphere and orbit error, respectively. The atmospheric effects are shown in Table 1.2. These error can be considered low to average in magnitude.

1.5 Thesis Outline

Chapter 2 discusses the fundamental background for this research. This information is required to fully understand the development in further chapters.

Table 1.2: RMS error of the L1 ionosphere and residual troposphere and orbit errors for June 8 and 14, 2001

	L1 Ionosphere	Residual Troposphere and Orbit
June 8	0.9 ppm	0.2 ppm
June 14	0.8 ppm	0.2 ppm

Chapter 3 discusses the development of an adaptive covariance function. This chapter begins with the selection of the form of the covariance function. It then shows that the coefficients of this function can be estimated in real-time to adapt to the changing environmental errors.

Chapter 4 shows the development of collocation equations for multiple reference station positioning first assuming that the adjustment misclosure is a function of the estimated parameters. Secondly, the equations are adapted for fixed ambiguities and again to also include special considerations inherent to ionospheric modelling. This development includes calculation of the variance-covariance matrix of the corrections, a method of applying the corrections and the theoretical mathematical effect of the corrections on a user given the variance-covariance matrix of the corrections.

Chapter 5 shows a comparison between the single reference station approach and the collocation-based multiple reference station approach using three days of data from the MAGNET network.

Chapter 6 discusses an alternate method of multiple reference station positioning using a tightly coupled approach. Results demonstrate the performance of the tightly coupled approach compared to the single reference station approach using three days of data from the MAGNET network.

Chapter 7 discusses theoretical differences between the collocation-based approach and the tightly coupled approach. A comparison follows using data from the SAN

network.

Chapters 8 draws conclusions from this work, including recommendations for future work.

Chapter 2

Fundamentals

2.1 GPS Error Sources

The precision, accuracy and reliability of GPS positioning and navigation is dependent on the level of errors present in the observations. The properties of observation errors change over time and geographic region. This section describes the error sources relevant to differential carrier phase positioning. When all of these errors are considered the resulting code and carrier phase measurement equations are

$$\begin{aligned} P &= \rho + d\rho + T + I_f + \varepsilon_{P_{mp}} + \varepsilon_{P_{noise}} \\ \phi &= \rho + d\rho + T - I_f + \varepsilon_{\phi_{mp}} + \varepsilon_{\phi_{noise}} + \lambda N \end{aligned} \tag{2.1}$$

where

P	is a code measurement in metres,
ϕ	is a carrier phase measurement in metres,
ρ	is the receiver to satellite range in metres
$d\rho$	is the satellite position error in metres
T	is the troposphere error in metres
I_f	is the ionospheric error at the frequency (f) in metres,
$\varepsilon_{P_{mp}}, \varepsilon_{\phi_{mp}}$	are the code and carrier phase multipath in metres,
$\varepsilon_{P_{noise}}, \varepsilon_{\phi_{noise}}$	is the code and carrier phase measurement noise in metres, and
λN	is the carrier phase ambiguity in metres.

Each error will now be discussed.

2.1.1 Ionosphere Errors

The ionosphere is a region of the atmosphere which contains weakly ionized plasma (Klobuchar, 1996). The ion content (free electrons) in this region has various effects on electromagnetic signals, such as GPS.

The ion content of the ionosphere is distributed from 60 to more than 1000 km above the surface of the Earth (Klobuchar, 1996) however the peak density is located around 300 to 450 km. The effect of the ionosphere on radio-navigation signals is a function of the integration of the electron density along the signal's path as shown for the pseudorange code measurement as follows

$$I(f) = \frac{40.3}{cf^2} \int_{path} N dl, \tag{2.2}$$

where $I(f)$ is the pseudorange ionospheric delay in metres, f is the wavelength of the signal and N is the electron density of the ionosphere. Equation 2.2 shows that the ionospheric delay is a function of the frequency of the signal for L-band signals. A multiple frequency navigation system can use this dispersive property to estimate the ionospheric effect on the measurements.

The ionospheric phenomenon affects the code and carrier phase measurements differently. Carrier phase measurements are advanced by the ionosphere by the same amount that the code is delayed. This property is commonly used to estimate the ionospheric effect in the following code minus carrier phase combination

$$P - \phi = 2I_f + \varepsilon_{P_{mp}} - \varepsilon_{\phi_{mp}} + \varepsilon_{P_{noise}} - \varepsilon_{\phi_{noise}} - \lambda N. \tag{2.3}$$

The ionosphere's variability is due to the number of free electrons, which is a function of solar radiation. As a result, there is a daily variation of the ionosphere such that it is relatively calm at night and is most active around 14:00 local time.

There are also regional effects due to the Sun. These effects can be seen in Figure 2.1, which shows the estimated global ionospheric error on January 1, 2004 at 0:00 UTC. This is derived from a Global Ionosphere Map (GIM) produced by the Center for Orbit Determination in Europe (CODE). There is a significant ionspheric gradient at low geomagnetic latitudes which is amplified at approximately 14:00 local time.

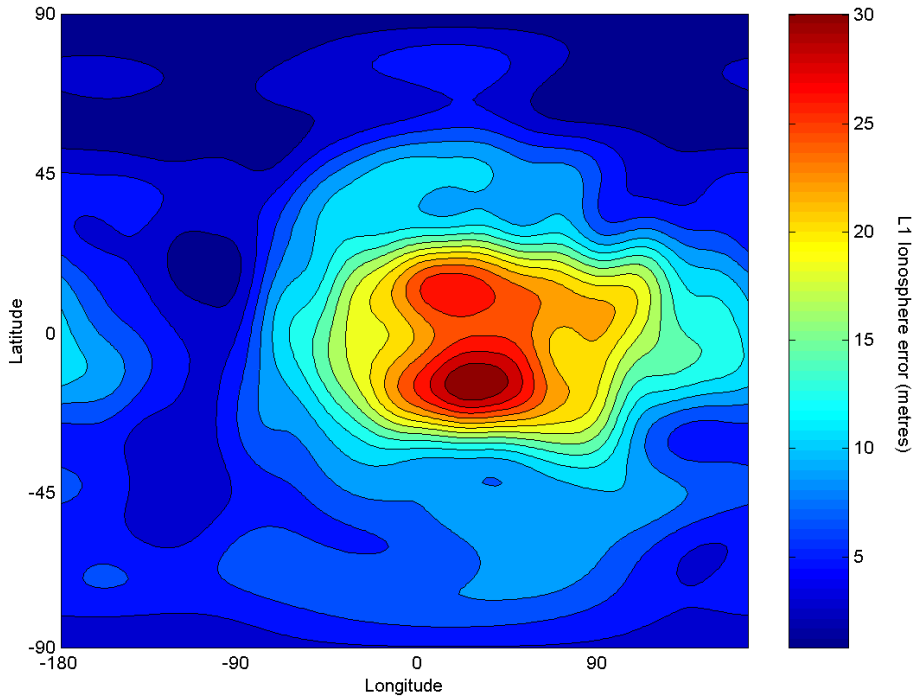

Figure 2.1: L1 ionosphere error for Jan 1, 2004 at 0:00 UTC derived from a Global Ionosphere Map from the Center for Orbit Determination in Europe (CODE)

The ionosphere is the largest error source for differential GPS ranging less than 1 part per million (ppm) of the inter-antenna distance during low ionospheric periods at mid latitudes to greater than 10 ppm at low geomagnetic latitudes during midday. Figure 2.2 shows the level of ionosphere error for data collected from the MAGNET network in Turkey (October 26, 2001). The daily variation and effect of

baseline length are shown figure. In the early morning and late evening the error is approximately 0.6 ppm and increases to approximately 4.1 ppm at midday. The values shown in Tables 1.1 and 1.2 are the averages for the 24 hour data sets and the many baselines. For example, the ionosphere given in Table 1.1 is 1.4 ppm, which is the average of the ppm for the network baselines throughout the day.

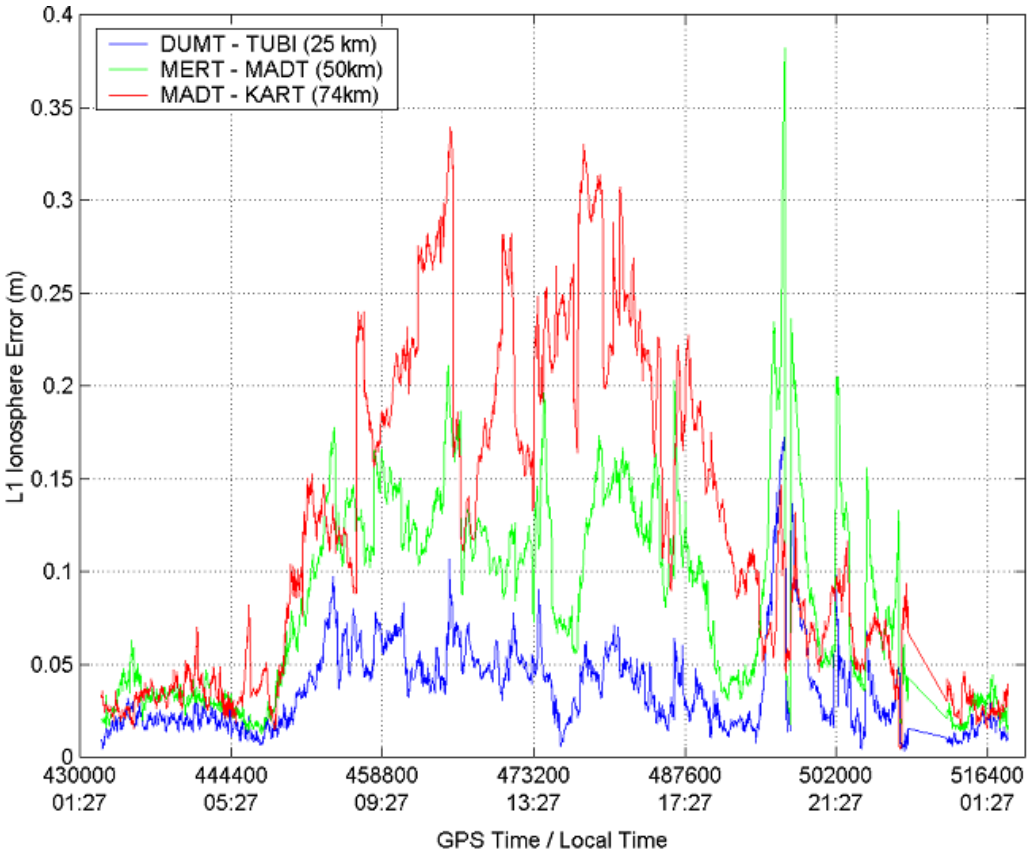

Figure 2.2: L1 ionosphere error for three baselines of the October 26, 2001 data set

2.1.2 Troposphere Errors

The troposphere is a region of the atmosphere that spans from the Earth's surface to 12 to 14 km above the surface (Spilker, 1996). The composition of the gases in this region has an impact on GPS signals. As the signal travels through these

tropospheric gases, the signal refracts and slows the transmission speed of the signal, which both lengthen the measurement's path causing a delay in the time that the signal is received. The magnitude of the delay is relative to the atmospheric profile along the signal path.

This delay can be characterized through two effects, the dry and wet delays. The dry part is due to the non-water content and the wet delay is caused by the water content in the atmosphere. The dry delay is the larger of the effects, however it is predictable and stable over time. The remaining wet part is relatively unstable and unpredictable over time but only constitutes 10 percent of the total tropospheric effect. The wet delay varies by 10 to 20 percent in a few hours (Spilker, 1996).

Many models have been developed to reduce the effect of the troposphere on GPS measurements. The model used in this research is the modified Hopfield model (Goad and Goodman, 1974) using standard atmospheric parameters for temperature and pressure (derived from the station height) and a relative humidity of 50 percent. This is the same model used in Raquet (1998). The differential residual troposphere error (after modelling) is on the order of 0.1 to 0.4 ppm of the inter-antenna distance (e.g. Tables 1.1 and 1.2).

2.1.3 Orbit Errors

The orbit error is due to inaccuracies in the satellite position reported by the broadcast ephemeris. The effect of a satellite position error on the differential position is the projection of this error onto the direction of the observation vector (Parkinson, 1996). Raquet (1998) shows that orbit error is usually less than 0.1 ppm of the inter-antenna distance.

2.1.4 Multipath and Measurement Noise

Multipath error is caused by the interference of a reflected signal mixing with the direct satellite signal. The level of multipath is a function of the receiver tracking technology, the antenna type, and the antenna environment.

The noise term consists of receiver measurement noise and the sum of all other unmodelled and second order effects. This is also a function of the receiver technology used. Raquet (1998) shows the code and carrier phase noise and multipath root mean squared errors (Table 2.1) from sample data. These are consistent with the level of multipath and noise shown in Petovello (2003).

Table 2.1: Code and carrier phase noise and multipath RMS error shown in Raquet (1998)

Measurement type	RMS Error
L1 CA code	0.4 m
L2 P code	1.0 m
L1 phase	4.3 mm
L2 phase	6.2 mm

2.2 Least Squares Estimation

Least squares estimation is one method of unbiased parameter estimation. There are many forms of the estimation equations for different applications. This research focuses on real-time estimation of the parameters over time. To accommodate this requirement, an epoch-by-epoch approach is used. There are two forms of least squares estimation that allow for real-time estimation, Bayes filtering (Gelb, 1974) and Kalman filtering (Gelb, 1974; Brown and Hwang, 1997; Salychev, 1998). These two methods have differing properties; however, their solutions are equivalent (Koch,

2000; Brown and Hwang, 1997). The Bayes filter is more computationally efficient than Kalman filtering when the number of measurements exceeds the number of parameters and a Kalman filter is more efficient than a Bayes filter when the number of parameters exceeds the number of measurements.

2.2.1 Kalman/Bayes Filtering

A Bayes filter has been used over a Kalman filter in this research because there are usually more measurements than parameters in the models employed.

The measurement matrix (B) relates the measured observations (l) to the linear combination which observes the estimated parameters. Each column in the matrix represents an untransformed (raw) measured observation. Each row of the matrix represents a transformed linear combination of the measured observations. Each element of the matrix is the partial derivative of the observation equations with respect to the untransformed (raw) observations. Double difference observations are commonly used in carrier phase GPS estimation. As an example, the (raw) undifferenced observations from Table 2.2 are used to create the double difference observations shown in Table 2.3.

Table 2.2: Example set of undifferenced (raw) observations

Observation	Station	PRN
l_a^1	a	1
l_a^2	a	2
l_a^3	a	3
l_b^1	b	1
l_b^2	b	2
l_b^3	b	3

The double difference measurement matrix for this example is

Table 2.3: Example set of double difference observations

Difference observation	Undifferenced combination
$\Delta\nabla l_{ab}^{12}$	$l_a^1 - l_a^2 - (l_b^1 - l_b^2)$
$\Delta\nabla l_{ab}^{13}$	$l_a^1 - l_a^3 - (l_b^1 - l_b^3)$

$$\begin{aligned} \Delta\nabla l &= Bl \\ &= \begin{bmatrix} 1 & -1 & 0 & -1 & 1 & 0 \\ 1 & 0 & -1 & -1 & 0 & -1 \end{bmatrix} \begin{bmatrix} l_a^1 \\ l_a^2 \\ l_a^3 \\ l_b^1 \\ l_b^2 \\ l_b^3 \end{bmatrix}. \end{aligned} \tag{2.4}$$

The design matrix (A) relates the double difference observations to the estimated parameters. Each column represents an estimated parameter and each row represents an observation. Elements of the matrix are the partial derivatives of the observation equations with respect to the estimated parameters. A set of parametric equations is

$$\begin{aligned} \Delta\nabla l_{ab}^{12} &= \Delta\nabla\rho_{ab}^{12} + \lambda\Delta\nabla N_{ab}^{12} + \varepsilon_{ab}^{12} \\ \Delta\nabla l_{ab}^{13} &= \Delta\nabla\rho_{ab}^{13} + \lambda\Delta\nabla N_{ab}^{12} + \varepsilon_{ab}^{12}, \end{aligned} \tag{2.5}$$

where λ is the wavelength of the signal in metres, N is the carrier phase ambiguity is cycles and ε is the unestimated residual errors in metres. An example design matrix

(A) given these measurement equations is

$$\begin{aligned}\Delta\nabla l_{ab}^{12} &= Ax \\ &= \begin{bmatrix} \frac{\partial\Delta\nabla l_{ab}^{12}}{\partial x_b} & \frac{\partial\Delta\nabla l_{ab}^{12}}{\partial y_b} & \frac{\partial\Delta\nabla l_{ab}^{12}}{\partial z_b} & \frac{\partial\Delta\nabla l_{ab}^{12}}{\partial\Delta\nabla N_{ab}^{12}} & \frac{\partial\Delta\nabla l_{ab}^{12}}{\partial\Delta\nabla N_{ab}^{13}} \\ \frac{\partial\Delta\nabla l_{ab}^{13}}{\partial x_b} & \frac{\partial\Delta\nabla l_{ab}^{13}}{\partial y_b} & \frac{\partial\Delta\nabla l_{ab}^{13}}{\partial z_b} & \frac{\partial\Delta\nabla l_{ab}^{13}}{\partial\Delta\nabla N_{ab}^{12}} & \frac{\partial\Delta\nabla l_{ab}^{13}}{\partial\Delta\nabla N_{ab}^{13}} \end{bmatrix} \begin{bmatrix} x_b \\ y_b \\ z_b \\ \Delta\nabla N_{ab}^{12} \\ \Delta\nabla N_{ab}^{13} \end{bmatrix}. \end{aligned} \tag{2.6}$$

The Bayes filter estimation equations are

$$\hat{x} = x^\circ + (A^T(BC_{ll}B^T)^{-1}A + C_{x^\circ x^\circ}^{-1})^{-1}A^T(BC_{ll}B^T)^{-1}(Ax^\circ - Bl), \tag{2.7}$$

where $\hat{x}$ is a vector of adjusted parameters, x° is a vector of the parameters prior to adjustment, C_{ll} is the variance-covariance matrix of the raw observations and $C_{x^\circ x^\circ}$ is the variance-covariance matrix of the parameters prior to the adjustment. This equation takes into account a-priori information contained within the vector of the parameters prior to adjustment (x°) and its variance-covariance matrix, $C_{x^\circ x^\circ}$. In the processing of data in real-time, these equations are used at each epoch to update the current solution with new observations.

2.2.2 Collocation

Least squares collocation is derived from the concept of dividing residual errors into two components: signal and noise. This suggests that in addition to the functional model that is represented as Ax there are additional unmodelled errors. In this case, ionosphere, troposphere, and orbit errors are all signal components, which are due to artifacts external to the measurement instrument.

Although a deterministic function for the signal components is unknown, the second moment of the expected value of the signal $(E\{ss^T\})$ must be known for

collocation. The second moment of the signal can be derived from a signal covariance function.

Separating the measurements into a signal component and a noise component gives

$$l = l_\circ + l_s + l_n \tag{2.8}$$

where $l_\circ$ is the deterministic bias including the true range, l_s is the signal, and l_n is the observation noise. The variance-covariance matrix of the observations is

$$\begin{aligned} C_{ll} &= \mathrm{E}\{(l - \mathrm{E}\{l\})(l - \mathrm{E}\{l\})^T\} \\ &= \mathrm{E}\{(l_\circ + l_s + l_n - l_\circ)(l_\circ + l_s + l_n - l_\circ)^T\} \\ &= \mathrm{E}\{l_s l_s^T\} + \mathrm{E}\{l_n l_n^T\} \\ &= C_{l_s l_s} + C_{l_n l_n}. \end{aligned} \tag{2.9}$$

This assumes that the signal and noise are uncorrelated. In comparison the covariance between two vectors of observations is

$$\begin{aligned} C_{l_1,l_2} &= \mathrm{E}\{(l_1 - \mathrm{E}\{l_1\})(l_2 - \mathrm{E}\{l_2\})^T\} \\ &= \mathrm{E}\{(l_{1s} + l_{1n})(l_{2s} + l_{2n})^T\} \\ &= \mathrm{E}\{l_{1s} l_{2s}^T\} = C_{l_{1s} l_{2s}}. \end{aligned} \tag{2.10}$$

It is assumed that the noise components of the observations are uncorrelated in this example. The covariance between the two observation vectors is simply the signal covariance.

Using the definitions of the signal and noise components in the least squares estimation gives the estimation component of least squares collocation. This is the

substitution of Equations 2.9 and 2.10 into Equation 2.7:

$$\begin{aligned}\hat{x} &= x^{\circ} + (A^T(B(C_{l_s l_s} + C_{l_n l_n})B^T)^{-1}A + C_{x^{\circ}x^{\circ}}^{-1})^{-1} \\ & \quad A^T(B(C_{l_s l_s} + C_{l_n l_n})B^T)^{-1}(Ax - Bl). \end{aligned} \tag{2.11}$$

Moritz (1980) gives an intuitive derivation for the prediction of the signal. The estimated signal is defined as a linear function of the data (l),

$$\hat{s} = Hl, \tag{2.12}$$

where H is the linear transformation matrix which relates the data to the signal. The error of this estimate is

$$\varepsilon = \hat{s} - s. \tag{2.13}$$

The linear transformation matrix used is that which minimizes the error covariance. The error covariance of the estimated signal is

$$\begin{aligned} C_{\varepsilon\varepsilon} &= \mathrm{E}\{\varepsilon\varepsilon^T\} \\ &= \mathrm{E}\{(Hl - s)(Hl - s)^T\} \\ &= H\mathrm{E}\{ll^T\}H^T - \mathrm{E}\{sl^T\}H^T - H\mathrm{E}\{ls^T\} + E\{ss^T\} \\ &= HC_{ll}H^T - C_{sl}H^T - HC_{ls} + C_{ss}. \end{aligned} \tag{2.14}$$

This equation can be rearranged to simplify the evaluation of the minimum:

$$C_{\varepsilon\varepsilon} = C_{ss} - C_{sl}C_{ll}^{-1}C_{ls} + (H - C_{sl}C_{ll}^{-1})C_{ll}(H - C_{sl}C_{ll}^{-1})^T. \tag{2.15}$$

From this equation it is easy to see that to find a value of H that minimizes the error covariance of the estimated signal, the term $(H - C_{sl}C_{ll}^{-1})C_{ll}(H - CslC_{ll}^{-1})^T$ must be minimized. As a result

$$H = C_{sl}C_{ll}^{-1}. \tag{2.16}$$

The estimate that minimizes the error covariance of the signal is

$$\hat{s} = C_{sl} C_{ll}^{-1} l. \tag{2.17}$$

Replacing the definition for H from Equation 2.16 into the equation of the error covariance of the signal (Equation 2.15) gives

$$C_{\varepsilon\varepsilon} = C_{\hat{s}\hat{s}} = C_{ss} - C_{sl} C_{ll}^{-1} C_{ls}. \tag{2.18}$$

2.2.3 Temporal Models

Temporal models are used to relate one epoch's states to the next. This is accomplished using an assumption about the stochastic behaviour of the estimated parameter over time. If a parameter is static and constant over time then one epoch will directly relate to the next. Consequently, the one epoch's estimated parameters and estimated variance-covariance can be used as a-priori information for the following epoch.

The reverse case (infinite white noise) is also trivial. If the parameters from one epoch have no relationship with the next epoch's parameters then no information from one epoch can be passed to the next. In this case the state vector from the one epoch can be used as a point of expansion for the next epoch with an infinite variance (i.e., no information).

All the cases in between can be described by a system of differential equations that relate one epoch to the next. This system of differential equations defines the transition from one epoch to the next and, to some extent, the change in variance-covariance from one epoch to the next. Two common, time-varying systems are a random walk process and a first order Gauss-Markov process. These processes are described in Gelb (1974).

A random walk process is best described by a roaming value that changes by a discrete step randomly increasing or decreasing from the previous value. All the future values are tied to the current value; however, the likelihood that the future value and the current value are the same decreases over time. In terms of temporal modelling, the current value of the parameter is used as the a-priori estimate for the next epoch but due to the decreased likelihood that the value is the same, the estimated variance of the parameter is increased from one epoch to the next. The update equations from one epoch to the next for a random walk process is

$$\begin{aligned} x_{k+1} &= x_k, \\ \sigma^2_{x_{k+1}} &= \sigma^2_{x_{k+1}} + q\Delta t, \end{aligned} \tag{2.19}$$

where x is the value of the random walk parameter, σ^2 is the estimated variance of the parameter, q is the spectral density, which describes the variability of the parameter over time, and Δt is the difference in time between the last update and the next.

A Gauss-Markov process is described by the differential equation (Gelb, 1974)

$$\dot{x} = -\beta x + w. \tag{2.20}$$

It produces a characteristic decreasing autocorrelation function. It is commonly used in prediction because of the behaviour of the estimate over time. Initially, the predicted update is the same as the latest estimate and over time the estimate converges to zero. For this reason, it is a conservative estimation choice for many estimated parameters. Consider as an example the velocity of a person walking as the lights go out being estimated as a first order Gauss-Markov process. Initially, it is safe to walk blindly forward at the same speed as before the lights went out and over time (as the person's confidence in their current position or changing surroundings decreases) the person slows to a stop. The rate at which the individual slows depends on their

environment, for example, if the person is walking in an empty field then they could walk with confidence knowing that they will not encounter any obstacles. However, a person walking in a crowded room would stop immediately because of the variability of their surroundings. The update equations for a first order Gauss-Markov process are (Gelb, 1974)

$$\begin{aligned} x_{k+1} &= e^{-\beta\Delta t}x_k \\ \sigma^2_{x_{k+1}} &= \sigma^2_{x_k} + \tfrac{q}{2\beta}(1 - e^{-2\beta\Delta t}). \end{aligned} \tag{2.21}$$

In the precise carrier phase positioning filters used in this research there are four types of states: ambiguities, slant ionosphere error, position and velocity. Ambiguities and static positions are usually modelled as random constants (static states) (described above), whereby one epoch's parameter estimate is used as a-priori information for the next epoch. Slant ionosphere error and velocity are time varying states which change somewhat from epoch to epoch. Skone (1998) shows that ionospheric error behaves like a first order Gauss-Markov process based on its autocorrelation function.

A kinematic (mobile) receiver is modelled temporally to propagate and relate the estimation solution from one epoch to the next. This requires some assumptions about the general dynamic behaviour of the vehicle. In a position and velocity model the position is propagated over time using the integration of velocity over time. This is not as simple for the velocity states, which must be propagated using an assumption about the vehicle behaviour. Two common models for the velocity states are the random walk velocity model and the first order Gauss-Markov model.

The random walk velocity model assumes that the vehicle will travel in the same trajectory from one epoch to the next. Although this may be true in a majority of situations this can be detrimental if the vehicle changes speed or direction. The first

order Gauss-Markov process assumes that the velocity will decrease at an exponential rate from one epoch to the next. Although this is an unlikely vehicle behaviour, it allows for a near constant velocity model when the data rate is high or the correlation time is long. This model is also safer when the data rate is low or the correlation time is low because the predicted vehicle's velocity decreases, which will reduce propagation errors in the event that the vehicle does not maintain a constant trajectory or speed.

As the update equations for the velocity will also affect the position estimates, the transition must be determined by solving the system of differential equations. The system dynamics model for the position and velocity states, when the velocity is estimated as a first order Gauss-Markov process is

$$\begin{aligned} \dot{x} &= \dot{x} \\ \ddot{x} &= -\beta\dot{x} + w \end{aligned} \tag{2.22}$$

where x is the position state, $\dot{x}$ is the velocity state, $\ddot{x}$ is the acceleration, β is the rate of decline of the velocity over time and w is the white noise error associate with the propagation error.

In matrix form the system model is

$$\begin{bmatrix} \dot{x} \\ \ddot{x} \end{bmatrix} = \begin{bmatrix} 0 & 1 \\ 0 & -\beta \end{bmatrix} \begin{bmatrix} x \\ \dot{x} \end{bmatrix} + \begin{bmatrix} 0 \\ w \end{bmatrix}. \tag{2.23}$$

This system of equations can be solved using a Taylor series expansion (Gelb, 1974). The expansion about t_0 is

$$x(t) = x(t_0) + \dot{x}\Delta t + \ddot{x}\frac{\Delta t^2}{2!} + ... \tag{2.24}$$

The expansion can be related to the system model by

$$x(t) = x(t_0) + F\Delta t x(t_0) + \frac{F^2\Delta t^2}{2!}x(t_0) + ... \tag{2.25}$$

where

$$F = \begin{bmatrix} 0 & 1 \\ 0 & -\beta \end{bmatrix}. \tag{2.26}$$

This expansion in terms of the matrix F is

$$\begin{aligned} \begin{bmatrix} x \\ \dot{x} \end{bmatrix} &= \left(I + \sum_{i=1}^{\infty} \begin{bmatrix} 0 & (-\beta)^{i-1} \\ 0 & (-\beta)^{i} \end{bmatrix} \frac{\Delta t^i}{i!} \right) \begin{bmatrix} x(t_0) \\ \dot{x}(t_0) \end{bmatrix} \\ &= \begin{bmatrix} 1 & a \\ 0 & b \end{bmatrix} \begin{bmatrix} x(t_0) \\ \dot{x}(t_0) \end{bmatrix} \end{aligned} \tag{2.27}$$

where a and b are the elements of the matrix to be simplified in the following derivation.

$$a = \Delta t - \beta \frac{\Delta t^2}{2!} + \beta^2 \frac{\Delta t^3}{3!} + ... \tag{2.28}$$

$$1 - \beta a = 1 - \beta \Delta t + \frac{\beta^2 \Delta t^2}{2!} - \frac{\beta^3 \Delta t^3}{3!} + ... \tag{2.29}$$

which can be replaced using the definition of the Taylor series expansion of an exponential decay function:

$$e^A = 1 + A + \frac{A^2}{2!} + \frac{A^3}{3!} + ... \tag{2.30}$$

resulting in

$$a = \frac{1 - e^{-\beta \Delta t}}{\beta} \tag{2.31}$$

A similar derivation can be made for the solution of b:

$$\begin{aligned} b &= 1 - \beta \Delta t + \frac{\beta^2 \Delta t^2}{2!} - \frac{\beta^3 \Delta t^3}{3!} + ... \\ &= e^{-\beta \Delta t} \end{aligned} \tag{2.32}$$

The transition matrix, which relates one epoch to the next is then

$$\Phi = \begin{bmatrix} 1 & \frac{1 - e^{-\beta \Delta t}}{\beta} \\ 0 & e^{-\beta \Delta t} \end{bmatrix} \tag{2.33}$$

The propagation's effect on the covariance matrix is based on the noise term (w). If

$$G = \begin{bmatrix} 0 & 0 \\ 0 & 1 \end{bmatrix}, \tag{2.34}$$

then the propagation's effect on the variance-covariance matrix is defined by the following. Hereafter the temporal propagation is assumed to be from $t = 0$ to t:

$$\begin{aligned} Q_{ww} &= \int_0^t \Phi G Q G^T \Phi^T \, dt \\ &= \int_0^t \begin{bmatrix} 1 & \frac{1-e^{-\beta t}}{\beta} \\ 0 & e^{-\beta t} \end{bmatrix} \begin{bmatrix} 0 & 0 \\ 0 & 1 \end{bmatrix} \begin{bmatrix} 1 & 0 \\ \frac{1-e^{-\beta t}}{\beta} & e^{-\beta t} \end{bmatrix} q \, dt \\ &= \int_0^t q \begin{bmatrix} \left(\frac{1-e^{-\beta t}}{\beta}\right)^2 & \frac{1-e^{-\beta t}}{\beta} e^{-\beta t} \\ \frac{1-e^{-\beta t}}{\beta} e^{-\beta t} & e^{-\beta t} \end{bmatrix} dt. \end{aligned} \tag{2.35}$$

The integrals of each of the elements of this matrix can be calculated independently as

$$\begin{aligned} Q_{w11} &= \int_0^t q \left(\frac{1}{\beta} - \frac{e^{-\beta t}}{\beta}\right)^2 dt \\ &= \int_0^t q \left(\frac{1}{\beta^2} - 2\frac{e^{-\beta t}}{\beta^2} + \frac{e^{-2\beta t}}{\beta^2}\right) dt \\ &= \frac{q}{\beta^3}(-\frac{3}{2} + \beta t + 2e^{-\beta t} - \frac{1}{2}e^{-2\beta t}), \end{aligned} \tag{2.36}$$

$$\begin{aligned} Q_{w12} = (\Gamma Q \Gamma^T)_{21} &= \int_0^t \frac{q}{\beta} \left(e^{-\beta t} - e^{-2\beta t}\right) dt \\ &= \frac{q}{\beta^2}(\frac{1}{2} - e^{-\beta t} + \frac{1}{2}e^{-2\beta t}), \text{ and} \end{aligned} \tag{2.37}$$

$$\begin{aligned} Q_{w22} &= \int_0^t q e^{-2\beta t} \, dt \\ &= \frac{q}{2\beta}(1 - e^{-2\beta t}). \end{aligned} \tag{2.38}$$

The update (using the transition matrix) of the state parameters is

$$\begin{aligned} x_{k+1} &= \Phi x_k, \\ C_{x_{k+1}x_{k+1}} &= \Phi C_{x_k x_k} \Phi^T + Q_{ww}. \end{aligned} \tag{2.39}$$

In terms of a position and velocity system, where the velocity is modelled as a first order Gauss-Markov process, the update equations are

$$\begin{bmatrix} x \\ \dot{x} \end{bmatrix}_{k+1} = \begin{bmatrix} 1 & \frac{1-e^{-\beta\Delta t}}{\beta} \\ 0 & e^{-\beta\Delta t} \end{bmatrix} \begin{bmatrix} x \\ \dot{x} \end{bmatrix}_k, \tag{2.40}$$

$$\begin{aligned} C_{x_{k+1}x_{k+1}} = & \begin{bmatrix} 1 & \frac{1-e^{-\beta\Delta t}}{\beta} \\ 0 & e^{-\beta\Delta t} \end{bmatrix} C_{x_k x_k} \begin{bmatrix} 1 & 0 \\ \frac{1-e^{-\beta\Delta t}}{\beta} & e^{-\beta\Delta t} \end{bmatrix} \\ & + \begin{bmatrix} \frac{q}{\beta^3}(-\frac{3}{2} + \beta t + 2e^{-\beta t} - \frac{1}{2}e^{-2\beta t}) & \frac{q}{\beta^2}(\frac{1}{2} - e^{-\beta t} + \frac{1}{2}e^{-2\beta t}) \\ \frac{q}{\beta^2}(\frac{1}{2} - e^{-\beta t} + \frac{1}{2}e^{-2\beta t}) & \frac{q}{2\beta}(1 - e^{-2\beta t}) \end{bmatrix}. \end{aligned} \tag{2.41}$$

2.3 Ambiguity Resolution

Carrier phase ambiguities are tracking biases induced by the measurement process of the carrier phase of the GPS signal. These biases have integer values (in cycles). These bias are random values that change with each loss of lock of the tracked signal. In other words, each satellite is assigned a random integer ambiguity that will be different every time the signal is tracked.

These biases must be estimated before the signal can be used effectively and if possible the ambiguities should be constrained (fixed) to their true integer values. This fixed ambiguity case will give the best possible performance when using carrier phase measurements.

There are many methods to determine the correct integer ambiguity. Erickson (1992) discusses many of the original methods for ambiguity resolution. Many of the

methods were developed to accommodate the limited computing power available at the time. Most of the methods described use the sum of squared residuals to decide, statistically if the ambiguity set should be accepted.

The latest methods for ambiguity resolution require a float estimate and a variance-covariance matrix of the ambiguities. They use the covariance matrix to statistically reject ambiguity sets. The Fast Ambiguity Search Filter (FASF) (Chen, 1994) uses the variance and covariance of the ambiguities to propagate the effect of one integer ambiguity onto the others. By propagating the effect of a fixed ambiguity onto the others this method will quickly detect and reject diverging solutions.

The LAMBDA method (Teunissen, 1994; de Jonge and Tiberius, 1996) decorrelates the ambiguities as much as possible while preserving the integer characteristics of the ambiguities. This reduces the number of possible integer ambiguity sets within the search space leaving a small set of remaining ambiguities to test. The search then uses the variance-covariance matrix of the float ambiguities to find the set of ambiguities that minimizes the sum of squared residuals.

Teunissen (1999, 2000) shows that the integer least squares estimator used in the LAMBDA method maximizes the probability that the selected integer ambiguity set is the correct integer ambiguity set given a real-value estimate of the ambiguities and the corresponding covariance matrix.

2.3.1 Observation Combinations for Ambiguity Resolution

GPS is currently a dual-frequency system, meaning that all of the measurement types are measured on two signals, which are at different frequencies. The advantage of having two frequencies is that different errors affect the signals differently. For example, the troposphere affects both of the frequencies to the same degree while the ionosphere

affects them differently. These error properties between the various measurements can be leveraged to reduce the overall measurement errors.

Frequency combinations are formed by linearly combining measurements from the two frequencies. This approach can be used to improve ambiguity resolution performance by reducing measurement errors in units of cycles. Specifically, if an error is small relative to the wavelength of the carrier, then its effect on the ambiguity resolution is reduced. Conversely, to improve positioning accuracy, the measurement errors should be reduced in units of metres.

If the carrier phase combination is represented as:

$$\phi_{a,b} = a \cdot \phi_{L1} + b \cdot \phi_{L2} \tag{2.42}$$

where a and b are constants, then the effective wavelength of the linear combination is given by

$$\lambda_{a,b} = \frac{\lambda_{L1} \cdot \lambda_{L2}}{b \cdot \lambda_{L1} + a \cdot \lambda_{L2}}. \tag{2.43}$$

Note that a and b must be integers in order for the resulting signal ambiguity to be an integer value. For example, the most common frequency combinations is the so-called wide-lane combination, which is the difference between the L1 phase and the L2 phase measurements in cycles ($a = 1$, $b =$ -1). The wide-lane combination has an effective wavelength of approximately 0.86 cm, which is much longer than either the L1 (0.19 cm) or L2 (0.24 cm) wavelengths.

The error characteristics for a generic linear combination of the L1 and L2 phase observations are shown in Table 2.4. Table 2.5 shows the errors in cycles as a function of the coefficients a and b, for several common frequency combinations. The troposphere error is represented relative to the tropospheric effect on the signal in metres (T) and the ionosphere is relative to the ionospheric effect on the L1 signal in metres

(I_{L1}).

From the table, the usefulness of the wide-lane combination is obvious, because it reduces the troposphere and ionosphere errors relative to the L1 measurement (in cycles) by factors of 0.22 ($1.16T/5.26T$) and -0.28 ($-1.49I_{L1}/5.26I_{L1}$), respectively. In a similar manner, the ionosphere-free (IF) and geometry-free (GF) combinations are commonly used to respectively evaluate the magnitude of the troposphere and ionosphere errors. The ionosphere-free combination is also commonly used to estimate the position states because the ionosphere is the largest differential error source.

To contrast with the results of Table 2.5, the effect of the errors on the same frequency combinations in metres is shown in Table 2.6. These values relate to the accuracy of the position estimates.

Table 2.4: Generic dual frequency combinations and their associated error characteristics

	cycles	metres
Wavelength	$\frac{\lambda_{L1}\lambda_{L2}}{b\lambda_{L1}+a\lambda_{L2}}$	$\frac{\lambda_{L1}\lambda_{L2}}{b\lambda_{L1}+a\lambda_{L2}}$
Troposphere	$\frac{b\lambda_{L1}+a\lambda_{L2}}{\lambda_{L1}\lambda_{L2}}T$	T
Ionosphere	$\frac{a\lambda_{L1}+b\lambda_{L2}}{\lambda_{L1}^2}I_{L1}$	$\lambda_{a,b}\frac{a\lambda_{L1}+b\lambda_{L2}}{\lambda_{L1}^2}I_{L1}$
Noise	$\sqrt{a^2+b^2}\sigma$	$\lambda_{a,b}\sqrt{a^2+b^2}\sigma$

Comparing Tables 2.5 and 2.6 shows an apparent contradiction, namely that reducing an error in cycles often comes at the cost of increasing the error in metres. For example, although the wide-lane ambiguity is relatively easy to fix because of the decreased ionosphere and troposphere errors in units of cycles, it increases the measurement noise and ionosphere error by factors of 6.42 ($1.22\sigma/0.19\sigma$) and -1.28 ($-1.28I_{L1}/I_{L1}$) relative to the L1 measurement terms, respectively (Table 2.6). In

Table 2.5: Common frequency combinations and their associated single satellite (undifferenced) error characteristics in cycles. T is the troposphere error in metres, I_{L1} is the L1 ionosphere error in metres, and σ is the standard deviation of the L1 and L2 measurement noise in cycles.

Ambiguity	Wavelength (m)	Troposphere	Ionosphere	Noise
$N_{L1} = N(1, 0)$	0.19	$5.26T$	$5.26I_{L1}$	σ
$N_{L2} = N(0, 1)$	0.24	$4.09T$	$6.74I_{L1}$	σ
$N_{WL} = N(1, -1)$	0.86	$1.16T$	$-1.49I_{L1}$	1.41σ
$N_{NL} = N(1, 1)$	0.11	$9.35T$	$12.00I_{L1}$	1.41σ
$N_{IF} = N(1, -\frac{\lambda_{L1}}{\lambda_{L2}})$	0.48	$2.08T$	0.00	1.27σ
$N_{GF} = N(1, -\frac{\lambda_{L2}}{\lambda_{L1}})$	∞	0.00	$-3.40I_{L1}$	1.63σ

contrast, the narrow-lane ambiguities show the inverse behaviour of the wide-lane ambiguities in that the narrow-lane ambiguities are very difficult to fix because of the increased ionosphere, troposphere and noise in cycles. However, once these ambiguities are resolved they give a very precise measure of the position. In general, the easier it is to resolve the ambiguities for a given frequency combination, the less useful that frequency combination will be to estimate the rover's position.

The magnitude of the troposphere and ionosphere errors (after double differencing) depends on the distance between the differenced stations. This baseline distance-dependent error is used in combination with the characteristics of the various frequency combinations to maximize the likelihood of resolving ambiguities and, more importantly, to maximize position accuracy. For example, if the rover is very close to a reference station, then it will experience little troposphere or ionosphere error. With this in mind, the receiver can construct a frequency combination that reduces the level of noise. For short baselines a receiver may use L1, L2, or the narrow-lane combination to reduce the effect of measurement noise because the ionosphere and

Table 2.6: Common frequency combinations and their associated single satellite (undifferenced) error characteristics in metres. T is the troposphere error in metres, I_{L1} is the L1 ionosphere error in metres, and σ is the standard deviation of the L1 and L2 measurement noise in cycles.

Ambiguity	Wavelength (m)	Troposphere	Ionosphere	Noise
$N_{L1} = N(1,0)$	0.19	T	I_{L1}	0.19σ
$N_{L2} = N(0,1)$	0.24	T	$1.65I_{L1}$	0.24σ
$N_{WL} = N(1,-1)$	0.86	T	$-1.28I_{L1}$	1.22σ
$N_{NL} = N(1,1)$	0.11	T	$1.32I_{L1}$	0.15σ
$N_{IF} = N(1,-\frac{\lambda_{L1}}{\lambda_{L2}})$	0.48	T	0.00	0.61σ
$N_{GF} = N(1,-\frac{\lambda_{L2}}{\lambda_{L1}})$	∞	$Undefined$	∞	∞

troposphere errors are low. Alternatively, if the rover is far from the nearest reference station then the receiver may use the wide-lane combination to reduce the effects of the correlated errors, but must sacrifice increased measurement noise. Another approach for long baselines is to use the ionosphere-free combination to reduce the effects of the ionosphere, which is the largest error source, especially for very long baselines.

The coefficients of the ionosphere-free and geometry-free combinations are not integer. As a result, the corresponding ambiguities are not integers and therefore cannot be resolved. Instead, these ambiguities are usually estimated as real numbers. In general, this will add more error to the estimated position due to the reduced number of degrees of freedom in the adjustment. However, this may be acceptable if the reduction in the measurement error is significant.

2.4 Ionosphere Modelling

The ability of the reference stations to resolve their integer ambiguities is a major factor affecting multiple reference station positioning. By definition, the reference stations for the multiple reference station approach will be spaced further apart than is typically reasonable for single reference station kinematic ambiguity resolution.

These longer baseline lengths are more likely to have higher levels of correlated errors. The largest of these is the effect due to the ionosphere. The pseudorange and carrier phase observations on two frequencies can be used in combination to model the frequency dependent bias induced by the ionosphere.

Teunissen (1997), Odijk (1999, 2000) and Liu and Lachapelle (2002) discuss three methods for modelling ionosphere biases: the ionosphere float, fixed, and weighted models. All of these models attempt to reduce the dual frequency slant ionospheric effect.

The ionosphere free model estimates the double difference slant ionosphere from the dual frequency code and carrier phase measurements. In this model there is no previous knowledge about the ionosphere or direct ionosphere observations.

The system model for the ionosphere float model is

$$\begin{aligned} \Delta\nabla\phi_{L1} - \Delta\nabla\rho &= \lambda_{L1}\Delta\nabla N_{L1} - I_{L1} + \varepsilon_{\phi_{L1}} \\ \Delta\nabla\phi_{L2} - \Delta\nabla\rho &= \lambda_{L2}\Delta\nabla N_{L2} - \tfrac{f_{L1}^2}{f_{L2}^2} I_{L1} + \varepsilon_{\phi_{L2}} \\ \Delta\nabla P_{L1} - \Delta\nabla\rho &= I_{L1} + \varepsilon_{P_{L1}} \\ \Delta\nabla P_{L2} - \Delta\nabla\rho &= \tfrac{f_{L1}^2}{f_{L2}^2} I_{L1} + \varepsilon_{P_{L2}} \end{aligned} \tag{2.44}$$

where $\Delta\nabla\phi$ is a double difference carrier phase measurement in metres, $\Delta\nabla\rho$ is a double antenna to satellite range in metres, λ is a measurement wavelength in metres, $\Delta\nabla N$ is a double difference ambiguity in cycles, f is the frequency of the signal, I_{L1}

is the ionosphere delay of the L1 signal in metres and ε is the sum of unmodelled measurement errors to be estimated as residuals.

The ionosphere weighted model is the ionosphere float model augmented with an external observation of the double difference slant ionosphere. This additional measurement has a variance that weights its effect relative to the code and carrier phase observations.

The ionosphere fixed model does not estimate the ionosphere but the code and carrier phase observations are reduced with an external ionosphere value. The external ionosphere value can be inserted from a variety of sources. Liu (2001) shows the effect of deriving the external estimate of the ionosphere from Global Ionosphere Maps (GIM) or the broadcast ionosphere model.

The ionosphere fixed and float models are extremes of the ionosphere weighted model. The ionosphere fixed model is the ionosphere weighted model when the variance of the external ionosphere observation is zero. Conversely, when the variance of external ionosphere observation is infinite the ionosphere weighted model is equivalent to the float model.

Odijk (2000) suggests that the ionosphere weighted model is the best for fast ambiguity resolution while the ionosphere float model gives the best coordinate estimation results. The additional ionosphere parameters in the ionosphere float model delay the resolution of the ambiguities. Odijk (2000) recommends the ionosphere weighted model because of the trade off between fast ambiguity resolution and coordinate estimation error.

Teunissen (1997) discusses the theoretical ambiguity search space for the three methods. In this approach the ionosphere fixed model is theoretically the best but it assumes that the input external ionosphere estimates are perfect. The ionosphere

fixed model is shown to have a low ambiguity success rate when using real data and real external ionosphere observations (Odijk, 2000) because of errors in the external ionosphere estimates. These biases propagate into the ambiguities, decreasing the success rate. Odijk (2000) also shows that the ionosphere weighted model gives the highest ambiguity success rates compared to the other models mentioned using real-data.

Landau et al. (2001) discuss wide area ionosphere modelling using a network of reference receivers where the zenith ionosphere estimates are reduced to a shell. The shell is modelled using simple two-dimensional polynomials as a function of the geomagnetic latitude and the hour angle of the sun. They conclude that this wide area model is effective in removing about fifty percent of the ionosphere delay but local ionosphere effects remain. In order to better estimate local ionosphere effects they integrate the wide area technique with stochastic modelling to estimate the residual, local area, effects. This system is similar to the ionosphere weighted model (Liu and Lachapelle, 2002) where the external ionosphere estimate is generated using the shell model.

The reduced error ambiguity resolution approach discussed by Landau et al. (2001) is a loosely coupled system where the troposphere and ionosphere errors are estimated in two independent filters. The ambiguity estimates from these two adjustments are combined to resolve the L1 and L2 ambiguities. This is opposite to the ambiguity resolution approach discussed by Wübbena et al. (2001a) where a tightly coupled system is implemented. Wübbena et al. (2001a) estimates the effects of many error sources including the ionosphere and troposphere effects in one large adjustment.

Teunissen (1997) discusses the temporal variation of the ionosphere in terms of ability to resolve ambiguities as a function of temporal correlation. However, he gives

no suggestion as to the type of temporal behaviour modelling that would represent typical ionospheric error.

Liu and Lachapelle (2002) discuss the observation error as a function of time for the three models. The ionosphere estimates were estimated as first order Gauss Markov noise processes where the process noise was derived as a function of baseline length. The three models are compared in terms of ambiguity error as a function of time. This shows that the ionosphere weighted model provides the best estimate of the ambiguities on average. The ionosphere float model preforms poorly at first and then converges to a value similar to the weighted ionosphere model in less than twenty minutes. The inaccuracy in the float ionosphere is due to the ionosphere estimate being initially driven by the code observation error.

Liu and Lachapelle (2002) add a short discussion about the similarity of performance between the ionosphere weighted model and the results when using the ionosphere free observable. The ionosphere free observable uses the frequency dispersion of the ionosphere to difference the ionosphere effect. This observable should be unbiased by the ionosphere providing any accurate position estimate. They suggest that the use of the ionosphere weighted pseudo-observable will achieve similar results as the ionosphere-free solution. Odijk (2000) discusses the use of the ionosphere float model instead of the ionosphere free combination because they will both produce position solutions that are free of ionosphere biases. With fixed ambiguities, Odijk (2000) shows that the position coordinate solution using the ionosphere float model produces more accurate results than the other models.

The external ionosphere estimates for the ionosphere fixed and ionosphere weighted models could be used from many different sources. Liu and Lachapelle (2002) examines two sources: the Broadcast Ionosphere Model (BIM) and an International GPS

Service (IGS) produced Global Ionosphere Map (GIM). The GIM appears to be effective in reducing the ionosphere effect under high and low ionosphere activity but the BIM only reduces the ionospheric effect during low ionosphere conditions. Odijk (2000) generated external ionosphere estimates using a surrounding network of GPS reference stations. The network-measured relative ionospheric effect was interpolated to the user positions using a linear interpolation scheme. Li and Gao (2000) use the ionosphere estimates calculated from one day of data to reduce the ionosphere effect on subsequent days.

2.5 Covariance Functions

A covariance function models the variance and covariance of observations. This function can be used to populate the variance covariance matrix of the observations for estimation and prediction. The covariance function calculates covariance between observations as a function of deterministic properties of the observations. Raquet (1998) parameterizes the covariance function as a function of elevation and relative position. Radovanovic et al. (2001) and Kennedy (2002) parameterized the covariance function as a function of the elevation and azimuth of the observations, and relative distance between the stations from which the observations are measured.

The variance of a random variable and the covariance between two random variables can be defined by the expected value operator:

$$\begin{aligned} C_{aa} &= \mathrm{E}\{(a - \mathrm{E}\{a\})(a - \mathrm{E}\{a\})^T\} \\ C_{ab} &= \mathrm{E}\{(a - \mathrm{E}\{a\})(b - \mathrm{E}\{b\})^T\}. \end{aligned} \tag{2.45}$$

If the probability density function is known then the expected value operator is

(Walpole and Myers, 1993)

$$E\{X\} = \int_{-\infty}^{\infty} x f(x)\, dx \tag{2.46}$$

where X is a random variable, $f(x)$ is the probability density of X, and x is an array of observed, sample values.

Practically, the probability density functions for the error sources that affect the observations are not known. The expected value can also be estimated given a set of random variables (Grimmett and Stirzaker, 2001), as follows

$$E\{X\} \approx \frac{1}{n} \sum_{i=1}^{n} X_i \tag{2.47}$$

where X_i is a random variable in the set of n random variables.

Equations 2.45 and 2.47 can be used to estimate the variance and covariance of random variables from data. As shown in Equation 2.45 the expected value of the product of two random variables is the covariance between them. The objective is to parameterize the covariance as a function of deterministic parameters. The covariance of the data must be evaluated as a function of some parameters. Initially the data is arranged as a function of an expected parameter (distance between the stations for example). This gives the product ab^T as a function of the correlating parameter. These sample values are located at discrete points. To convert the collection of products into standard deviations, the data is divided into bins. The expected value of the products from each bin gives an estimate of the standard deviation of the data. The expected value for each bin is then calculated using Equation 2.47. The shape of these expected value points as a function of the correlating parameter is an estimate of the covariance function. A mathematical function is then fit to the data. This function is later used to predict the correlation between observations that have not yet been observed. The covariance function is essential for prediction (Moritz, 1980)

because it defines the correlation between the network observations and the rover observations, which have not yet been observed.

Raquet (1998), Radovanovic et al. (2001) and Kennedy (2002) used this approach to estimate the coefficients of their respective covariance functions. In the case of Radovanovic et al. (2001) and Kennedy (2002) the covariance function is a function of more parameters than can be effectively plotted to expose the shape and consequently the mathematical form of the function. As a result, a exponential decay function is assumed and the multi-dimensional function's coefficients are estimated using batch least squares.

2.6 Multiple Reference Station Approach

Differential positioning significantly reduces the measurement errors, improving positioning accuracy and precision relative to single point positioning. When a network of reference stations is available then one reference station alone or some combination of the surrounding stations can be used to estimate the rover's position. A system that uses more than one reference station for precise carrier phase-based positioning is said to use a multiple reference station approach. This approach can be categorized into single baseline techniques and Network real-time kinematic (RTK) techniques. The single baseline techniques are methods for integrating the solutions from multiple single baseline solutions, whereas the Network RTK methods involve the integration of the network into corrections to be applied by a single baseline.

2.6.1 Single Baseline Techniques

Single baseline techniques are the simplest to implement because they require very little deviation from traditional carrier phase positioning. The single baseline approach

averages the single baseline solutions for baselines between the rover and multiple nearby reference stations. The technique attempts to average reference station measurement errors and to provide greater observability and availability for the rover.

The single baselines can be combined using a centralized or decentralized approach (Mutambara, 1998). The decentralized approach averages the position solutions from the various single baselines using the estimated variance-covariance matrices of the position solutions as weight matrices. This allows for any systematic biases to be averaged among the various baseline solutions. The decentralized approach allows for modularity and flexibility. It is easy to implement because it does not require any changes to the traditional single baseline methods.

The second approach is the centralized approach, where the measurements from each of the reference stations are combined into a single filter to estimate the rover's position. The centralized approach is better suited to allowing for correlations between the measurements to be used. It also allows for the use of reference stations that do not contain enough observations to provide an independent position solution, however, this situation is unlikely in practice.

2.6.2 Network-Based RTK Methods

Network-Based RTK methods use a network of reference stations to measure the correlated error over a region and to predict their effects spatially and temporally within the network. Although the name suggests that these methods are real-time specific, RTK refers to precise carrier phase positioning. Any of these methods can be used in post-mission. This process can reduce the effects of the correlated errors much better than the single reference station approach, thus allowing for reference stations to be spaced much further apart thereby covering a larger service area than the

traditional approach, while still maintaining the same level of performance. Network RTK is comprised of three main processes:

1. Network correction computation,
2. Correction interpolation, and
3. Virtual reference station calculation and data transmission

The network correction computation uses the network reference stations to precisely estimate the differential correlated errors for the region. This is usually accomplished using carrier phase observations with fixed ambiguities between the network stations. Thus, ambiguity fixing between these stations is a major part of this process. The correction interpolation process models the network corrections to determine the effects of the correlated errors at the rover's position. The third process is the generation of virtual reference station (VRS) measurements to relay the corrections to the rover receiver for use with standard RTK software.

Measuring Network Errors

The first step of Network RTK is to measure the errors at the reference stations. In most cases, the errors are measured as the difference between the carrier phase observations with fixed ambiguities and the theoretical range, which is calculated using the known reference stations' coordinates. These errors can be measured in terms of the raw L1 and L2 carrier phase observations or a linear combination of the L1 and L2 observations. Linear combinations are used to isolate the various error sources and to take advantage of their unique characteristics.

Interpolation of Measured Network Errors

Interpolation of the correlated errors to the location of the rover receiver assumes a stochastic and physical relationship between the errors. For example, all interpolation methods result in the closest reference stations having the most influence over the predicted value because a close reference station is more likely to experience the same error conditions as the rover receiver as opposed to a reference station which is further away.

Raquet (1998) proposed a method of interpolating the observed errors between the reference stations to a rover's position anywhere in the network. In this method, an exterior process determines the carrier phase integer ambiguities between the reference stations. These ambiguities are then used to estimate the differential errors between the reference stations. The measured errors are interpolated to a rover in the network using a linear least-squares prediction method. Covariance functions that represent the stochastic behaviour of the errors must be determined at the outset. This method has been implemented in a functional real-time system and provides good improvement in post-mission and real-time (Raquet, 1998; Raquet et al., 1998; Zhang, 1999; Fortes et al., 2000a,b, 2001; Cannon et al., 2001a,b; Alves et al., 2001; Zhang and Lachapelle, 2001).

Wanninger (1999), Vollath et al. (2000a), and Wübbena et al. (2001a) discuss a slightly different interpolation scheme where only the surrounding three stations are used to predict the corrections at the rover. In this simpler model, a plane is fit to the error estimates at the three surrounding stations. This plane represents the differential errors within the three-station triangle. This method has also proven to provide good positioning results under a quiet ionosphere and with a relatively high reference station density (Wanninger, 1999; Vollath et al., 2000a,b, 2002; Wübbena

et al., 2001b; Euler et al., 2001).

Dai et al. (2004) compare five common interpolating surfaces, including a least squares collocation approach. This paper concludes that each of the interpolation methods perform similarly with the exception of the distance dependent linear interpolation method, which performs slightly poorer.

Virtual Reference Station Calculation and Data Transmission

Once the corrections for the rover are determined, they still need to be transmitted to the rover receiver in a suitable format. The traditional single baseline approach has a large impact on this process because most off-the-shelf receivers are not designed to accept network corrections. To compensate, many Network RTK systems create a virtual reference station (VRS). A virtual reference station's data is the adjusted (corrected) data from one of the reference stations in the network. This data is usually geometrically translated to be close to the region for which it is to be applied. The rover receiver can then accept the virtual reference station data as a single reference station. This process is described in Fotopoulos (2000).

Figure 2.3 shows an example of the VRS approach. The left view shows the configuration of the network relative to the rover. To convert the network data into a receiver-acceptable format, the network is condensed into a single *virtual* reference station (shown on the right). The VRS is located closer to the rover than the nearest network reference station to represent the reduced differential errors due to the multiple reference station approach.

In general, the VRS approach creates a (virtual) reference station for use with standard off-the-shelf receivers that do not have the capability of accepting network corrections. There are many disadvantages to this approach:

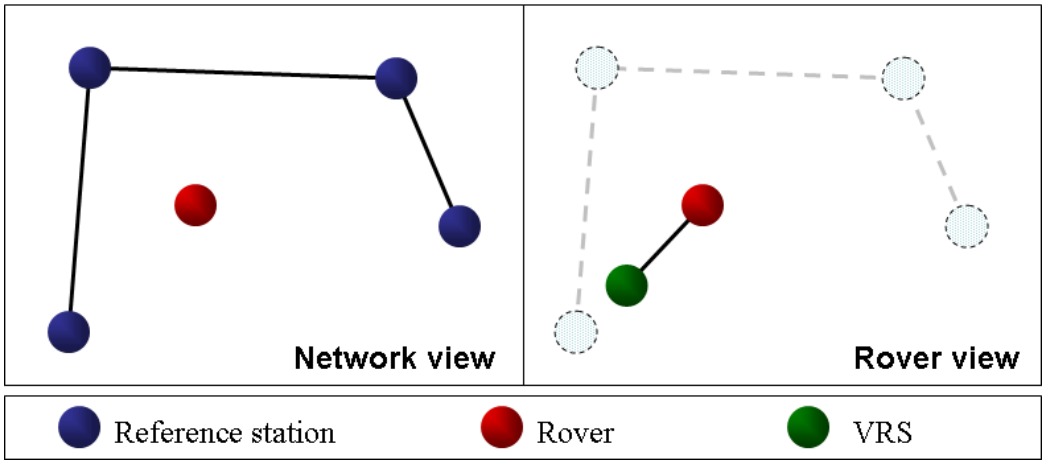

Figure 2.3: Example of the network and virtual reference station relationship. Left shows the network of actual network reference stations in relation to the rover. Right shows the rover's view whereby the reference station network is replaced by a single. *virtual* reference station.

1. The rover receiver will interpret the VRS as a single reference station, which may cause the rover to use a processing scheme that is not optimal (Townsend et al., 2000). Specifically, a GPS receiver will typically select a processing strategy based on its distance to the nearest reference station, which is closely related to the magnitude of the expected measurement errors. For a corrected reference station (VRS) however, the magnitude of the measurement error remaining after applying correction is less than if a physical reference station were present at the same location. This is most obvious if the rover receiver's position coincides with the VRS position. If a rover were at the location of a reference station then the differential errors would be limited to multipath and noise (since all other errors would be zero). As such, the rover will choose a positioning method which optimizes the performance based on this assumption. However the level of error remaining in the VRS data is a function of the network geometry and the relative position of the rover. Therefore, the distance between the VRS and

the rover receiver should be representative of the amount of error remaining after the network corrections have been applied.

2. A solution to the above problem would be to have the correction service provider ensure that the VRS is an appropriate distance away from the rover to optimize the processing scheme but this is not always possible with multiple rovers. This alternative requires that the service providers know the approximate position of the rover. In this case, the rover would be required to send its position (via National Marine Electronics Association (NMEA) messages for example) to the processing control centre to ensure that the interpolation is calculated for the correct position and to position the VRS appropriately. This increases the complexity of the communications network, as two-way communication is required. In addition, the service becomes user limited.

3. This method does not comply with the Radio technical commission for maritime services (RTCM) standard (RTCM, 1998) because the standard does not allow for the reference station data to be corrected for atmospheric or orbit errors (Townsend et al., 2000). However, if the data are corrected prior to being transmitted to the users, then this is in clear violation of the standard. Currently, network RTK specific RTCM corrections are under development to address these problems.

Implementation Options

Given the limitations discussed in the previous section, the multiple reference station approach can be implemented in many ways, which vary the order and location of the processing steps. The use of the various options depends mainly on the communication network and the rover equipment.

In the first approach, network corrections are sent to a computer located at the rover (Figure 2.4). The computer then interpolates the corrections based on the rover's position. To do this, the GPS receiver outputs its position to the computer so that the interpolation location is known. The interpolated corrections are then applied along with the reference station corrections to the data for one of the reference stations. The corrected observations are then translated to a VRS location which is selected to avoid the problems discussed above. Finally, the corrected VRS data is converted to RTCM format and is sent to the rover receiver. In this way, the rover receiver never knows that the data is corrected by the network.

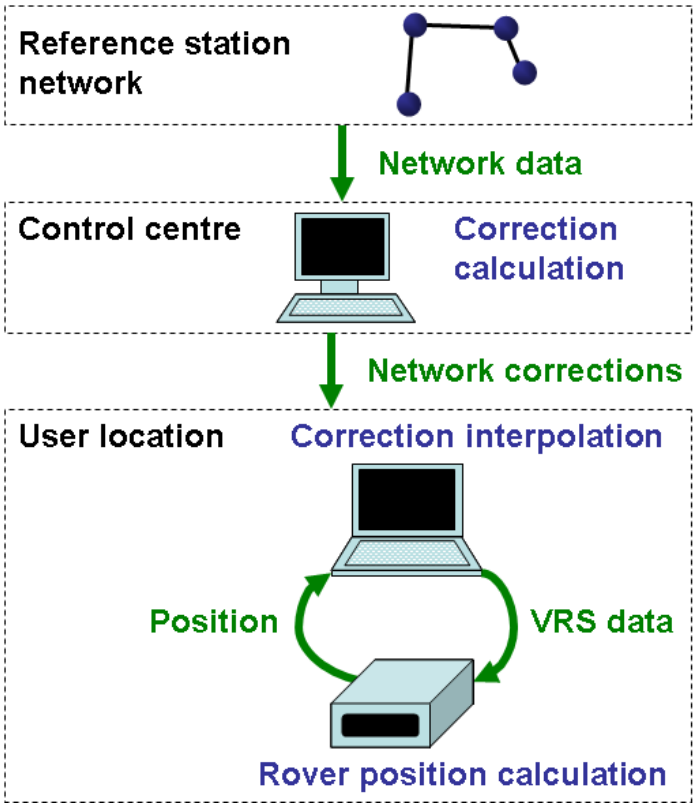

Figure 2.4: Implementation option for the virtual reference station approach, which requires a computer at the location of the rover and only one way communication between the rover and the control centre

The computer used to interpolate the corrections does not necessarily have to be

located at the rover receiver, since the interpolation and VRS generation can also be done at the control centre (Figure 2.5) . However, in this case the communication network would need to support two-way communication with all of the rovers in the region. This would also require the rovers to send their locations to the control centre.

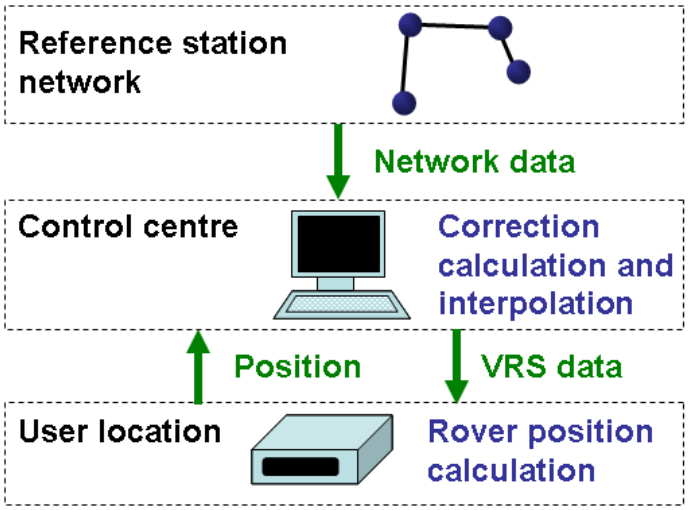

Figure 2.5: Implementation option for the virtual reference station approach, which requires two way communication between the rover and the control centre

If there is no computer available at the rover and the communication network only supports one way data transfer, then the corrections must be calculated for a range of rover location service areas. Multiple VRS data is broadcast to users without knowing their locations. Each service area requires a different VRS.

In order for this implementation to work effectively the distance between the VRS and the rover must be representative of the errors remaining in the observations (after applying the network corrections), or the rover receiver may select an inappropriate processing strategy. This implies that the VRS should be located within a minimum and maximum distance to the VRS service area (Figure 2.6). Specifically, if the VRS is too close to the rover, then the rover will select an inappropriate RTK method that will yield poor position performance. At the same time, the VRS cannot be too far

removed from the rover for the same reasons. Ideally, the VRS should be outside of the VRS's coverage area so that the minimum distance is not zero.

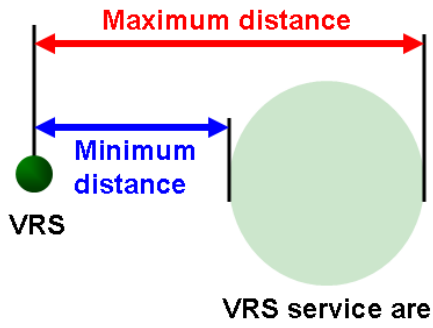

Figure 2.6: VRS in relation to the VRS service area for a broadcast service implementation

Unfortunately, when many VRSs are created to cover a large area then it is likely that a VRS for one coverage area will be inside of another VRS's coverage area (Figure 2.7). Traditionally, the rover receiver will select the closest reference station for differential positioning, because this reference station is likely to have similar error magnitudes as the rover, such that the differential errors are small. However, in this scenario if the rover selects the closest reference station (or VRS), then likely this station will likely be meant for a coverage area for which the rover does not belong.

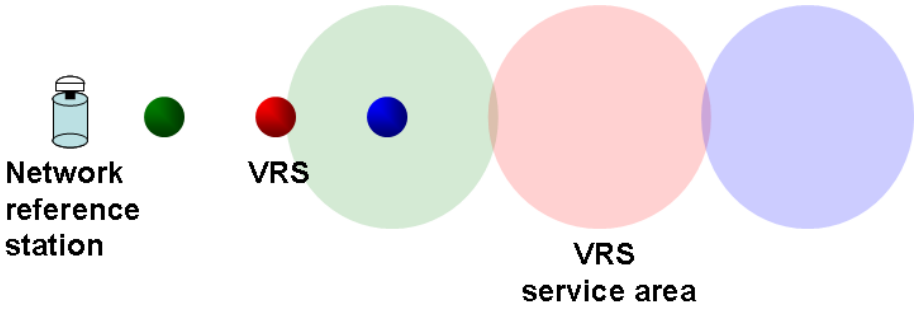

Figure 2.7: Example distribution of VRS and VRS service areas for a broadcast service implementation

FKP Methods

An alternative to the VRS method is to generate a regional correction model (Fotopoulos (2000) for example). FKP is an abbreviation of the German *Flächen Korrektur Parameter*, meaning area correction parameter (Odijk, 2002). This model is usually a representation of a two dimensional surface that covers the correction region. This model can be of any order; however, a first order model grid model is commonly used. This approach has many advantages over the VRS approach:

- It does not violate the RTCM standard (Townsend et al., 2000)
- One model can be sent to all of the users in the field.
- The receiver has control over the use of the corrections.

This approach has not been widely used and supported by receiver manufacturers because of disagreements over the message format. In the years ahead, when an accepted standard FKP format is available, this will likely become the preferred method for network-based RTK.

Network-Based RTCM Corrections

A new version of the RTCM standardized corrections is under development. Included in these standards are a set of correction formats for network RTK. The methodology for the use of these corrections transfers some of the operations that were previously performed at the control centre to the rover. The network control centre is responsible for resolving network ambiguities. With the ambiguities resolved, there are two types of corrections:

- Master corrections provide the absolute value of the corrections. These are the same correction format as the single reference station corrections.

- Auxiliary station corrections are the residual differences relative to the master station with the ambiguities removed. These corrections are divided into dispersive and non-dispersive corrections.

The master-auxiliary concept is described by Euler et al. (2004b).

Using these corrections, the control centre is responsible for resolving the network ambiguities. The interpolation of the measured network errors is performed by the roving receiver. This allows for one-way communication of the corrections to any number of rovers. It also allows the rover receiver to decide on the interpolating function.

External Network RTK Techniques

Due to infrastructure limitations, it may not be possible to send the reference station data to the control centre and return the corrections. An alternative may be to use an external network with better infrastructure to to generate corrections for the reference stations in the service network. In this case, the external network would calculate corrections for both the reference stations and the rover, similar to the original Network RTK procedure. The only difference being that in this case the reference stations in the service network are not used in the calculation of the network corrections. The external network is used purely for error modelling. The corrections calculated from this approach can be applied using any of the implementation options discussed above.

Chapter 3

Development of an Adaptive Covariance Function

A covariance function is used to calculate the covariance between observations. More specifically, the covariance function calculates the estimated covariance between the observation's signal components. This is used to populate the covariance matrix of the observations of a least squares adjustment. The covariance function is particularly important in least squares collocation because it is the prediction weighting function, however Fortes (2002) shows that least squares prediction is insensitive to the choice of the covariance function.

The least squares collocation equations for estimating the signal at a given set of GPS observations are (Raquet, 1998)

$$\hat{s} = -C_{sl_s} B^T (BC_{ll}B^T)^{-1}(A\hat{x} - Bl) \tag{3.1}$$

where $\hat{s}$ is a vector of the estimated signals (corrections), C_{sl_s} is the covariance matrix between the signal components of the network observations and the predicted signal, B is the observation matrix, C_{ll} is the variance-covariance matrix of the network observations, which is the sum of the signal covariance and the noise variance-covariance matrix, A is the design matrix of the estimated parameters, $\hat{x}$ is a vector of estimated parameters, and l is a vector of network observations. This equation can be broken down into two prediction weighting parts: $-C_{sl_s}B^T$ and $(BC_{ll}B^T)^{-1}$.

$(BC_{ll}B^T)^{-1}$ weights each double differenced observation based on their variance and covariance. This ensures that observations that are more precise have more weight than observations that are noisier. This is shown in the equation; observations with

low levels of error and noise have lower variance (diagonal of C_{ll}). When $BC_{ll}B^T$ is inverted the low variance values become large and the high variance values become small. When the inverse matrix is multiplied by the misclosures, $A\hat{x} - Bl$, the high weight for the precise observations and low weight for noisy observations is applied.

The second part of this equation, $C_{sl_s}B^T$, relates each of the network observations to the predicted signals of the observations. Again, these weights are determined by the covariance function, which defines the characteristic shape of the predictions throughout the geographic region. Different covariance functions will produce different shapes and prediction characteristics.

Fortes (2002) suggests that the only requirement of the covariance function is that it always produces a positive definite variance covariance matrix. In addition to positive definiteness the prediction should represent the likelihood that the errors measured at the reference stations are the same as the errors measured at the rover. To this end, the covariance should converge to zero with increasing distance (for example), meaning that errors measured at the reference stations are likely not the same as the errors measured at the rover (computation point). The policy of this covariance function is then, if no reference station is in a position to predict the errors at the rover, then the covariance of the signal and network observation's signal should be zero.

Given these desired characteristics, the following section describes the process of selecting and estimating the parameters of a covariance function.

3.1 Covariance Function Modelling

The covariance function gives the covariance between the signal components of two observations. This can be described using the expected value operator for observation ϕ_1 and ϕ_2 by

$$\begin{aligned} E\{(\phi_1 - E\{\phi_1\})(\phi_2 - E\{\phi_2\})\} &= E\{(s_1 + n_1)(s_2 + n_2)\} \\ &= E\{s_1 s_2\} \\ &= \sigma_{\phi_1,\phi_2} \end{aligned} \tag{3.2}$$

where s is the signal and n is the noise of the observations.

The covariance function attempts to model the covariance of the observation's signals (i.e., ϕ_1 and ϕ_2) as a function of deterministic parameters (distance or elevation for example) as follows

$$\sigma_{\phi_1,\phi_2} = f(\cdot). \tag{3.3}$$

3.1.1 Parameters of the Covariance Function

Before the form of the covariance function can be discussed, the deterministic parameters must first be chosen. The candidate parameters must be determined based on the physical properties governing the measurement errors. The function will give the relationship between the parameter and the covariance of the measurement errors. To calculate the variance of the measurement errors, measurement residuals are sorted by the candidate parameter. The covariance of the measurement residuals is found by dividing the residuals into bins of the parameter. This collection of points is modelled and reproduced by the covariance function. A plot of the measurement covariance as a function of the candidate parameter also exposes the functional form of the covariance function.

If the measurement error is a function of more than one parameter, then this procedure may not properly expose the covariance function form, because the effect of the other parameters may clutter the distribution of the residuals. For example, if the errors are a function of longitude distance and latitude distance then plotting as a function of longitude alone will average the effect of the latitude for each longitude bin. A more appropriate approach would be to create two dimensional bins of easting and northing and plot the two dimensional surface. This would also expose any possible correlation between the parameters.

The error sources found are precisely measured in differential form in this work. Equation 3.2 can be expanded for the double difference case:

$$\begin{aligned} & E\{(\Delta\nabla\phi_{ab}^{12} - E\{\Delta\nabla\phi_{ab}^{12}\}) \\ & (\Delta\nabla\phi_{cd}^{34^T} - E\{\Delta\nabla\phi_{cd}^{34^T}\})\} \;=\; E\{((s_a^1 - n_a^1) - (s_a^2 - n_a^2) \\ & \qquad -(s_b^1 - n_b^1) + (s_b^2 - n_b^2)) \\ & \qquad ((s_c^3 - n_c^3) - (s_c^4 - n_c^4) \\ & \qquad -(s_d^3 - n_d^3) + (s_d^4 - n_d^4))\} \end{aligned} \tag{3.4}$$

where a, b, c and d are receivers observing satellites 1, 2, 3 and 4. The expanded variance-covariance equation for this double difference equation is

$$\begin{aligned} & E\{(\Delta\nabla\phi_{ab}^{12} - E\{\Delta\nabla\phi_{ab}^{12}\}) \\ & (\Delta\nabla\phi_{cd}^{34} - E\{\Delta\nabla\phi_{cd}^{34}\})^T\} \;=\; \sigma_{\phi_a^1,\phi_c^3} - \sigma_{\phi_a^1,\phi_c^4} - \sigma_{\phi_a^1,\phi_d^3} + \sigma_{\phi_a^1,\phi_d^4} \\ & \qquad -\sigma_{\phi_a^2,\phi_c^3} + \sigma_{\phi_a^2,\phi_c^4} + \sigma_{\phi_a^2,\phi_d^3} - \sigma_{\phi_a^2,\phi_d^4} \\ & \qquad -\sigma_{\phi_b^1,\phi_c^3} + \sigma_{\phi_b^1,\phi_c^4} + \sigma_{\phi_b^1,\phi_d^3} - \sigma_{\phi_b^1,\phi_d^4} \\ & \qquad +\sigma_{\phi_b^2,\phi_c^3} - \sigma_{\phi_b^2,\phi_c^4} - \sigma_{\phi_b^2,\phi_d^3} + \sigma_{\phi_b^2,\phi_d^4}. \end{aligned} \tag{3.5}$$

In terms of covariance function modelling, each σ in this equation is a function of

deterministic parameters. This limits the ability to plot the product of two error sources as a function of some parameter, because each double difference involves a minimum of four parameters. However, there are particular models that will allow for the product to be plotted.

Assume that the correlation (correlated error model) is a linear function of the form

$$\sigma = mx + b \tag{3.6}$$

where x is the deterministic parameter, and m and b are coefficients of the model. If this functional model is inserted in Equation 3.5 the result can be factored into the form

$$\begin{aligned} E\{\Delta\nabla\phi_{ab}^{12}\Delta\nabla\phi_{cd}^{34^T}\} &= (x_{\phi_a^1,\phi_c^3} - x_{\phi_a^1,\phi_c^4} - x_{\phi_a^1,\phi_d^3} + x_{\phi_a^1,\phi_d^4} \\ &\quad -x_{\phi_a^2,\phi_c^3} + x_{\phi_a^2,\phi_c^4} + x_{\phi_a^2,\phi_d^3} - x_{\phi_a^2,\phi_d^4} \\ &\quad -x_{\phi_b^1,\phi_c^3} + x_{\phi_b^1,\phi_c^4} + x_{\phi_b^1,\phi_d^3} - x_{\phi_b^1,\phi_d^4} \\ &\quad +x_{\phi_b^2,\phi_c^3} - x_{\phi_b^2,\phi_c^4} - x_{\phi_b^2,\phi_d^3} + x_{\phi_b^2,\phi_d^4})m. \end{aligned} \tag{3.7}$$

The bias, b, cancels in the double difference. The slope of the function, m, can be estimated using the plotting method described above. This linear model will be used to expose the deterministic parameters to describe the covariance function.

To maximize the number of data elements, all available double difference residuals are used with all others. The double difference covariance shown in Equation 3.5 assumes that none of the observations from one of the double difference residuals (used in the product) are used in the other double difference residuals. If the same double difference residuals are used in the product then Equation 3.5 becomes

$$E\{(\Delta\nabla\phi_{ab}^{12} - E\{\Delta\nabla\phi_{ab}^{12}\})$$

$$
\begin{aligned}
(\Delta\nabla\phi_{ab}^{12} - E\{\Delta\nabla\phi_{ab}^{12}\})^T\} &= \sigma^2_{\phi_a^1} + \sigma^2_{\phi_a^2} + \sigma^2_{\phi_b^1} + \sigma^2_{\phi_b^2} \\
&\quad -2\sigma_{\phi_a^1,\phi_a^2} - 2\sigma_{\phi_a^1,\phi_b^1} + 2\sigma_{\phi_a^1,\phi_b^2} \\
&\quad +2\sigma_{\phi_a^2,\phi_b^1} - 2\sigma_{\phi_a^2,\phi_b^2} - 2\sigma_{\phi_b^1,\phi_b^2}. \qquad (3.8)
\end{aligned}
$$

The covariance terms in Equation 3.8 consist of only correlated errors and the variance terms contain both correlated and uncorrelated terms. The linear model shown in Equation 3.6 only models the correlated error terms therefore the variance elements of Equation 3.8 require an additional uncorrelated error term (σ_u^2). This assumes that the noise is uncorrelated between the measurements:

$$
\begin{aligned}
\sigma^2 &= mx + b + \sigma_u^2 \\
&= b + \sigma_u^2 \qquad (3.9)
\end{aligned}
$$

As with Equation 3.7, Equations 3.6 and 3.9 can be substituted into Equation 3.8 to give

$$
\begin{aligned}
&E\{(\Delta\nabla\phi_{ab}^{12} - E\{\Delta\nabla\phi_{ab}^{12}\}) \\
&(\Delta\nabla\phi_{ab}^{12} - E\{\Delta\nabla\phi_{ab}^{12}\})^T\} &= 4\sigma_u^2 + 2m(-x_{\phi_a^1,\phi_a^2} - x_{\phi_a^1,\phi_b^1} \\
&\quad +x_{\phi_a^1,\phi_b^2} + x_{\phi_a^2,\phi_b^1} - x_{\phi_a^2,\phi_b^2} - x_{\phi_b^1,\phi_b^2}). \qquad (3.10)
\end{aligned}
$$

The uncorrelated error term ($4\sigma_u^2$) will bias the analysis when the variance terms are combined with the purely covariance terms. Fortunately, the measurement residual products that include the variance terms have lower double difference parameters than residual products that do not. This effect is apparent in the following analysis plots.

The differential error sources have two main components. These will be modelled individually to better model the changing effects of each. These two error components are the dispersive (ionospheric error) and non-dispersive (tropospheric and

orbital errors) effects. Two parameters are proposed to described the covariance of the troposphere and orbit components: the baseline length and the angle between the measurements. The angle between the measurements represents the variation in the signal path as a function of the separation of the signal paths.

The first parameter to investigate is for distance dependant errors. The effect of baseline length on differential errors is well known. This example will deviate from the linear model described above because a distance only dependent covariance function has the same generalized properties with any model. Replacing the σ terms in Equation 3.5 with functions of the distance between the stations as the functional form of Equation 3.3 gives

$$\begin{aligned} E\{(\Delta\nabla\phi_{ab}^{12} - E\{\Delta\nabla\phi_{ab}^{12}\}) & \\ (\Delta\nabla\phi_{cd}^{34} - E\{\Delta\nabla\phi_{cd}^{34}\}^T\} &= f(a,c) - f(a,c) - f(a,d) + f(a,d) \\ &\quad -f(a,c) + f(a,c) + f(a,d) - f(a,d) \\ &\quad -f(b,c) + f(b,c) + f(b,d) - f(b,d) \\ &\quad +f(b,c) - f(b,c) - f(b,d) + f(b,d) \\ &= 0. \end{aligned} \tag{3.11}$$

Each covariance is a function of the locations of the two stations and can more specifically be replaced by a function of the distance between the stations. However, this will still result in a value of zero for any double difference combinations.

This shows that the covariance function can not be modelled as a function of baseline distance alone. This observability problem can be overcome if assumptions are made. For example, Raquet (1998) assumes that there is only correlation between the same satellites observed at different stations. Applying this assumption, the

following model can be used:

$$\begin{aligned} & E\{(\Delta\nabla\phi_{ab}^{12} - E\{\Delta\nabla\phi_{ab}^{12}\}) \\ & (\Delta\nabla\phi_{ab}^{12} - E\{\Delta\nabla\phi_{ab}^{12}\})^T\} &=& \ {\sigma_{\phi_a^1}}^2 + {\sigma_{\phi_a^2}}^2 + {\sigma_{\phi_b^1}}^2 + {\sigma_{\phi_b^2}}^2 \\ & & & -2\sigma_{\phi_a^1,\phi_b^1} - 2\sigma_{\phi_a^2,\phi_b^2}. \end{aligned} \tag{3.12}$$

Replacing the σ terms with a function of the distance between the stations gives

$$\begin{aligned} & E\{(\Delta\nabla\phi_{ab}^{12} - E\{\Delta\nabla\phi_{ab}^{12}\}) \\ & (\Delta\nabla\phi_{ab}^{12} - E\{\Delta\nabla\phi_{ab}^{12}\})^T\} &=& \ f(d_{a,a}) + f(d_{a,a}) + f(d_{b,b}) + f(d_{b,b}) \\ & & & -2f(d_{a,b}) - 2f(d_{a,b}) \\ & & =& \ 4f(0) - 4f(d_{a,b}) \end{aligned} \tag{3.13}$$

where $d_{a,b}$ is the distance between stations a and b. Although this assumption solves the observability problem it is overly simplified. Two satellites that are observed from the same station but are relatively close to one another are highly correlated. The paths of these signals will be similar and, consequently, the observations will be correlated.

The other covariance function components are analyzed using the linear model approach described above. Figure 3.1 shows the troposphere and orbit errors modelled as a function of the double difference angle between the vector of the satellite-receiver measurements, as shown in Equation 3.7. The data for this analysis is from the MAGNET network.

The linear arrangement of data points suggests that a linear model is a valid covariance model for this parameter. The the data points with double difference angles less than -20 degrees include variance components.

The baseline length could also be a parameter to incorporate into the covariance

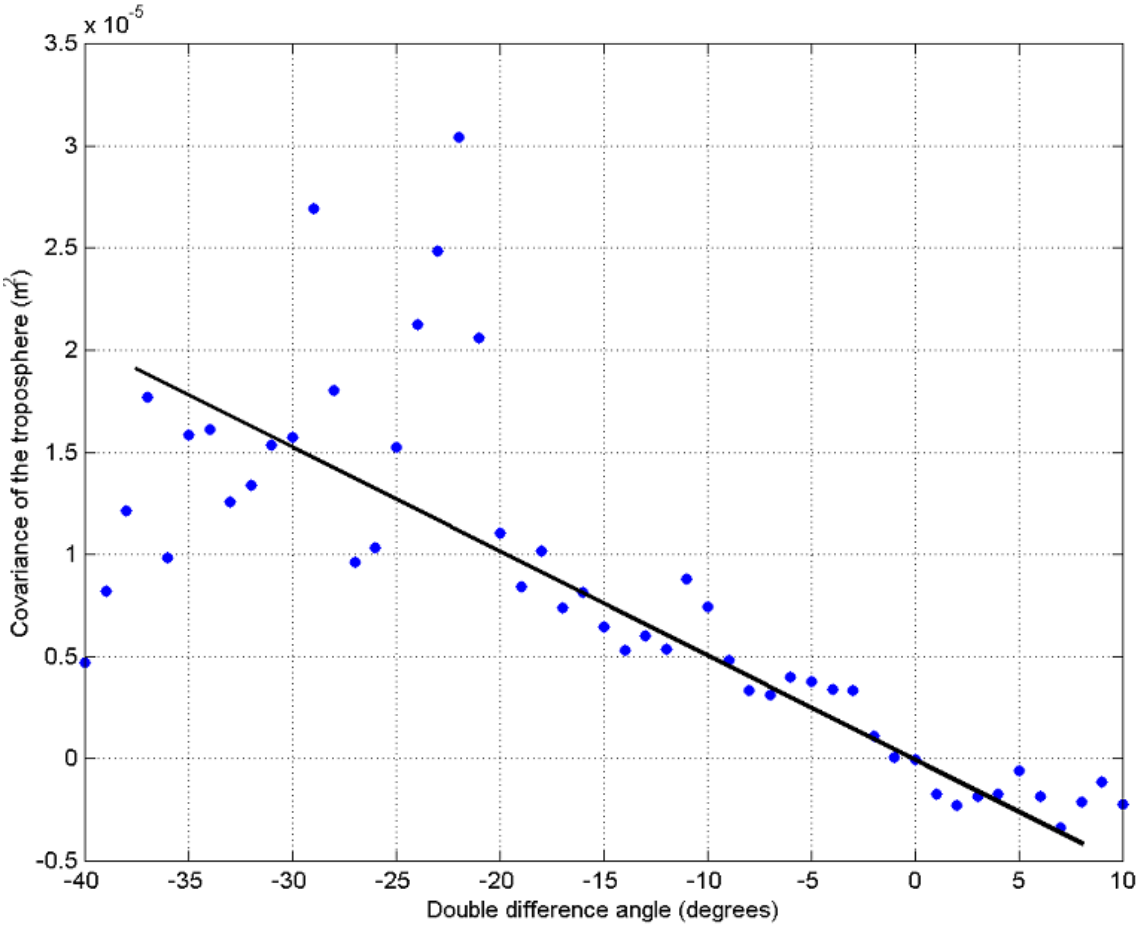

Figure 3.1: The double difference troposphere error modelled as a linear function of the great circle angle between two measurements.

model; Unfortunately, it cannot be shown with this method of analysis for reasons already discussed.

The parameter chosen for the ionospheric error is the distance between the pierce points of two zenith observations on an ionospheric shell located 350 km above the surface of the Earth. This height was chosen because it is in the vertical region that contains the usual maximum electron density (Klobuchar, 1996). The zenith value is calculated using the mapping function derived by Skone (1998). The distance between two pierce points includes both the angle between the observations and the distance between the two stations. This is the most logical metric for the ionosphere because this is a representation of the separation of the paths through the ionosphere. Figure 3.2 shows the linear model as a function of the double difference ionospheric pierce point distance. This parameterization shows a linear trend although with less slope than the troposphere model. Again the effect of the variance bias can be seen when the double difference distance is less than -220 kilometres.

The linear model appears to be a reasonable model for both the tropospheric and ionospheric errors but, unfortunately, the linear model does not result in a positive definite covariance matrix, which is a requirement for this covariance function. The angle and pierce point distance functions need to be modelled by a function that is positive definite.

3.1.2 Form of the Covariance Function

The covariance function used in Raquet (1998) is a double difference specific function that is dependent on the location of the fictional P0 point. The function used to predict the distance dependent errors cannot be separated from P0. The covariance functions compared by Fortes (2002) are increasing as a function of distance because

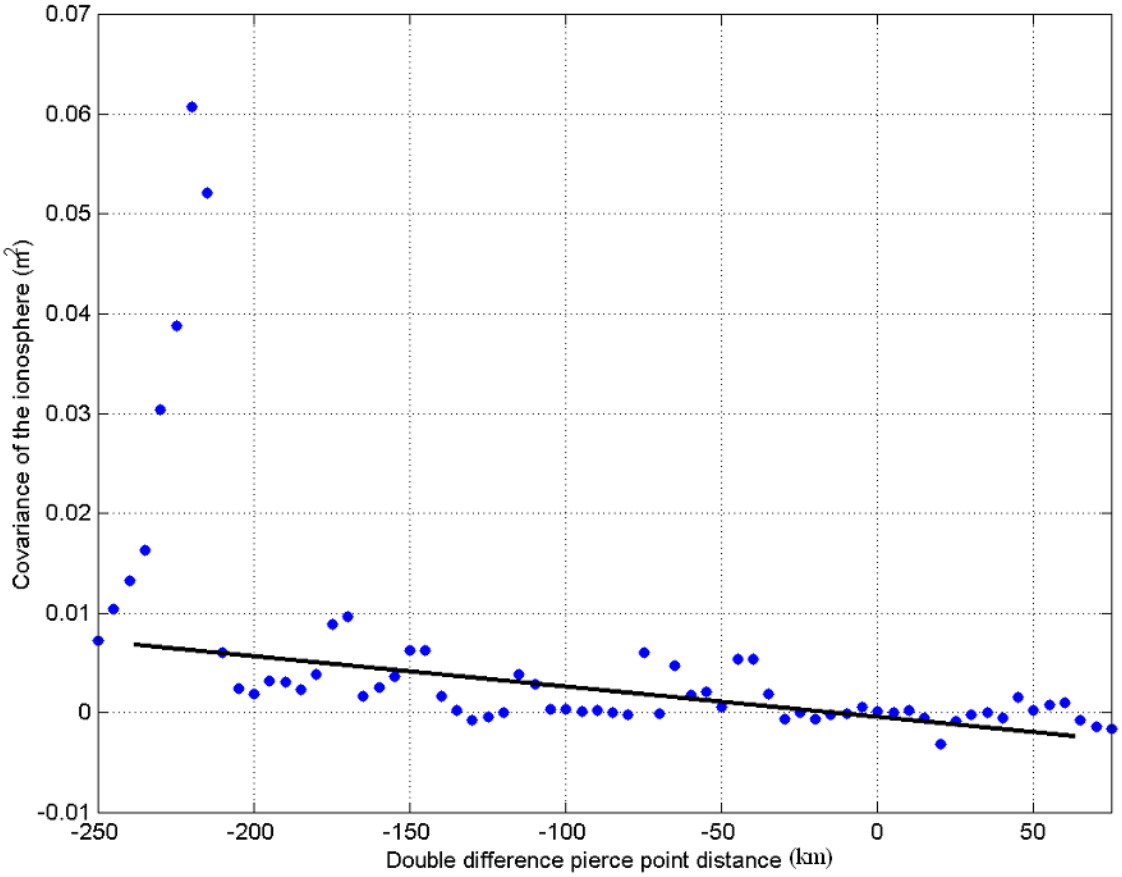

Figure 3.2: The double difference zenith ionosphere error modelled as a linear function of the pierce point distance between two measurements

they are in relation to the distance in relation to P_0 and the separation of the two measurement stations. If P_0 is not used then the covariance functions must be a decreasing function in order to produce a positive define variance covariance matrix. The covariance functions shown below are similar in form to the covariance function used in Raquet (1998) and Fortes (2002). Unfortunately, these functions may not produce a positive definite covariance matrix in all cases but will be used to compare the prediction characteristics against other potential covariance functions:

$$\begin{aligned} CF_1(d) &= 1 - \frac{d}{\tau} \\ CF_2(d) &= 1 - \left(\frac{d}{\tau}\right)^2 \\ CF_3(d) &= 1 - \frac{d}{\tau} - \left(\frac{d}{\tau}\right)^2 \end{aligned} \tag{3.14}$$

where d is the distance between two measurements and τ is the correlation distance.

Radovanovic (2002) and Kennedy (2002) use a decreasing exponential function as the functional model. This will be tested in two forms:

$$\begin{aligned} CF_4(d) &= e^{\left(-\frac{d}{\tau}\right)} \\ CF_5(d) &= e^{\left(-\left(\frac{d}{\tau}\right)^2\right)}. \end{aligned} \tag{3.15}$$

To demonstrate the prediction properties of these covariance functions, a simple observation and prediction test is shown. In this scenario two observations of the signal are predicted. The observations are shown in Table 3.1.

Table 3.1: Observations of the signal for a simple prediction characteristic test of the covariance functions.

Location (x location)	Observation (measured y value)
-2	1
2	5

This test simulates the prediction of observations from two reference stations for a region using the covariance functions shown in Equations 3.14 and 3.15. Two scenarios are shown. The first represents a closely spaced network with a large correlation length. The results of this test are shown in Figure 3.3. The predicted values are very similar between the observation locations for each of the covariance functions. Each of the covariance functions has a particular extrapolation characteristic but, in general, they either use the observation from one station or both to predict outside of the observation locations.

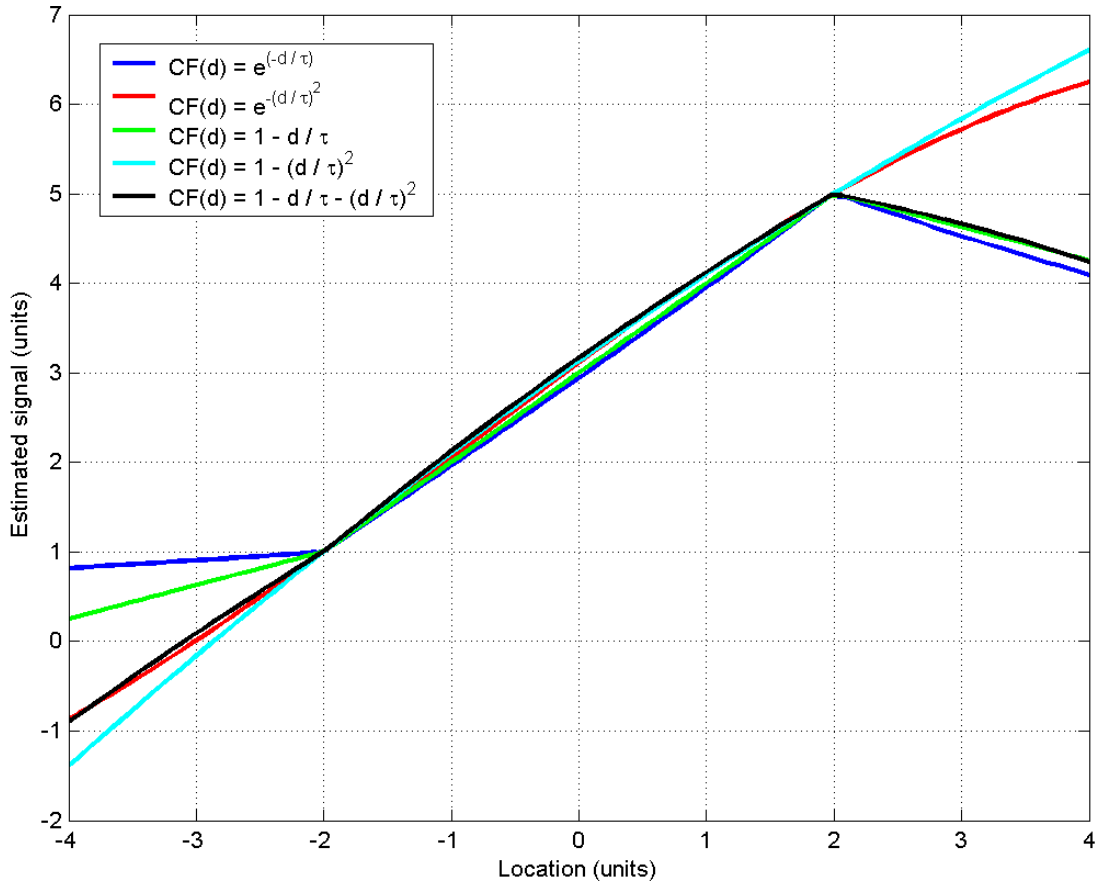

Figure 3.3: Prediction characteristics for various covariance functions with a long correlation length (10 units)

The greatest differences in the prediction characteristics between the covariance

functions will be when the network is sparse or the correlation length is short. In this case the reference stations are not close enough to observe the errors throughout the entire network. Figure 3.4 shows the prediction characteristics for the various covariance functions with a short correlation distance. Each of the covariance functions provides slightly different prediction qualities between and outside the control (reference) stations. The exponential covariance functions from Equation 3.15 have the best characteristics, because if the reference stations do not measure the same errors as the predicted location, then the corrections converge to zero. This is the best prediction behaviour because it is better to provide no improvement than it is to degrade the performance. These covariance functions also provide similar behaviour when extrapolating outside of the observation points.

This test demonstrates the prediction behaviour between the various covariance function forms assuming that the observations are undifferenced at each of the observed locations. In practice the regional errors are predicted though differential measurements. This affects the shape and behaviour of the predictions. In this next test the signal is measured using the difference between the measurements. This is similar to the double differenced observations that are used to measure the signal in network RTK. Only single differenced observations are used in this evaluation because double differenced observations require azimuths and elevations of the measurements, which would overly complicate the location-based evaluation. Now that differential measurements are used, the P_0-based covariance function used by Raquet (1998) and Fortes (2002) can be compared to the functions in Equations 3.14 and 3.15.

The P_0 covariance function used for this comparison is

$$\sigma_{\phi_1,\phi_2} = \frac{\sigma(P_1, P_0) + \sigma(P_2, P_0) + \sigma(P_1, P_2)}{2} \tag{3.16}$$

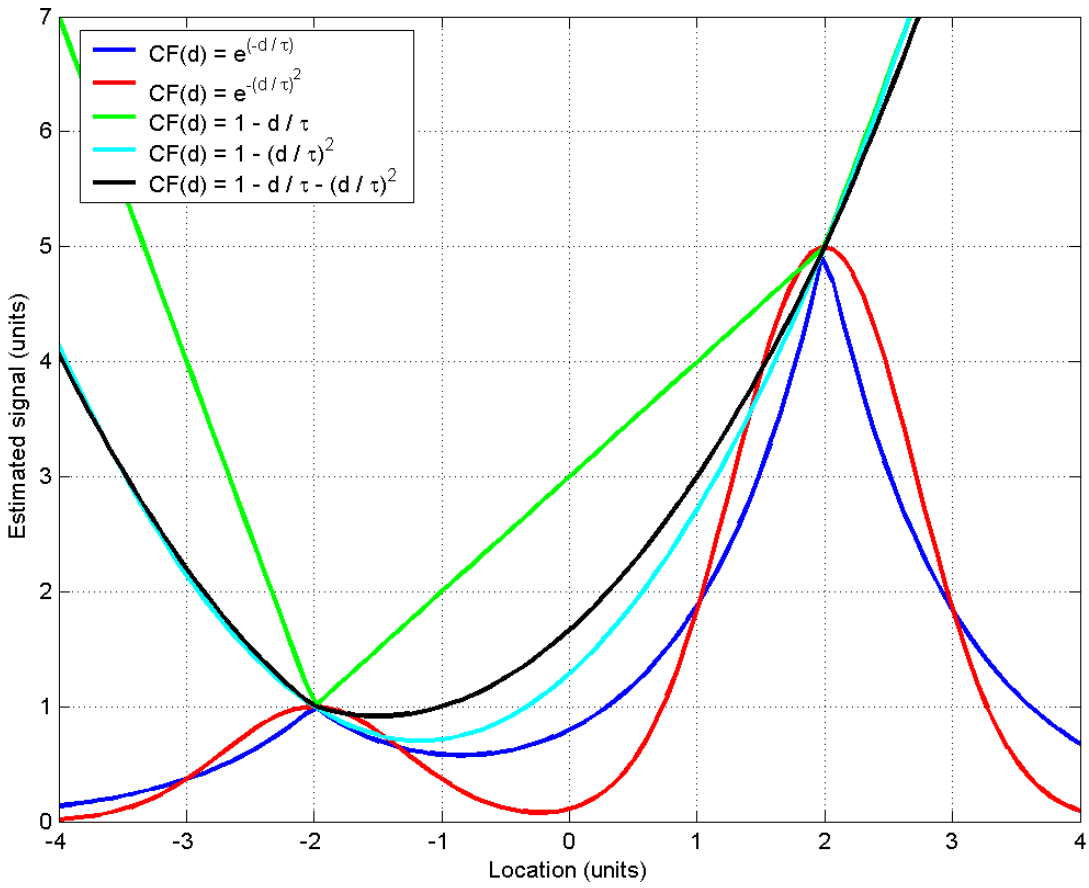

Figure 3.4: Prediction characteristics for various covariance functions with a short correlation length (1 units)

where $\sigma(P_a, P_b)$ is a distance dependant function and P_0 is the location of an arbitrary point which should be located in or around the network. The distance dependant function used in this evaluation is

$$\sigma(P_a, P_b) = \frac{d_{a,b}}{\tau} + \left(\frac{d_{a,b}}{\tau}\right)^2. \tag{3.17}$$

This covariance function limits the magnitude of the variance and covariance values such that they are allowed to increase as the location moves further away from the P_0 location. This covariance function is inappropriate for undifferenced observations because the observations from any reference station located at the P_0 location would have variances and covariances of zero.

Figure 3.5 shows the predicted signal for each of the covariance functions when estimated using single differenced observations from Table 3.1. In the differenced solution the linear functions provide the same predicted solution within the observation points. The exponential functions now converge to the average value of all the measurements. These functions again show a prediction that is a function of the expected correlation around each of the observation points. When the computation point is outside of the influence of the nearest observation point then the exponential functions converge to the average network measurement. In practice, the average of all double differenced residuals should be zero, in which case the prediction converges to zero. As in the undifferenced test, the estimated signal within the observation points is very similar; however, outside of the observation points the prediction for the functions is considerably different.

To expose the differences between the functions, a third observation is added to the observations shown in Table 3.1. The observations used for the following tests are shown in Table 3.2.

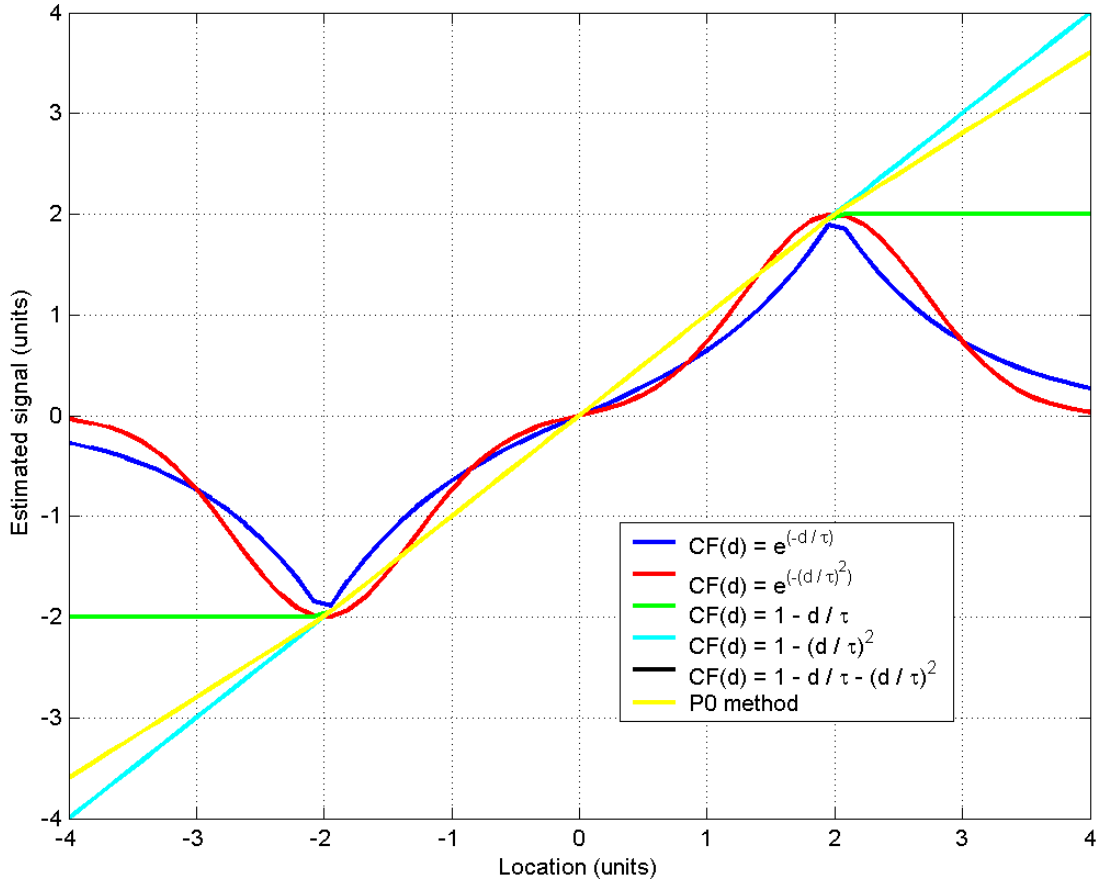

Figure 3.5: Prediction characteristics for various covariance functions with a short correlation length (1 units) using single difference observations

Table 3.2: Observations of the signal for a simple differential prediction characteristic test of the covariance functions.

Location (x location)	Observation (measured y value)
-2	1
2	5
4	6

Figure 3.6 shows the differential prediction characteristics for the various covariance functions. The datum used by each of the covariance functions differs, shown in the figure by the vertical biases between the solutions. This bias has no effect on the performance of the covariance functions, because the corrections are only applicable in differential form. This shows that the spatial shape of the predictions for the P_0-based covariance function is the same as the linear covariance function, $CF_2(d) = 1 - \left(\frac{d}{\tau}\right)^2$. The distance weighting function of the P_0-based covariance function and the linear function are very similar in form.

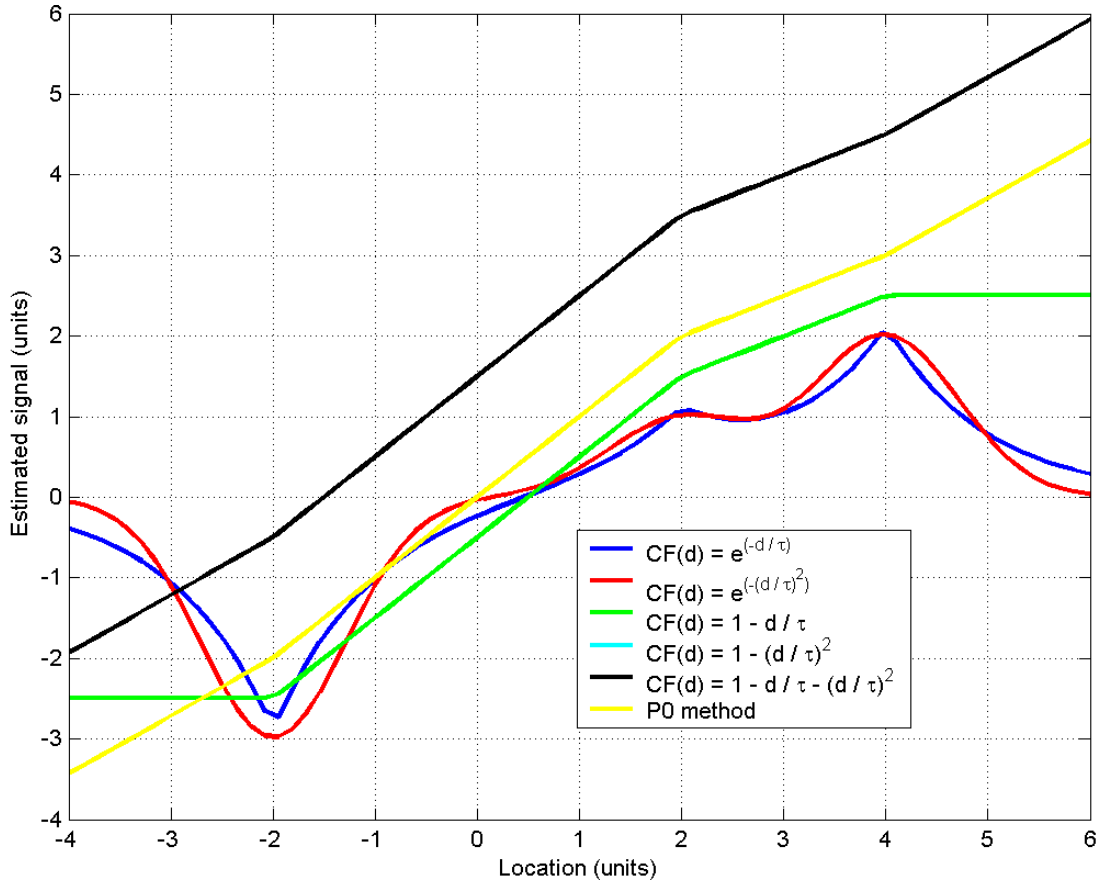

Figure 3.6: Prediction characteristics for various covariance functions with a short correlation length (1 units) using single difference observations

When the corrections are differenced (to be applied) the bias is removed from

each of the solutions. Figure 3.7 shows the normalized prediction characteristics for the covariance functions. The predicted signal at the first observation point (−2) is constrained to zero. This is used to compare the shape of the functions and their performance when applied. Once again the linear covariance functions provide the same prediction between the observation points. The second order exponential decay function provides a better prediction shape than the first order function, because the local values are preserved for a longer distance before converging to the mean value.

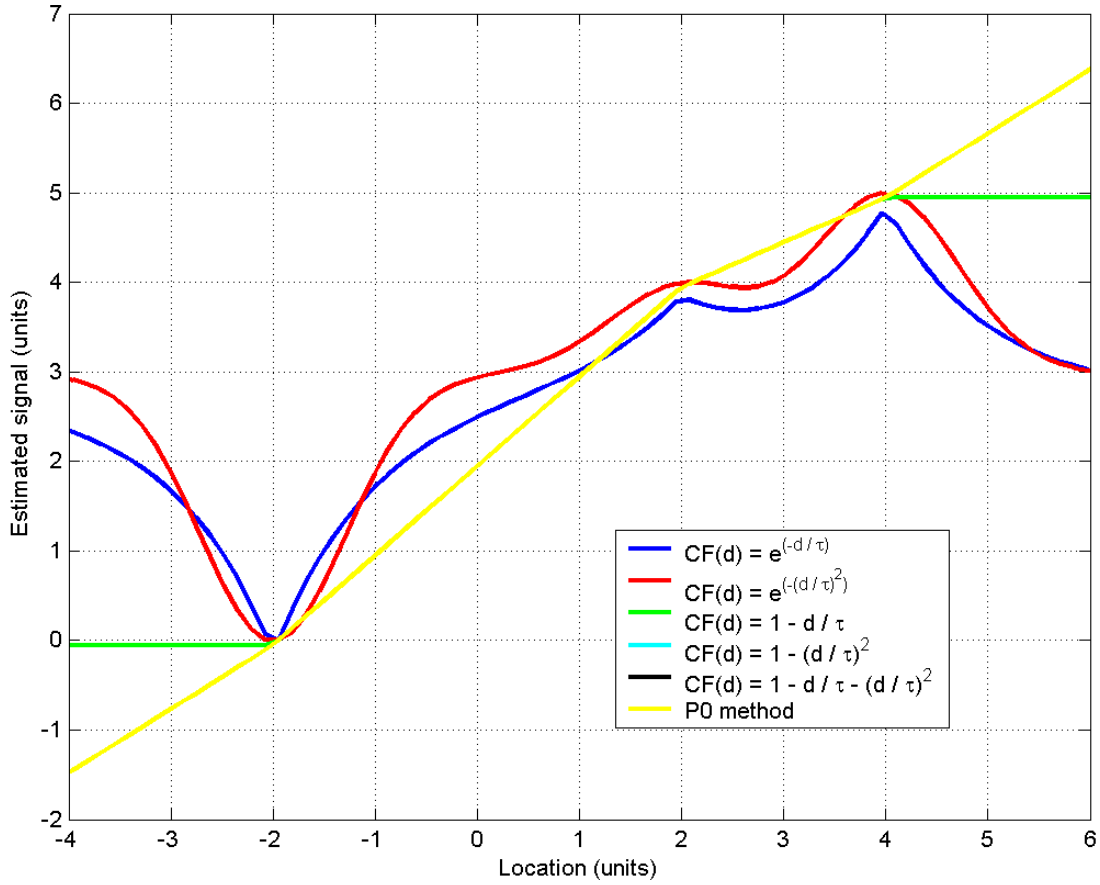

Figure 3.7: Prediction characteristics for various covariance functions normalized at location -2 with a short correlation length (1 units) using single differenced observations

This test also illustrates how the prediction is tied to the observation points. Figure 3.8 shows the prediction for one of the covariance functions in the previous test.

The corrections are only valid when differenced and in practice they are differenced with a reference station in the network. The figure shows the value of the differential correction for each of the two closest measurement points. The value of the differenced correction is the difference between the correction at the rover's computation point and the correction at the observation point. This is shown as Correction A and Correction B. As shown by this test, the difference of the corrections at the measurement points is the difference in the observations of the two points. In this way the corrections applied to the rover from either station A or station B are tied together through the stations' measurements. This means that the rover will get the same correction when using either station A or station B.

In the network approach the rover solution is thus tied to every station in the network. The performance of the network approach is often compared to that of the single baseline approach. The network approach and the single reference station approach are similar in terms of the representation of the corrections. An example is shown in Figure 3.9. Using this error profile allows the network approach to mimic the single baseline approach.

In the single reference station approach the errors measured by the single reference station are assumed to be the same as the errors measured by surrounding stations. This is why each reference station has a horizontal estimated signal. The vertical discontinuities are the locations at which the user would switch from one reference station to the next. These transition locations are shown at the midpoint between the two adjacent reference stations.

This generalization is limited by the resolution of the network ambiguities. The corrections are tied to each of the reference stations because the differenced corrections from one station are the corrections from another station minus the difference

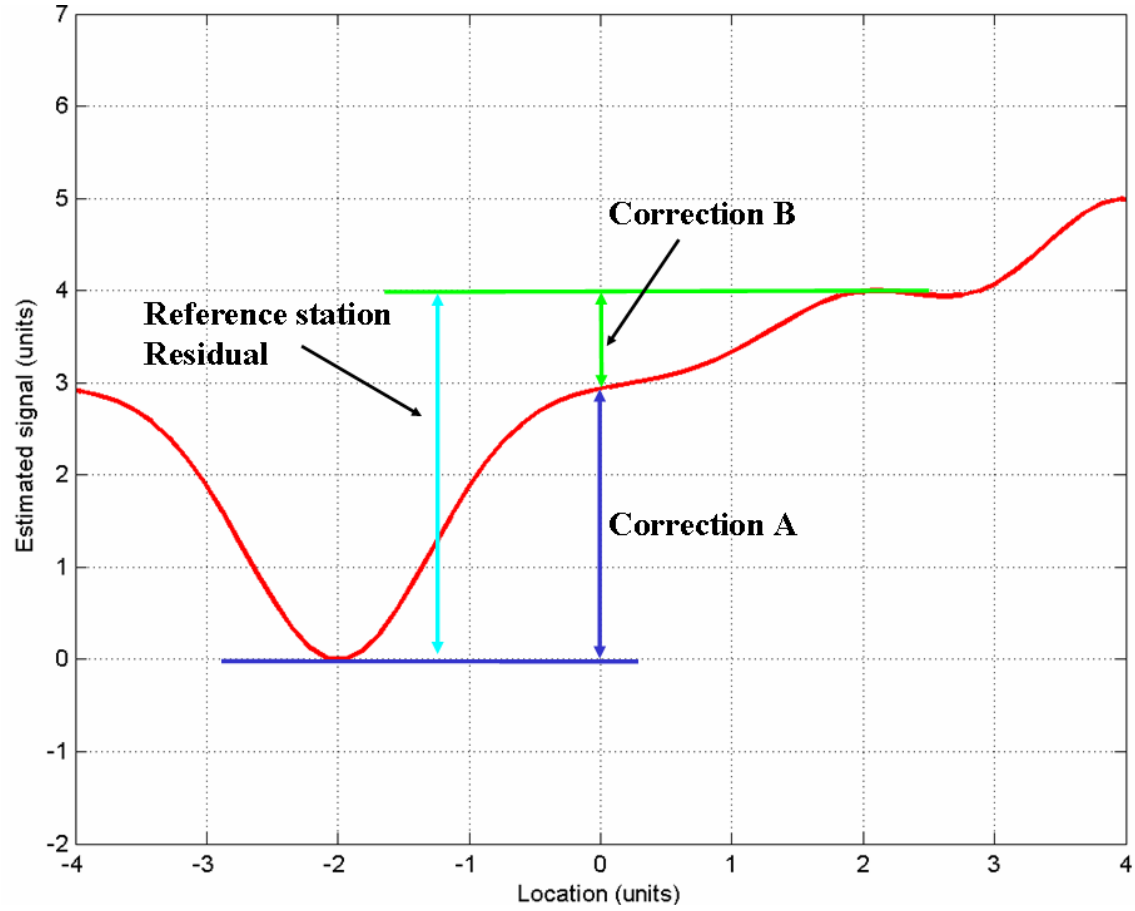

Figure 3.8: Differential prediction values in relation to the observation point corrections

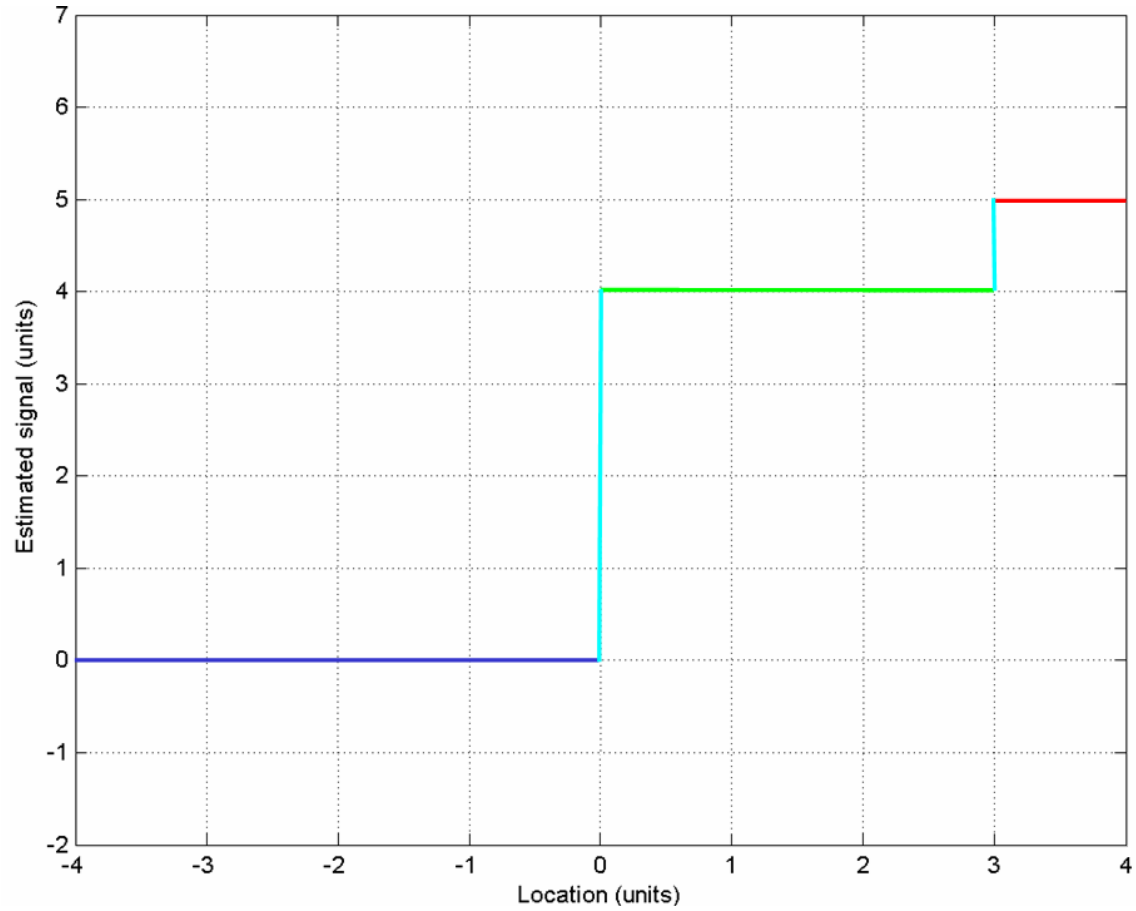

Figure 3.9: Differential prediction values in relation to the observation point corrections for the single baseline approach

in station observations. The differences in station observations, in practice, are a function of the estimated or fixed ambiguities between the two stations. If the ambiguities are incorrectly estimated or resolved then the difference in the errors from one station to the other will contain ambiguity estimation error as well as atmospheric errors.

The logical alternative for small to medium scale networks would be to only generate corrections using fixed ambiguities. If this is the case then it is important to ensure that the observations that have corrections are not differenced from observations for which corrections were not calculated because then the undifferenced form of the corrections will be used. For example, if two corrected observations, $\phi_1 - s_1$ and $\phi_2 - s_2$, are differenced then the corrections (s_1 and s_2) are also differenced. In the case of double differenced observations, the result is the double difference observation minus the double difference correction. If only one satellite has corrections then the resulting adjusted (corrected) observation is the double difference measurement minus the single difference correction. In this way the network correction generation is either an all or nothing process.

3.1.3 Final Covariance Function

The previous sections have shown that the troposphere covariance is a function of the angle between the observations and the ionosphere covariance is a function of the pierce point distance on the ionosphere shell. The troposphere covariance is also a function of the inter-antenna separation, however this cannot be taken into account using the linear model technique.

The exponential covariance functions shown in Equation 3.15 provide the desired characteristics, namely

- the function is positive definite,
- the function converges to zero as the distance increases, and
- the function represents the statistical likelihood that the signal observed is the same as the signal at the computation point.

The coefficient of this covariance function will need to be calibrated using a least squares adjustment. Although the second order exponential decay function provides a better prediction shape, the coefficients of the first order function will be easier to estimate because they are linear.

When all of the covariance function terms are included the first order covariance function is

$$CF_6(d, \alpha, d_I) = e^{-\left(\frac{d}{\beta_d}\right)} e^{-\left(\frac{\alpha}{\beta_\alpha}\right)} \sigma_T^2 + e^{-\left(\frac{d_I}{\beta_{d_I}}\right)} \sigma_I^2 \tag{3.18}$$

and the second order covariance function is

$$CF_7(d, \alpha, d_I) = e^{-\left(\frac{d}{\beta_d}\right)^2} e^{-\left(\frac{\alpha}{\beta_\alpha}\right)^2} \sigma_T^2 + e^{-\left(\frac{d_I}{\beta_{d_I}}\right)^2} \sigma_I^2 \tag{3.19}$$

where d is the inter-antenna distance between the stations, β_d is the correlation length for the inter-antenna distance between the stations for the troposphere, α is the angle between the observations, β_α is the correlation angle for the great circle angle of the troposphere, σ_T^2 is the variance of the troposphere error, d_I is the distance between the pierce points on the ionosphere shell, β_{d_I} is the correlation length for the pierce point distance for the ionosphere, and σ_I^2 is the variance of the ionosphere. These covariance functions are a function of the inter-antenna distance, the great circle angle between the observations, and the pierce point distance between the observations. They can calculate the correlation between any two observations.

3.2 Estimating the Coefficients of the Covariance Function

The coefficients of the covariance function can be estimated using a least squares adjustment (Radovanovic, 2002). The coefficients of the covariance function in Equations 3.18 and 3.19 are the correlation angle, β_α, the two correlation lengths, β_d and β_{d_I}, and the two variances, σ_T and σ_I. The following section shows how the coefficients of the covariance function are estimated using the covariance function in Equation 3.18 as an example. A similar procedure is used for the covariance function in Equation 3.19.

To assist with the linearization of the covariance function in terms of the coefficients, the correlation lengths and angle are estimated as their inverses. The estimated covariance function is then

$$CF(d, \alpha, d_I) = e^{-d\beta'_d} e^{-\alpha\beta'_\alpha} \sigma_T^2 + e^{-d_I\beta'_{d_I}} \sigma_I^2 \tag{3.20}$$

where

$$\begin{aligned} \beta'_d &= \frac{1}{\beta_d} \\ \beta'_\alpha &= \frac{1}{\beta_\alpha} \\ \beta'_{d_I} &= \frac{1}{\beta_{d_I}} \end{aligned}$$

The vector of estimated parameters is

$$x = \begin{bmatrix} \beta'_d & \beta'_\alpha & \sigma_T^2 & \beta'_{d_I} & \sigma_I^2 \end{bmatrix}^T \tag{3.21}$$

These parameters are estimated using the ionosphere-free and geometry-free linear combinations. These are used instead of the raw L1 and L2 observations because the linear combinations can observe the tropospheric and ionospheric coefficients independently. This simplifies the estimation procedure because the tropospheric coefficients

can be estimated in a separate filter than the ionospheric coefficients. For simplicity, this example will estimate all of the coefficients in one filter however the filter may be partitioned into two independent parts.

The ionosphere-free linear combination is used to estimate the coefficients of the tropospheric covariance. The ionosphere-free combination residual is

$$\begin{aligned} \Delta\nabla r_{IF} &= \Delta\nabla\phi_{L1} + \lambda_{L1}\Delta\nabla N_{L1} - \Delta\nabla\rho + \varepsilon_{L1} \\ &\quad -\tfrac{f_{L2}^2}{f_{L1}^2}(\Delta\nabla\phi_{L2} + \lambda_{L2}\Delta\nabla N_{L2} - \Delta\nabla\rho + \varepsilon_{L2}) \\ &= \left(1 - \tfrac{f_{L2}^2}{f_{L1}^2}\right)\Delta\nabla T + \varepsilon_{IF}. \end{aligned} \tag{3.22}$$

The geometry-free linear combination is used to estimate the ionospheric coefficients of the covariance function. The geometry free combination residual is

$$\begin{aligned} \Delta\nabla r_{GF} &= \Delta\nabla\phi_{L1} + \lambda_{L1}\Delta\nabla N_{L1} + \varepsilon_{L1} - (\Delta\nabla\phi_{L2} + \lambda_{L2}\Delta\nabla N_{L2} + \varepsilon_{L2}) \\ &= \left(1 - \tfrac{f_{L1}^2}{f_{L2}^2}\right)\Delta\nabla I + \varepsilon_{GF}. \end{aligned} \tag{3.23}$$

These frequency combinations are equivalent to those shown in Tables 2.5 and 2.6. In this case the measurements in units of length (m) are differenced and in Tables 2.5 and 2.6 the carrier phase ambiguities are differenced in units of length (cycles). The frequency ratio between L1 and L2 is the property that is used to isolate (geometry-free) or remove (ionosphere-free) the ionosphere error in all cases.

Each of these frequency combination equations involves four observations. To observe the covariance function from a linear combination, the expected value of the product of two ionosphere free or geometry free observations is calculated in a similar way to Equation 3.5. Each σ is estimated as the covariance from Equation 3.18. Let i and j represent each of the undifferenced observations of the double difference combination, a and b, respectively. The misclosure for the estimation of the covariance

function coefficients is

$$w_{IFab} = \left(1 - \frac{f_{L2}^2}{f_{L1}^2}\right)^2 \sum_{i=1}^{4}\sum_{j=1}^{4}(\text{Sign}(i)\text{Sign}(j)e^{-\alpha_{i,j}\beta'_{\alpha}}e^{-d_{i,j}\beta'_{d}}\sigma_T^2) - \Delta\nabla r_{IFa}\Delta\nabla r_{IFb} \tag{3.24}$$

$$w_{GFab} = \left(1 - \frac{f_{L1}^2}{f_{L2}^2}\right)^2 \sum_{i=1}^{4}\sum_{j=1}^{4}(\text{Sign}(i)\text{Sign}(j)e^{-d_{I\,i,j}\beta'_{d_I}}\sigma_I^2) - \Delta\nabla r_{GFa}\Delta\nabla r_{GFb} \tag{3.25}$$

where Sign is an array that represents the order in the double difference:

$$\text{Sign}(i) = \begin{bmatrix} 1 & -1 & -1 & 1 \end{bmatrix} \tag{3.26}$$

The elements of the design matrix are the partial derivatives of w_{IF} and w_{GF} with respect to the estimated parameters (Equation 3.21).

Each observation for this estimation contains the product of two double difference residuals. The total number of observations is the number of combinations that can be formed from all of the double differences with fixed carrier phase ambiguities. In this case, only linearly independent ambiguities are estimated.

The correlation between these observations cannot be properly modelled because the observations are not linear combinations of the untransformed observations. As a result, each of the observations is given a unit weight and observation correlations are ignored. This means that the values of the variance-covariance matrix of the estimated parameters will not be correct in an absolute sense.

When the covariance function parameters are estimated in real-time using a Bayes filter, the variance-covariance matrix of the estimated parameters smooths the parameters from one epoch to the next. When process noise is added to the variance-covariance matrix of the estimated parameters then they will adapt to changing error

conditions. This adaptive property allows the covariance function coefficients to dynamically tune themselves to changing atmospheric conditions.

The observability of this filter is a function of the number of reference stations, spacing of the reference stations, and the distribution of satellites in view. As a result, the contribution of the update for each epoch may vary. To prevent the filter from applying too much process noise and weakening the estimates, the variance terms of the variance-covariance matrix are multiplied by a process noise factor. The process noise factor used herein is 1.01 for the variance components and 1.001 for the correlation lengths and angle. These values are chosen through trial and error. A low value for the process noise factor constrains the estimated parameters and limits their adaptation to changing conditions. A value that is too large gives too much variability to the estimated parameters, which may lead to divergence. This applies a process noise relative to the level of convergence of the filter. This will ensure that a reasonable level of process noise is added regardless of the contribution of the update. A similar approach is shown in Gertler (1998) whereby a *forgetting factor* is used to gradually deweight previous solutions by multiplying the variance-covariance matrix from the previous epoch by a factor.

As stated earlier, the correlations in this matrix are not properly calculated because the correlation between the observations are not properly modelled. Consequently, the covariance components of the variance-covariance matrix of the estimated parameters are set to zero after each update. This also prevents the parameters from becoming overly correlated.

The range of the covariance function coefficients are limited because they must be positive. This can be a problem if the errors are small. To ensure that the range of the estimated parameters is enforced, the change in the parameter values due to the

update is restricted so that the parameter remains positive after the update.

In addition, to prevent divergence of the filter, the change in value due to the update is limited to a percentage of the value of the parameter. This forces the estimated parameters to vary slowly over time, which prevents them from oscillating around the correct value or diverging due to one large update. The variance components are limited to a maximum change due to one epoch of 20 percent and the correlation lengths and angle are limited to a change of 5 percent. These values were chosen by evaluating the rate of change of the estimated parameters before and during divergence.

3.3 Results

The above covariance function coefficient estimation was applied to three consecutive days of data from the MAGNET network for both 3.18 and 3.19 covariance functions.

Figure 3.10 shows the estimated value of the troposphere standard deviation component of the covariance function. The absolute value of these estimates are smaller than expected for the troposphere. This is not an absolute estimate of the undifferenced variance of the troposphere because it is measured through the double difference residuals. There are no unexpected trends in these estimates however the visual similarities in the values between the days suggests a small influence of multipath error in the estimates. The covariance functions each provide a similar estimate of the troposphere standard deviation. The values at the end of one day and the beginning of the next day should be the same. This is somewhat true in these plots however, the initial convergence time of the estimated parameters will distort this validation.

Figure 3.11 shows the estimated ionosphere standard deviation. The standard

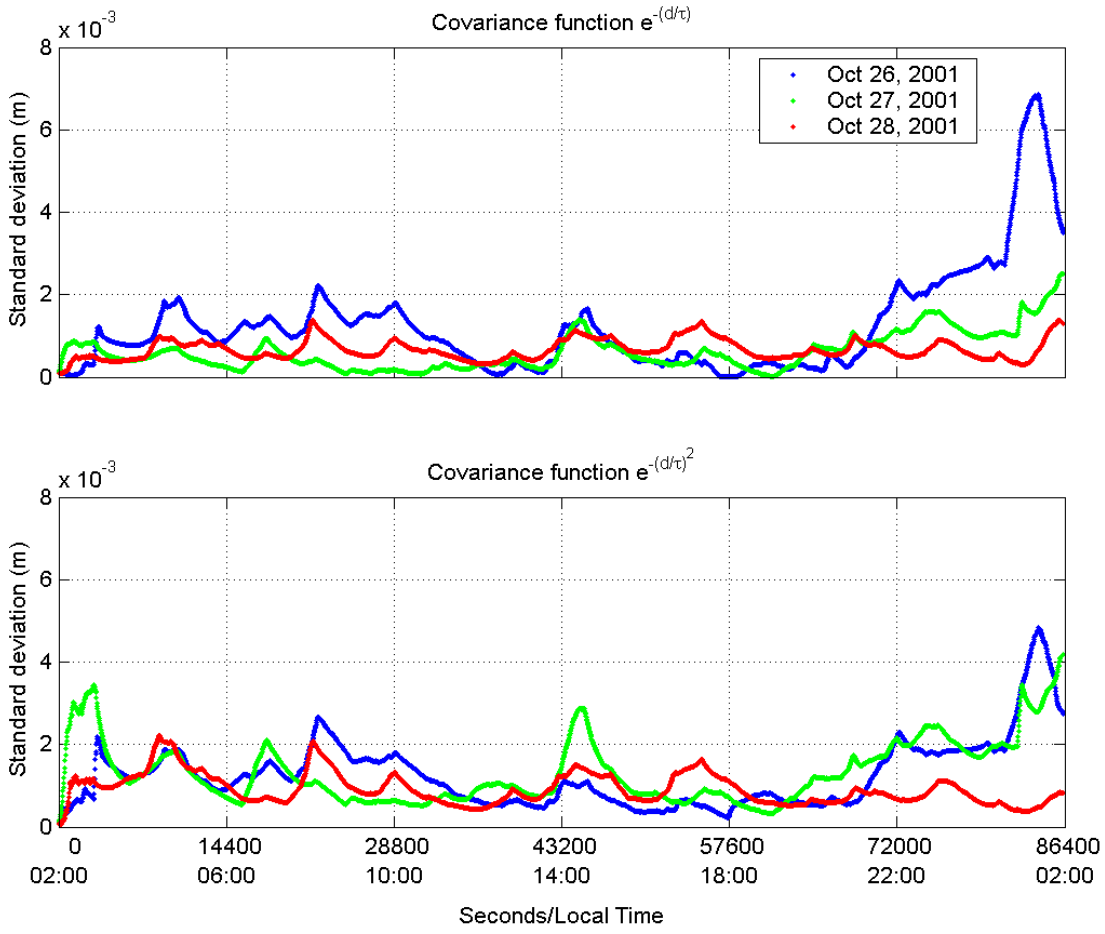

Figure 3.10: Estimated standard deviation of the troposphere error (covariance function coefficient) for Oct 26, 27, and 28 for a first order exponential decay (top) and second order exponential decay (bottom) covariance functions

deviation estimates show the expected daily variation of the ionosphere. The ionosphere error is relatively low at night and high during the day. This pattern is very repeatable from one day to the next, as expected. The two covariance functions have very similar estimates of the ionosphere standard deviation, however the magnitude of the estimates are very different. This is discussed in Section 3.5. Similar to the troposphere standard deviation, the values at the end of one day should be similar to those at the beginning of the following day. This is again, somewhat true in these plots, however, the values will differ because of the initial convergence of the estimated parameters.

Figures 3.12, 3.13, and 3.14 show the correlation angle and length of the troposphere and the correlation length of the ionosphere, respectively. These coefficients converge to a value and vary only a little for the remainder of the data set. This may be due to the low separability of these parameters. For example, the correlation length for the troposphere is only measured at the discrete intervals defined by the reference station spacing. The correlation angle and correlation length have very similar variations. This may be because these parameters are difficult to separate due to their low observability. Further results show that although the separability of the estimated parameters is low the double difference covariance is effectively modelled.

The variances of the L1 and L2 pseudorange measurements are also tracked using the code residuals with fixed positions. This is to allow the software to adapt to the wide variety of code qualities from various receivers and reference station networks. Figure 3.15 shows the estimated standard deviation of the L1 and L2 pseudorange measurements. The day-to-day repeatability shows the effect of day-to-day multipath on the estimate.

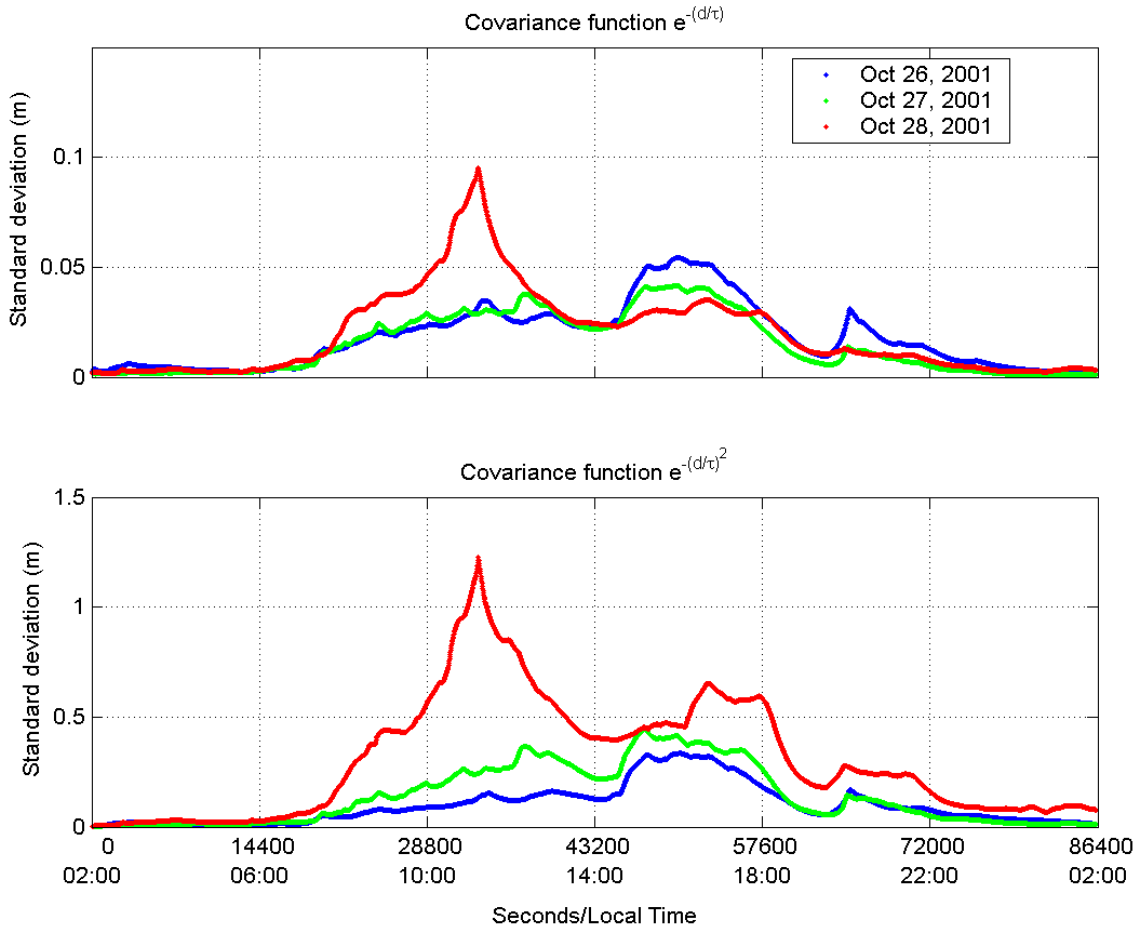

Figure 3.11: Estimated standard deviation of the ionosphere error (covariance function coefficient) for Oct 26, 27, and 28 for a first order exponential decay (top) and second order exponential decay (bottom) covariance functions

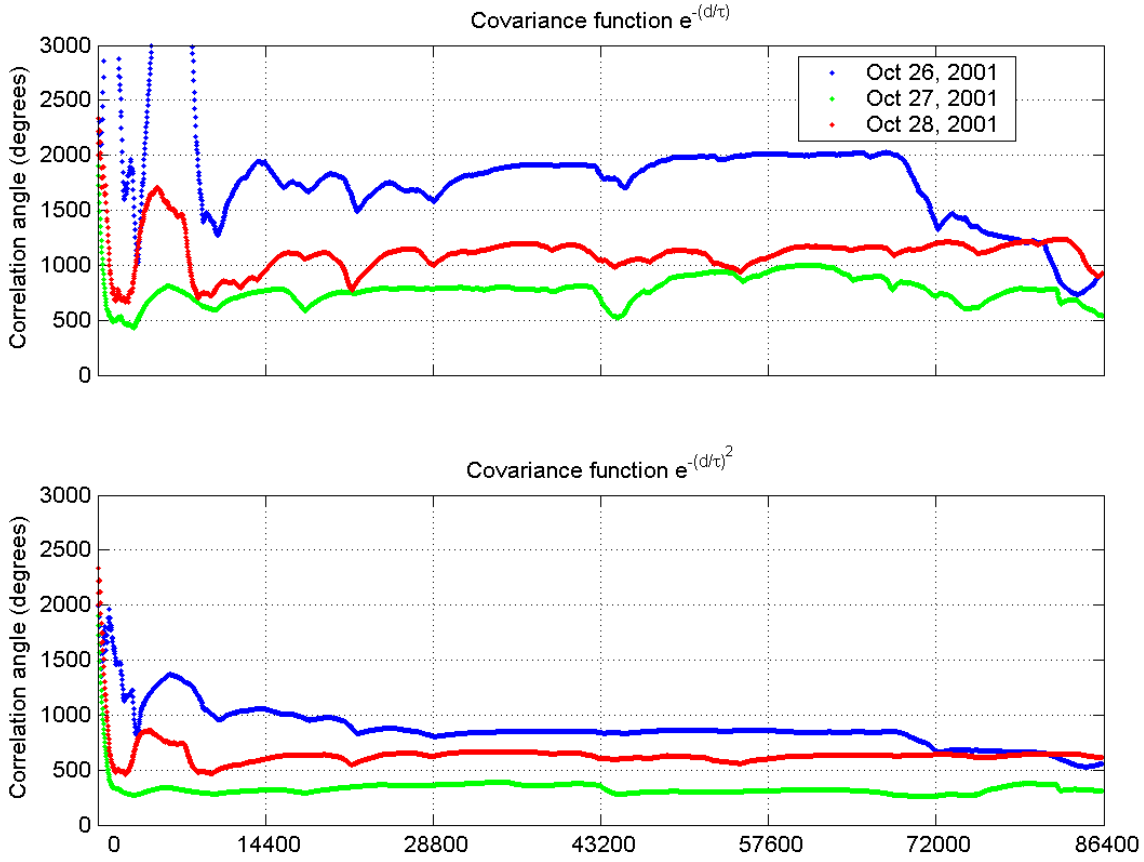

Figure 3.12: Estimated correlation angle of the troposphere error (covariance function coefficient) for Oct 26, 27, and 28 for a first order exponential decay (top) and second order exponential decay (bottom) covariance functions

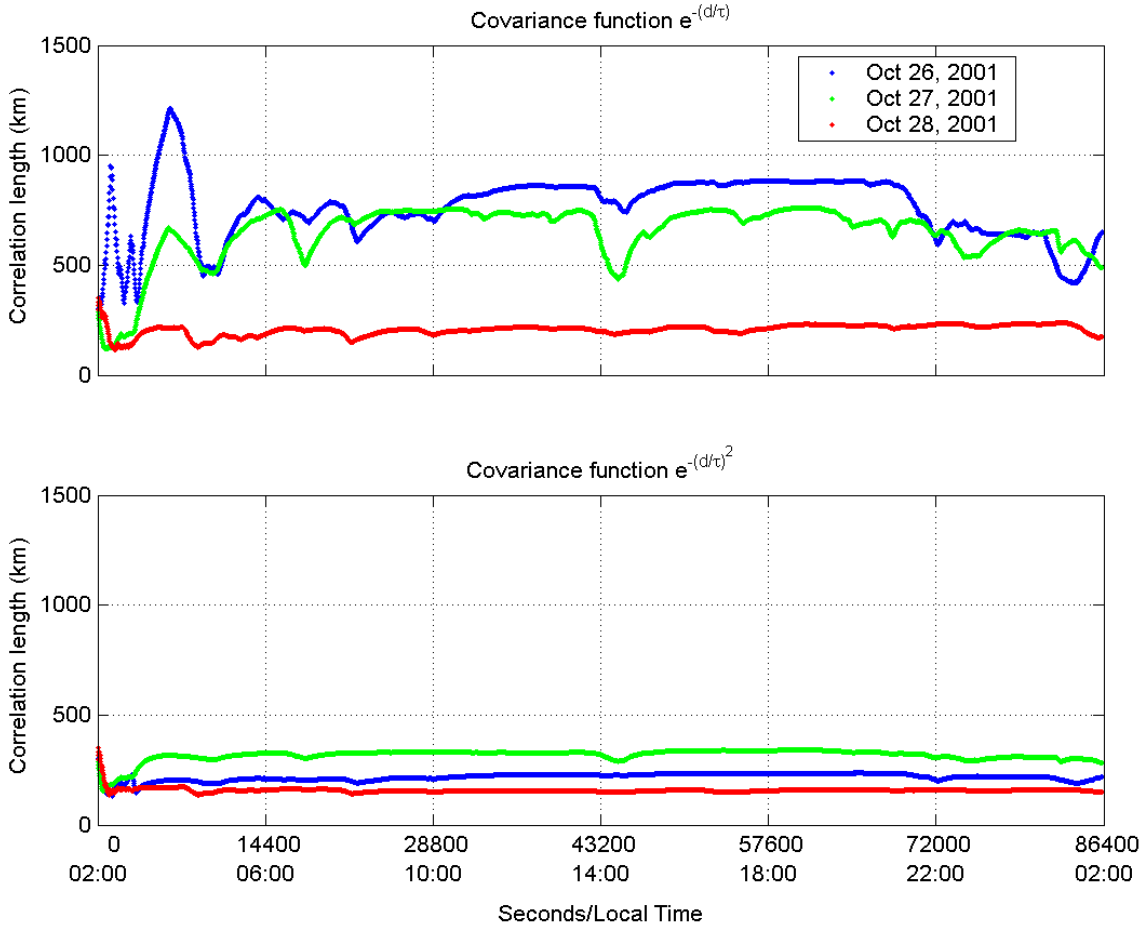

Figure 3.13: Estimated correlation length of the troposphere error (covariance function coefficient) for Oct 26, 27, and 28 for a first order exponential decay (top) and second order exponential decay (bottom) covariance functions

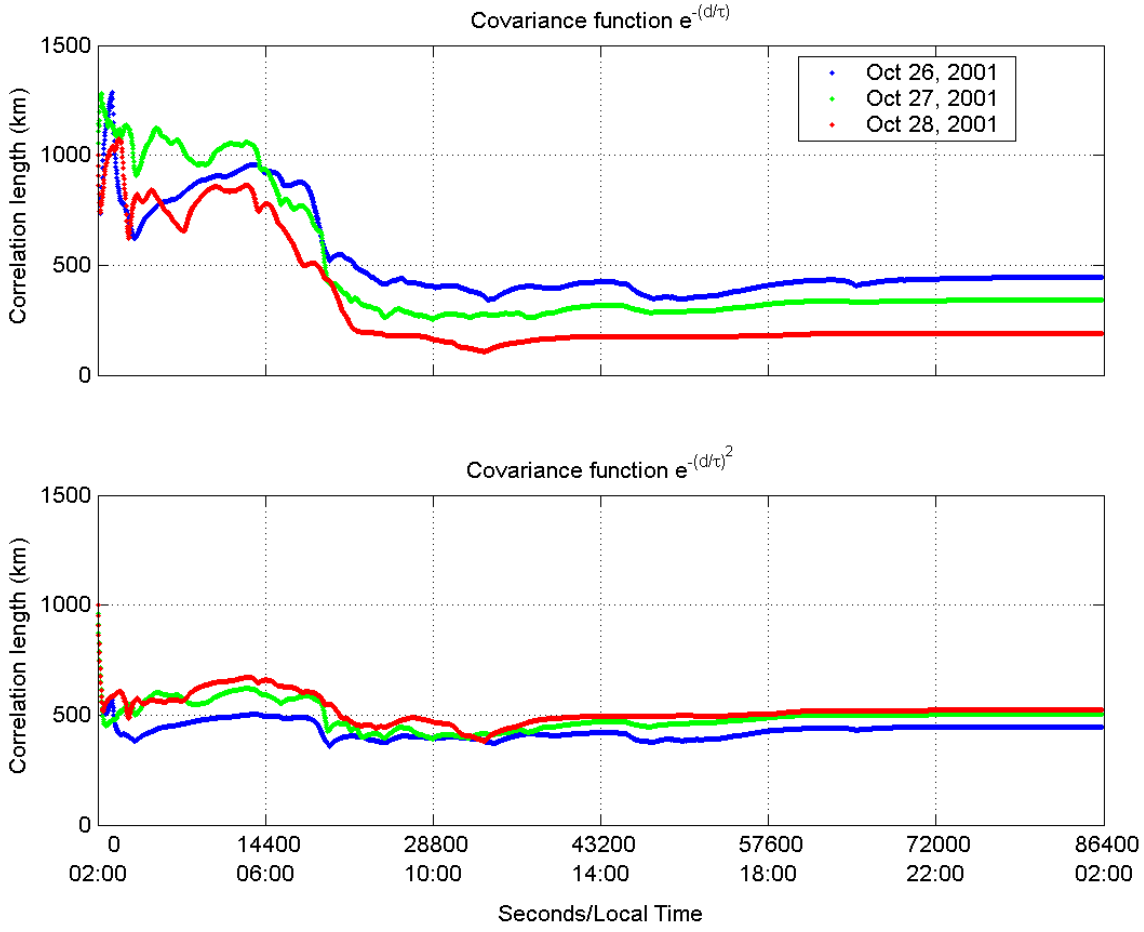

Figure 3.14: Estimated correlation length of the ionosphere error (covariance function coefficient) for Oct 26, 27, and 28 for a first order exponential decay (top) and second order exponential decay (bottom) covariance functions

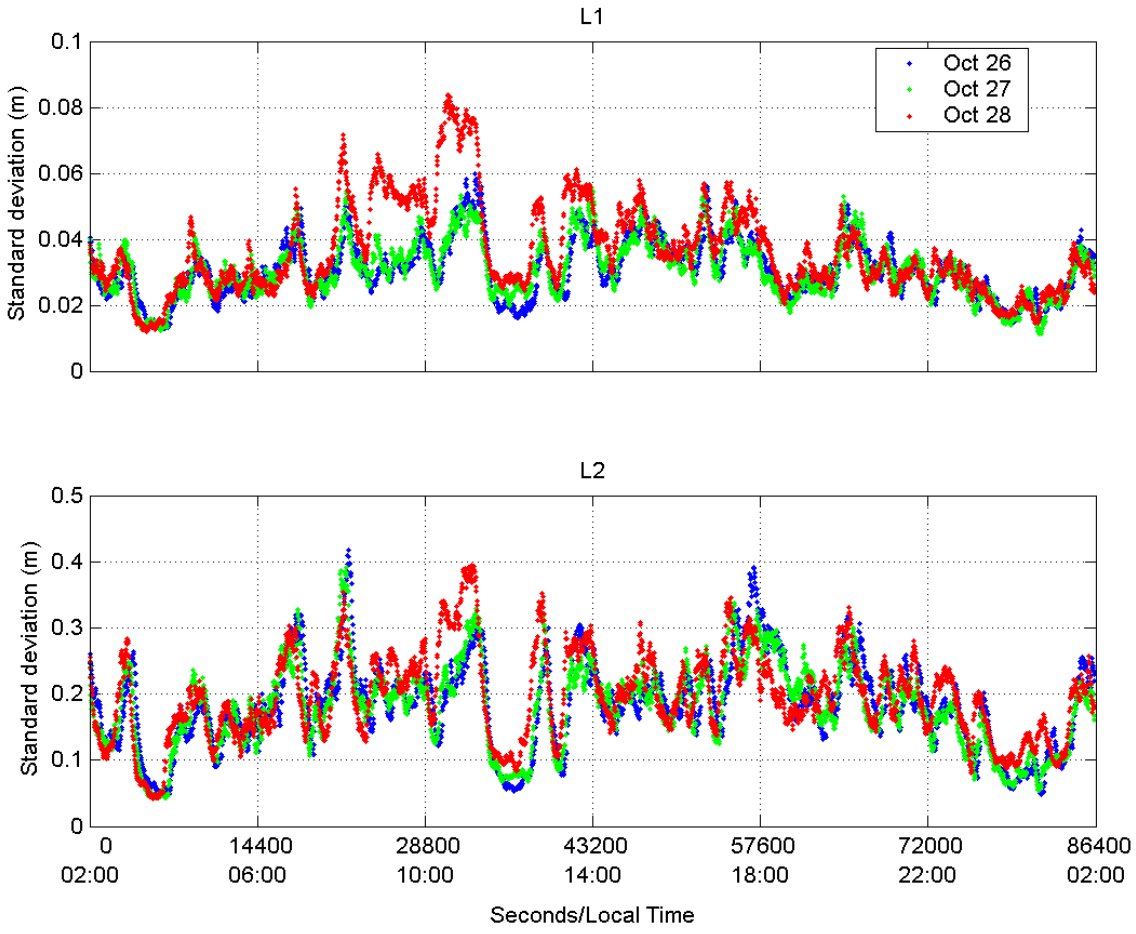

Figure 3.15: Estimated pseudorange standard deviation for Oct 26, 27, and 28 for L1 and L2

3.4 Validation

The covariance functions produce an estimate of the variance and covariance of each observation. This can be compared to the measured error of the observation to validate the covariance function as a model.

This test compares the estimated standard deviation of an observation versus the standard deviation calculated directly by the measured data. The measured errors are derived from the measurement residuals using fixed positions and ambiguities. With all fixed parameters there is no difference between the variance-covariance of the residuals and the variance-covariance of the observations. To calculate the standard deviation of the residuals as a function of the estimated standard deviations produced from the covariance function, the residuals are divided into bins. Bins with less than 300 observations are rejected.

A plot of the standard deviation of the residuals versus the estimated standard deviation of the observations calculated from the covariance function should be linear with a slope of one meaning that the estimated double difference standard deviation using the covariance function is equal to the actual double difference standard deviation of the data.

Figure 3.16 shows a comparison of the standard deviation of the residuals and the estimated standard deviation of the observations for the two covariance functions for Oct 26, 27 and 28. Each of these covariance functions provide a linear relationship between the actual and estimated standard deviations. This shows that as the measurement errors increase so does the estimated standard deviations of the measurements. This relationship is due to the covariance function and the adaptive method. The lines shown in the figure are a least squares fit to the points. The

slopes of these lines are greater than one showing that these covariance functions are optimistic; the standard deviations provided by the covariance function are generally less than the actual measurement errors.

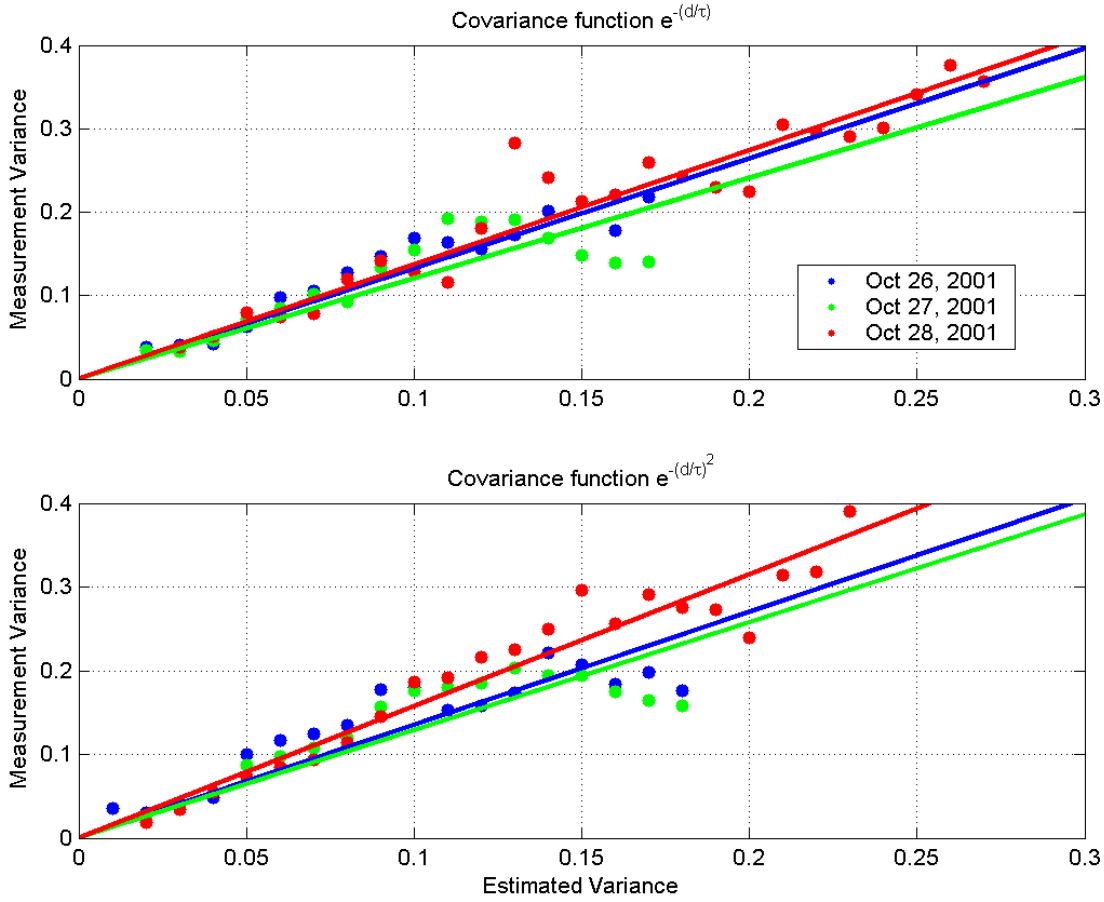

Figure 3.16: Comparison of the standard deviation of the residuals and the estimated standard deviation of the observations calculated from a first order and second order exponential decay covariance functions for Oct 26

3.5 Discussion of Observability

There are many issues that affect the observability of the covariance function coefficients. In general, these estimated parameters are weakly determined because the

single observation covariance function is estimated using the double difference residuals from the network. Although the absolute values of the estimated parameters are weakly observable, the relative values of the covariance function coefficients can be estimated, which provide an accurate double difference covariance function.

The range of observations with respect to the covariance function coefficients is also an important factor in observability. For example, the correlation length of the troposphere error is estimated. This parameter requires a wide range of baseline lengths in order to be observable. Unfortunately, the networks generally used usually consist of less than ten stations, which does not allow for a wide variety of observations.

To illustrate the ability of the covariance function filter to estimate the relative values of the coefficients, the a-priori ionosphere standard deviation is changed without changing the a-priori ionosphere correlation length. Figure 3.17 shows the estimated standard deviation of the ionosphere for the three different initial a-priori values for Oct 26. Figure 3.18 shows the estimated correlation length of the ionosphere for three different initial a-priori ionosphere standard deviations. The ionosphere variance was doubled (shown in red) and divided by two (shown in blue) relative to the previous results (shown in green). This provides a range of initial estimates. The a-priori correlation length is the same for these three tests.

The correlation length is biased for each of the tests, however the error behaviour remains the same. This is because the correlation length is compensating for changes in the standard deviation. The relative values of the parameters are being estimated such that the double difference variance-covariance is correctly modelled. The double difference is a function of the variances and covariance between the observations. The variances are all positively added and the covariance terms are mixed between being

added or subtracted (depending on the order of the observations) to calculate the double difference variance. With this in mind, an increase in the standard deviation requires an increase in the correlation length to maintain a similar double difference observation variance. This results in the behaviour shown in Figures 3.17 and 3.18.

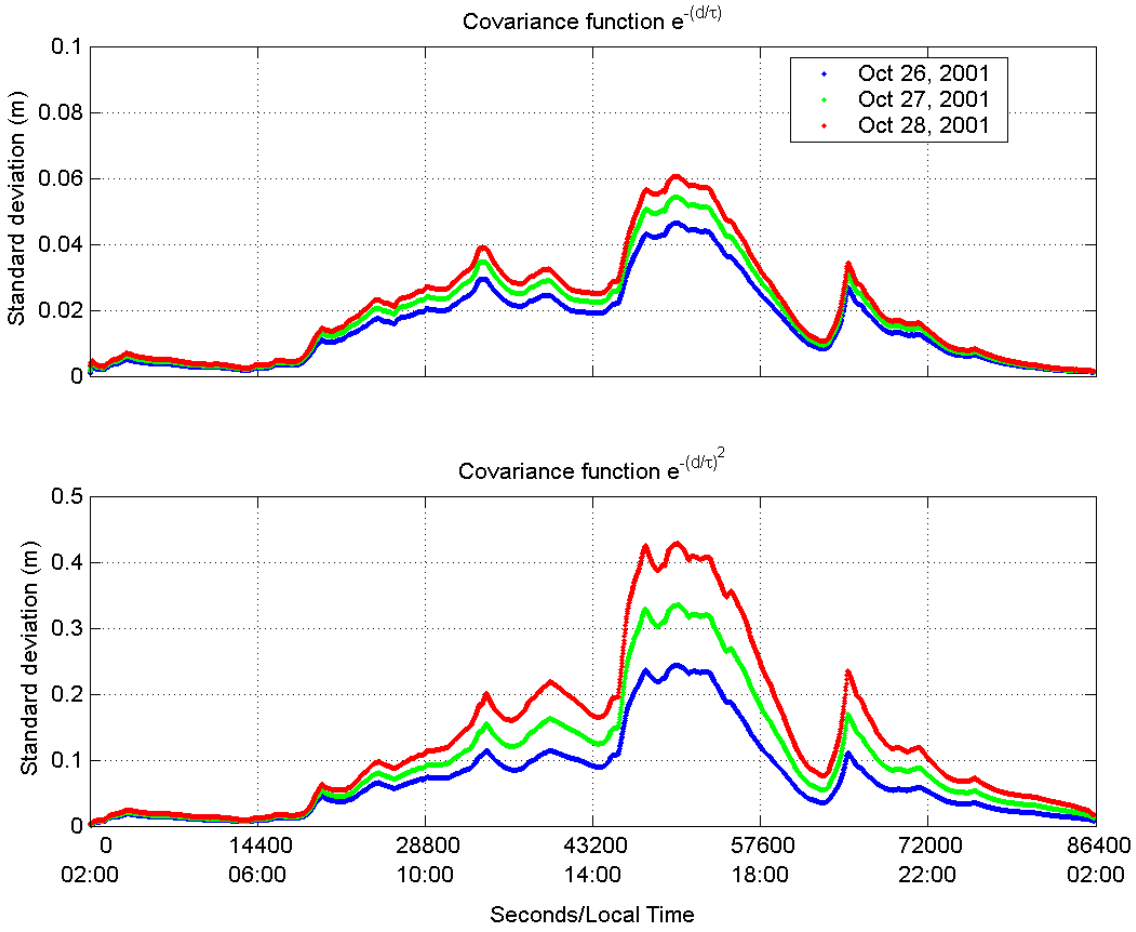

Figure 3.17: Estimated standard deviation of the ionosphere error (covariance function coefficient) for Oct 26 for a first order exponential decay (top) and second order exponential decay (bottom) covariance functions using different a-priori estimates

Figure 3.19 shows a comparison of the standard deviation of the residuals and the estimated standard deviation of the observations for the two covariance functions for Oct 26. As expected, each tests shows a linear relationship between the actual

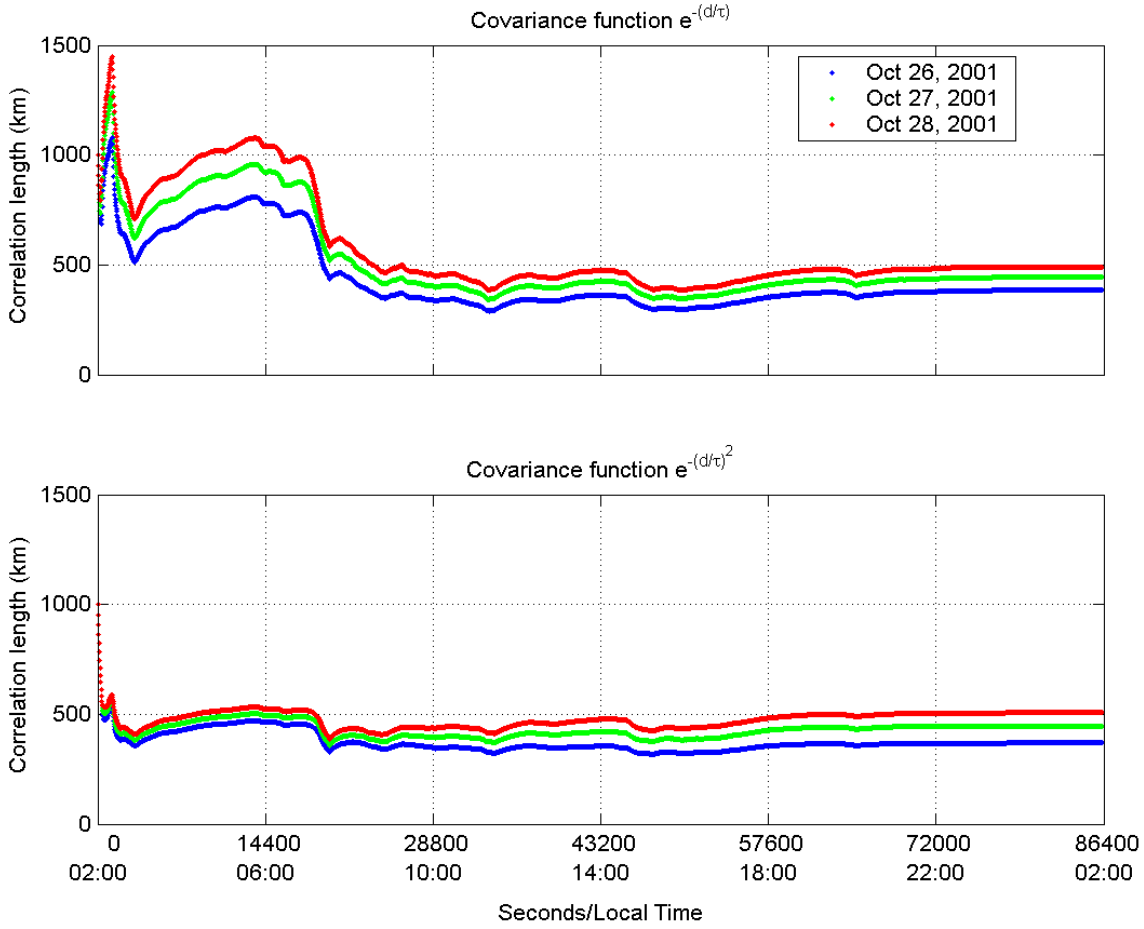

Figure 3.18: Estimated correlation length of the ionosphere error (covariance function coefficient) for Oct 26 for a first order exponential decay (top) and second order exponential decay (bottom) covariance functions using different a-priori estimates for the ionosphere standard deviation (covariance function coefficient)

and estimated standard deviations. In general, there is very little change in the double difference covariance functions when changing the a-priori value of the standard deviation of the ionosphere.

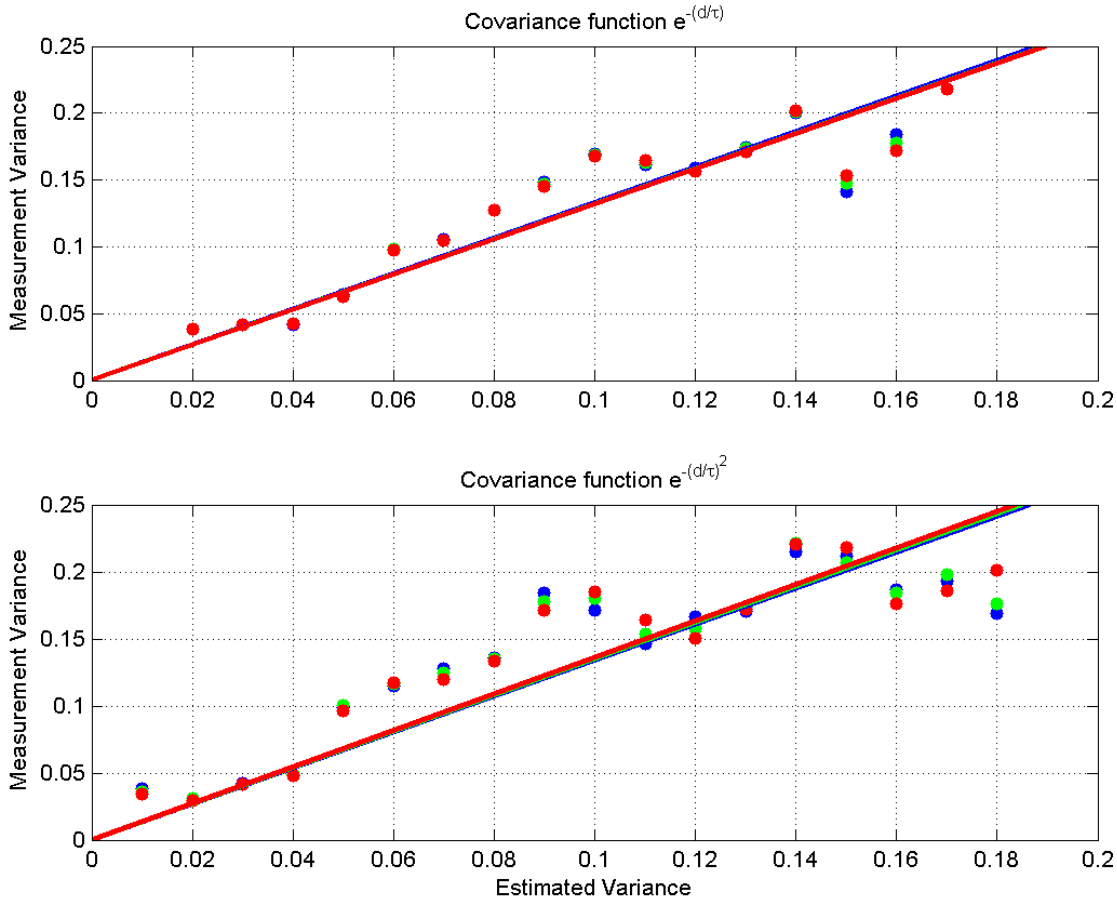

Figure 3.19: Comparison of the standard deviation of the residuals and the estimated standard deviation of the observations calculated from a first order and second order exponential decay covariance functions for Oct 26 for three a-priori ionosphere standard deviations

3.6 Prediction

Real-time estimation of the coefficients of the function allows for adaptive modelling of the changing error conditions. This change is most substantial with the ionosphere

error because it varies greatly throughout the day.

This adaptive modelling is especially useful for prediction in the collocation-based approach to multiple reference station positioning. The collocation-based approach uses the correlation between the reference stations' and the rover's observations to interpolate the errors (signals) measured at the reference stations to the rover's observation's signals. This adaptive covariance function model uses the covariance between the reference stations' observations to estimate the covariance between the reference stations' observations and the rover's observations. Given a well distributed network of reference station this approach could provide significant improvement over other methods, especially in the presence of changing environmental conditions or ionospheric storms. For example, if an atmospheric event occurs that causes large spatial variations of the errors then the reference stations will measure the event, and the covariance function will adapt and provide appropriate corrections.

The collocation equations used in previous work assume that the values of all estimated parameters are known. Taking into account the uncertainly of the estimated parameters is important in the calculation of the estimated variance-covariance of the corrections.

The relationship between the estimated parameters and the prediction collocation equations is especially important when predicting using estimated parameters. When using stochastic ionosphere modelling only a subset of the estimated parameters and observations are used to predict the corrections. The development of the collocation equations with estimated parameters is discussed in the following chapter.

Chapter 4

Correction Equations for Collocation-Based Multiple Reference Station Approaches

4.1 Introduction

The generalized least squares collocation equations for prediction of a signal s that is observed by a process y where $\mathrm{E}\{s\} = 0$ and $\mathrm{E}\{y\} = 0$ are derived in Section 2.2.2. The collocation prediction general formula is repeated from Equation 2.17.

$$\hat{s} = C_{sy} C_{yy}^{-1} y \tag{4.1}$$

where C_{yy} is the variance-covariance matrix of y and C_{sy} is the covariance matrix between the predicted signal and y (Moritz, 1980; Raquet, 1998).

In terms of carrier phase-based differential positioning using the multiple reference station approach proposed by Raquet (1998), the correlated error at an arbitrary position for an arbitrary satellite is the stochastic process observed through the double differenced carrier phase estimated residuals.

$$\hat{s} = C_{s\hat{r}} C_{\hat{r}\hat{r}}^{-1} \hat{r} \tag{4.2}$$

where $\hat{s}$ is a vector of the estimated signals, otherwise referred to as the corrections. In terms of differential carrier phase-based positioning, the $\hat{s}$ vector contains the corrections for observations that are to be used in the estimation of the rover's parameters, namely the observations for the rover and one reference station. $\hat{r}$ is a vector of the estimated residuals. In the case of network positioning the estimated residuals are

the double differenced carrier phase range plus double differenced estimated carrier phase ambiguities minus the double differenced carrier phase observations.

4.2 Correction Computation

The calculation of residuals can be generalized for the residuals for any linear implicit adjustment

$$\hat{r} = A\hat{x} - Bl \tag{4.3}$$

where A is a design matrix, $\hat{x}$ is a vector of estimated parameters, B is a linear transformation of the measurements, and l is a vector of measurements.

$\hat{x}$ is a vector of estimated parameters after the observations, l, have been applied. In other words, these are the best estimates of the parameters at the time. These parameters are updated with the current observations using sequential least squares (Krakiwsky, 1990), also referred to as the alternative form of the discrete Kalman filter (Brown and Hwang, 1997). From Equation 2.11 the estimation of the parameters is

$$\begin{aligned} \hat{x} &= x^\circ + \hat{\delta} \\ &= x^\circ - (A^T(BC_{ll}B^T)^{-1}A + C_{x^\circ x^\circ}^{-1})^{-1}A^T(BC_{ll}B^T)^{-1}(Ax^\circ - Bl) \qquad (4.4) \\ C_{\hat{x}} &= (A^T(BC_{ll}B^T)^{-1}A + C_{x^\circ x^\circ}^{-1})^{-1} \qquad (4.5) \end{aligned}$$

where x° is the a-priori estimate of the parameters and $C_{x^\circ x^\circ}$ is its associated variance-covariance matrix. The variance-covariance of the measurements is the sum of the signal covariance and noise variance components:

$$C_{ll} = \mathrm{E}\{(l - \mathrm{E}\{l\})(l - \mathrm{E}\{l\})^T\}. \tag{4.6}$$

It is necessary to separate the observations into a systematic component that is

the true measurement range ($l_\circ$) and signal (l_s) and noise (l_n) components as follows

$$l = l_\circ + l_s + l_n. \tag{4.7}$$

The expected value of the observations is the bias component because the expected values of the random components equals to zero. Using the observation components gives

$$\begin{aligned} C_{ll} &= \mathrm{E}\{(l_\circ + l_s + l_n - l_\circ)(l_\circ + l_s + l_n - l_\circ)^T\} \\ &= \mathrm{E}\{(l_s + l_n)(l_s + l_n)^T\} \\ &= C_{l_s} + C_{l_n}. \end{aligned} \tag{4.8}$$

It is assumed throughout that the signal and the noise are zero mean as follows

$$\mathrm{E}\{s\} = 0 \tag{4.9}$$

$$\mathrm{E}\{n\} = 0 \tag{4.10}$$

as well as that the expected value of an estimated or random variable is equal to the true value as shown in the following cases

$$\mathrm{E}\{\hat{x}\} = \mathrm{E}\{x\} = x \tag{4.11}$$

$$\mathrm{E}\{\hat{s}\} = \mathrm{E}\{s\} = 0 \tag{4.12}$$

$$\mathrm{E}\{l\} = l_\circ. \tag{4.13}$$

Equations 4.3 and 4.4 can be used to calculate the conditional estimation equations. The covariance matrix of the residuals ($C_{\hat{r}\hat{r}}$) can be calculated using error propagation

$$\begin{aligned} C_{\hat{r}\hat{r}} &= E\{(A\hat{x} - Bl - \mathrm{E}\{A\hat{x} - Bl\})(A\hat{x} - Bl - \mathrm{E}\{A\hat{x} - Bl\})^T\} \\ &= \mathrm{E}\{(A\hat{x} - Bl - (Ax - Bl_\circ))(A\hat{x} - Bl - (Ax - Bl_\circ))^T\} \end{aligned}$$

$$
\begin{aligned}
&= \mathrm{E}\{(A(\hat{x}-x)-B(l_s+l_n))(A(\hat{x}-x)-B(l_s+l_n))^T\} \\
&= A\mathrm{E}\{(\hat{x}-x)(\hat{x}-x)^T\}A^T + B\mathrm{E}\{(l_s+l_n)(l_s+l_n)^T\}B^T \\
&\quad -A\mathrm{E}\{(\hat{x}-x)(l_s+l_n)^T\}B^T - B\mathrm{E}\{(l_s+l_n)(\hat{x}-x)^T\}A^T \\
&= AC_{\hat{x}\hat{x}}A^T + BC_{ll}B^T - 2A\mathrm{E}\{(\hat{x}-x)(l_s+l_n)^T\}B^T. \qquad (4.14)
\end{aligned}
$$

$\mathrm{E}\{(\hat{x}-x)(l_s+l_n)^T\}$ can be calculated using Equation 4.4 as follows

$$
\begin{aligned}
\mathrm{E}\{(\hat{x}-x)(l_s+l_n)^T\} &= \mathrm{E}\{(x^\circ+\hat{\hat{\delta}}-x)(l_s+l_n)^T\} \\
&= \mathrm{E}\{x^\circ(l_s+l_n)^T\} + \mathrm{E}\{\hat{\hat{\delta}}(l_s+l_n)^T\} \\
&\quad -x\mathrm{E}\{(l_s+l_n)^T\}. \qquad (4.15)
\end{aligned}
$$

The last term in this equation is zero because the expected value of the observation signal and noise is zero.

It is assumed that the parameter estimates from the previous epoch, x°, are not correlated to the observations at this epoch, l:

$$E\{x^\circ(l_s+l_n)^T\} = 0. \qquad (4.16)$$

The level of correlation is a function of the measurement rate and although may not be zero, is small for typical GPS data rates of one second or more. This is one of the assumptions required for sequential least squares estimation.

For ease of reading the following substitution is used

$$M = BC_{ll}B^T. \qquad (4.17)$$

$$
\begin{aligned}
\mathrm{E}\{(\hat{x}-x)(l_s+l_n)^T\} &= 0 + \mathrm{E}\{\hat{\delta}(l_s+l_n)^T\} \\
&= \mathrm{E}\{-C_{\hat{x}\hat{x}}A^TM^{-1}(Ax^\circ-Bl)(l_s+l_n)^T\} \\
&= C_{\hat{x}\hat{x}}A^TM^{-1}BC_{ll}. \qquad (4.18)
\end{aligned}
$$

Substituting Equation 4.18 into Equation 4.14 gives

$$\begin{aligned} C_{\hat{r}\hat{r}} &= AC_{\hat{x}\hat{x}}A^T + BC_{ll}B^T - 2AC_{\hat{x}\hat{x}}A^T(BC_{ll}B^T)^{-1}BC_{ll}B^T \\ &= AC_{\hat{x}\hat{x}}A^T + BC_{ll}B^T - 2AC_{\hat{x}\hat{x}}A^T \\ &= BC_{ll}B^T - AC_{\hat{x}\hat{x}}A^T. \end{aligned} \tag{4.19}$$

A similar derivation can be made to determine $C_{s\hat{r}}$:

$$\begin{aligned} C_{s\hat{r}} &= \mathrm{E}\{(s - \mathrm{E}\{s\})(r - \mathrm{E}\{r\})^T\} \\ &= \mathrm{E}\{(s-0)(A\hat{x} - Bl - (Ax - Bl_\circ))^T\} \\ &= \mathrm{E}\{s(A(\hat{x} - x) - B(l_s + l_n))^T\} \\ &= \mathrm{E}\{s(\hat{x} - x)^T\}A^T - \mathrm{E}\{s(l_s + l_n)^T\}B^T \\ &= \mathrm{E}\{sx^{\circ T}\}A^T + \mathrm{E}\{s\hat{\delta}^T\}A^T - \mathrm{E}\{sx^T\} - C_{sl_s}B^T. \end{aligned} \tag{4.20}$$

It is assumed that the estimated signal, $\hat{s}$, is not correlated to the estimate of the parameters at the previous epoch, x°. This is similar to the assumption in Equation 4.16 except that in this case the correlation refers to only the signal instead of the observation:

$$\mathrm{E}\{sx^{\circ T}\} = 0 \tag{4.21}$$

In addition the expected value of s is zero therefore

$$\mathrm{E}\{sx^T\} = \mathrm{E}\{s\}x^T = 0. \tag{4.22}$$

$$\begin{aligned} C_{s\hat{r}} &= \mathrm{E}\{-s(Ax^\circ - Bl)^T\}M^{-1}AC_{\hat{x}\hat{x}}A^T - C_{sl_s}B^T \\ &= C_{sl_s}B^TM^{-1}AC_{\hat{x}\hat{x}}A^T - C_{sl_s}B^T \\ &= C_{sl_s}B^TM^{-1}(AC_{\hat{x}\hat{x}}A^T - M) \\ &= -C_{sl_s}B^TM^{-1}C_{\hat{r}\hat{r}}. \end{aligned} \tag{4.23}$$

The combined generalized conditional estimation equation from Equation 4.2 is

$$\begin{aligned}\hat{s} &= -C_{sl_s}B^TM^{-1}C_{\hat{r}\hat{r}}C_{\hat{r}\hat{r}}^{-1}(A\hat{x}-Bl)\\ &= -C_{sl_s}B^TM^{-1}(A\hat{x}-Bl). \qquad (4.24)\end{aligned}$$

Equation 4.24 can be used to derive the error covariance of the estimated signal,

$$\begin{aligned}C_{\varepsilon_{\hat{s}}\varepsilon_{\hat{s}}} &= \mathrm{E}\{(\hat{s}-s)(\hat{s}-s)^T\}\\ &= \mathrm{E}\{\hat{s}\hat{s}^T\}+\mathrm{E}\{ss^T\}-\mathrm{E}\{\hat{s}s^T\}-\mathrm{E}\{s\hat{s}^T\}. \qquad (4.25)\end{aligned}$$

This is separated into components,

$$\begin{aligned}\mathrm{E}\{\hat{s}\hat{s}^T\} &= C_{sl_s}B^TM^{-1}\mathrm{E}\{(A\hat{x}-Bl)(A\hat{x}-Bl)^T\}M^{-1}BC_{l_ss}\\ &= C_{sl_s}B^TM^{-1}C_{\hat{r}\hat{r}}M^{-1}BC_{l_ss}\\ &= C_{sl_s}B^TM^{-1}(M-AC_{\hat{x}\hat{x}}A^T)M^{-1}BC_{l_ss}, \qquad (4.26)\end{aligned}$$

$$\mathrm{E}\{ss^T\}=C_{ss} \qquad (4.27)$$

where covariance matrix of the signal is calculated by the covariance function.

$$\begin{aligned}\mathrm{E}\{\hat{s}s^T\} &= -\mathrm{E}\{C_{sl_s}B^TM^{-1}(A\hat{x}-Bl)s^T\} \qquad (4.28)\\ &= -C_{sl_s}B^TM^{-1}(A\mathrm{E}\{\hat{x}s^T\}-B\mathrm{E}\{ls^T\}). \qquad (4.29)\end{aligned}$$

Similar to previous cases

$$\begin{aligned}\mathrm{E}\{ls^T\} &= \mathrm{E}\{(l_\circ+l_s+l_n)s^T\}\\ &= l_\circ\mathrm{E}\{s^T\}+\mathrm{E}\{l_ss^T\}+\mathrm{E}\{l_ns^T\}\\ &= C_{l_ss}. \qquad (4.30)\end{aligned}$$

The covariance between the estimated parameters and the signal at the computation point can be determined by expanding the least squares solution for the estimated parameters:

$$\mathrm{E}\{\hat{x}s^T\} = \mathrm{E}\{(x^\circ - C_{\hat{x}\hat{x}}A^T M^{-1}(Ax^\circ - Bl))s^T\}. \tag{4.31}$$

After applying the assumption in Equation 4.21 whereby the estimated parameters from the previous epoch not correlated with the signal

$$\mathrm{E}\{\hat{x}s^T\} = C_{\hat{x}\hat{x}}A^T M^{-1}BC_{l_s s}. \tag{4.32}$$

Substituting Equation 4.32 into Equation 4.28 gives

$$\begin{aligned}
\mathrm{E}\{\hat{s}s^T\} &= -C_{sl_s}B^T M^{-1}(AC_{\hat{x}\hat{x}}A^T M^{-1}BC_{l_s s} - BC_{l_s s}) \\
&= -C_{sl_s}B^T M^{-1}(AC_{\hat{x}\hat{x}}A^T - M)M^{-1}BC_{l_s s}.
\end{aligned} \tag{4.33}$$

Comparing Equations 4.33 and 4.26 shows that these are equivalent:

$$\mathrm{E}\{\hat{s}s^T\} = \mathrm{E}\{\hat{s}\hat{s}^T\}. \tag{4.34}$$

This is used to simplify Equation 4.25 into

$$\begin{aligned}
C_{\varepsilon_{\hat{s}}\varepsilon_{\hat{s}}} &= \mathrm{E}\{\hat{s}\hat{s}^T\} + \mathrm{E}\{ss^T\} - \mathrm{E}\{\hat{s}s^T\} - \mathrm{E}\{s\hat{s}^T\} \\
&= \mathrm{E}\{\hat{s}\hat{s}^T\} + \mathrm{E}\{ss^T\} - \mathrm{E}\{\hat{s}\hat{s}^T\} - \mathrm{E}\{\hat{s}\hat{s}^T\} \\
&= \mathrm{E}\{ss^T\} - \mathrm{E}\{\hat{s}\hat{s}^T\} \\
&= C_{ss} - C_{sl_s}B^T M^{-1}(M - AC_{\hat{x}\hat{x}}A^T)M^{-1}BC_{l_s s} \\
&= C_{ss} - C_{sl_s}B^T M^{-1}BC_{l_s s} + C_{sl_s}B^T M^{-1}AC_{\hat{x}\hat{x}}A^T M^{-1}BC_{l_s s}.
\end{aligned} \tag{4.35}$$

This shows that the variance of the estimated signal (estimated corrections) decreases as the estimated parameters converge. In the case of ambiguities, the variance of the estimated signal is lowest when the ambiguities are fixed to their correct values.

Equation 4.24 matches that derived by Raquet (1998) and are the same as the equations to calculate the residuals from an implicit adjustment (Krakiwsky and Abousalem, 1995; Krakiwsky, 1990).

4.3 Applying Corrections

The corrections determined in the previous section are applied to the observations of one reference station and the mobile remote user. The corrections from Equation 4.24 are subtracted from the observations. In practice the corrections are applied to the rover station and one reference station however in theory corrections could be calculated for any location or any station. The adjusted (corrected) observations are

$$\hat{l} = l - \hat{s}$$

where $\hat{l}$ is a vector of the adjusted observations. The variance-covariance matrix for the corrected observations can be determined via error propagation:

$$C_{\hat{l}\hat{l}} = \mathrm{E}\{(\hat{l} - \mathrm{E}\{\hat{l}\})(\hat{l} - \mathrm{E}\{\hat{l}\})^T\}. \tag{4.36}$$

The components of this expectation can be reduced to

$$\begin{aligned} \hat{l} - \mathrm{E}\{\hat{l}\} &= l - \hat{s} - \mathrm{E}\{(l - \hat{s})\} \\ &= l - \hat{s} - l_\circ \\ &= l_s + l_n - \hat{s}. \end{aligned} \tag{4.37}$$

Assuming the signal in the observations and the true signal are equal and replacing it into Equation 4.36 gives

$$C_{\hat{l}\hat{l}} = \mathrm{E}\{(l_n - (\hat{s} - s))(l_n - (\hat{s} - s))^T\}$$

$$= C_{l_n l_n} + C_{\varepsilon_{\hat{s}}\varepsilon_{\hat{s}}} \tag{4.38}$$

$$= C_{l_n l_n} + C_{ss} + C_{sl_s} B^T M^{-1} (A C_{\hat{x}\hat{x}} A^T - M) M^{-1} B C_{l_s s}$$

$$= C_{ll} - E\{\hat{s}\hat{s}^T\}. \tag{4.39}$$

The variance of the corrected observations has an interesting form in Equation 4.38. The corrected observations are a function of the noise variance and the accuracy of the estimated signal. If the signal is known then it is completely removed from the observations and all that remains is measurement noise.

There is an interesting relationship between the convergence of the estimated parameters and the accuracy of the estimated corrections and the resulting accuracy of the adjusted observations. When a least squares solution (Bayes or Kalman filter based) has no redundancy the observations and the parameters have the same precision or $BC_{ll}B^T - AC_{\hat{x}\hat{x}}A^T = 0$. When additional observations are included then $(BC_{ll}B^T - AC_{\hat{x}\hat{x}}A^T)_{i,i} > 0$ for any i. This is a result of the added information given by the estimated parameters and the system model defined in the design matrix and the a-priori information. As Equation 4.35 shows, when $BC_{ll}B^T - AC_{\hat{x}\hat{x}}A^T = 0$ the variance of the corrections is equal to the variance of the signal. Moreover, Equation 4.39 shows that under the same conditions the variance of the adjusted measurements equals the variance of the uncorrected measurements. In other words, the corrections have no effect. Equation 4.35 also shows that as long as redundant observations are used then the error variance of the corrections will be less than the variance of the signal.

As the network parameters become better known, the error variance of the corrections decreases and the variance of the rover's observations decreases. This decrease in the rover's observation variance will directly impact the variance of the rover's

estimated parameters, as follows

$$\begin{aligned}
(C_{\overline{xx}})_{i,i} &\leq (C_{\hat{x}\hat{x}})_{i,i} \\
((A^T C_{\hat{l}\hat{l}}^{-1} A + C_{x^\circ x^\circ})^{-1})_{i,i} &\leq ((A^T C_{ll}^{-1} A + C_{x^\circ x^\circ})^{-1})_{i,i} \\
((A^T (C_{ll} - \mathrm{E}\{\hat{s}\hat{s}^T\})^{-1} A + C_{x^\circ x^\circ})^{-1})_{i,i} &\leq ((A^T C_{ll}^{-1} A + C_{x^\circ x^\circ})^{-1})_{i,i} \qquad (4.40)
\end{aligned}$$

where subscript i, i represent each variance element of the variance-covariance matrix and $\overline{x}$ is the vector of estimated parameters when the adjusted observations are used. This clearly shows the improvement due to the multiple reference station corrections and, ultimately, the multiple reference station approach.

4.4 Estimating the reference station corrections

The correction-based multiple reference station approach is usually regarded as a three step process: resolution of the network ambiguities, correction calculation, and rover station estimation. The covariance function, which is used to calculate the variance-covariance matrix of the signal (C_{ss} and C_{sl}), must remain consistent throughout these three steps in order to achieve the simplifications and reductions shown. It is common to separate these processes but they must share information and, consequently, must be consistent in terms of stochastic and mathematical models. In other words, the covariance function, the design matrix (A), and the linear measurement transformation matrix (B) for the ambiguity estimation and corrections generation processes must be the same.

The correlations between the reference stations' corrections and the rover corrections should not be overlooked. Raquet (1998) separates the generation of rover and network station corrections because the correction equation allows for independent determination of each correction set. However, this separation is not valid when the

variance-covariance matrix of the corrections is considered because of correlations between the rover and reference station corrections. This correlation is especially important in the determination of the double difference observation variance between the stations. Due to this correlation induced inseparability, the corrections for both the reference stations and the rover are contained in the correction vector ($\hat{s}$). If the correction (signal) vector $\hat{s}$ is divided into a rover correction and network station corrections then Equation 4.38 must be adjusted because the noise of the reference station is correlated with the estimated corrections. It is more appropriate to estimate the signal at the control point (reference stations in this case) as well as filter the noise of these observations. In this case the predicted value is not only the observation signal but also the observation noise. It is then necessary to separate the predicted control point observations from the complete set of control points. Predicted control points will be denoted with a *.

From Equation 4.2 the estimated signal and noise for a control point is

$$\hat{l}_s^* + \hat{l}_n^* = C_{(l_s^*+l_n^*)\hat{r}} C_{\hat{r}\hat{r}} r. \tag{4.41}$$

As shown, the variance of the residuals remains unchanged, however the covariance between the estimated quantities and the residuals is changed. Similar to Equation 4.30

$$\begin{aligned} \mathrm{E}\{l(l_s^* + l_n^*)^T\} &= C_{l_s l_s^*} + C_{l_n l_n{}^*} \\ &= C_{ll^*}. \end{aligned} \tag{4.42}$$

Replacing s for $l_s^* + l_n^*$ in Equation 4.23 gives

$$C_{(l_s^*+l_n^*)r} = \mathrm{E}\{-(l_s^* + l_n^*)(Ax^\circ - Bl)^T\} M^{-1} A C_{\hat{x}\hat{x}} A^T - C_{l^* l} B^T$$

$$
\begin{aligned}
&= C_{l^*l}B^TM^{-1}(AC_{\hat{x}\hat{x}}A^T - M) \\
&= -C_{l^*l}B^TM^{-1}C_{\hat{r}\hat{r}}. \qquad (4.43)
\end{aligned}
$$

The estimated value of the signal and the noise is

$$
\begin{aligned}
\hat{l}_s^* + \hat{l}_n^* &= -C_{l^*l}B^TM^{-1}C_{\hat{r}\hat{r}}C_{\hat{r}\hat{r}}^{-1}(A\hat{x} - Bl) \\
&= -C_{l^*l}B^TM^{-1}(A\hat{x} - Bl) \\
&= -(C_{l_s^*l_s} + C_{l_n^*l_n})B^TM^{-1}(A\hat{x} - Bl). \qquad (4.44)
\end{aligned}
$$

The final solution for the estimated signal has a very similar form to the estimated signal in Equation 4.24. If this equation is applied for observations that are not used in the prediction then the matrix $C_{l_n^*l_n}$ would equal zero and this equation would match the equation for the estimated signal of the rover only (Equation 4.24). Estimated signal and noise is analogous to predicting the complete error at the computation point or the control point.

The resulting error variance is

$$
C_{\varepsilon_{\hat{s}}\varepsilon_{\hat{s}}} = C_{ss} - C_{l^*l}B^TM^{-1}(M - AC_{\hat{x}\hat{x}}A^T)M^{-1}BC_{ll^*}. \qquad (4.45)
$$

The adjusted observations are still the differences between the raw observations and the estimated observation error (signal plus noise). However the noise component in calculating the estimated variance of the adjusted observations (Equation 4.38) is not correct because observation noise component is correlated with the noise component of the estimated error.

$$
\begin{aligned}
C_{\hat{l}^*\hat{l}^*} &= \mathrm{E}\{(l_n^* - (\hat{s} - s))(l_n^* - (\hat{s} - s))^T\} \\
&= C_{l_n^*l_n^*} + C_{\varepsilon_{\hat{s}}\varepsilon_{\hat{s}}} - \mathrm{E}\{l_n^*\hat{s}^T\} - \mathrm{E}\{\hat{s}l_n^{*T}\}. \qquad (4.46)
\end{aligned}
$$

where

$$\begin{aligned} \mathrm{E}\{\hat{s}l_n^{*T}\} &= -C_{l^*l}B^TM^{-1}\mathrm{E}\{(A\hat{x}-Bl)l_n^{*T}\} \\ &= -C_{l^*l}B^TM^{-1}C_{\hat{r}\hat{r}}M^{-1}BC_{l_nl_n^*}, \end{aligned} \tag{4.47}$$

$$\begin{aligned} C_{\hat{l}^*\hat{l}^*} &= C_{l_n^*l_n^*} + C_{\varepsilon_{\hat{s}}\varepsilon_{\hat{s}}} + C_{l^*l}B^TM^{-1}C_{\hat{r}\hat{r}}M^{-1}BC_{l_nl_n^*} \\ &\quad + C_{l_n^*l_n}B^TM^{-1}C_{\hat{r}\hat{r}}M^{-1}BC_{ll^*} \\ &= C_{l_n^*l_n^*} + C_{l_s^*l_s^*} - (C_{l_s^*l_s} + C_{l_n^*l_n})B^TM^{-1}C_{\hat{r}\hat{r}}M^{-1}B(C_{l_s^*l_s} + C_{l_n^*l_n}) \\ &\quad + C_{l^*l}B^TM^{-1}C_{\hat{r}\hat{r}}M^{-1}BC_{l_nl_n^*} + C_{l_n^*l_n}B^TM^{-1}C_{\hat{r}\hat{r}}M^{-1}BC_{ll^*} \\ &= C_{l_n^*l_n^*} + C_{l_s^*l_s^*} - C_{l_s^*l_s}B^TM^{-1}C_{\hat{r}\hat{r}}M^{-1}BC_{l_sl_s^*}. \end{aligned} \tag{4.48}$$

This equation is the same as the equation for the prediction of the signal in Equation 4.39. Only the covariance of the signal influences the level of increased accuracy due to the prediction.

4.5 Fixed Ambiguities

The previous derivation uses the adjustment residuals from the float ambiguity solution to determine the corrections for the rover. For the most precise corrections, the fixed carrier phase ambiguities should be used. For this case a fixed solution is denoted by a check ($\check{\cdot}$). The reference network parameters are now determined using the fixed ambiguities

$$\check{x} = \hat{x} - C_{\hat{x}\hat{a}}C_{\hat{a}\hat{a}}^{-1}(\hat{a}-\check{a}) \tag{4.49}$$

$$C_{\check{x}\check{x}} = C_{\hat{x}\hat{x}} - C_{\hat{x}\hat{a}}C_{\hat{a}\hat{a}}^{-1}C_{\hat{a}\hat{x}} + C_{\hat{x}\hat{a}}C_{\hat{a}\hat{a}}^{-1}C_{\check{a}\check{a}}C_{\hat{a}\hat{a}}^{-1}C_{\hat{a}\hat{x}} \tag{4.50}$$

where a is a vector of ambiguities, which have fixed ambiguity values. The a vector only contains ambiguities for which fixed ambiguities could be determined to a certain

level of statistical confidence. In a practical sense, the covariance matrix of the fixed ambiguities, $C_{\check{a}\check{a}}$, can not be determined. The covariance of the fixed ambiguities would be a function of the confidence of the validation of the ambiguity set. The fixed ambiguities are discrete processes because they are limited to integer values. The probability distribution of the fixed ambiguities is also discrete (Joosten and Tiberius, 2000), therefore Equation 4.50 cannot be evaluated in the continuous sense as shown. The discrete covariance of the fixed ambiguities is a function of the likelihood that a fixed ambiguity value is indeed the correct value. To overcome these difficulties, the fixed ambiguities are assumed to be correct (deterministic) for the remainder of this derivation. As a result, all further results shown are slightly optimistic. The resulting variance-covariance matrix of the parameters is

$$C_{\check{x}\check{x}} = C_{\hat{x}\hat{x}} - C_{\hat{x}\hat{a}} C_{\hat{a}\hat{a}}^{-1} C_{\hat{a}\hat{x}}. \tag{4.51}$$

In the case where the integer ambiguities are fixed, and assumed to be known, the residuals are calculated as

$$\check{r} \;=\; A_{\check{x}}\check{x} - Bl + A_{\check{a}}\check{a}. \tag{4.52}$$

The design matrix for the fixed and float parameters are separated from the unscripted design matrix, which was used to determine the float parameters.

The corrections to the signal using the fixed ambiguities can be determined using the variance-covariance matrix of the fixed-ambiguity residuals and the covariance matrix between the rover's observations and the network residuals as in the previous derivation. The variance-covariance matrix of the residuals is calculated as

$$\begin{aligned} C_{\check{r}\check{r}} \;=\; & \mathrm{E}\{(A_{\check{x}}\check{x} - Bl + A_{\check{a}}\check{a} - \mathrm{E}\{A_{\check{x}}\check{x} - Bl + A_{\check{a}}\check{a}\}) \\ & (A_{\check{x}}\check{x} - Bl + A_{\check{a}}\check{a} - \mathrm{E}\{A_{\check{x}}\check{x} - Bl + A_{\check{a}}\check{a}\})^T\}, \end{aligned} \tag{4.53}$$

$$\begin{aligned} A_{\check{x}}\check{x} - Bl + A_{\check{a}}\check{a} - \mathrm{E}\{A_{\check{x}}\check{x} - Bl + A_{\check{a}}\check{a}\} &= A_{\check{x}}\check{x} - Bl + A_{\check{a}}\check{a} \\ &\quad -(A_{\check{x}}x - Bl_\circ + A_{\check{a}}a) \\ &= A_{\check{x}}(\check{x} - x) - B(l_s + l_n) \\ &\quad +A_{\check{a}}(\check{a} - a). \end{aligned} \tag{4.54}$$

The expected value terms that contain a vector of the fixed ambiguities are zero because

$$\mathrm{E}\{\check{a} - a\} = \mathrm{E}\{\check{a}\} - a = a - a = 0 \tag{4.55}$$

$$\mathrm{E}\{\check{a}\check{a}\} = 0, \tag{4.56}$$

$$\begin{aligned} C_{\check{r}\check{r}} &= A_{\check{x}}\mathrm{E}\{(\check{x} - x)(\check{x} - x)^T\}A_{\check{x}}^T + B\mathrm{E}\{(l_n + l_s)(l_n + l_s)^T\}B^T \\ &\quad -A_{\check{x}}\mathrm{E}\{(\check{x} - x)(l_s + l_n)^T\}B^T - B\mathrm{E}\{(l_s + l_n)(\check{x} - x)^T\}A_{\check{x}}^T \\ &= A_{\check{x}}C_{\check{x}\check{x}}A_{\check{x}}^T + BC_{ll}B^T \\ &\quad -A_{\check{x}}\mathrm{E}\{(\check{x} - x)(l_s + l_n)^T\}B^T - B\mathrm{E}\{(l_s + l_n)(\check{x} - x)^T\}A_{\check{x}}^T, \end{aligned} \tag{4.57}$$

$$\begin{aligned} \mathrm{E}\{(\check{x} - x)(l_s + l_n)^T\} &= \mathrm{E}\{(\hat{x} - x)(l_s + l_n)^T\} \\ &\quad -C_{\hat{x}\hat{a}}C_{\hat{a}\hat{a}}^{-1}\mathrm{E}\{(\hat{a} - \check{a})(l_s + l_n)^T\}. \end{aligned} \tag{4.58}$$

$\mathrm{E}\{(\hat{x} - x)(l_s + l_n)^T\}$ and $\mathrm{E}\{\hat{a}(l_s + l_n)^T\}$ can be determined by expanding the definitions of $\hat{x}$ and $\hat{a}$. As with the previous section, the state vector from the previous epoch is uncorrelated with the observations from this epoch.

In this method of applying fixed ambiguity information through a conditional reduction, x and a are initially estimated in the same adjustment, but in later steps the fixed ambiguities are removed. For this reason, the definitions of $\hat{x}$ and $\hat{a}$ are shown using matrix partitioning:

$$\begin{aligned} \mathrm{E}\{(\hat{x}-x)(l_s+l_n)^T\} &= -\begin{bmatrix} C_{\hat{x}\hat{x}} & C_{\hat{x}\hat{a}} \end{bmatrix} A^T M^{-1} \mathrm{E}\{(Ax^\circ - Bl)(l_s+l_n)^T\} \\ &= \begin{bmatrix} C_{\hat{x}\hat{x}} & C_{\hat{x}\hat{a}} \end{bmatrix} A^T M^{-1} B C_{ll}, \end{aligned} \tag{4.59}$$

$$\begin{aligned} \mathrm{E}\{\hat{a}(l_s+l_n)^T\} &= -\begin{bmatrix} C_{\hat{a}\hat{x}} & C_{\hat{a}\hat{a}} \end{bmatrix} A^T M^{-1} \mathrm{E}\{(Ax^\circ - Bl)(l_s+l_n)^T\} \\ &= \begin{bmatrix} C_{\hat{a}\hat{x}} & C_{\hat{a}\hat{a}} \end{bmatrix} A^T M^{-1} B C_{ll}. \end{aligned} \tag{4.60}$$

The expected values in Equations 4.59 and 4.60 are replaced into Equation 4.58 to give

$$\begin{aligned} \mathrm{E}\{(\check{x}-x)(l_s+l_n)^T\} &= \left(\begin{bmatrix} C_{\hat{x}\hat{x}} & C_{\hat{x}\hat{a}} \end{bmatrix} - C_{\hat{x}\hat{a}} C_{\hat{a}\hat{a}}^{-1} \begin{bmatrix} C_{\hat{a}\hat{x}} & C_{\hat{a}\hat{a}} \end{bmatrix} \right) A^T M^{-1} B C_{ll} \\ &= \left(\begin{bmatrix} C_{\hat{x}\hat{x}} & C_{\hat{x}\hat{a}} \end{bmatrix} - \begin{bmatrix} C_{\hat{x}\hat{a}} C_{\hat{a}\hat{a}}^{-1} C_{\hat{a}\hat{x}} & C_{\hat{x}\hat{a}} \end{bmatrix} \right) A^T M^{-1} B C_{ll} \\ &= \begin{bmatrix} C_{\hat{x}\hat{x}} - C_{\hat{x}\hat{a}} C_{\hat{a}\hat{a}}^{-1} C_{\hat{a}\hat{x}} & C_{\hat{x}\hat{a}} - C_{\hat{x}\hat{a}} \end{bmatrix} A^T M^{-1} B C_{ll} \\ &= \begin{bmatrix} C_{\check{x}\check{x}} & 0 \end{bmatrix} A^T M^{-1} B C_{ll} \end{aligned} \tag{4.61}$$

The zero sub-matrix in this equation removes the effect of the once floating ambiguities when multiplied by A^T. As a result

$$A_{\check{x}}^T = \begin{bmatrix} I & 0 \end{bmatrix} A^T \tag{4.62}$$

This relationship is used to reduce Equation 4.61 to

$$\mathrm{E}\{(\check{x}-x)(l_s+l_n)^T\} = C_{\check{x}\check{x}} A_{\check{x}}^T M^{-1} B C_{ll}. \tag{4.63}$$

Equation 4.63 is inserted into Equation 4.57 to give

$$\begin{aligned} C_{\check{r}\check{r}} &= A_{\check{x}} C_{\check{x}\check{x}} A_{\check{x}}^T + B C_{ll} B^T - 2 A_{\check{x}} C_{\check{x}\check{x}} A_{\check{x}}^T M^{-1} B C_{ll} B^T \\ &= A_{\check{x}} C_{\check{x}\check{x}} A_{\check{x}}^T + B C_{ll} B^T - 2 A_{\check{x}} C_{\check{x}\check{x}} A_{\check{x}}^T \\ &= B C_{ll} B^T - A_{\check{x}} C_{\check{x}\check{x}} A_{\check{x}}^T. \end{aligned} \tag{4.64}$$

The variance-covariance matrix of the residuals with fixed ambiguities, Equation 4.64, has the same form as the variance-covariance matrix of the residuals with float ambiguities, Equation 4.19.

The covariance between the signal and the residuals, $C_{s\check{r}}$, can be determined in a similar manner

$$\begin{aligned} C_{s\check{r}} &= \mathrm{E}\{s\check{r}^T\} \\ &= \mathrm{E}\{(s - \mathrm{E}\{s\})(A_{\check{x}}\check{x} - Bl + A_{\check{a}}\check{a} - \mathrm{E}\{A_{\check{x}}\check{x} - Bl + A_{\check{a}}\check{a}\})^T\}, \end{aligned} \tag{4.65}$$

$$\begin{aligned} A_{\check{x}}\check{x} - Bl + A_{\check{a}}\check{a} - \mathrm{E}\{A_{\check{x}}\check{x} - Bl + A_{\check{a}}\check{a}\} &= A_{\check{x}}\check{x} - Bl + A_{\check{a}}\check{a} \\ &\quad -(A_{\check{x}}x - Bl_\circ + A_{\check{a}}a \\ &= A_{\check{x}}(\check{x} - x) - B(l_s + l_n) \\ &\quad + A_{\check{a}}(\check{a} - a), \end{aligned} \tag{4.66}$$

$$\begin{aligned} C_{s\check{r}} &= \mathrm{E}\{s(\check{x} - x)^T\} A_{\check{x}}^T - \mathrm{E}\{s(l_s + l_n)^T\} B^T \\ &= C_{sl_s} B^T M^{-1} A_{\check{x}} C_{\check{x}\check{x}} A_{\check{x}}^T - C_{sl_s} B^T \\ &= C_{sl_s} B^T M^{-1} (A_{\check{x}} C_{\check{x}\check{x}} A_{\check{x}}^T - M) \\ &= -C_{sl_s} B^T M^{-1} C_{\check{r}\check{r}}. \end{aligned} \tag{4.67}$$

Equations 4.64 and 4.67 can be used to determine the corrections and the error covariance matrix of the corrections:

$$\begin{aligned} \check{s} &= C_{s\check{r}} C_{\check{r}} \check{r} \\ &= C_{sl_s} B^T M^{-1} C_{\check{r}\check{r}} C_{\check{r}\check{r}}^{-1} (A_{\check{x}} \check{x} - Bl + A_{\check{a}} \check{a}) \\ &= -C_{sl_s} B^T M^{-1} (A_{\check{x}} \check{x} - Bl + A_{\check{a}} \check{a}), \end{aligned} \tag{4.68}$$

$$C_{\varepsilon_{\check{s}} \varepsilon_{\check{s}}} = C_{ss} - C_{sl_s} B^T M^{-1} (BC_{ll} B^T - A_{\check{x}} C_{\check{x}\check{x}} A_{\check{x}}^T) M^{-1} BC_{l_s s}. \tag{4.69}$$

The corrections determined using float or fixed ambiguities only differ by the ambiguities used in the calculation of the residuals. This difference is shown in the error covariance matrix of the signal where each is dependant on the variance-covariance of the remaining floating parameters. If all the parameters are fixed to known quantities then the error covariance matrix of the signal (Equation 4.69) reduces to

$$C_{\varepsilon_{\check{s}} \varepsilon_{\check{s}}} = C_{ss} - C_{sl_s} B^T (BC_{ll} B^T)^{-1} BC_{l_s s}. \tag{4.70}$$

Equation 4.70 is the error covariance matrix for a conditional model adjustment where there are no estimated parameters (Krakiwsky and Abousalem, 1995).

4.5.1 Applying Corrections

The application of the corrections is identical to the float ambiguity case except with fixed ambiguity corrections and variance-covariance matrix of the corrections. The corrected observations and variance-covariance matrix of the corrected observations are

$$\check{l} = l - \check{s}, \tag{4.71}$$

$$C_{\check{l}\check{l}} = C_{l_n l_n} + C_{\varepsilon_{\check{s}}\varepsilon_{\check{s}}}. \quad (4.72)$$

The most precise adjusted measurements will have the minimum observation variance. In terms of the precision of the corrections, the error covariance matrix of the corrections should be as small as possible. Comparing Equations 4.69 and 4.70 shows that the variance of the corrections is smaller when all the parameters are known (fixed). As one would expect, a solution with fixed parameters will provide the best corrections and the lowest, correction applied, measurement variance for the rover.

4.6 Practical Considerations

The derivation from the previous section makes two assumptions: (1) that the estimated parameters are not predicted and (2) that all the observations that were used to determine the network parameters are used to predict the residual errors and the computation point corrections. However, in practice the network adjustment may estimate parameters to absorb correlated errors in an attempt to better resolve the network ambiguities. These correlated errors should be predicted along with the remaining correlated errors to reduce their effects on the rover. For example, the slant ionosphere error may be estimated to reduce the effect of the ionosphere on ambiguity resolution. The residuals of the parameter estimation would not contain ionosphere error. However the rover's corrections should contain ionosphere error and need to be reintroduced into the predicted residuals.

The second assumption may also be false. The weighted ionosphere model outlined by Odijk (2000) requires the addition of ionosphere pseudo-observations to assist with the convergence of the filter. In general, these observations should not be used to predict correlated errors. Especially with fixed (integer) ambiguities, it is unnecessary

to include pseudo-range code observations because of their high noise and multipath characteristics.

The derivation from the previous section is repeated with these assumptions removed. The complete list of estimated parameters are in the state vector, $\hat{x}$, and the complete list of observations are in the vector l. Two different design matrices, A and A_g, are used to distinguish between estimated parameters used in the estimation and the prediction. This assumes that a subset of the estimated parameters is used in the prediction. This is an obvious assumption because unknown parameters that are not estimated would not contribute to the prediction. Two observation matrices, B and B_g, are used to distinguish between the observations used in the estimation and prediction. Subscript g represents the design matrix and observation matrix used specifically for generating corrections (prediction).

The variance-covariance matrix of the residuals is now defined as

$$\begin{aligned} C_{\hat{r}\hat{r}} &= \mathrm{E}\{(A_g\hat{x} - B_g l - \mathrm{E}\{A_g\hat{x} - B_g l\})(A_g\hat{x} - B_g l - \mathrm{E}\{A_g\hat{x} - B_g l\})^T\} \\ &= A_g C_{\hat{x}\hat{x}} A_g^T + B_g C_{ll} B_g^T - A_g \mathrm{E}\{(\hat{x})(l_s + l_n)^T\} B_g^T \\ &\quad - B_g \mathrm{E}\{(l_s + l_n)(\hat{x})^T\} A_g^T. \end{aligned} \tag{4.73}$$

$\mathrm{E}\{\hat{x}(l_s + l_n)^T\}$ is the same as shown in Equation 4.18 giving

$$\begin{aligned} C_{\hat{r}\hat{r}} &= A_g C_{\hat{x}\hat{x}} A_g^T + B_g C_{ll} B_g^T - A_g C_{\hat{x}\hat{x}} A^T (B C_{ll} B^T)^{-1} B C_{ll} B_g^T \\ &\quad - B_g C_{ll} B^T (B C_{ll} B^T)^{-1} A C_{\hat{x}\hat{x}} A_g^T. \end{aligned} \tag{4.74}$$

It is already apparent that this derivation is much less elegant than the previous. The covariance matrix relating the signal and the residuals, C_{sr}, is similar to that of the previous section:

$$C_{s\hat{r}} = \mathrm{E}\{(l_s + l_n)x^{\circ T}\} A_g^T + \mathrm{E}\{(l_s + l_n)\hat{\delta}^T\} A_g^T - C_{ll} B_g^T$$

$$= \quad C_{sl_s}B^T(BC_{ll}B^T)^{-1}AC_{\hat{x}\hat{x}}A_g^T - C_{sl_s}B_g^T. \tag{4.75}$$

The conditional estimation equation without the assumptions is

$$\begin{aligned} s \quad = \quad & (C_{sl_s}B^T(BC_{ll}B^T)^{-1}AC_{\hat{x}\hat{x}}A_g^T - C_{sl_s}B_g^T) \\ & (A_gC_{\hat{x}\hat{x}}A_g^T + B_gC_{ll}B_g^T - A_gC_{\hat{x}\hat{x}}A^T(BC_{ll}B^T)^{-1}BC_{ll}B_g^T \\ & -B_gC_{ll}B^T(BC_{ll}B^T)^{-1}AC_{\hat{x}\hat{x}}A_g^T)^{-1}(A_g\hat{x} - B_gl). \end{aligned} \tag{4.76}$$

This equation cannot be reduced as in the previous derivation without the assumptions taking affect. The conditional estimation equation is much more cumbersome in this case.

The complications in this derivation are due to two factors: the parameters estimated are not used in the prediction and the observations used to estimate the parameters are not used in the prediction. The first of these factors can be removed by decorrelating the estimated parameters that are not to be predicted similar to the decorrelation of the ambiguities shown in Equation 4.49. Decorrelating the parameters removes their effect on the remaining parameters as though the removed parameters had not been estimated but constrained to their final values.

Using this technique, the parameters that are not used in the prediction are decorrelated from the remaining, predicted parameters. In the case of ambiguities, the decorrelation is meant to constrain their estimated float values to their integer values. The estimated ionosphere parameters, for example, should be decorrelated from the other estimated parameters using their correct values, which are unknown. The best estimate of the ionosphere is its current estimated value. As a result, the decorrelation performed by Equation 4.49 will not adjust the remaining parameters because the difference between the estimated value and the constrained value is zero. The decorrelation will, however, remove the effect of estimating these parameters from the

variance covariance matrix of the remaining parameters (Equation 4.51). Assuming that all of the observations that were used to estimate the parameters are being used in prediction, the unwanted parameters can be decorrelated to simplify the prediction equations to Equations 4.24 and 4.38.

4.7 Properties of the collocation-based approach

This section describes important properties of the collocation-based corrections. These properties are important because they affect or validate the use and application of the corrections.

4.7.1 Differencing the undifferenced corrections

A vector of undifferenced corrections is calculated through the collocation-based multiple reference station approach. The undifferenced corrections are biased by an arbitrary value determined by the inner constraints of the solution. Consequently, the undifferenced corrections are only valid in differential form and any double difference combination produces valid double difference corrections. This is shown in the following proof.

Any double difference combination of the corrections would be the same if the single observation corrections were generated with a different double difference combination. The simple correction equations for the network reference stations are

$$s = -C_{ll}B^T(BC_{ll}B^T)^{-1}(A\hat{x} - Bl). \tag{4.77}$$

Network corrections are used because if they are transformed into the double difference combinations used in the misclosures $(A\hat{x} - Bl)$ then the double difference corrections are equal to the double difference misclosures, as shown in the following

equation:

$$\begin{aligned} Bs &= -BC_{ll}B^T(BC_{ll}B^T)^{-1}(A\hat{x} - Bl) \\ &= -(A\hat{x} - Bl). \end{aligned} \tag{4.78}$$

When the corrections are transformed into double differenced corrections the vector of corrections is multiplied by a linear transformation matrix, B', giving

$$B's = -B'C_{ll}B^T(BC_{ll}B^T)^{-1}(A\hat{x} - Bl). \tag{4.79}$$

The transformation matrix B' can be represented in the form $A'B$ where A' is a linear transformation matrix. $A'B$ is substituted for B' in Equation 4.79 to yield

$$\begin{aligned} B's &= -A'BC_{ll}B^T(BC_{ll}B^T)^{-1}(A\hat{x} - Bl) \\ &= -A'(A\hat{x} - Bl) \\ &= -(A'A\hat{x} - A'Bl) \\ &= -(A'A\hat{x} - B'l). \end{aligned} \tag{4.80}$$

It is obvious from these equations that the solution is the same as though the original observations were calculated using the linear transformation B'. It is also obvious from these equations that since the observations are transformed into the double difference space defined by B', the transformation of $A'A$ must also transform it into the same double difference observations.

4.7.2 Correction and ambiguity convergence

The objective of the variance-covariance estimate of the corrections is to provide a correction measurement weight to correction users. The error variance of the corrections decreases as the ambiguities of the network converge and are resolved. A

decrease in the error variance of the corrections results in a decrease in the variance of the rover's corrected observations.

Figure 4.1 shows the prediction values for a zero baseline test. Zero baseline means that the rover is located at a reference station in the network. The focus of this figure is the standard deviation of the corrected rover measurements. The convergence of the network ambiguities is shown in the slowly decreasing estimated rover measurement standard deviation prior to 3:00 local time. At approximately 3:00 local time the network ambiguities are resolved, which removes the uncertainty in the ambiguities from the corrections. The estimated standard deviation of the rover's measurements are then reduced to the magnitude of the carrier phase measurement noise because this is a zero baseline and the rover is located at a network reference station.

This is an interesting property of the collocation-based approach that has not be previously explored. This allows for a mixed group of float and fixed ambiguity measurements to be weighted when applied by the rover.

4.7.3 Choice of reference station

The choice of reference station in the network to use in the rover baseline calculation is arbitrary. Any reference station in the network provides the same solution given a few assumptions, which will be discussed shortly.

Consider for example that a rover is at a network reference station. This is a zero baseline with respect to the network. The corrections of the co-located reference station are within the measurement noise level to the corrections of the rover, therefore if the co-located reference station is used as the corrected single reference station then this is indeed a standard zero baseline. However, if a different reference station in the network is used then the difference in the corrections between this reference station

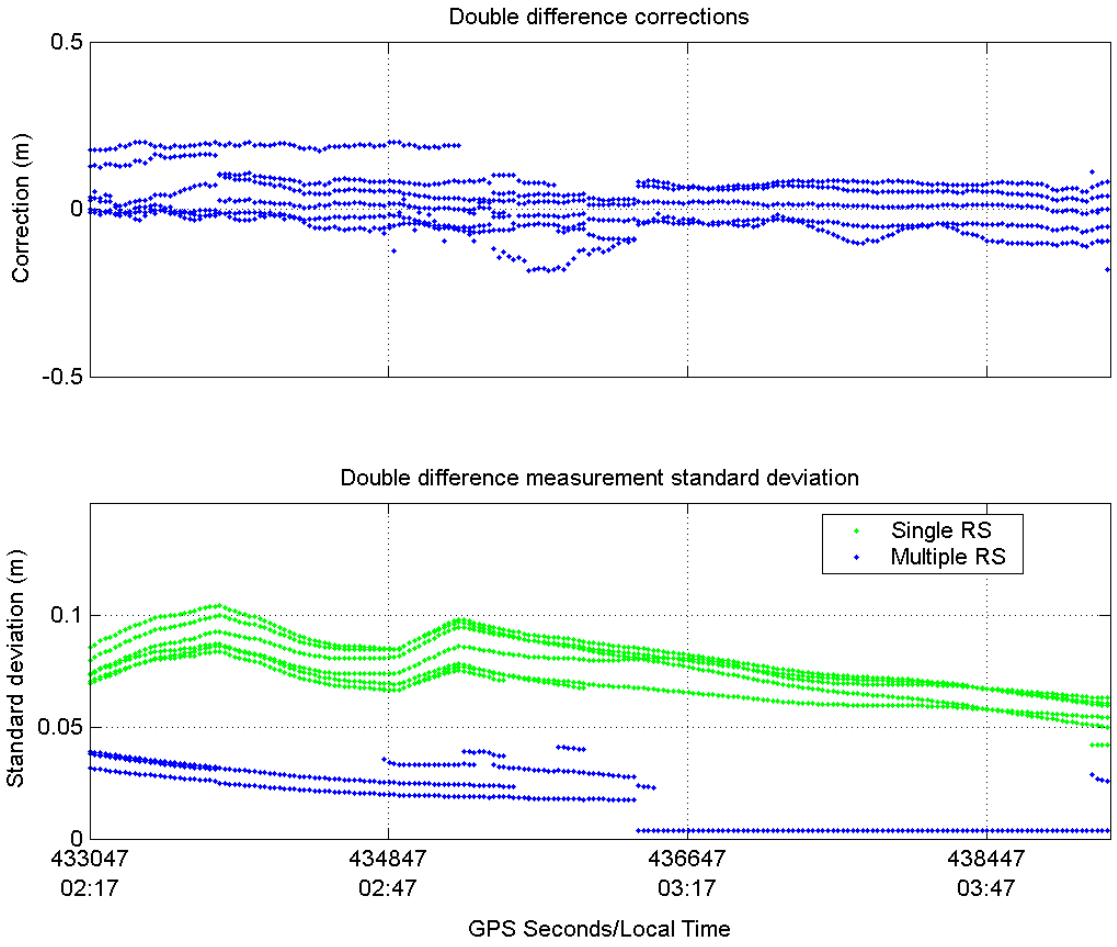

Figure 4.1: Sample double difference and the estimated standard deviations of the rover's corrected and uncorrected measurements for a zero baseline.

and the rover is equivalent to the residuals between the reference station and the co-located reference station. Assuming that the station coordinates are correct and that the ambiguities are fixed correctly, this residual difference is the difference between the measurement errors at the reference stations. When this correction is applied to the non co-located reference station, the errors in the station become the errors at the co-located station, hence the errors at the rover.

Once again, this assumes that the reference station coordinates are correct and that the ambiguities between the stations are correctly resolved. This may not be the case for every baseline in the network and it may not be practical to transmit the data from all of the reference stations to the user - depending on the setup this may be required. It is the best practice to use the closest reference station to the rover as the corrected single reference station when estimating the rover's position. If this is not possible then a station in the centre of the network is preferable to a station near the edge of the network to reduce the accumulation of ambiguity errors across multiple baselines.

Chapter 5

Results for the Collocation-Based Multiple Reference Station Approach

Data from the MAGNET network are used to show the effectiveness and properties of the collocation-based multiple reference station approach described in the previous chapter. A 15 degree elevation cutoff angle was used for all cases.

5.1 Test methodology and figures of merit

The multiple reference station approach is performed in a series of steps that must each be monitored to properly describe the effectiveness of the method. The first step is the resolution of the network integer carrier phase ambiguities. The ability of the network to resolve ambiguities affects the accuracy of the corrections. The magnitude of the corrections and their estimated variances constitute a measure of the difference between the single reference station approach and the network approach. This chapter demonstrates improvement due to this technique. This section describes how each of these quality measures are obtained and why they are important.

All of the processing in the following section simulates real-time performance by processing using an epoch-by-epoch approach.

5.1.1 Network ambiguity resolution

The ability of the network to resolve ambiguities is a function of the network geometry, satellite geometry, accuracy of the network reference station positions and magnitude

of the measurement errors. The network ambiguity resolution performance shown in the following results shows the percentage of fixed ambiguities for the network when calculating network corrections. The percentage of fixed ambiguities considers every epoch of every ambiguity as opposed to each pass of the satellites. This measure is used because it includes convergence time of the filter in real-time.

The accuracy of the ambiguities affects the accuracy of the corrections and the estimated error variances of the corrections. If the network is unable to resolve the network ambiguities then less improvement is to be expected from the calculated corrections using float ambiguities. This is represented in the variance of the corrections but will degrade the quality of the rover's solution.

5.1.2 Rover corrections

In the network approach the single observation corrections are generated so that they can be applied to the raw observations of a network reference station. However, the corrections are only valid in differenced form. Consequently, the double difference corrections are shown using the nearest network reference station and the rover receiver. The variances of the double difference corrections are also calculated, however the rover's measurement variances before and after applying corrections are shown. This is a more intuitive presentation of the variance of the corrections. These two figures are shown together to correlate periods with high measurement errors and the given variances of the measurements.

5.1.3 Observation domain

The effect of the corrections on the rover measurement errors is shown. To remove the effect of the changing rover position, the rover and nearest network reference

station positions are fixed. The best known fixed or float ambiguities are used to calculate the double difference measurement residuals. The residuals are shown for the L1 code measurements, L1 phase measurements, L2 phase measurements, as well as the following linear phase combinations: wide-lane, ionosphere-free, and geometry free. No code corrections are applied because the code observations are dominated by uncorrelated measurement errors and these can delay or prevent convergence of the positioning filter.

The L1 and L2 phase residuals show the reduction of measurement errors on the raw rover measurements. The wide-lane linear combination is commonly used in GPS carrier phase positioning. The ionosphere-free and geometry-free linear combinations are included to separate the effect of the corrections into troposphere plus orbit errors, and ionosphere error, respectively. The ionosphere and troposphere plus orbit errors have significantly different magnitudes, as shown in the following figures. Separating the errors into the two components shows the ability of the method to predict the differing error types.

5.1.4 Position domain

The position accuracy is, in most cases, the ultimate performance measure of concern to GPS users. This is the most important quality shown and is a function of all the previous quality measures. The positions are estimated using the method described in the following chapter with the exception that only a single baseline is used. This positioning filter estimated the L1 and L2 ambiguities, and the dual frequency slant ionosphere bias for each satellite pair. This is an ionosphere-free approach. It is one of the best positioning methods as evaluated by Liu (2003) in the assessment of various carrier phase positioning techniques.

The best available float or fixed ambiguities are used at each epoch in a Bayes filter approach. A first order Gauss Markov process is used to model the temporal behaviour of the rover velocity. Although the position is static, it is estimated assuming a kinematic mode. This simulates the accuracy of the real-time rover position using either the single reference station or multiple reference station approaches.

5.2 MAGNET Network with TU as a rover

The configuration of the MAGNET network shown in Figure 5.1 is used to demonstrate the effectiveness of the collocation-based multiple reference station approach. The rover is completely surrounded by reference stations and is 25 km from the nearest reference station. 25 km is an unreliable inter-antenna distance for single reference station fixed ambiguity carrier phase positioning. The network baseline lengths of this medium scale network range from 50 to 75 km.

5.2.1 Percentage of fixed network ambiguities

The percentages of fixed ambiguities are shown in Table 5.1, whereby 55 to 92 percent of the network ambiguities are resolved. This is a high level of fixed ambiguities for a network of this scale, with baselines ranging from 50 to 74 km. The increased error on October 28 has a noticeable affect on the ambiguity resolution performance.

5.2.2 Network corrections and variances of rover observations

Figures 5.2 to 5.4 shows the double difference L1 phase corrections and standard deviations of the rover's, and corrected rover's, double difference measurements for October 26 to October 28. The magnitudes of the corrections are as expected for a 25 km baseline. The measurement errors are smallest at night. The measurement

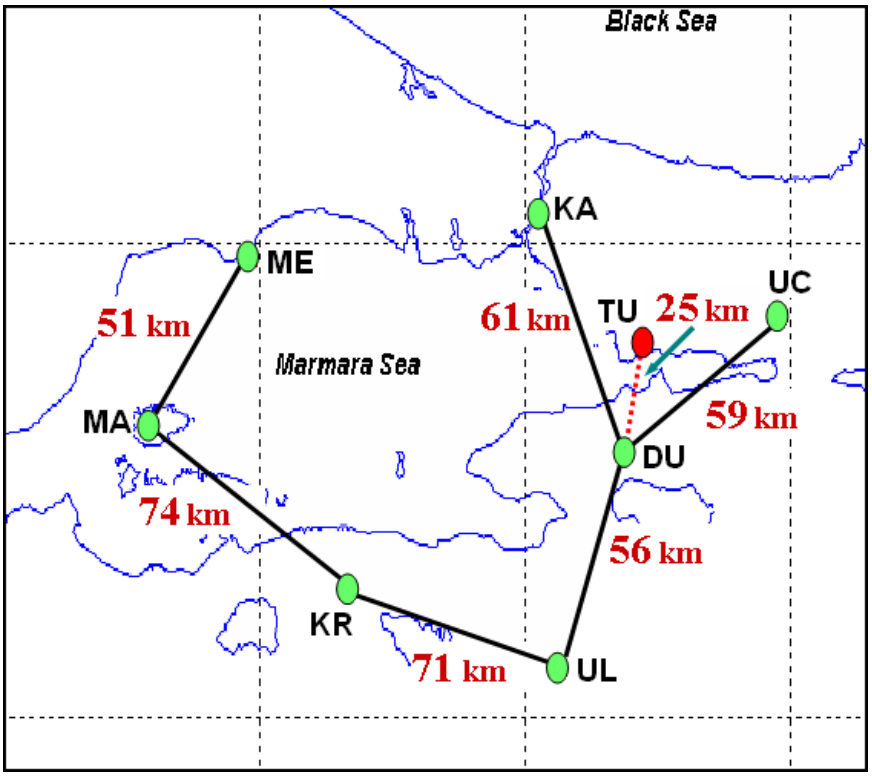

Figure 5.1: MAGNET network configuration with TU as the rover

Table 5.1: Percentage of fixed ambiguities.

Station 1	Station 2	Distance	Oct 26	Oct 27	Oct 28
MA	ME	50.6 km	82.1 %	87.3 %	86.8 %
DU	UL	55.9 km	81.8 %	92.4 %	72.4 %
DU	UC	58.8 km	82.2 %	87.5 %	87.1 %
DU	KA	60.9 km	83.6 %	72.3 %	62.8 %
KR	UL	70.6 km	72.9 %	85.8 %	54.5 %
KR	MA	74.0 km	81.0 %	77.6 %	73.1 %

corrections vary up to 3 ppm with the exception of a few satellite corrections of up to 15 ppm. Discontinuities in the double difference corrections are due to changes in the base satellite. For these examples, the base satellite with the lowest PRN number was selected. The corrections are larger on October 28 when the measurement errors are larger.

The estimated standard deviation of the rover measurements decrease when the corrections are applied. This is the estimated improvement due to the network corrections. The method suggests that the corrections will provide approximately a 20 percent reduction in the measurement errors over the single reference station case. The reduction of the measurement standard deviation is due to the correlation of the atmospheric errors and the network geometry.

5.2.3 Observation domain

Table 5.2 shows the RMS of the measurement residuals for the rover, and corrected rover's, measurements. The improvement due to the corrections is 6 to 26 percent for the raw L1 and L2 phase measurements. This improvement is due to a reduction of the ionosphere errors, evident by the 5 to 22 percent improvement in the geometry-free residuals and a negative improvement in the ionosphere-free residuals. The degradation of the troposphere and orbit components is because these components are very small in magnitude; The negative improvement is less than 0.1 cm in all cases. Figures 5.5 to 5.7 show the residuals for the single reference station and multiple reference station approaches for the three days. There is a noticeable reduction in the error magnitude and a few large magnitude residuals are removed. Although there is the an overall reduction of the measurement residuals, there are still large remaining residuals in the corrected data. These are errors that either the

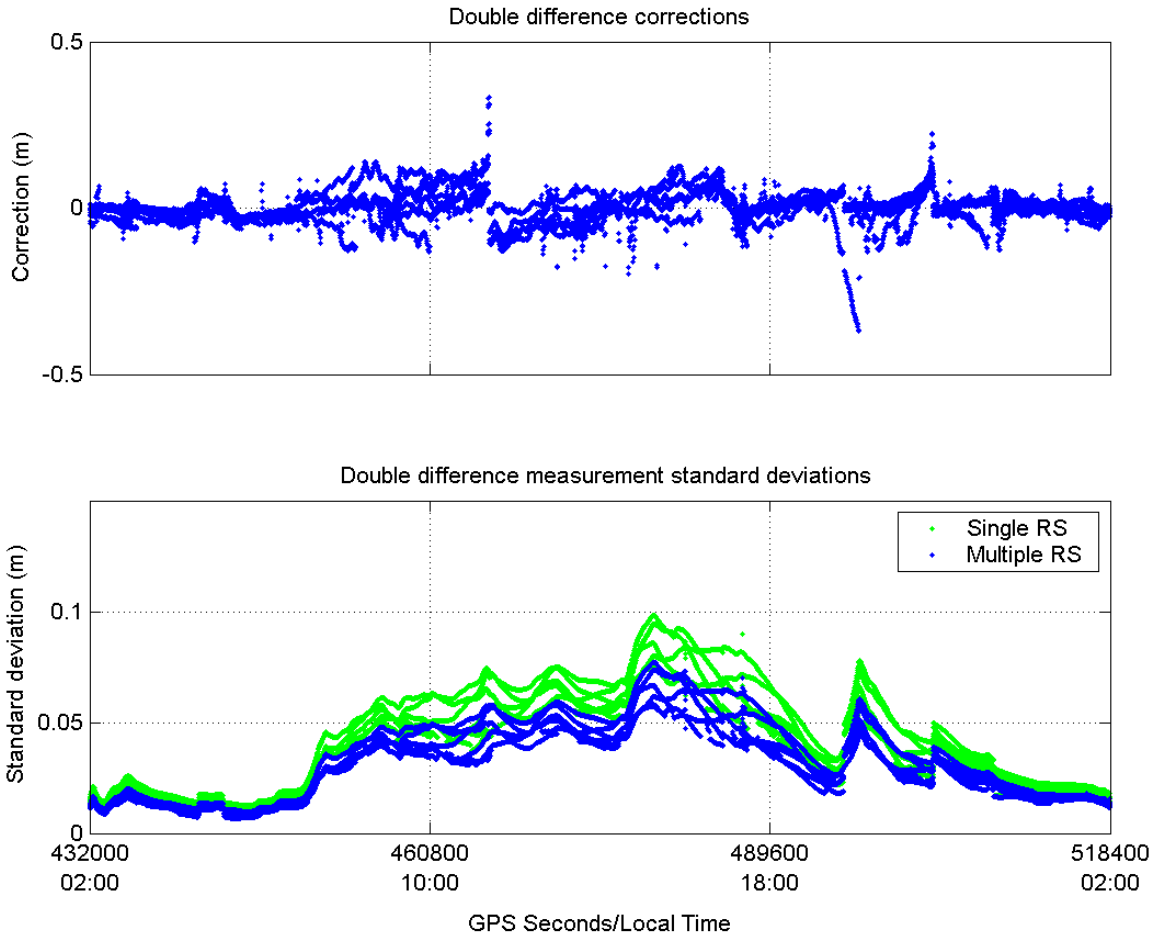

Figure 5.2: Double difference L1 phase corrections and double difference rover measurement standard deviations for the single reference station and corrected reference station observations for Oct 26

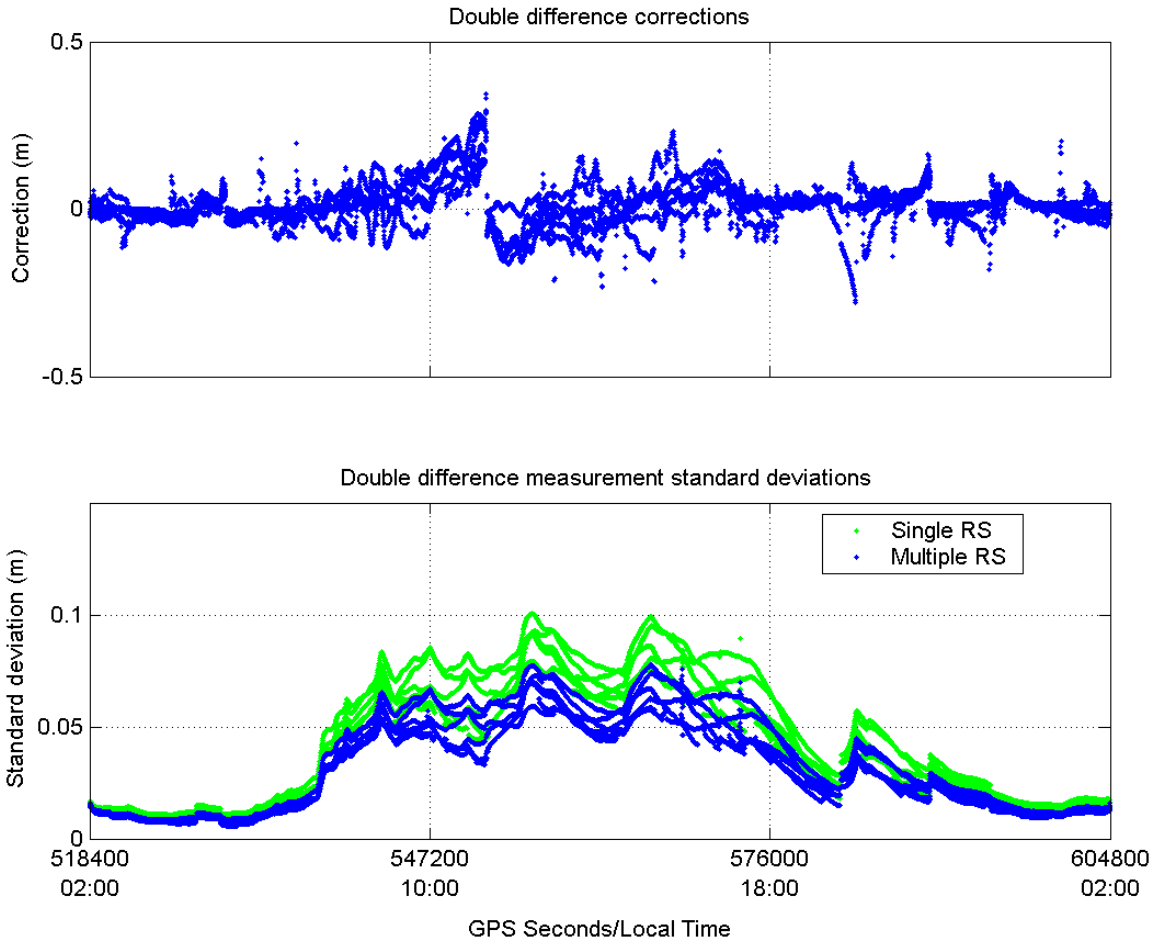

Figure 5.3: Double difference L1 phase corrections and double difference rover measurement standard deviations for the single reference station and corrected reference station observations for Oct 27

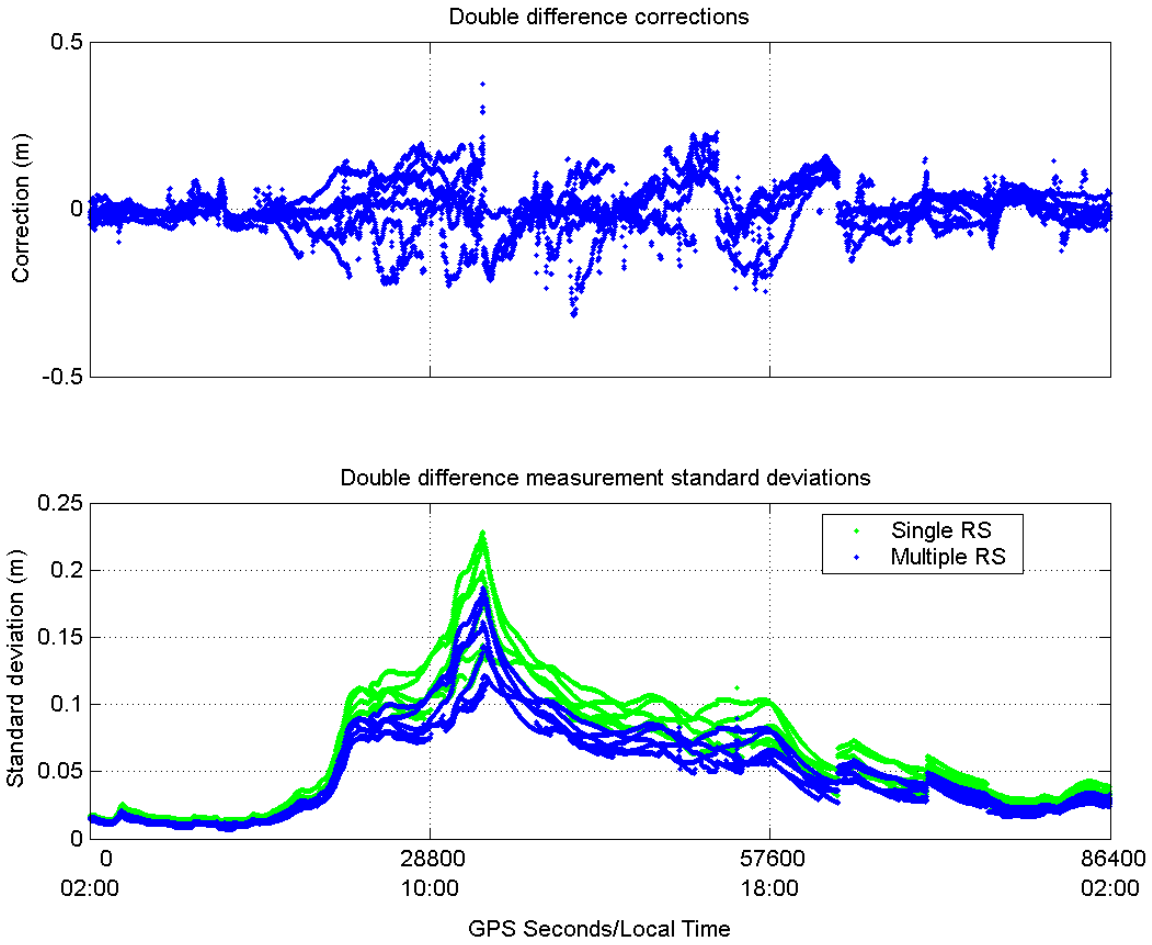

Figure 5.4: Double difference L1 phase corrections and double difference rover measurement standard deviations for the single reference station and corrected reference station observations for Oct 28

network was not able to measure or was not able to predict.

Table 5.2: RMS residuals for the single and corrected rover station baseline measurements

		L1	L2	WL	IF	GF
Oct 26	Single RS	3.7 cm	6.0 cm	4.7 cm	0.3 cm	2.4 cm
	Multiple RS	2.7 cm	4.5 cm	4.0 cm	0.4 cm	1.8 cm
	Improvement	27 %	25 %	15 %	-33 %	25 %
Oct 27	Single RS	4.1 cm	6.6 cm	5.1 cm	0.4 cm	2.6 cm
	Multiple RS	3.5 cm	5.6 cm	4.7 cm	0.4 cm	2.2 cm
	Improvement	15 %	15 %	8 %	¿ -1 %	15 %
Oct 28	Single RS	8.4 cm	13.8 cm	10.8 cm	0.4 cm	5.4 cm
	Multiple RS	7.9 cm	13.0 cm	10.4 cm	0.4 cm	5.1 cm
	Improvement	6 %	6 %	4 %	¿ -1 %	6 %

5.2.4 Position domain

Table 5.3 shows the RMS position errors for the north, east, up and 3D components and the percentage of fixed ambiguities. There is an 11 to 33 percent improvement in the 3D position accuracy when the network corrections are applied, relative to the single baseline approach using the nearest network reference station. In general, there is an improvement in all cases when the corrections are applied however the reduction of 3D position RMS errors ranges from 0.7 cm to 2.5 cm. There is also an improvement in the percentage of fixed ambiguities, however the improvement is at most 21 percent and is usually less than 5 percent.

The level of improve decreases as the measurement errors increase. This is because as the measurement errors increase the spatial correlation decreases. The measurement errors can not be interpolated as effectively when the spatial correlation decreases. The network approach would provide the greatest improvement when the measurement errors are high and the spatial correlation is also high. Further tests

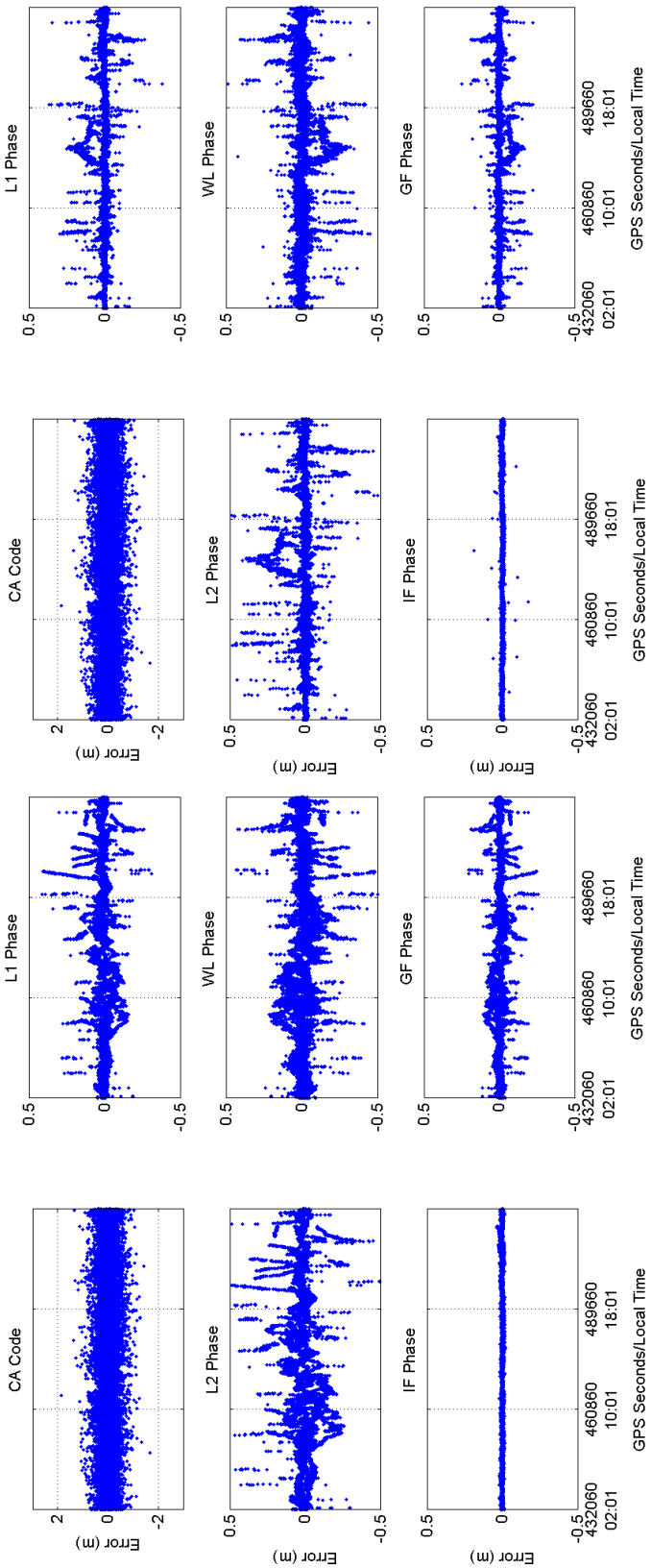

Figure 5.5: Residuals of the single (left) and multiple (right) reference station measurements for Oct 26

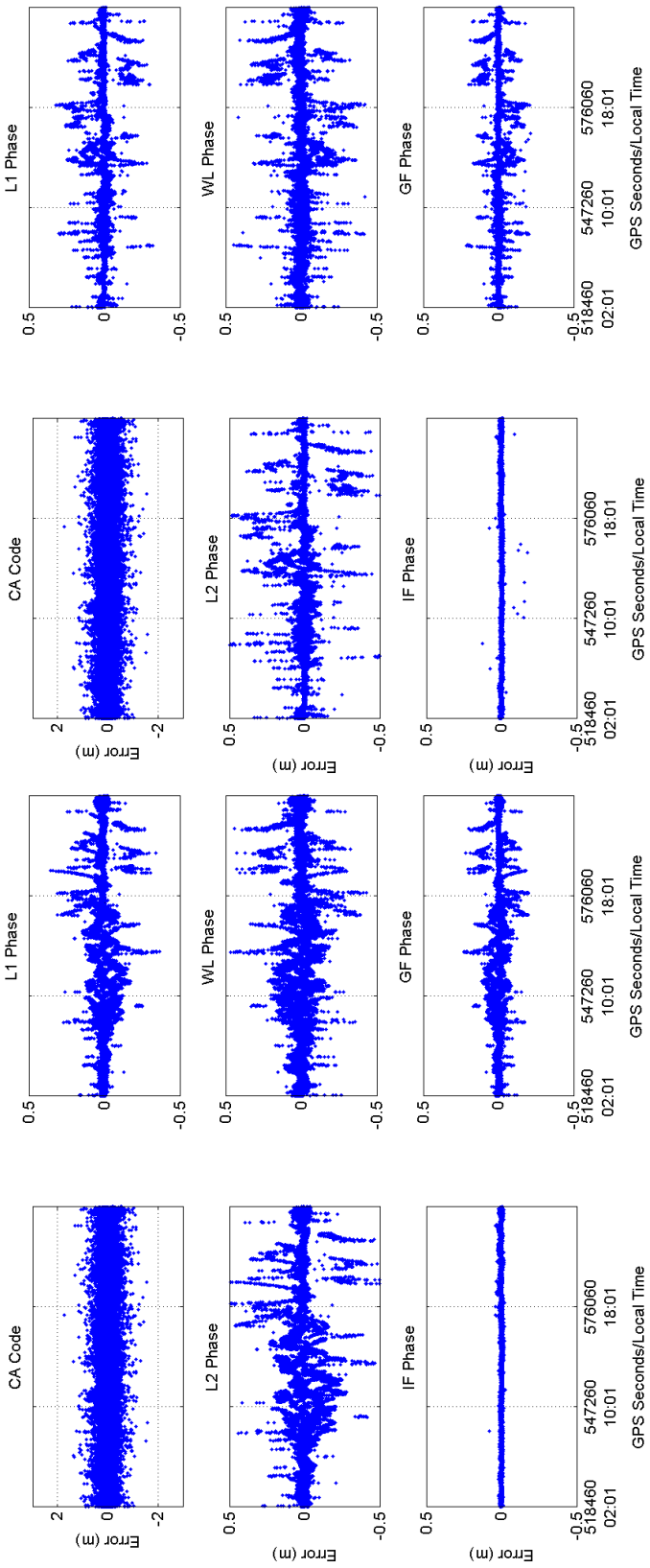

Figure 5.6: Residuals of the single (left) and multiple (right) reference station measurements for Oct 27

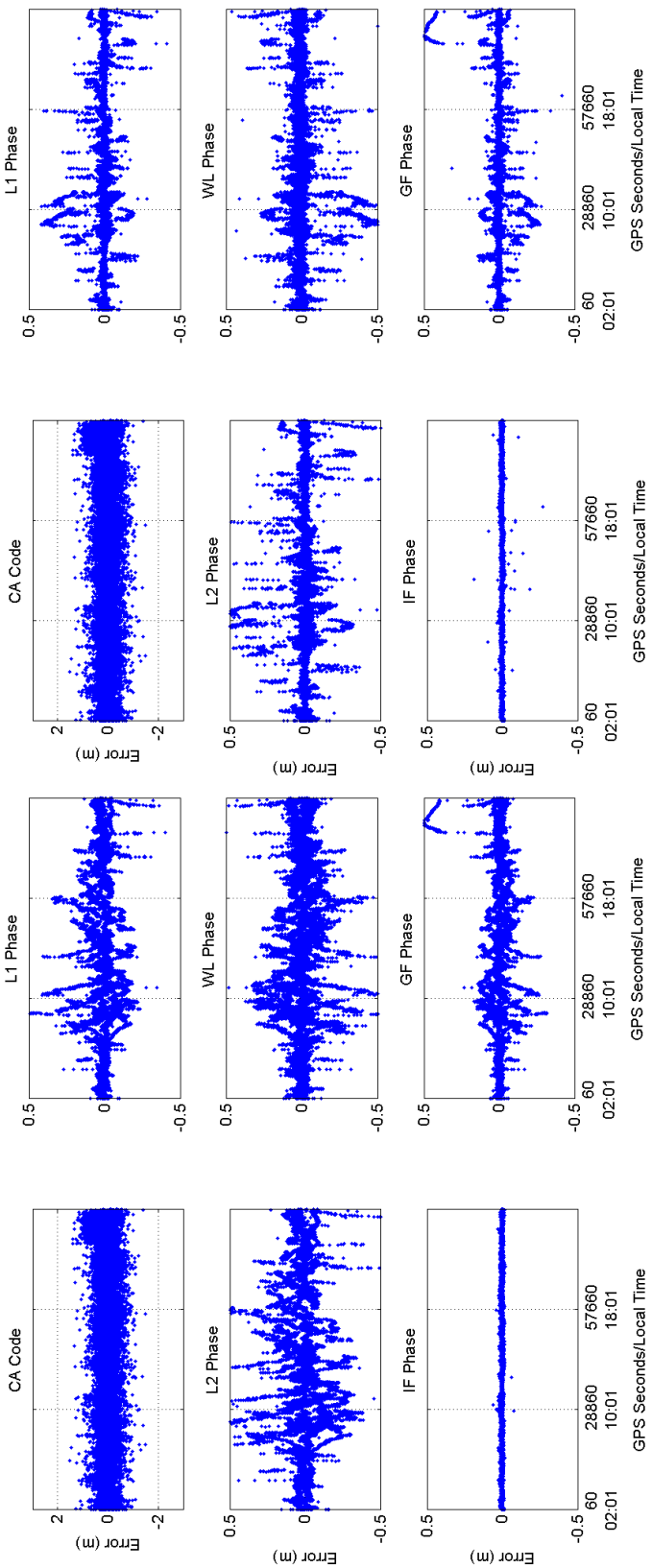

Figure 5.7: Residuals of the single (left) and multiple (right) reference station measurements for Oct 28

would be required to determine if the high measurement error, high spatial correlation occurs in GPS network data. The results do suggest that using the network of reference stations improves performance relative to the single baseline approach.

Table 5.3: RMS position errors and percentage of fixed ambiguities for the single and corrected rover station baseline measurements

		North	East	Up	3D	% fixed
Oct 26	Single RS	2.2 cm	4.6 cm	5.8 cm	7.7 cm	37 %
	Multiple RS	1.7 cm	2.8 cm	4.0 cm	5.2 cm	58 %
	Improvement	24 %	40 %	31 %	33 %	21 %
Oct 27	Single RS	2.0 cm	2.8 cm	6.5 cm	7.3 cm	50 %
	Multiple RS	1.5 cm	3.0 cm	4.7 cm	5.8 cm	50 %
	Improvement	25 %	-6 %	27 %	21 %	< 1 %
Oct 28	Single RS	1.8 cm	3.4 cm	4.9 cm	6.3 cm	43 %
	Multiple RS	1.7 cm	2.1 cm	4.9 cm	5.6 cm	48 %
	Improvement	10 %	39 %	< 1 %	11 %	5 %

Figures 5.8 to 5.10 show the north, east, up, and 3D position errors and the percentage of fixed ambiguities as a function of time for the three days. The improvement in the position accuracy is obvious in these figures. There is also a noticeable improvement in the convergence time on October 26. Some of the main position errors are reduced when the corrections are applied. Similar remaining position errors common to both the single and multiple reference station solutions suggest that some of the measurement errors could not be predicted by the network. Some of these characteristics may also be geometry effects, which include multipath and changes in dilution of precision. Similarities in the position errors from one day to the next also suggest related geometry effects. For example, the single reference station position errors are similar between October 27 and 28.

The ambiguity resolution performance is also similar between the single and multiple reference station approaches however the multiple reference station approach

generally resolves more ambiguities than the single reference station approach. There is low level of fixed ambiguities for both approaches around 16:00 because of the increase in measurement errors.

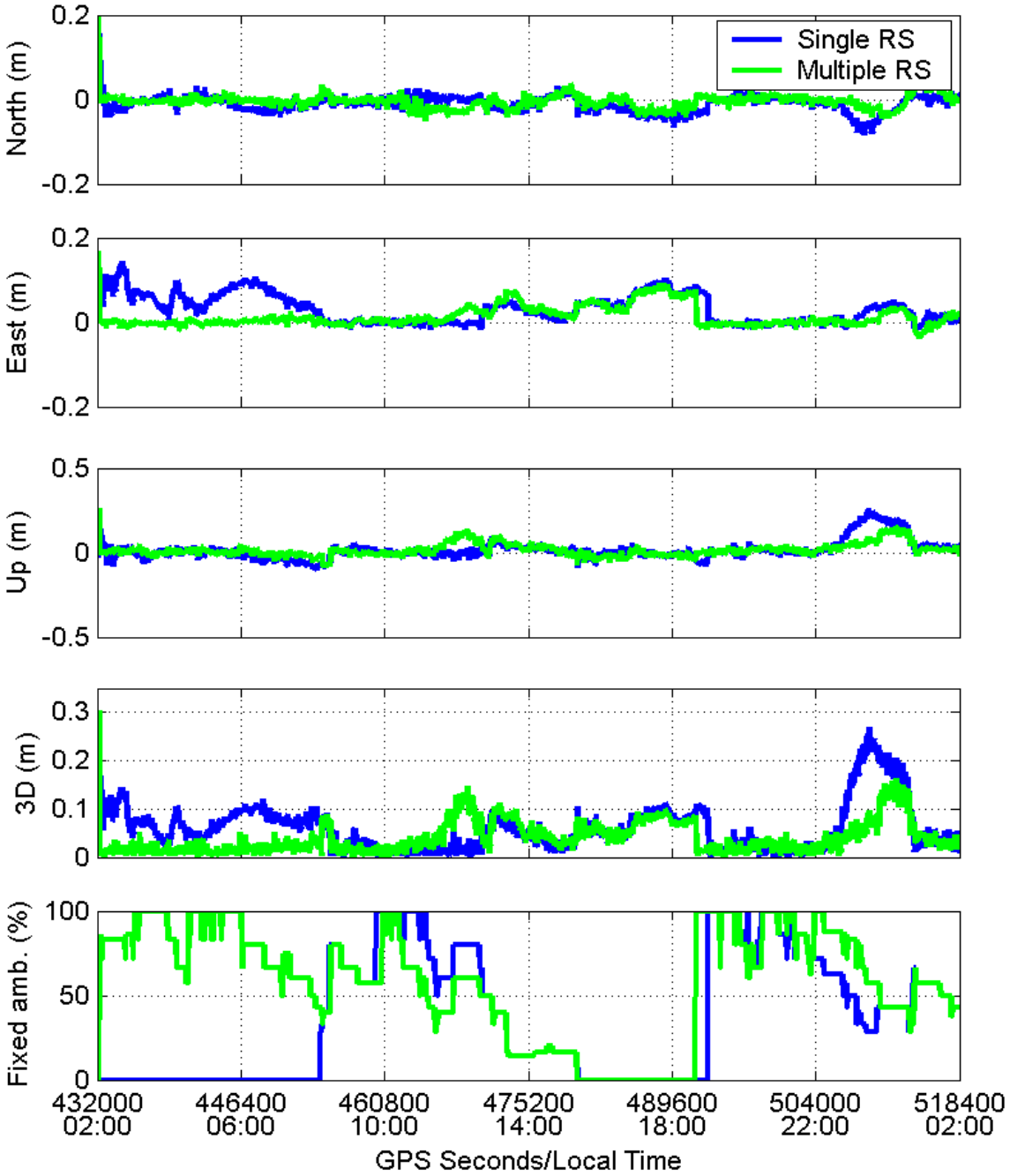

Figure 5.8: North, east, up, and three dimensional position errors and percentage of fixed ambiguities for single and corrected reference station solutions for Oct 26

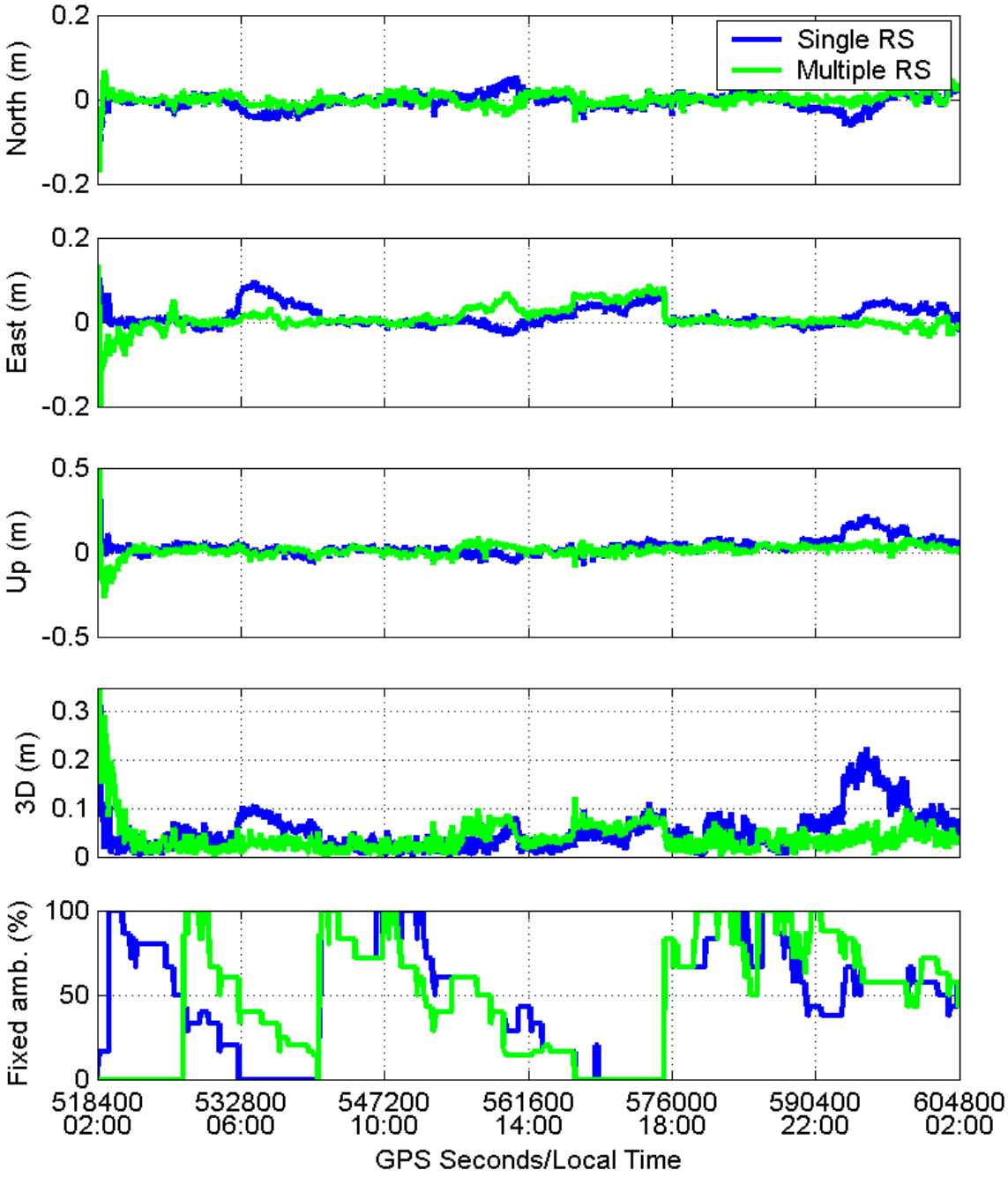

Figure 5.9: North, east, up, and three dimensional position errors and percentage of fixed ambiguities for single and corrected reference station solutions for Oct 27

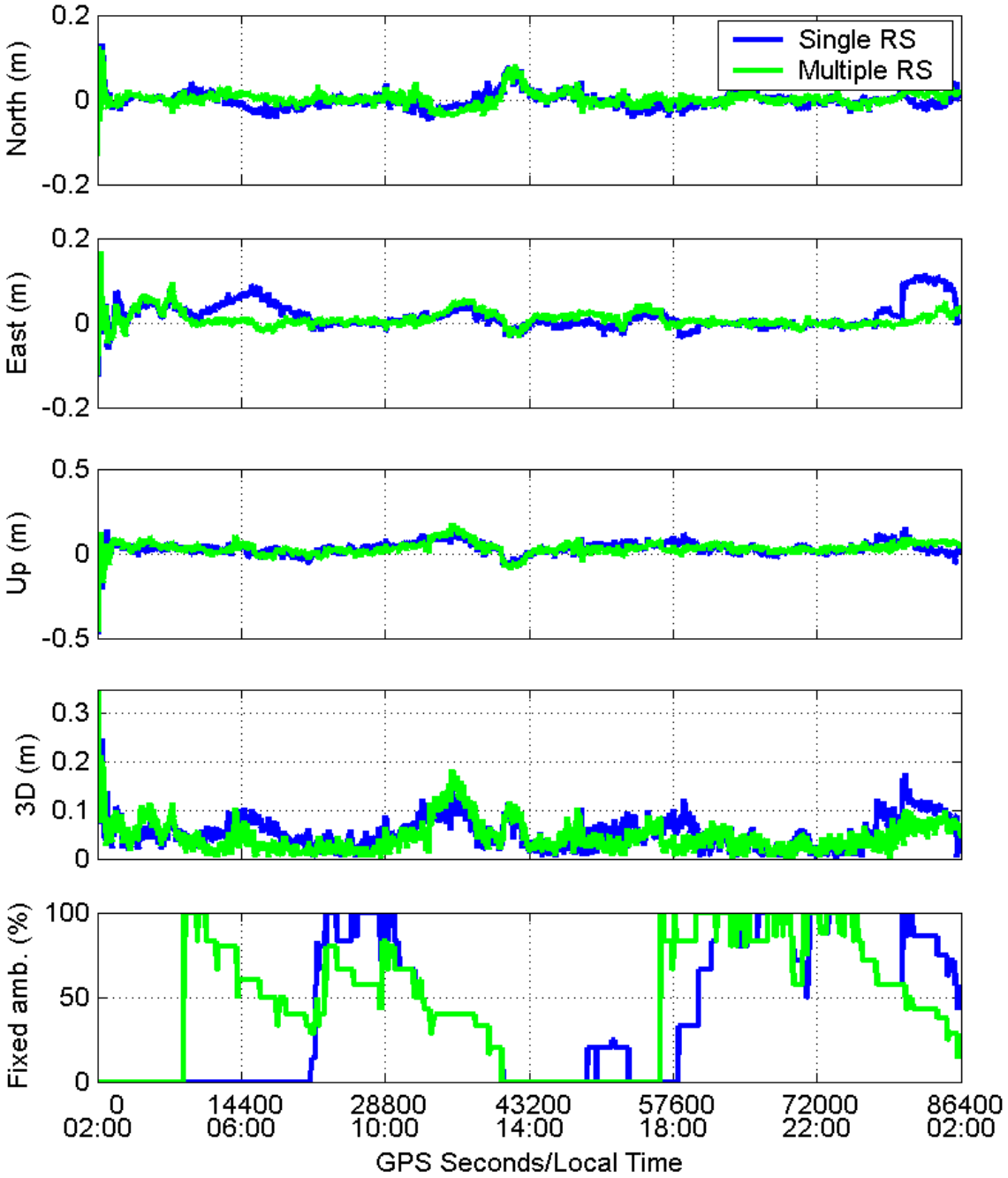

Figure 5.10: North, east, up, and three dimensional position errors and percentage of fixed ambiguities for single and corrected reference station solutions for Oct 28

Chapter 6

Tightly Coupled Approach

Network RTK implementation consists of three main steps (Lachapelle and Alves, 2002). In the first step, the errors at the reference stations are estimated using carrier-phase observations. The second step interpolates these errors to the rover receiver location whereas the third step is to transmit the corrections to the rover. This is usually carried out by generating virtual reference station data that the rover can accept, using a single reference station data format.

Real-time network kinematic positioning is limited by many factors, one of which is the communication network used between the network control centre and the rovers. Due to bandwidth limitations with multiple rovers and an attempt to allow for user privacy, real-time network kinematic positioning methods have attempted so far to operate a broadcast-only system (one-way communication), whereby the network corrections are broadcast to all rovers and there is no information communicated from the rover back to the network.

If two-way communication is used, not only can the network stations assist the rover but the rover can also assist the network with additional information. In this case, the rover actually becomes part of the network and the reduced inter-receiver distances and additional ambiguity constraints provided by the rover improve the overall ambiguity resolution process very significantly using the now established receiver multiplicity concept initially proposed by Lachapelle et al. (1993) and further tested by Luo and Lachapelle (2003). This enhanced procedure is also ideal for post-mission applications that are numerous for verification of hydrographic surveys,

airborne surveys and land surveying.

Network RTK systems use reference stations to precisely measure the correlated errors affecting the region. These errors can only be measured when all other parameters are precisely determined, namely the station position and carrier phase ambiguities. With this in mind, the better a station's position and ambiguities are known, the more accurately one can separate measurement errors and systematic biases. Reference stations are an obvious choice because their positions are known, but any receiver can be used to estimate measurement errors. For example, a static or kinematic rover can be treated as a reference station. In terms of error modelling, multiple rovers in an area can each give an indication of the local environmental error conditions. Combining all of this information into a coherent model allows for new network rovers, with less defined position and velocity estimates, to benefit from decreased measurement error.

The assistance of the rover to the network can be seen in the baseline configurations for the network. Ambiguity resolution performance is a function of inter-receiver distance separation because the correlated errors increase in magnitude as the separation increases. In a broadcast-only Network RTK system, baselines are formed between the various reference stations. Rovers within the network will, by definition, be between two or more reference stations. Therefore connecting baselines to the rovers as well as the reference stations will shorten the overall network inter-receiver separations within the network, thus giving a higher likelihood of resolving the carrier phase ambiguities.

Instead of applying a weighted average (prediction) approach, the rover's data and estimated states are added to the network filter. The network filter is used solely to estimate and resolve the network ambiguities in the real-time approach. The addition

of the rover's information into the network filter maintains all the information used in the least-squares collocation approach and adds the rover information. The difference is that the network not only assists the rover but the rover also assists the network.

In the loosely coupled approach network ambiguities (and other nuisance parameters, such as the ionosphere) are estimated using Bayes filtering. The ambiguities estimates are then searched and, if validated, resolved. The resulting ambiguities are then used to predict the errors to the locations of the rovers.

The integrated approach does not require the error prediction phase of the loosely coupled approach because the error estimates are reduced from the rover's estimates when the rover's position is estimated. This is accomplished by the covariance function, which is used to evaluate the contribution of each of the reference station's observations on the rover. The covariance function determines the level of correlation between measurements. If two measurements are highly correlated then when they are differenced the variance of the resulting, differenced, observation becomes low. Consider the case where the rover is involved in every baseline in the network. The reference station observations that are highly correlated with the rover be assigned a low variance and as a result, will be given more weight in the adjustment than an observation whose errors are different than those of the rover. This method of weighting produces an error model using all of the surrounding reference station's data.

6.1 Implementation

The design matrix of the integrated (tightly coupled) approach has the form

$$A = \begin{bmatrix} \frac{\partial \Delta\nabla\phi_1}{\partial x} & \frac{\partial \Delta\nabla\phi_1}{\partial y} & \frac{\partial \Delta\nabla\phi_1}{\partial z} & \lambda & 0 & & 0 & 0 & \\ \frac{\partial \Delta\nabla\phi_2}{\partial x} & \frac{\partial \Delta\nabla\phi_2}{\partial y} & \frac{\partial \Delta\nabla\phi_2}{\partial z} & 0 & \lambda & & 0 & 0 & \\ & & & & & \ddots & & & \\ 0 & 0 & 0 & 0 & 0 & & \lambda & 0 & \\ 0 & 0 & 0 & 0 & 0 & & 0 & \lambda & \\ & & & & & & & & \ddots \end{bmatrix} \tag{6.1}$$

where the first n rows correspond to the double difference observations between the rover and one of the reference stations, and the second set of m rows correspond to double difference observations between the fixed reference stations with known coordinates. n is the number of double difference observations between the rover and the reference station(s) and m is the number of double difference observations between reference stations. The first three columns correspond to the rover's position estimates and the following $n+m$ columns correspond to the ambiguities of all of the double difference observations. No partial derivatives with respect to the coordinates exist between reference stations because their coordinates are assumed known and held fixed.

The design matrix can be extended to accept any number of reference stations and rovers. The processing results shown include the code and carrier phase observations processed in a single Bayes filter. This model can be expanded to incorporate any observation (system) model (estimating troposphere delay, ionosphere error, or the rover's velocity estimates, for example). The selection of the double difference observables is based on the shortest inter-receiver separations, with the conditions

of linear independence and connectivity being preserved. Thus a rover may be connected to one or several reference stations, depending on the reference station-rover receiver configuration. Short distances are selected to minimize the magnitude of the differential errors. As an example, in the case of four reference stations and one rover, the double differences over the shortest four linearly independent receiver separations would be used. The rover may be involved in one to four sets of double differences.

The mathematical and stochastic information are used in the integrated approach. The mathematical correlation is due to inter-receiver separations that share a common reference station (or rover station) which use the same observations in their double difference measurements. This is represented in the filter by the double difference measurement matrix, B. This matrix is not block diagonal because the observations from one station may be used in multiple baselines. The measurement matrix shown below is for the scenario where there are four stations and each station is used in a maximum of two baselines, as follows

$$B = \begin{bmatrix} B_{sd} & -B_{sd} & 0 & 0 \\ 0 & B_{sd} & -B_{sd} & 0 \\ 0 & 0 & B_{sd} & -B_{sd} \end{bmatrix} \tag{6.2}$$

where B_{sd} is the single difference measurement matrix for each of the stations assuming each station has the same satellites in view. This correlation is often neglected in multiple baseline processing.

Stochastic correlation is defined by the covariance function. The covariance function states the likelihood of two values being the same based on a physical process. For example, it is known that the ionosphere is a spatially correlated error, therefore two stations close to each other are likely to have a similar ionospheric error. Stochastic correlation is represented in the Bayes filter in the variance-covariance matrix of

the observations. This is a fully populated matrix because each of the measurements should be somewhat correlated through their correlated errors.

6.2 Ionosphere Modelling

This model has been extended in this research to estimate the dual frequency slant ionosphere delay using the ionosphere free model Odijk (1999). In addition to the rover's position, velocity and ambiguity states, and the network's ambiguity states, an ionosphere parameter for each dual frequency satellite pair is estimated. The corresponding rows and columns are added to the design matrix in Equation 6.1.

The design matrix is partitioned into sub-matrices as shown

$$A = \begin{bmatrix} A_{(1,1)} & A_{(1,2)} \\ A_{(2,1)} & A_{(2,2)} \end{bmatrix} \tag{6.3}$$

where the first row of matrices refer to the measurements of baselines that include the rover as one of the stations. The second row refers to measurements of baselines with only network stations. As there are no common estimated parameters between the network and rover, one can write

$$A_{(1,2)} = A_{(2,1)} = 0. \tag{6.4}$$

The first sub-matrix is

$$A_{(1,1)} = \begin{bmatrix} A_{pos} & \lambda_{L1} I & 0 & I \\ A_{pos} & 0 & \lambda_{L2} I & \frac{f_{L1}^2}{f_{L2}^2} I \\ A_{pos} & 0 & 0 & -I \\ A_{pos} & 0 & 0 & -\frac{f_{L1}^2}{f_{L2}^2} I \end{bmatrix} \tag{6.5}$$

where the four row of the sub matrix ($A_{(1,1)}$) represent the four different measurement types L1 phase, L2 phase, L1 code, and L2 code, respectively. A_{pos} is a 3 column sub

matrix that includes the partial derivatives of the double difference measurements with respect to the three position components of the rover (similar to Equation 6.1). This matrix is repeated because the satellite geometry is the same for each measurement type from the same satellites. $\frac{f_{L1}^2}{f_{L2}^2}$ is the scalar transformation of the L2 ionosphere in metres to the L1 ionosphere.

The sub matrix for the network observations ($A_{(2,2)}$) has a similar form as $A_{(1,1)}$) without the first column:

$$A_{(2,2)} = \begin{bmatrix} \lambda_{L1}I & 0 & I \\ 0 & \lambda_{L2}I & \frac{f_{L1}^2}{f_{L2}^2}I \\ 0 & 0 & -I \\ 0 & 0 & -\frac{f_{L1}^2}{f_{L2}^2}I \end{bmatrix}. \tag{6.6}$$

As with $A_{(1,1)}$) each of the four rows represent the four measurement types: L1 phase, L2 phase, L1 code, and L2 code, respectively.

6.3 Practical Real-Time Use

The tightly coupled approach to multiple reference station GPS positioning is a natural extension of the single reference station approach. Users in an array of single operating reference stations commonly transition from one reference station to another. There is an ambiguous transition zone when the rover is between the reference stations. In this zone the rover has the option to estimate the baseline between the rover and one reference station or the other. The tightly coupled approach is a method for estimating both baseline parameters to improve positioning performance and remove the ambiguous zone.

Although the multiple reference station approach is usually regarded as a large

infrastructure method with a control centre, this method incorporates a network of reference stations without the need for a centralized control center.

6.3.1 Implementation with RTCM Version 3.0

The latest version of the standardized RTCM differential GPS messages was recently released. Included in these messages is tentative proposed messages for multiple reference station positioning. These messages implement the master-auxiliary concept (Euler et al., 2004b). The master-auxiliary concept uses two types of messages:

- The master station corrections are the standard single reference station correction data. Using this message as both the the master and single reference station messages allow for seamless integration of the multiple reference station and single reference station messages.

- The auxiliary messages provide observation differences relative to the master station with the ambiguities removed.

The master-auxiliary concept requires a control centre to estimate and remove the ambiguities between the reference stations. All of the auxiliary stations within the same network or sub-network are on the same ambiguity level, meaning that the ambiguities have been removed relative to the same master station.

The intended implementation of these messages are to model the differential errors using either a surface or least squares collocation and interpolate the errors to the location of the rover. Although this model focuses on the usual definition of the multiple reference station approach, it can easily be adapted with the tightly coupled approach. There are a few options for this model.

The reduced reference station network ambiguities can be eliminated from the tightly coupled filter estimation or the ambiguities can be estimated and compared to zero. The ambiguity values should be zero because they are removed from the control centre processing. This allows for an additional stage of reliability testing of the ambiguity values when incorporating the additional information provided by the rover data.

Also included in the master-auxiliary concept is an ambiguity flag to signify the confidence of the ambiguity values. These possibly incorrect ambiguities may cause significant errors in the multiple reference station prediction. This is not an issue in the tightly coupled approach because the network's float ambiguities can be estimated and may be further refined using the rover's data.

This is a main advantage of the tightly coupled approach over the modelling approach. The modelling approach constrains the solution to the fixed (or float) network ambiguities as well as the spatial model. Any errors in the ambiguities or interpolation model will directly impact the rover's corrections. The tightly coupled approach can assign relative weights to the network ambiguities to reduce the effects of ambiguity errors. It also allows for a relative weight for network ambiguities that may be better determined than others.

6.4 Results of the Tightly Coupled Approach

The improvement due to the tightly coupled approach is shown in this chapter using the three days of the MAGNET network. This consists of two comparisons. Firstly the improvement relative to the single baseline approach. Secondly, the improvement due to the estimation of multiple rovers.

The collocation-based approach, and generally all correction-based methods are independent of the number of rovers estimated. However, the tightly coupled approach can estimate multiple rover stations at the same time. This may have significant advantages for the relative positioning of rover stations.

6.5 Test methodology and figures of merit

To test the two objectives two rovers are removed from the network. Each rover is processed in three separate tests:

- single baseline test using the closest network reference station,
- tightly coupled multiple reference station approach,
- tightly coupled multiple reference station approach with multiple rovers.

A comparison of the single baseline solution and the tightly coupled solution shows the improvement due to the incorporation of the network data. Many of the performance measures that were used to compare the single reference station approach to the collocation-based are not applicable when comparing the tightly coupled approach to the single reference station approach. Only two performance measures are shown, the ambiguity resolution performance and the position domain accuracy.

6.5.1 Ambiguity resolution

The ambiguity resolution performance is shown as the percentage of fixed ambiguities. The percentage of fixed ambiguities includes each epoch for each ambiguity as opposed to each satellite path. This ambiguity resolution performance measure includes time to fix ambiguities.

6.5.2 Position domain

The position domain accuracy is shown as the root mean squared error and plots of the north, east, up and 3D position errors over time. The position domain accuracy is the most important criteria for most DGPS RTK users.

6.6 MAGNET network with TU as a rover

The network configuration shown in Figure 6.1 is used to compare the single reference station approach to the tightly coupled approach. Station DU is removed because it will be used as the secondary rover to determine the effect of estimating multiple rovers at the same time. The baseline lengths range from 44 to 74 km and the single reference station baseline is between stations TU and UC.

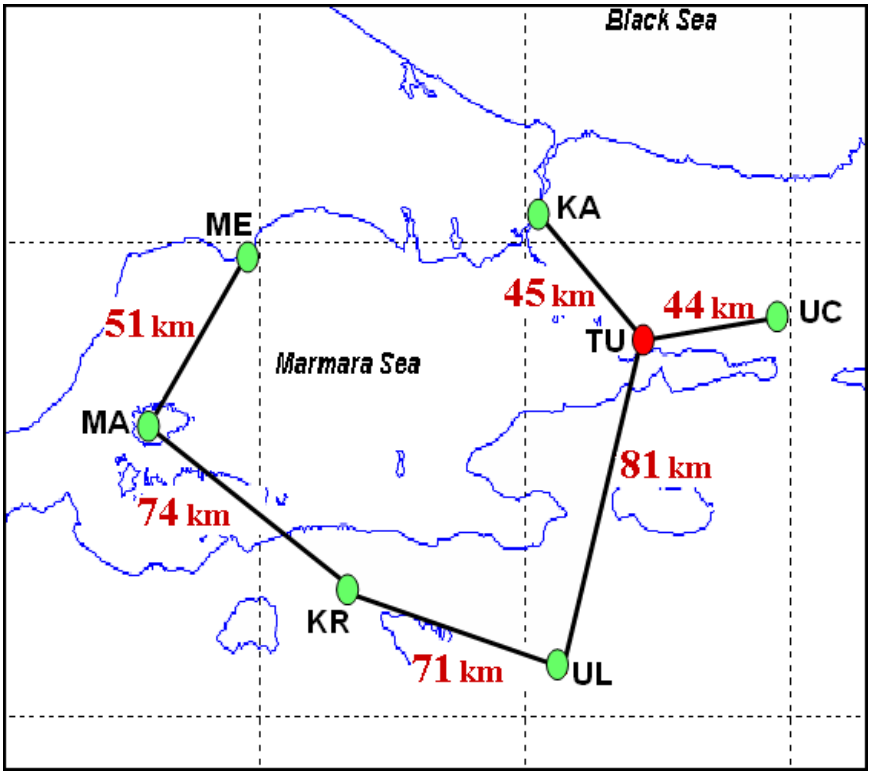

Figure 6.1: MAGNET network configuration with TU as the rover and DU removed

6.6.1 Percentage of fixed ambiguities

The percentages of fixed ambiguities for the single reference station and multiple reference station approaches are shown in Table 6.1. The single reference station approach resolves 29.5 percent of the ambiguities, while the tightly coupled approach is able to resolve 43.6 percent of the ambiguities on the same baseline. This is a significant increase in the number of fixed ambiguities for this baseline. In addition, the tightly coupled approach has the advantage of two additional baselines that connect the rover to the network. The baseline lengths that connect to the rover have a lower percentage of fixed ambiguities than baselines that connect between two reference stations. This is because of the errors in the rover receiver's coordinates.

Table 6.1: Percentage of fixed ambiguities for the single reference station and multiple reference station approach with TU as the rover.

	Station 1	UC	KA	MA	KR	KR	UL
	Station 2	TU	TU	ME	UL	MA	TU
	distance (km)	43.6	48.2	81.9	72.8	80.6	24.5
Oct 26	Single RS (%)	29.5					
	Multiple RS (%)	43.6	48.2	81.9	72.8	80.6	24.5
Oct 27	Single RS (%)	30.3					
	Multiple RS (%)	44.0	42.5	88.1	87.6	75.0	21.1
Oct 28	Single RS (%)	27.5					
	Multiple RS (%)	38.0	26.8	86.3	70.6	73.5	21.7

6.6.2 Position domain

Table 6.2 shows the RMS position errors for the north, east, up and 3D components for the single and multiple reference station approaches for the three days. The level of improvement varies between the days. On the first day, the improvement is very high (42 percent), which is a nearly 3 cm reduction of the 3D position RMS. The worst case is on the third day where the tightly coupled approach increases the 3D

RMS by 0.7 cm. When DU is processed at the same time as TU, the 3D position RMS error for TU is reduced to 4.7 cm. This is an improvement of 23 percent relative to the single reference station approach.

Table 6.2: Root mean squared position errors for the single and corrected rover station baseline measurements with TU as the rover.

		North	East	Up	3D
Oct 26	Single RS	2.3 cm	2.5 cm	5.1 cm	6.1 cm
	Multiple RS	1.6 cm	1.4 cm	2.8 cm	3.5 cm
	Improvement	30 %	44 %	45 %	43 %
Oct 27	Single RS	1.7 cm	3.2 cm	4.4 cm	5.7 cm
	Multiple RS	1.5 cm	1.6 cm	3.1 cm	3.8 cm
	Improvement	12 %	50 %	30 %	33 %
Oct 28	Single RS	2.1 cm	3.2 cm	4.8 cm	6.1 cm
	Multiple RS	1.6 cm	3.5 cm	5.6 cm	6.8 cm
	Improvement	24 %	-9 %	-17 %	-11 %

Figures 6.2 to 6.4 show the north, east, up and 3D position accuracies as a function of time for the three days. The tightly coupled approach appears to converge faster than the single reference station approach. In most cases the converged position accuracy is better than the single reference station solution.

6.7 MAGNET network with DU as a rover

The network configuration shown in Figure 6.5 is used to compare the single reference station approach to the tightly coupled approach. The station DU is removed because it will be used as the secondary rover to determine the effect of estimating multiple rovers at the same time. The baseline lengths range from 51 to 74 km and the single reference station baseline is between stations DU and UL (56 km).

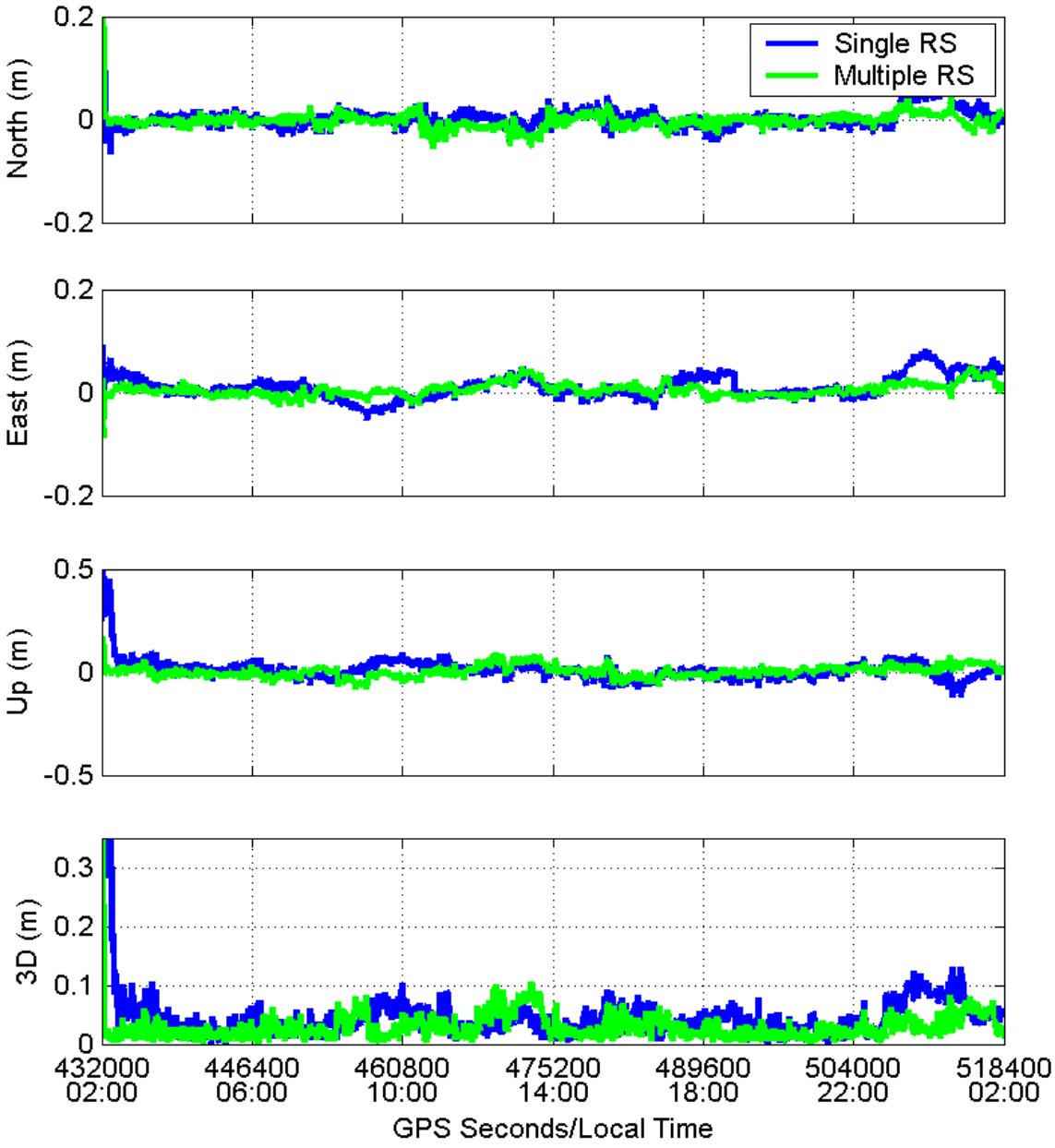

Figure 6.2: North, east, up and three dimensional position errors for single and multiple reference station solutions for Oct 26 network with TU as the rover

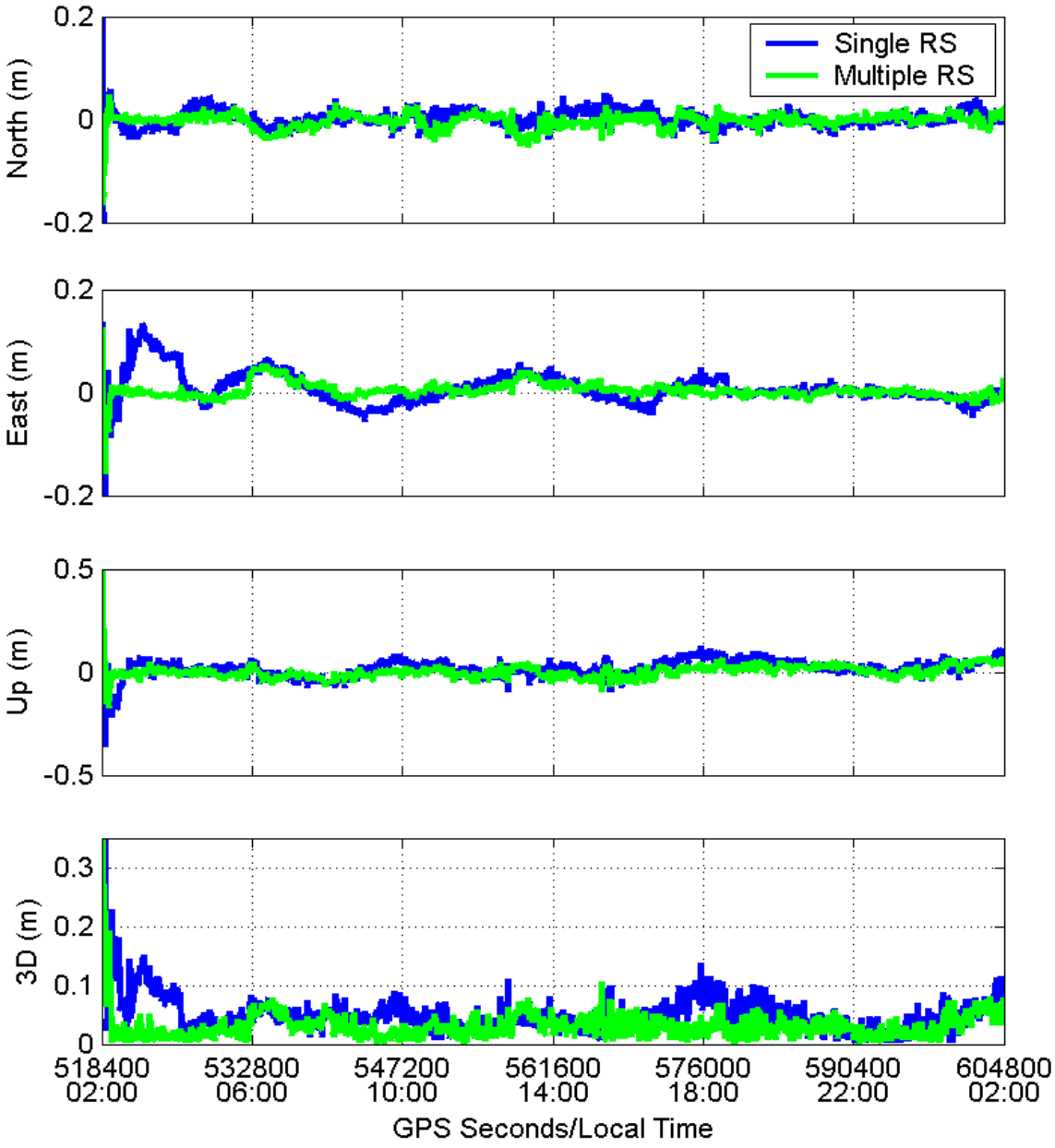

Figure 6.3: North, east, up and three dimensional position errors for single and multiple reference station solutions for Oct 27 network with TU as the rover

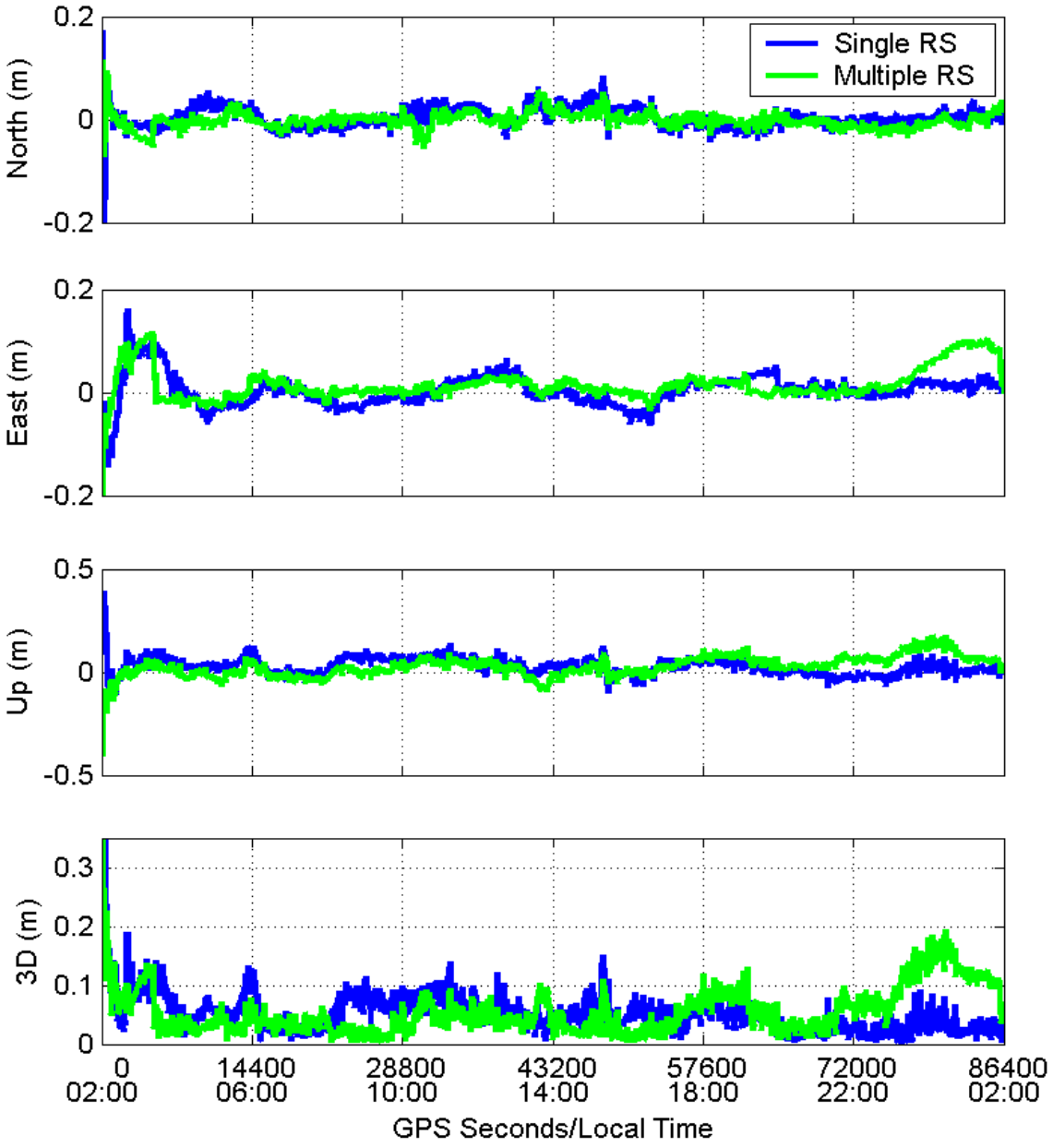

Figure 6.4: North, east, up and three dimensional position errors for single and multiple reference station solutions for Oct 28 network with TU as the rover

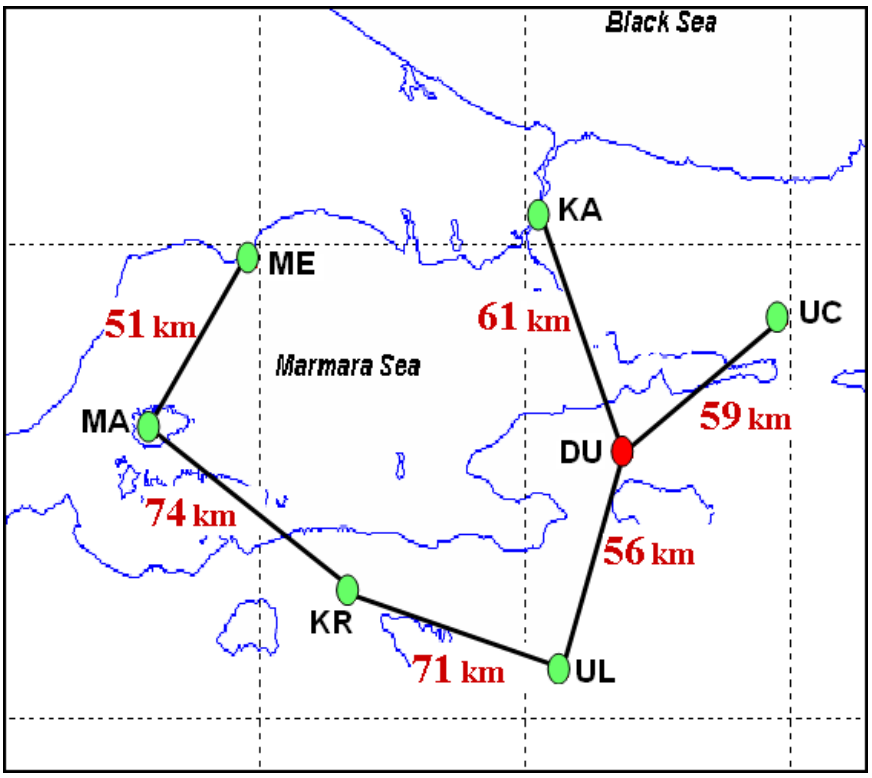

Figure 6.5: MAGNET network configuration with DU as the rover and TU removed

6.7.1 Percentage of fixed ambiguities

The percentage of fixed ambiguities for the single reference station and multiple reference station approaches are shown in Table 6.3. The single reference station approach resolves 49 to 71 percent of the ambiguities, while the tightly coupled approach is able to resolve 74 to 78 percent of the ambiguities on the same baseline. For October 26 and 27 the improvement in the percentage of fixed ambiguities is small. When the atmospheric errors increase on October 28 there is a large improvement due to the tightly coupled approach. In this case both approaches resolve a high percentage of ambiguities. As expected, the multiple reference station approach is able to resolve more ambiguities than the single reference station approach.

Table 6.3: Percentage of fixed ambiguities for the single reference station and multiple reference station approach with DU as the rover.

	Station 1	UL	MA	UC	KA	KR	KR
	Station 2	DU	ME	DU	DU	UL	MA
	distance (km)	55.9	50.6	58.8	60.9	70.6	74.0
Oct 26	Single RS (%)	71.2					
	Multiple RS (%)	75.4	81.3	74.4	65.1	73.2	81.3
Oct 27	Single RS (%)	73.4					
	Multiple RS (%)	77.5	87.9	81.2	70.3	86.8	77.0
Oct 28	Single RS (%)	49.3					
	Multiple RS (%)	74.4	85.5	83.6	55.4	52.9	74.3

6.7.2 Position domain

Table 6.4 shows the RMS position errors for the north, east, up and 3D components for the single and multiple reference station approaches. The position errors are decreased by 31 to 57 percent (3D RMS) due to the incorporation of the network data. The level of improvement does not appear to be a function of the atmospheric errors. This suggests that this method is effective regardless of the magnitude of the

measurement errors. The absolute position accuracy is a function of the measurement errors but the percentage of improvement is consistent. This may change under a wider range of measurement errors, in different geographical regions or with different network configurations.

Table 6.4: Root mean squared position errors for the single and corrected rover station baseline measurements with DU as the rover.

		North	East	Up	3D
Oct 26	Single RS	1.8 cm	2.2 cm	4.1 cm	5.0 cm
	Multiple RS	0.9 cm	0.9 cm	2.1 cm	2.4 cm
	Improvement	50 %	59 %	49 %	52 %
Oct 27	Single RS	2.2 cm	1.5 cm	3.5 cm	4.4 cm
	Multiple RS	1.1 cm	0.8 cm	2.7 cm	3.0 cm
	Improvement	50 %	47 %	23 %	32 %
Oct 28	Single RS	3.1 cm	2.4 cm	8.8 cm	9.7 cm
	Multiple RS	1.0 cm	2.7 cm	2.9 cm	4.1 cm
	Improvement	68 %	-13 %	67 %	58 %

Figures 6.6 to 6.8 show the north, east, up and 3D position accuracy as a function of time. The tightly coupled approach performs much better than the single reference station approach. Most of the main position errors in the single reference station solution are significantly reduced or completely removed by the tightly coupled approach. Although the improvement is noticeable on all three days the improvement is greatest on October 28.

6.8 MAGNET network with both TU and DU as rovers

This section will investigate the performance of the tightly coupled approach when the positions of two rovers are estimated at the same time. Figure 6.9 shows the network configuration used in this test. The baseline lengths for this test are considerably shorter when the two rovers are processed at the same time. This decrease in the

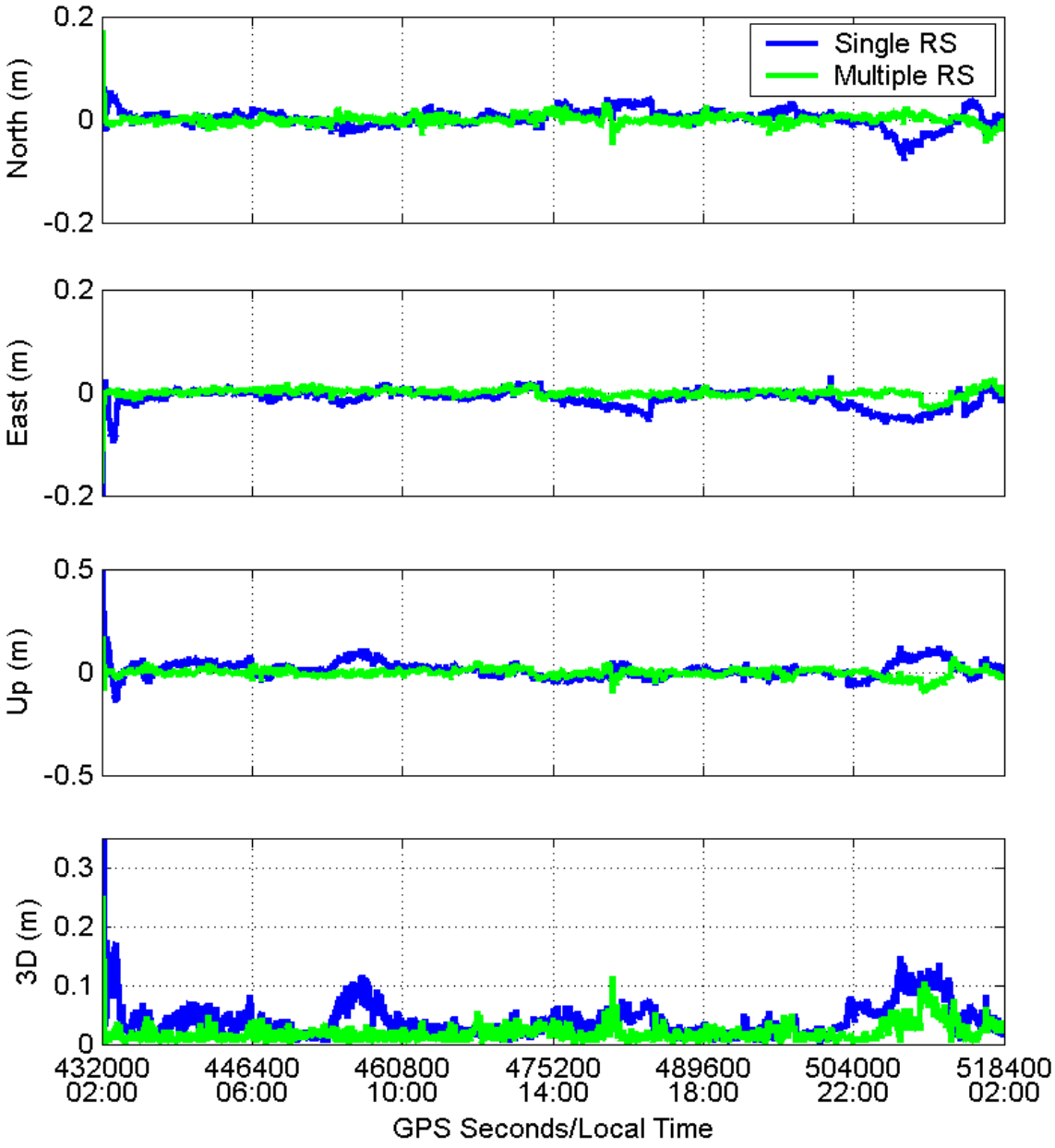

Figure 6.6: North, east, up and three dimensional position errors for single and multiple reference station solutions for Oct 26 network with DU as the rover

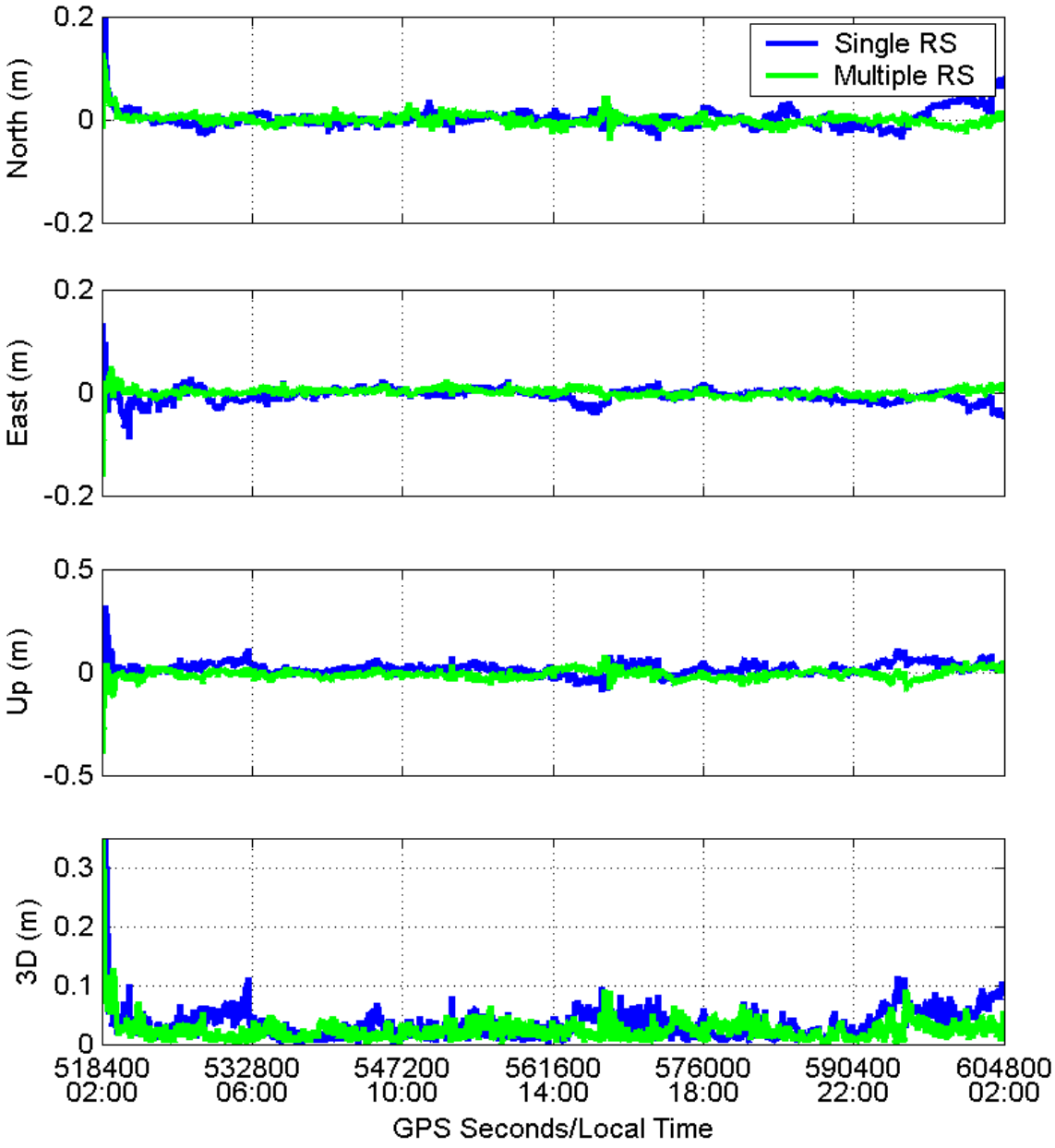

Figure 6.7: North, east, up and three dimensional position errors for single and multiple reference station solutions for Oct 27 network with DU as the rover

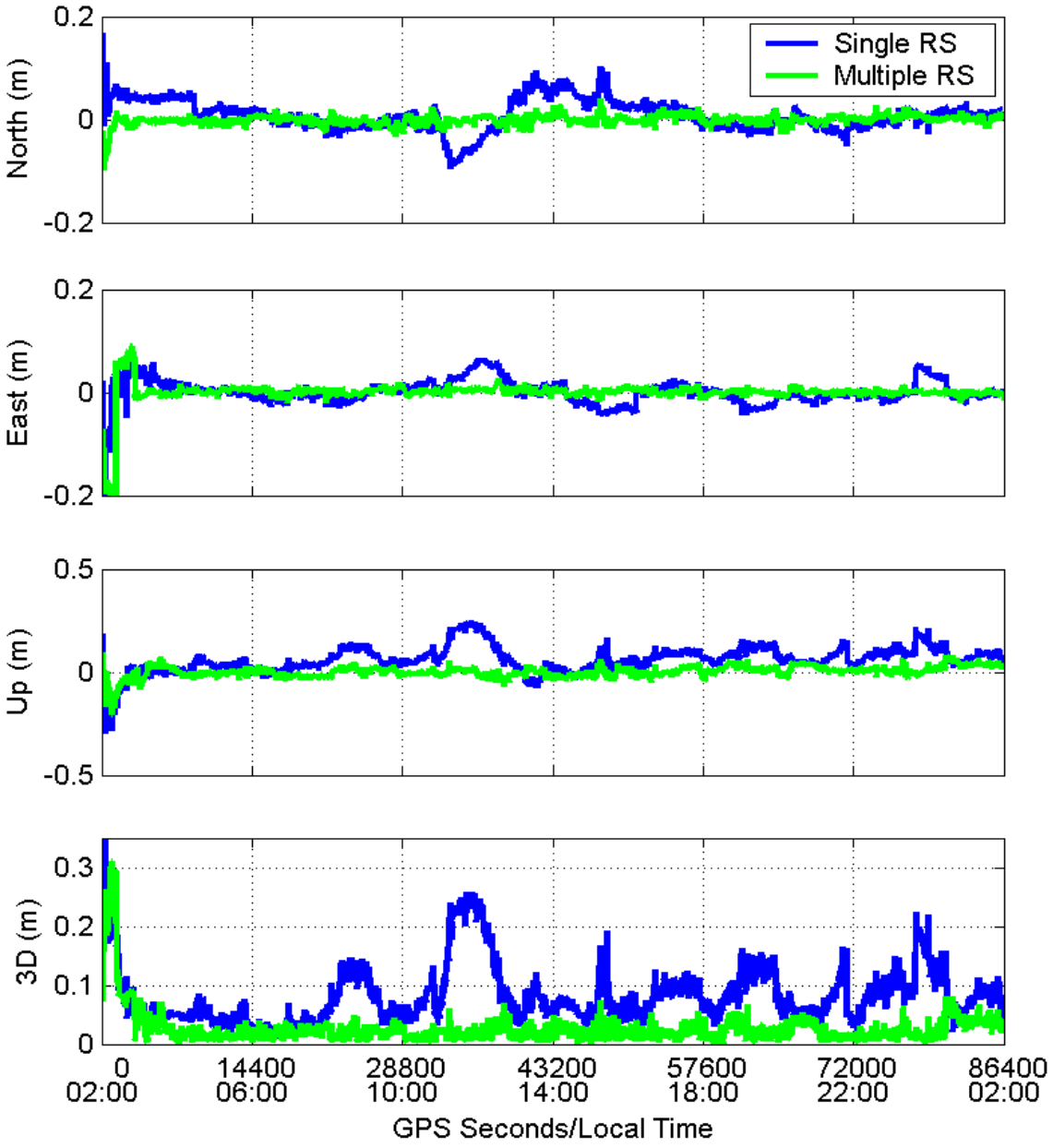

Figure 6.8: North, east, up and three dimensional position errors for single and multiple reference station solutions for Oct 28 network with DU as the rover

baseline lengths suggests that the position accuracy may be improved when multiple rovers are used. In this case the rovers are connected by a baseline. This may not always be the case. For all of these tests, the shortest baselines are used to connect the stations regardless of whether or not the stations are rover or reference stations.

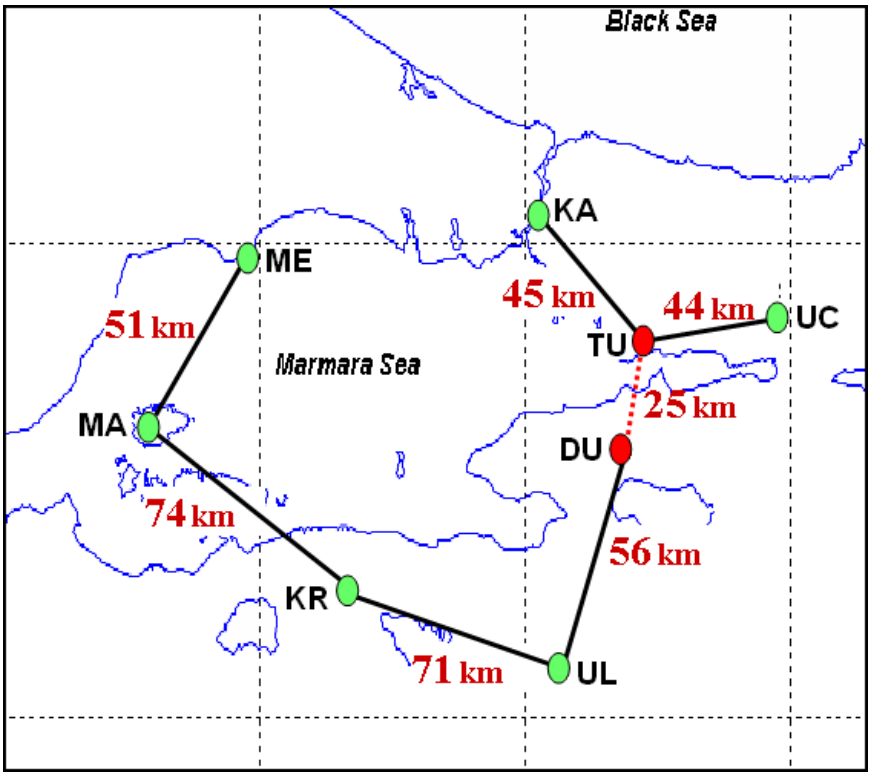

Figure 6.9: MAGNET network configuration with TU and DU rovers

6.8.1 Percentage of fixed ambiguities

Table 6.5 shows a summary of the ambiguity resolution performance for the three methods. In general, the ambiguity resolution performance for common baseline lengths is no significantly difference between the solutions. The percentage of fixed ambiguities in the baseline connecting the two rovers is particularly low (41 to 45 percent). The baselines that connect to one rover and one reference station resolve

noticeably less ambiguities than the baselines that connect two reference stations. It may be better to estimate ambiguities between reference stations instead of connecting them directly to the rover, although there would be a trade off between the reduction of baseline lengths and increased errors due to the rover position.

Table 6.5: Percentage of fixed ambiguities for the tightly coupled method when the rovers are processed independently and together.

	Station 1	DU	UC	KA	MA	UL	UC	DA	KR	KR	UL
	Station 2	TU	TU	TU	ME	DU	DU	DU	UL	MA	TU
	Dist. (km)	25.5	43.7	44.7	50.6	55.9	58.8	60.9	70.6	74.0	81.2
Oct	TU Only		43.6	48.2	81.9				72.8	80.6	24.5
26	DU Only				81.3	75.4	74.4	65.1	73.2	81.3	
	Both	41.2	45.5	54.2	81.9	69.6			73.1	81.7	
Oct	TU Only		44.0	42.5	88.1				87.6	75.0	21.1
27	DU Only				87.9	77.5	81.2	70.2	86.8	77.0	
	Both	44.7	43.4	44.1	88.5	74.3			86.6	77.3	
Oct	TU Only		38.0	26.8	86.3				53.9	73.5	21.7
28	DU Only				85.5	74.4	83.6	55.4	52.9	74.3	
	Both	41.2	34.7	32.5	86.5	73.9			53.6	74.0	

6.8.2 Position domain

Table 6.6 shows the RMS position errors for the tightly coupled approach using TU only, DU Only and both TU and DU as rovers. There is very little difference in the performance between the solutions. Both solutions provide exceptional positioning performance. In general, the position errors are slightly higher when the two rovers are processed at the same time. Interestingly, the only case that produced a negative improvement relative to the single reference station approach is significantly improved by processing both rovers. The TU 3D RMS position error is reduced from 6.8 cm to 4.7 cm on the Oct 28 data set when processed with DU. This suggests that there may be an increase in the reliability of the method when processing multiple rovers,

although there is a slight decrease in performance.

Table 6.6: Root mean squared position errors for the tightly coupled approach using TU only and both TU and DU as rovers for the MAGNET Oct 26 data set.

		TU Only	TU (Both)	Percent Improve.	DU Only	DU (Both)	Percent Improve.
Oct 26	North	1.6 cm	1.6 cm	¿ -1 %	0.9 cm	1.3 cm	-44 %
	East	1.4 cm	1.1 cm	21 %	0.9 cm	1.3 cm	-44 %
	Up	2.8 cm	2.8 cm	¡ 1 %	2.1 cm	3.3 cm	-57 %
	3D	3.5 cm	3.4 cm	3 %	2.4 cm	3.8 cm	-58 %
Oct 27	North	1.5 cm	1.6 cm	-7 %	1.1 cm	1.4 cm	-27 %
	East	1.6 cm	1.8 cm	-13 %	0.8 cm	1.3 cm	-63 %
	Up	3.1 cm	3.4 cm	-10 %	2.7 cm	3.1 cm	-19 %
	3D	3.8 cm	4.1 cm	-8 %	3.0 cm	3.6 cm	-20 %
Oct 28	North	1.6 cm	1.3 cm	19 %	1.0 cm	1.7 cm	-70 %
	East	3.5 cm	1.7 cm	51 %	2.7 cm	2.0 cm	26 %
	Up	5.6 cm	4.2 cm	25 %	2.9 cm	4.3 cm	-48 %
	3D	6.8 cm	4.7 cm	31 %	4.1 cm	5.0 cm	-22 %

Figures 6.10 to 6.15 show the north, east, up and 3D position errors over time for the tightly coupled approach with TU only, DU only, and both TU and DU. The differences between the solutions is usually on the level of the noise with the exception of a few cases.

The most noticeable difference in the solutions is shown in Figure 6.14. This is the only test case that performed worse than the single reference station approach. When the two rover stations are processed at the same time the tightly coupled solution performs better than the single reference station approach.

Figure 6.15 also shows a significant difference between the two solutions. The errors beginning slightly after 10:00 local time are similar to the position errors shown in the single reference station approach (Figure 6.8). The a small percentage of the errors that caused the increased measurement errors in the single reference station approach reappear when the rover is connected to another roving receiver. Comparing

Figures 6.14 and 6.15 shows that increased position error in DU does not have a negative effect on the position accuracy of TU for the same epochs.

In these cases, both rovers are initialized at the same time. This approach may become more effective when some rovers are converged when new rovers are introduced. In this case, the convergence of the initial rover may assist in the convergence and performance of the additional rovers.

6.8.3 Relative position domain

This next test shows the relative position accuracy between the two rovers. Processing the two rovers in the same filter may provide an increase in the relative position accuracy even if the absolute position accuracy for the DU station is slightly decreased.

Table 6.7 shows the relative position RMS accuracy between TU and DU alone and between TU and DU when they are estimated at the same time. Extrapolating from the previous results, there is little difference between the results for the TU station and the accuracy of DU is better when DU is processed alone, therefore the relative accuracy of the stations when processed alone would be better then when processed together. This is shown in the following results, however the difference in performance is small and both stations provide high position accuracies for baseline lengths of this scale.

The considerable improvement in the October 28 data set is similar to the improvement in the two rover solutions shown in the previous section. This improvement is not an increase in the relative position accuracy but an improvement in the absolute accuracy of TU.

Figures 6.16 to 6.18 show the north, east up and 3D relative position errors between TU and DU when they are processed independently or at the same time for the

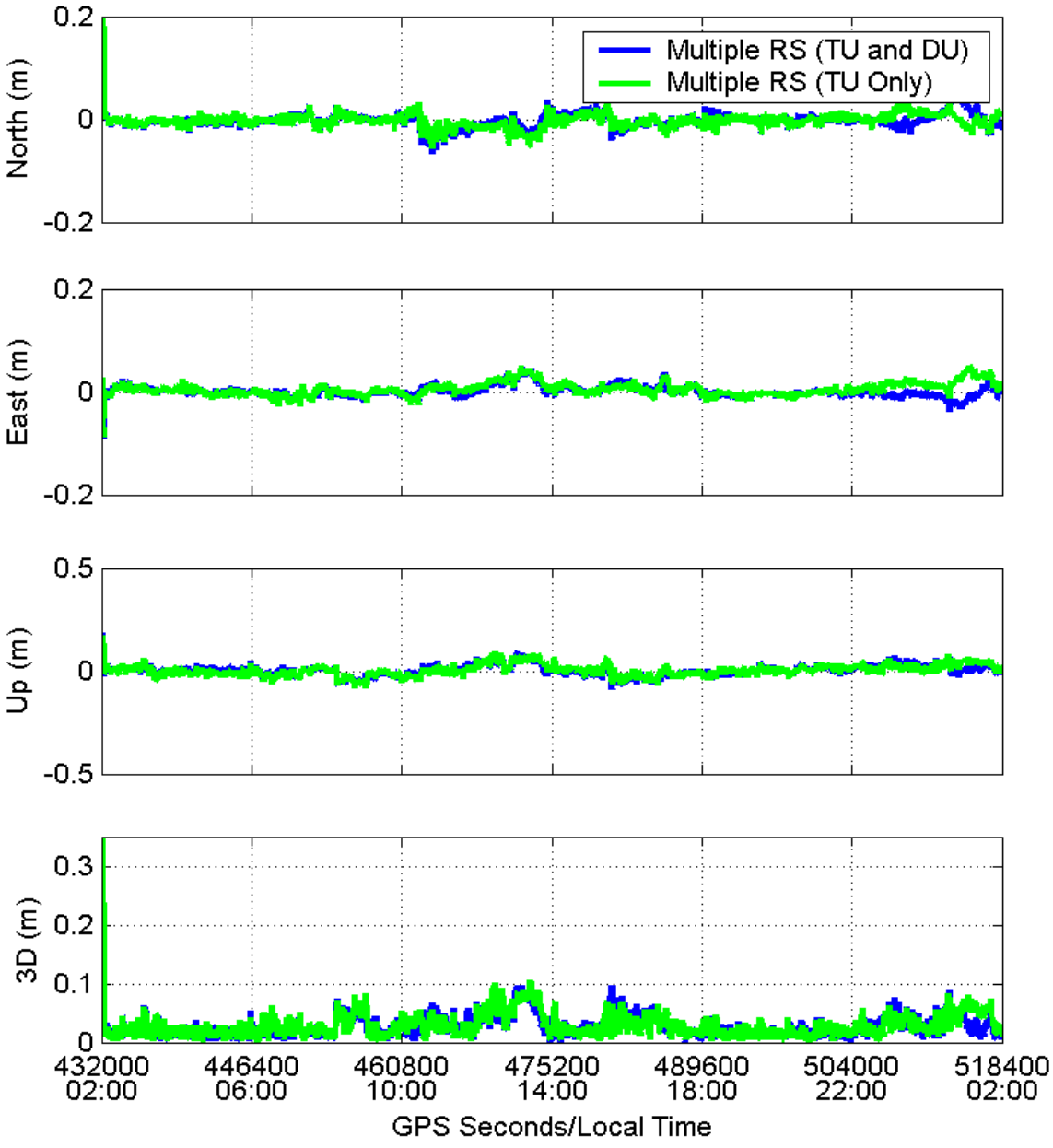

Figure 6.10: North, east, up and three dimensional position errors for tightly coupled approach with TU only as the rover and both TU and DU as rovers for Oct 26.

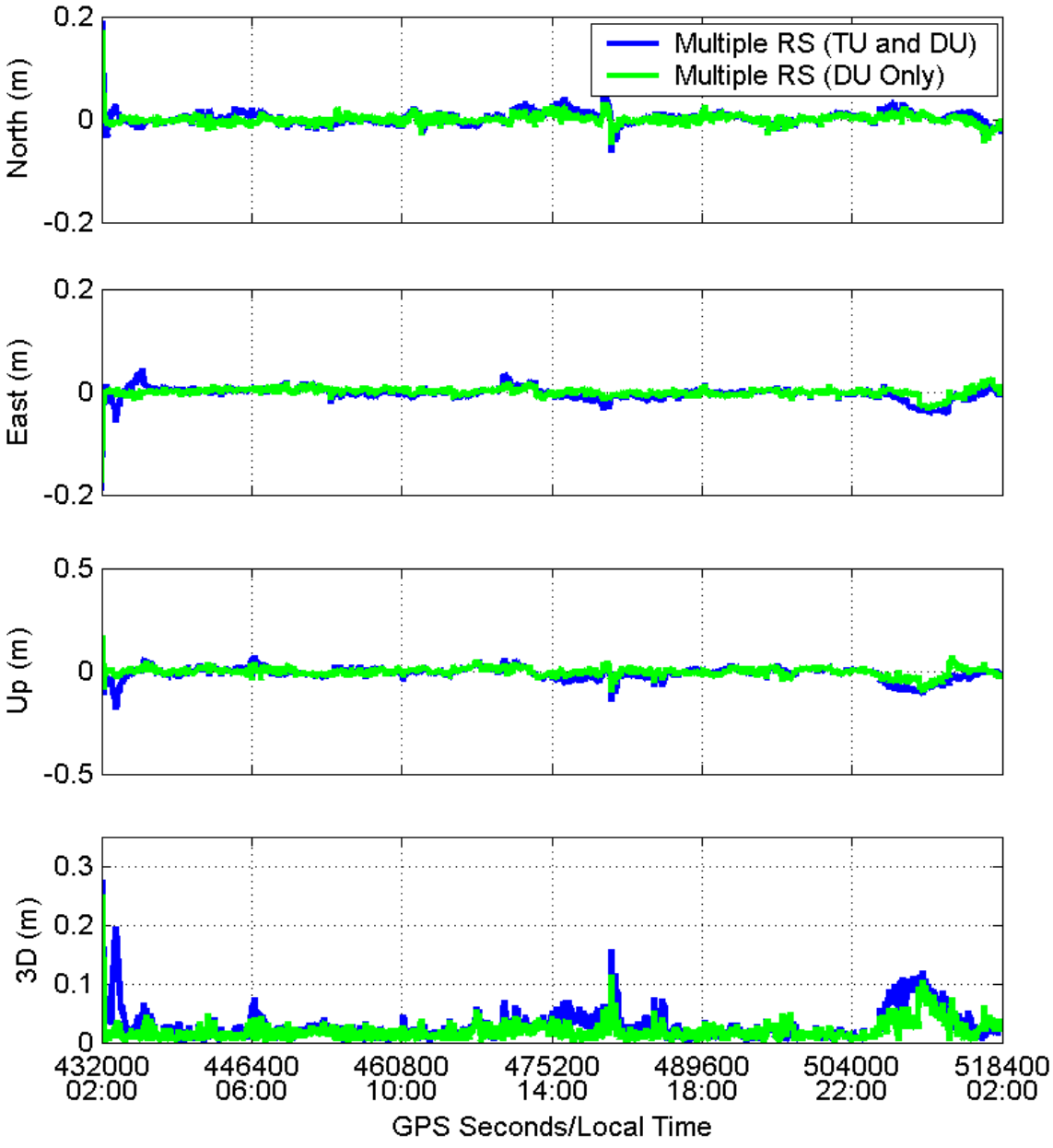

Figure 6.11: North, east, up and three dimensional position errors for tightly coupled approach with DU only as the rover and both TU and DU as rovers for Oct 26.

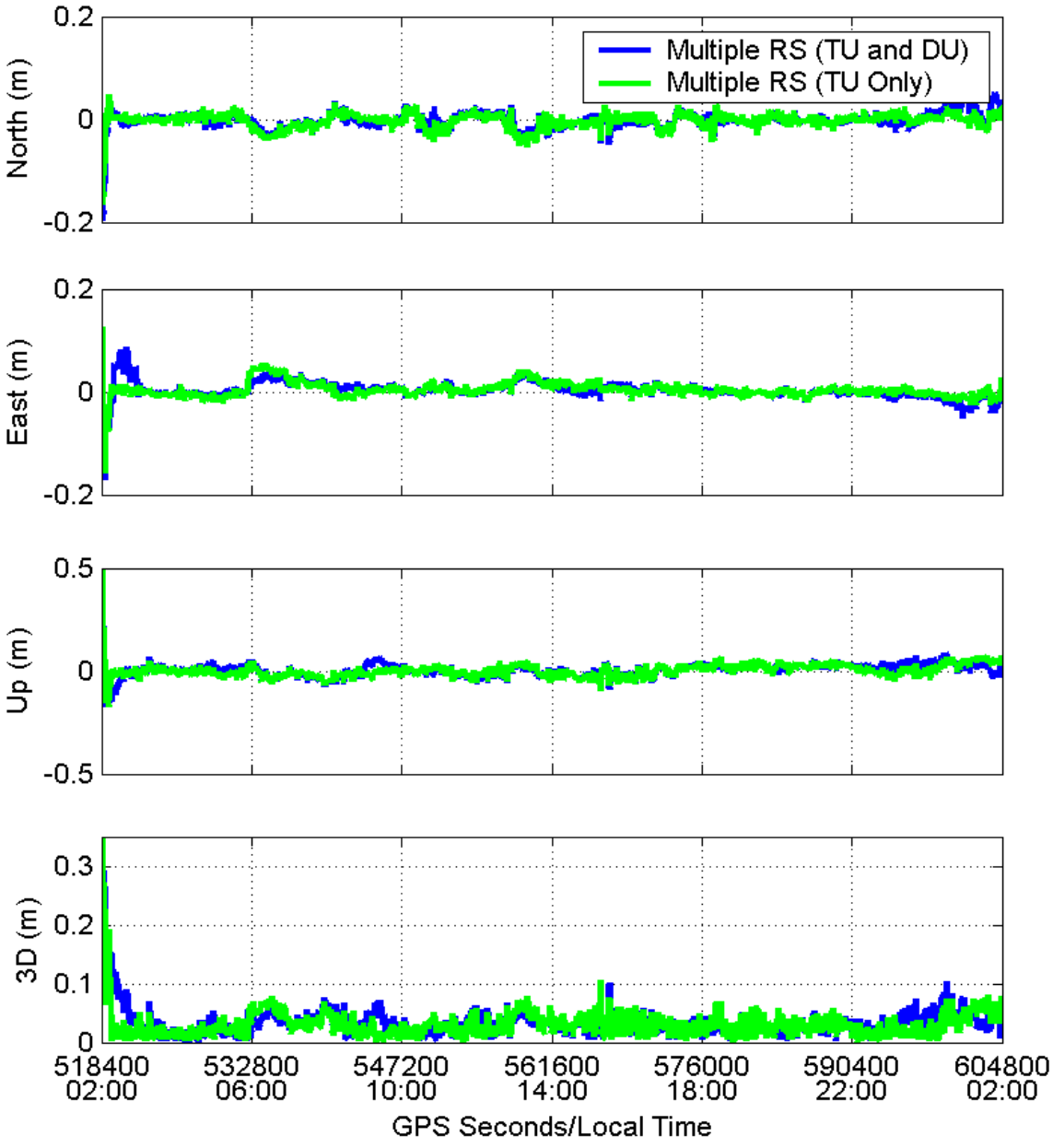

Figure 6.12: North, east, up and three dimensional position errors for tightly coupled approach with TU only as the rover and both TU and DU as rovers for Oct 27.

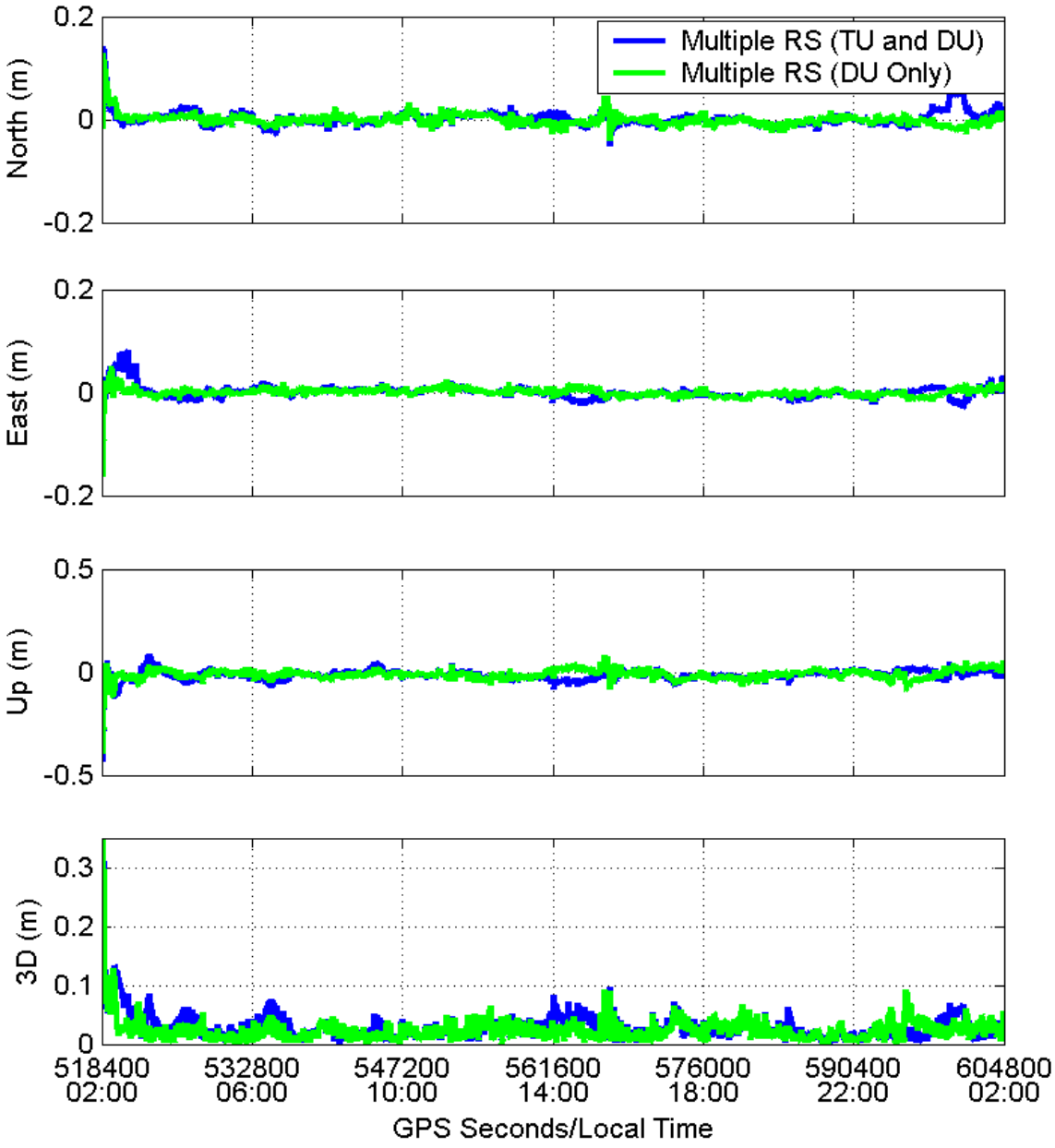

Figure 6.13: North, east, up and three dimensional position errors for tightly coupled approach with DU only as the rover and both TU and DU as rovers for Oct 27.

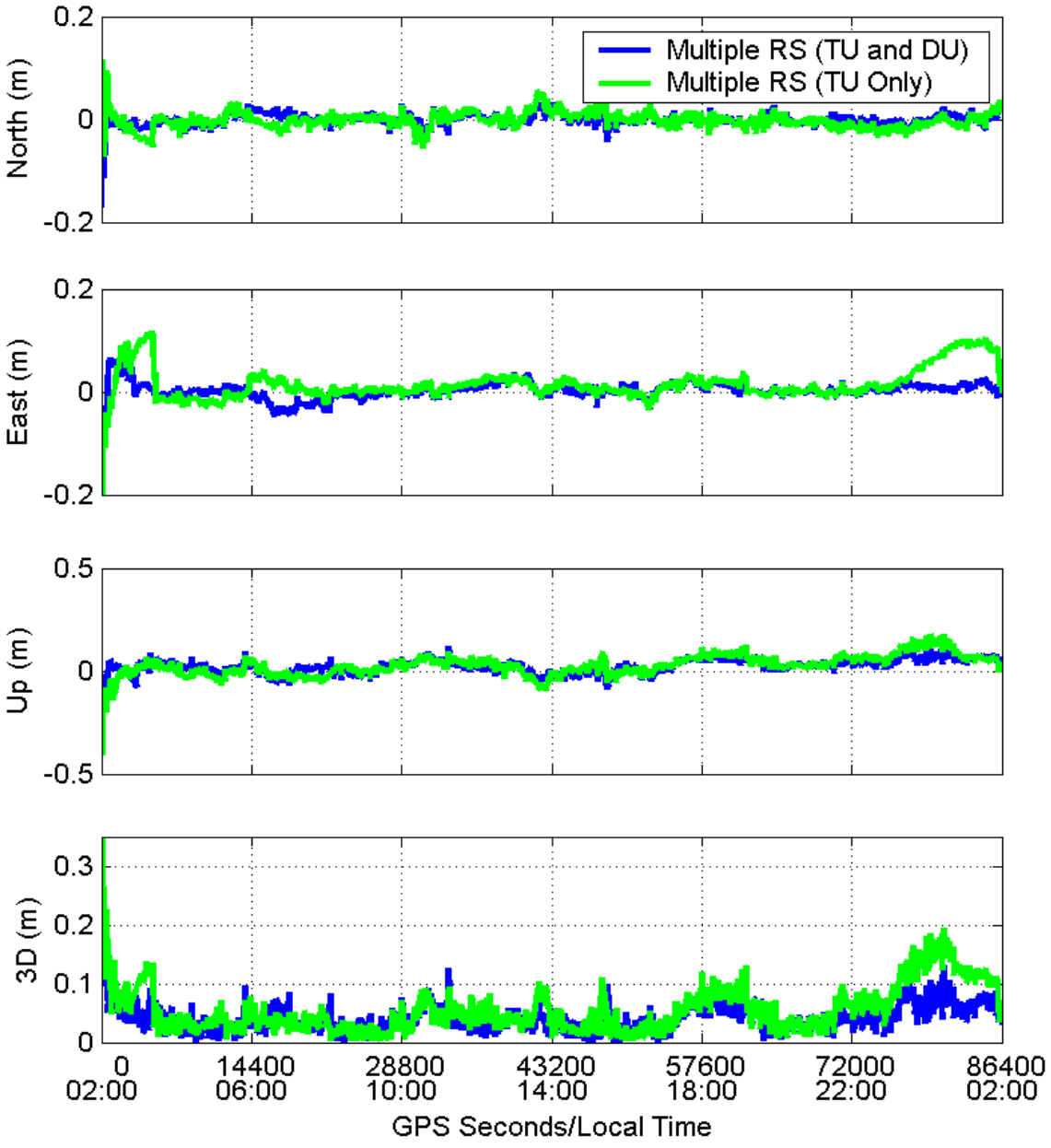

Figure 6.14: North, east, up and three dimensional position errors for tightly coupled approach with TU only as the rover and both TU and DU as rovers for Oct 28.

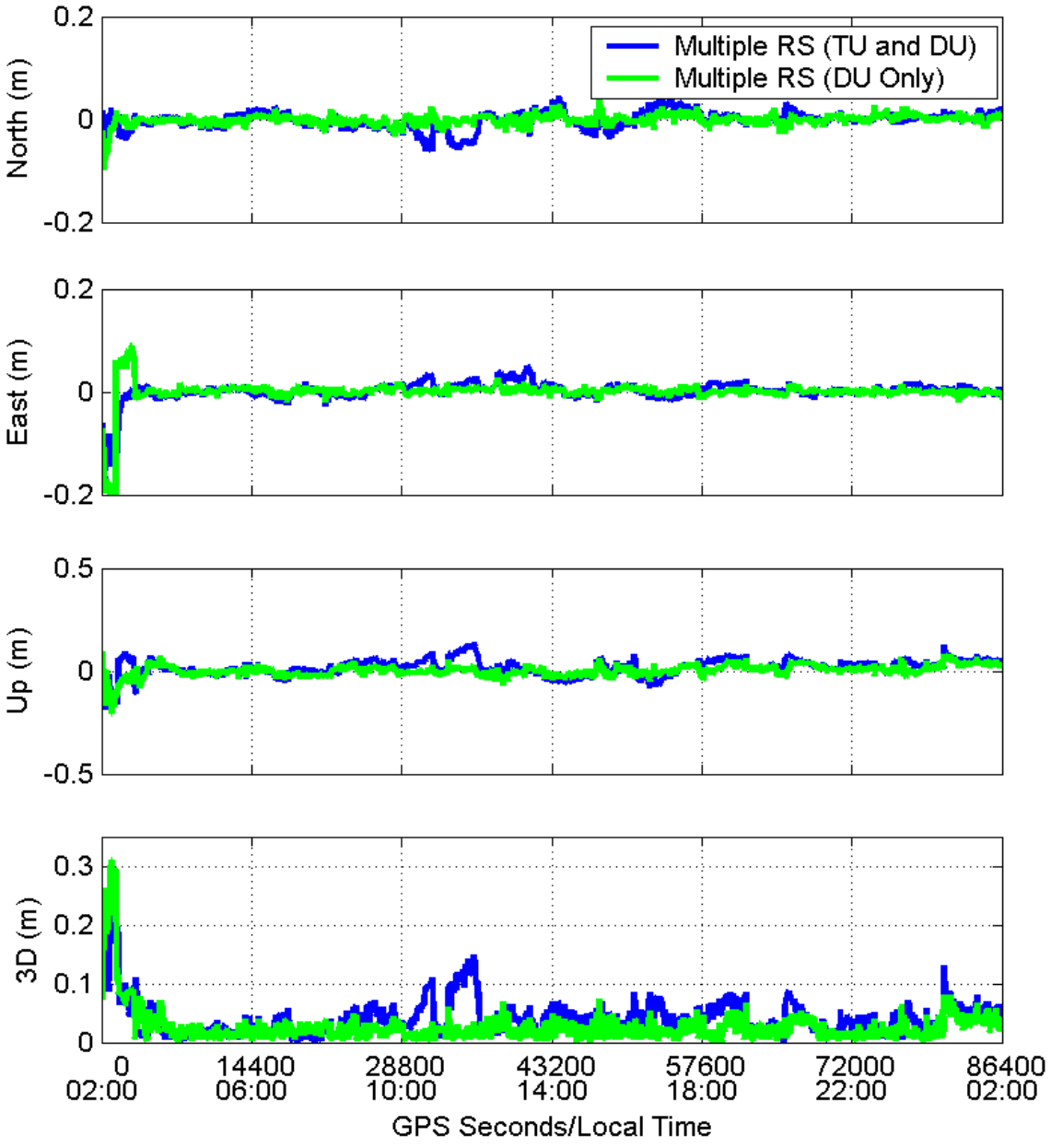

Figure 6.15: North, east, up and three dimensional position errors for tightly coupled approach with DU only as the rover and both TU and DU as rovers for Oct 28.

Table 6.7: Root mean squared relative position errors between TU and DU for the tightly coupled approach using DU only and TU only, and both TU and DU as rovers.

		TU and DU Only	Both	Percent Improvement
Oct 26	North	1.5 cm	1.6 cm	-7 %
	East	1.6 cm	1.4 cm	13 %
	Up	3.3 cm	4.3 cm	-30 %
	3D	3.9 cm	4.9 cm	-26 %
Oct 27	North	1.7 cm	1.9 cm	-12 %
	East	1.6 cm	1.7 cm	-6 %
	Up	4.2 cm	4.4 cm	-5 %
	3D	4.8 cm	5.0 cm	-4 %
Oct 28	North	1.8 cm	1.8 cm	¡ 1 %
	East	3.9 cm	2.4 cm	38 %
	Up	4.9 cm	3.8 cm	22 %
	3D	6.6 cm	4.9 cm	26 %

three days. Comparing these figures to the position errors over time shown in Figures 6.10 to 6.15 shows that there is no apparent improvement in the relative position accuracies by processing both rovers at the same time. This may be a function of the low ambiguity resolution performance for the baseline between the rovers.

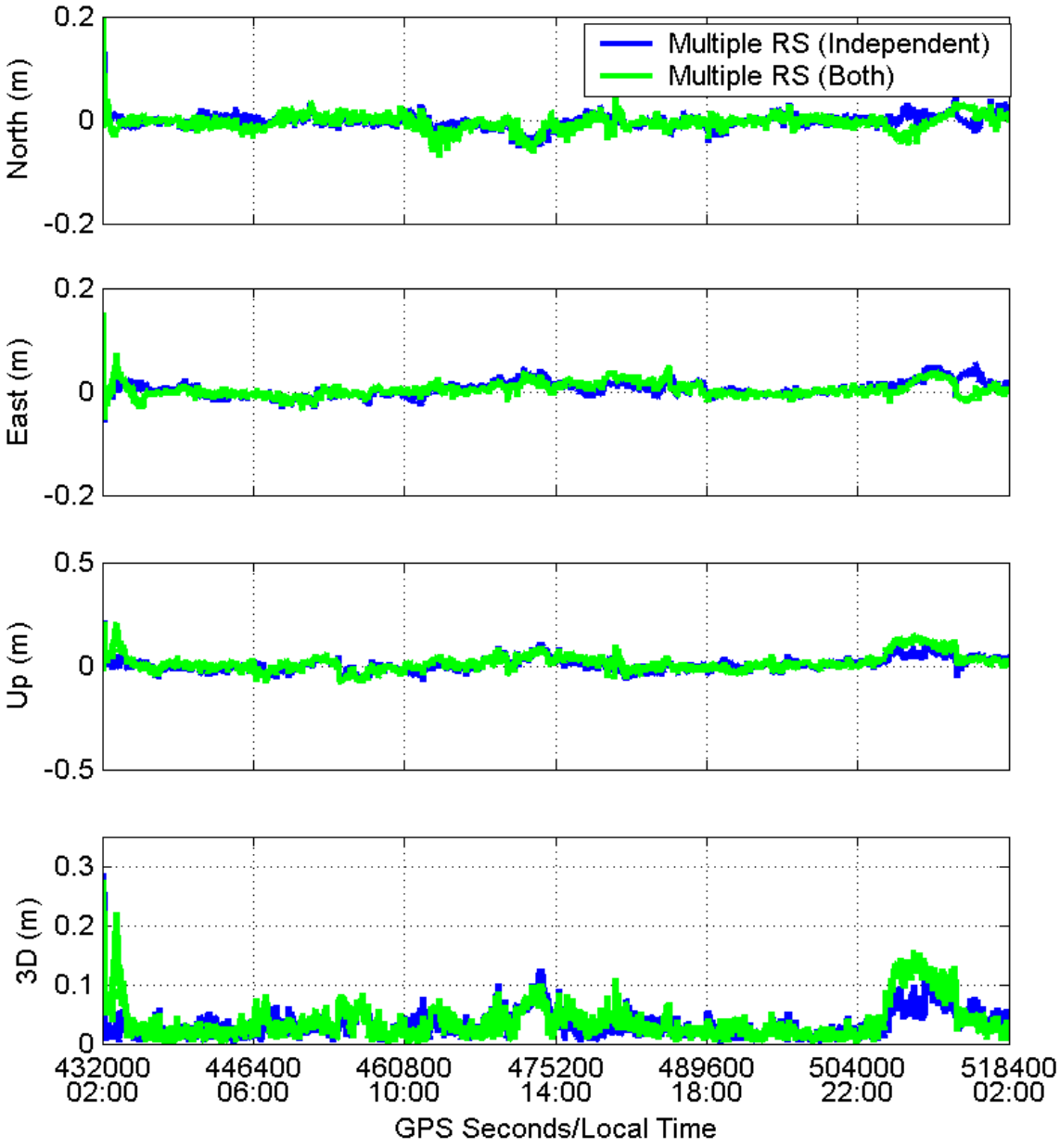

Figure 6.16: North, east, up and three dimensional relative position errors between TU and DU for the tightly coupled approach using DU only and TU only, and both TU and DU as rovers for Oct 26.

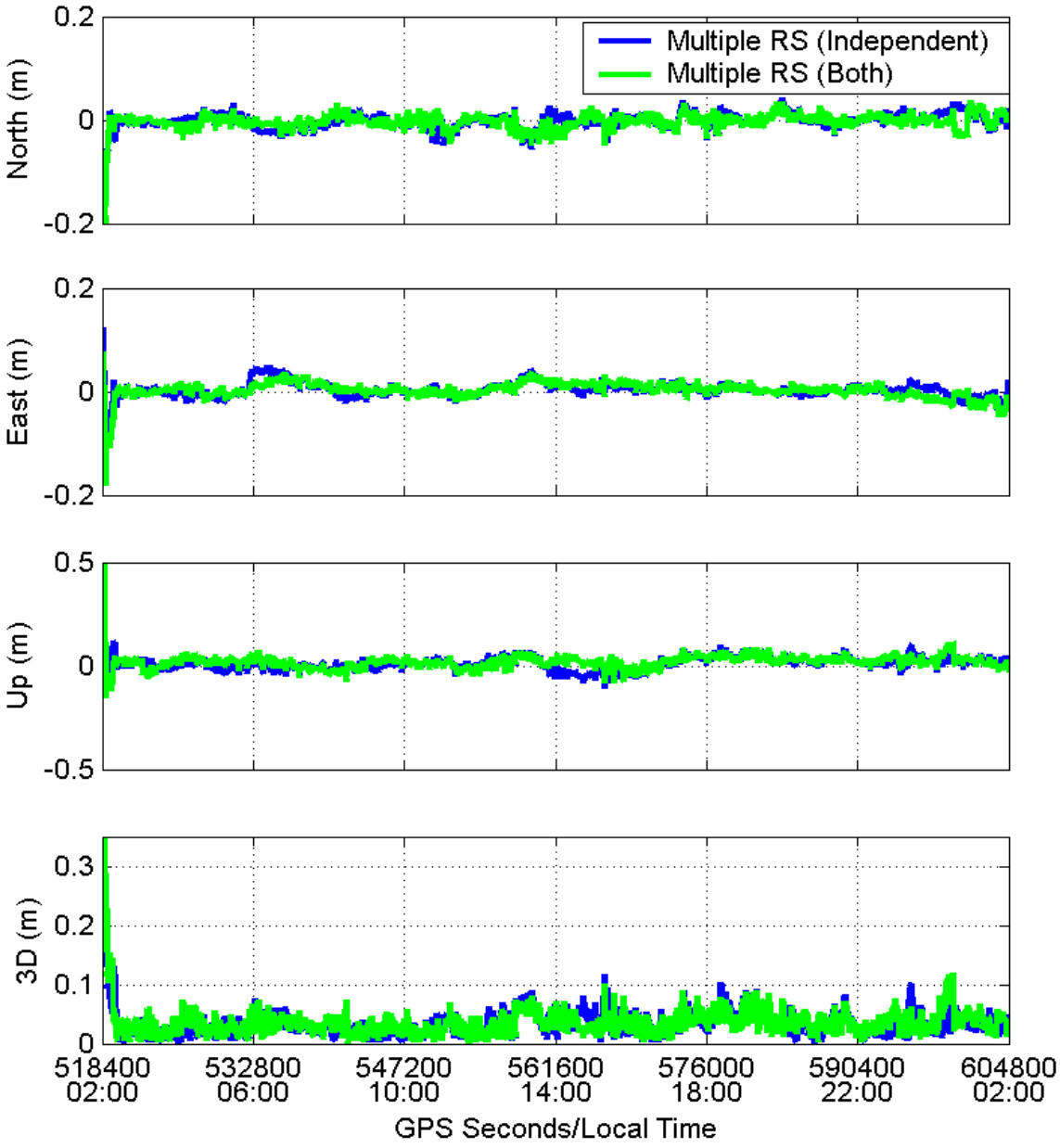

Figure 6.17: North, east, up and three dimensional relative position errors between TU and DU for the tightly coupled approach using DU only and TU only, and both TU and DU as rovers for Oct 27.

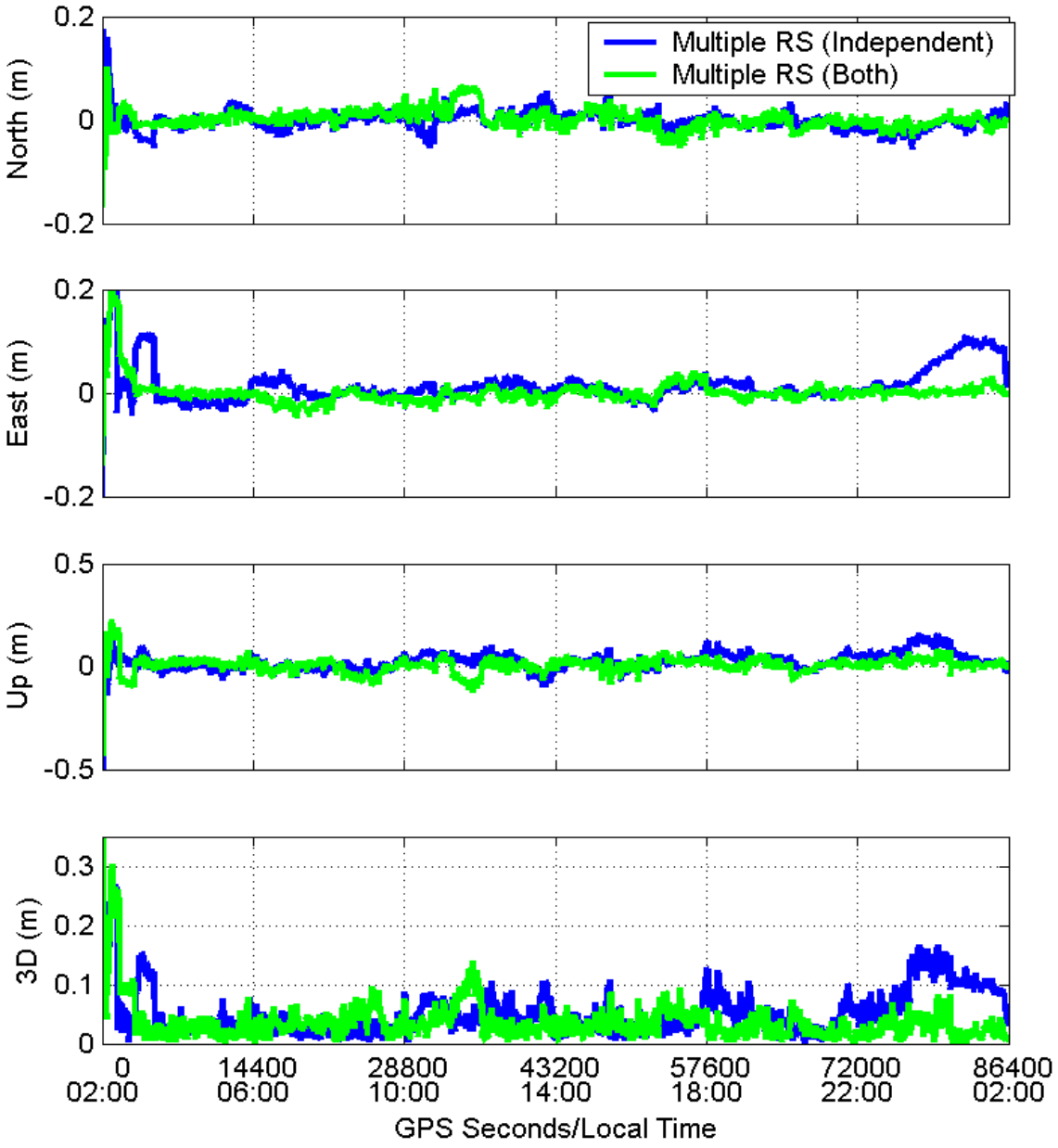

Figure 6.18: North, east, up and three dimensional relative position errors between TU and DU for the tightly coupled approach using DU only and TU only, and both TU and DU as rovers for Oct 28.

Chapter 7

Comparison of the Collocation-Based and Tightly Coupled Approaches

The two approaches discussed in this work use the same information as input to estimate the position of the rover. Although they have the same objectives and input they produce different solutions. This chapter discusses the difference between the methods and shows a comparison of them using data from a network in Southern Alberta, Canada.

7.1 Limitations of the collocation-based approach

The collocation-based approach has a few issues that limit its effectiveness. When the corrections are calculated using this approach, any errors in the network ambiguities are transferred into the corrections. This is a problem when the rover attempts to resolve ambiguities because the biases introduced by the network are not absorbed by the ambiguities. Float ambiguities in the network create non-integer biases in the measurements, and incorrect integer fixes may create long term, non-integer, ambiguities when the incorrect integer biases are interpolated to the user's location. The simple approach to solving this problem is the removal of observations with float ambiguities. Although this would resolve the problem of incorrect ambiguity biases, it may introduce availability problems. The first potential solution is to provide a single baseline observation (i.e., a correction value of zero) for observations without fixed ambiguities. Unfortunately, it is not possible to mix zero corrections with valid

undifferenced corrections because at the rover, the zero corrections will be differenced with the valid corrections to produce an incorrect, invalid correction. It is also not possible to create a correction that when differenced with the valid corrections would equal to zero because there is no way to make it equal to zero for every station in the network. This was described in more detail in Section 3.1.2.

Euler et al. (2004a) discusses the effect of integer ambiguity biases, due to incorrect ambiguities fixes, on the rover corrections as a function of the interpolating surface. In general, the surface with the fewest degrees of freedom, the linear plane surface, provided the greatest reduction of the introduced bias. This thesis does not discuss the possibility that the bias experienced by the reference station, which is ambiguity error in this case, may instead be local area atmospheric disturbances. There is a trade off between predicting the correlated errors and rejecting or reducing unwanted uncorrelated errors.

This problem is most obvious in the zero baseline case. If the network and rover are both using float ambiguities then the rover will naturally adopt the same ambiguities as the network. In general, the network is using more information to calculate these ambiguities such that this bias may be an improvement as compared to the single baseline ambiguity estimation. However, if the rover is able to resolve the ambiguities before the network then any ambiguity error in the network will become a bias in the rover observations. Assuming once again that the network ambiguities are better known than the rover's estimated ambiguities, one would expect the network to resolve ambiguities before the rover. Unfortunately, there are practical problems in validating the set of potentially fixed ambiguities, especially if the ambiguity set is particularly large or small. These problems are discussed by Julien et al. (2004) in the context of triple frequency GPS and Galileo.

7.2 Rover data assisting the network

The network data in both approaches is used to improve the estimation of the rover's parameters. In the correction-based approach (collocation-based approach) there is a one way communication between the network and rover. The network gives corrections to the rover and no information is returned. One option of the tightly coupled approach requires a two way communication system between the network and the rover. In this system the rover sends their data to the control centre, where the rover's position is calculated and sent back to the rover. Alternatively, if all the network reference station data is sent to the rover then the rover can calculate a multiple reference station solution without a centralized control centre.

With this method the rover can assist the network in estimating the network parameters, in this case ambiguities and ionosphere. With a floating position estimate the rover will likely take more information from the network than it gives back. However, this approach attempts to incorporate as much information as possible into the estimation of the network and rover parameters.

Consider for example a static rover. Initially, the rover position is unknown and therefore the rover will mainly be taking information from the network. However, as the rover position become better known, it gives equally to the adjoining baselines until its position is fixed, at which time it becomes a reference station. In the correction-based approach this static rover would never contribute to the surrounding network and surrounding rover stations.

7.3 Comparison of the collocation-based and tightly coupled approaches using SAN data

In this section data from the SAN network is used to compare the position solutions from the single reference station, collocation-based multiple reference station, and tightly coupled multiple reference station techniques. The processing approaches and performance measures are similar to those used in Chapters 5 and 6.4.

7.3.1 Network configurations

The network configuration used for the collocation-based multiple reference station test is shown in Figure 7.1. This is a medium scale network with baseline lengths ranging from 34 to 59 km. UofC is the rover station which is 24.3 km from the nearest reference station. When the rover is included in the tightly coupled approach (shown in Figure 7.2) the baseline lengths are somewhat reduced, ranging from 24 to 49 km.

7.3.2 Ambiguity resolution

Table 7.1 shows the percentage of fixed ambiguities for the three approaches. The ambiguity resolution performance for the tightly coupled approach is higher than the collocation-based approach for the common network baseline. There is an almost 40 percent difference in the percentage of fixed ambiguities for the STRA-AIRD baseline for June 8. The improvement for June 14 is slightly smaller with only a ten percent improvement. The baselines that are used are very different between the collocation-based and tightly coupled approaches so it is difficult to compare the effect that the rover baseline has on the network.

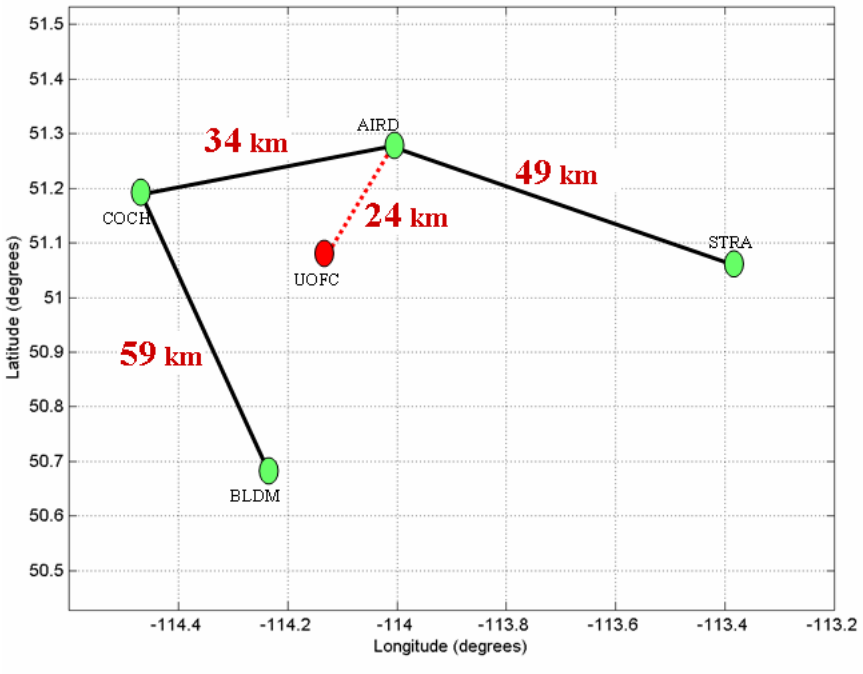

Figure 7.1: Network configuration of the SAN network used in the collocation-based approach.

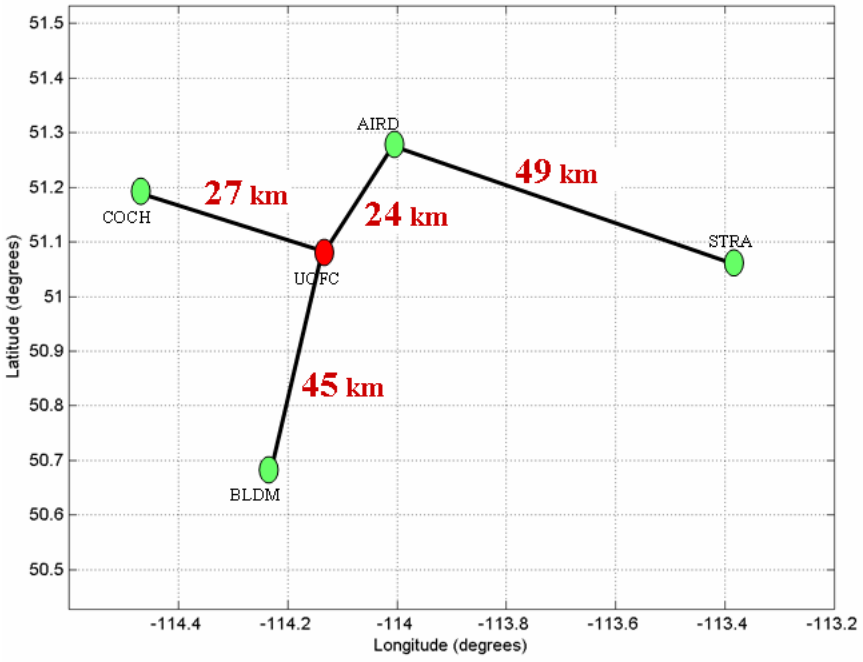

Figure 7.2: Network configuration of the SAN network used in the tightly coupled approach.

Table 7.1: Percentage of fixed ambiguities for the single reference station, collocation-based multiple reference station, tightly coupled multiple reference station approaches.

	Station 1	AIRD	COCH	AIRD	BLDM	STRA	COCH
	Station 2	UOFC	UOFC	COCH	UOFC	AIRD	BLDM
	Distance (km)	24.3	26.6	34.1	45.2	49.7	59.2
June 8	Single RS	94.6					
	Collocation-based	93.9		53.9		53.7	40.3
	Tightly coupled	91.4	59.8		83.7	93.4	
June 14	Single RS	89.1					
	Collocation-based	89.3		58.8		74.1	35.9
	Tightly coupled	93.4	80.6		74.5	84.8	

7.3.3 Position domain

Table 7.2 shows the north, east, up, and 3D RMS position error for the single reference station, collocation-based multiple reference station, and tightly coupled multiple reference station approaches. There is a progression in the level of improvement. The collocation-based approach improves the 3D position accuracy by 10 to 35 percent and the tightly coupled approach further improves the performance by improving single reference station approach by 33 to 44 percent. Both network methods provide a high level of position accuracy of better than 5 cm, 3D RMS.

This level of position accuracy and improvement due to the various methods is a function of the network scale and the environmental conditions. Changes in either the network scale or the magnitude of the environmental conditions may change the level of improvement and absolute performance of the various methods.

Figures 7.3 and 7.4 show the north, east, up and 3D position errors over time for June 8 and June 14, respectively. These show that the difference in the methods is only due to a few short time periods. Each of the methods perform well on a network of this scale and atmospheric conditions. There are few significant differences between

Table 7.2: Root mean squared position errors for the single and collocation-based multiple reference station, and tightly coupled reference station approaches for the SAN data set.

		Single RS	Collocation Based	Percent Improvement	Tightly Coupled	Percent Improvement
June 8	North	2.4 cm	1.8 cm	25 %	1.3 cm	46 %
	East	1.9 cm	1.8 cm	5 %	0.9 cm	53 %
	Up	4.6 cm	4.3 cm	7 %	3.4 cm	26 %
	3D	5.5 cm	5.0 cm	9 %	3.7 cm	33 %
June 14	North	1.9 cm	2.1 cm	-11 %	1.4 cm	26 %
	East	2.5 cm	1.3 cm	48 %	0.9 cm	64 %
	Up	5.2 cm	3.1 cm	40 %	3.0 cm	42 %
	3D	6.1 cm	4.0 cm	34 %	3.4 cm	44 %

the solutions.

7.3.4 Convergence analysis

The convergence of the positioning filter is an important criteria for GPS users in the field. The convergence time is the time required for a user to wait before achieving the highest available position accuracy. The convergence is tested through a series of one hour trials. The rover processing is restarted every hour and the initial position error is reset to one meter of error. The results from these trials are averaged to produce the results shown in Figure 7.5. All of the methods show the expected convergence behaviour. The collocation-based approach converges generally faster than the single reference station approach and the tightly coupled approach is clearly the best approach in terms of convergence.

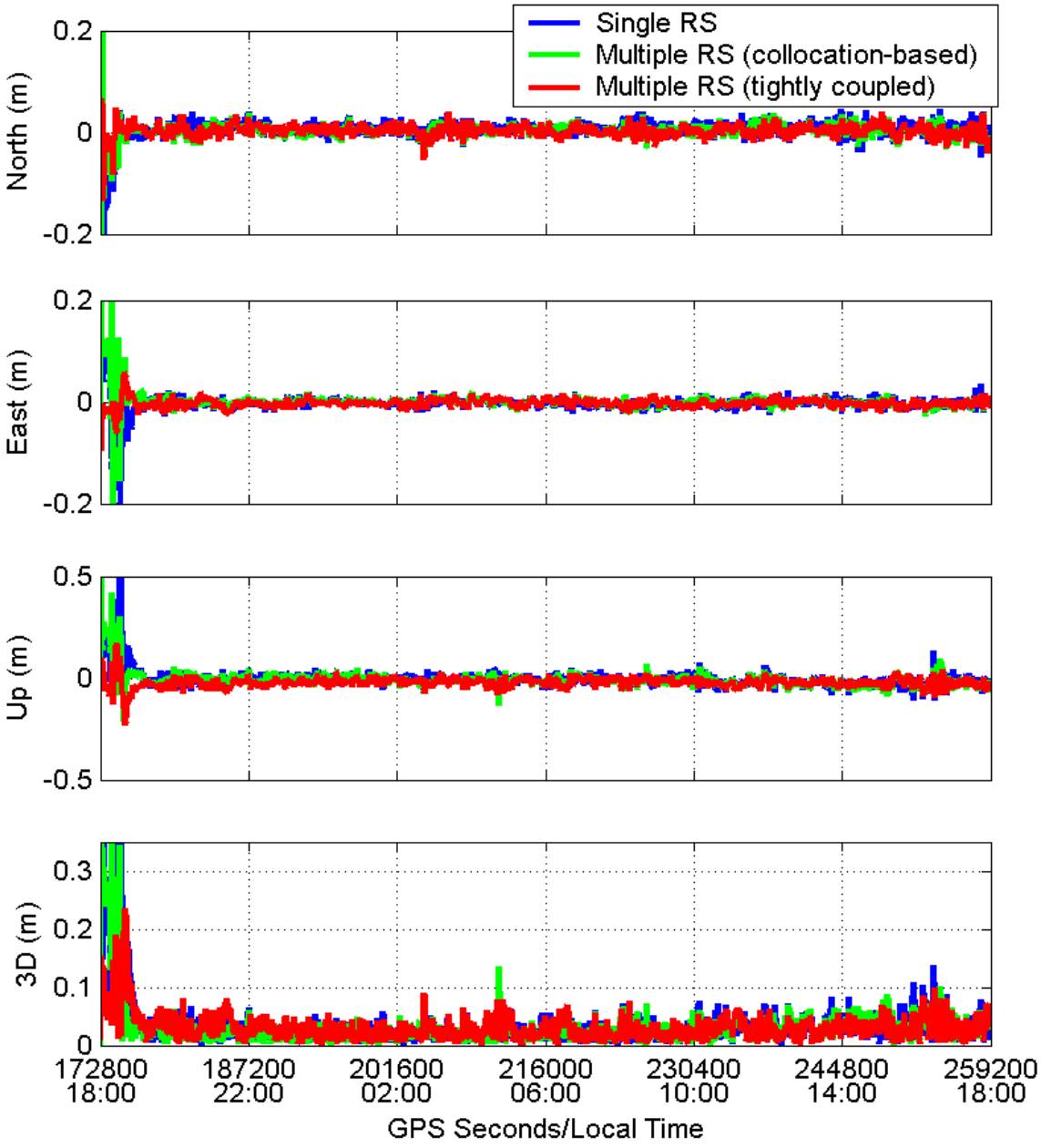

Figure 7.3: North, east, up and three dimensional position errors for single reference station, collocation-based multiple reference station, and tightly coupled multiple reference station approaches for June 8.

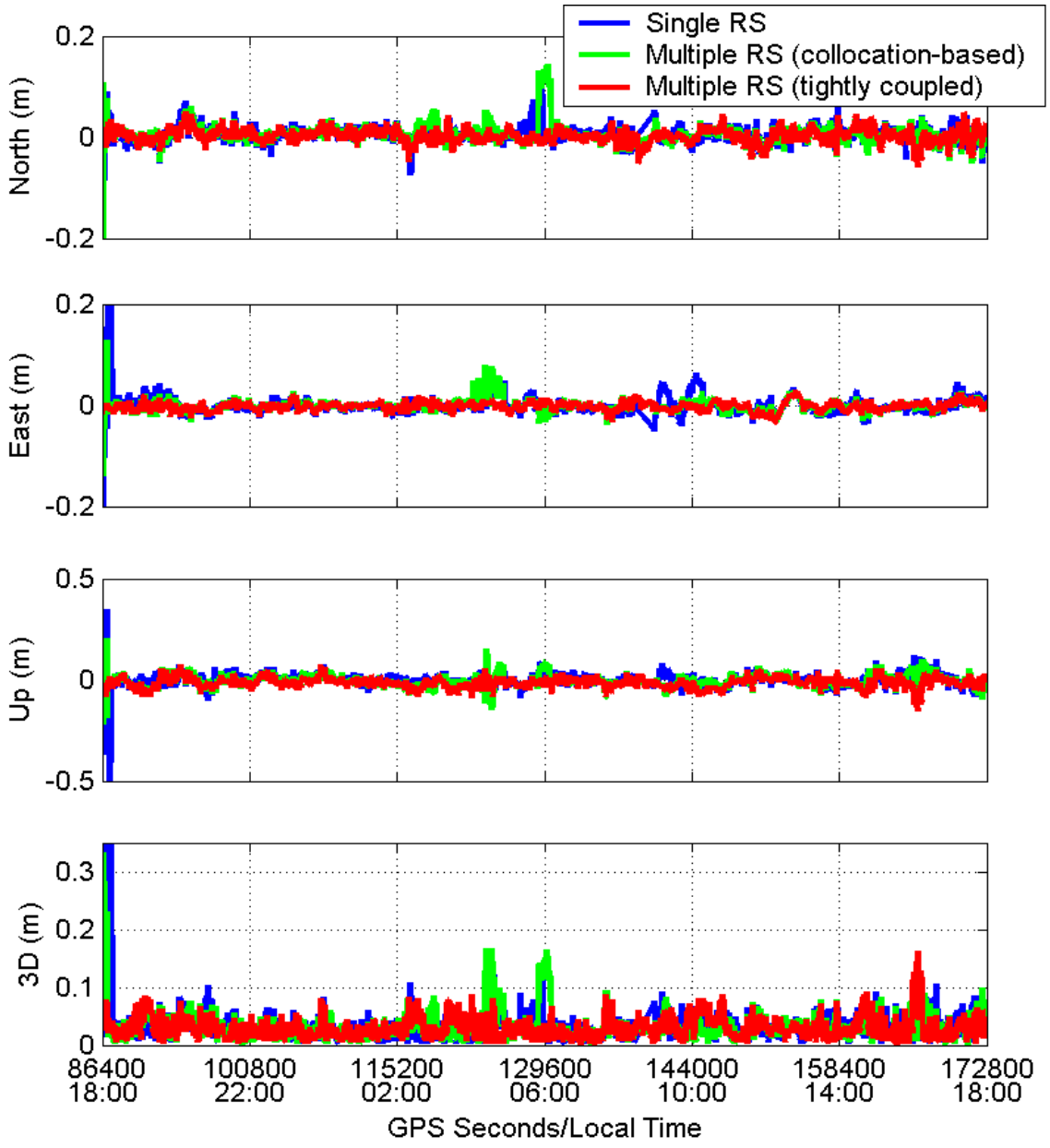

Figure 7.4: North, east, up and three dimensional position errors for single reference station, collocation-based multiple reference station, and tightly coupled multiple reference station approaches for June 14.

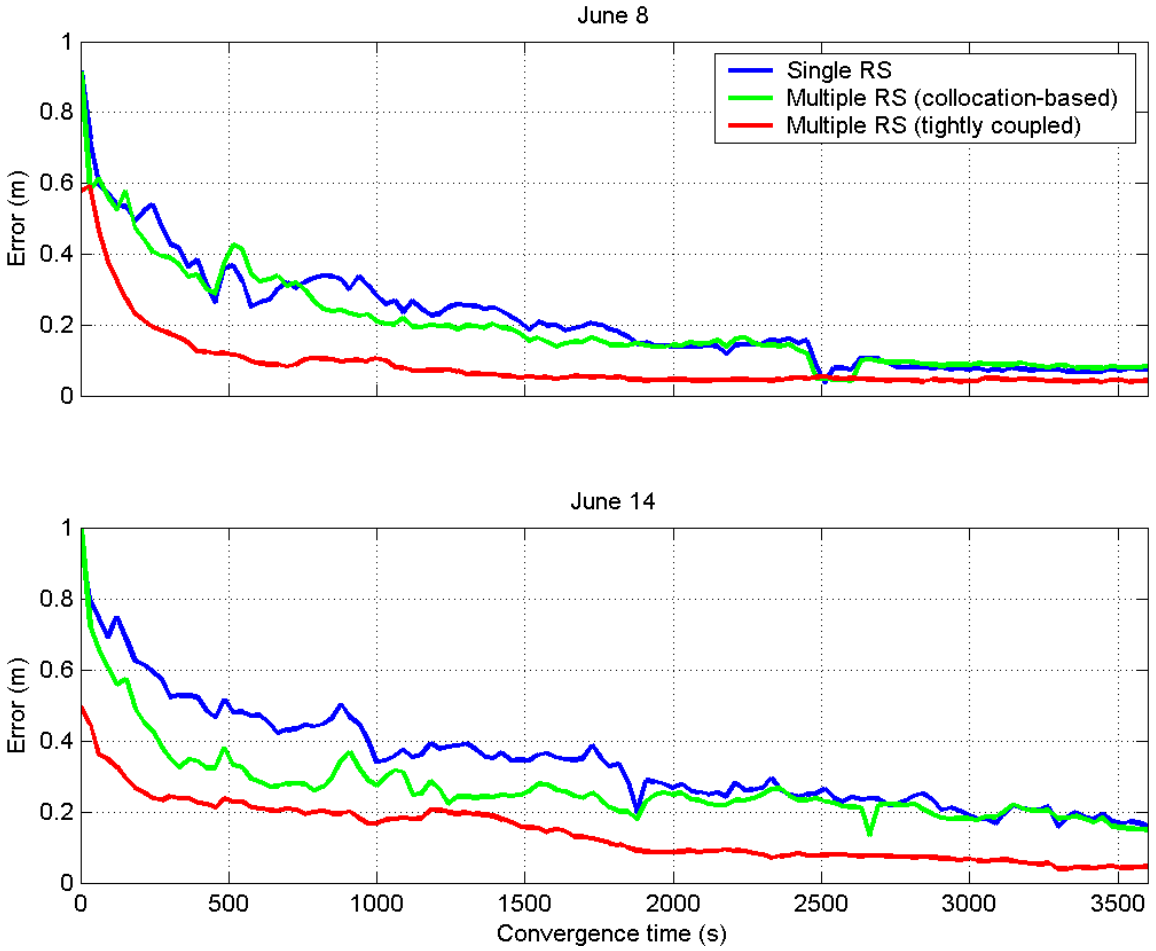

Figure 7.5: Average convergence for the single reference station, collocation-based multiple reference station, and tightly coupled multiple reference station approaches for the SAN network.

Chapter 8

Conclusions and Recommendations

8.1 Conclusions

This thesis derives two methods for multiple reference station positioning. The two main methods are a collocation-based multiple reference station technique (Chapter 4), which requires the definition of a covariance function (Chapter 3), and a tightly coupled multiple reference station technique (Chapter 6). This section summarizes the results of these methods.

8.1.1 Adaptive covariance function

The backbone of least squares estimation and collocation is the variance covariance matrix of the observations. In least squares estimation this matrix is used to weight the measurements. The relative measurement weighting defines the variance covariance matrix of the estimated parameters including the float ambiguities. The estimated variance covariance matrix of the float ambiguities are used for the LAMBDA decorrelation.

The values of the covariance matrix can be determined using a covariance function, which defines the covariance between measurements given a set of deterministic parameters. The covariance function is essential for least squares collocation because the signals of the control points are predicted without observing the signal at the prediction point. Although the covariance function is an important component, the performance of the least squares prediction is insensitive to the covariance function

used. The covariance function is a method for determining the covariance between two measurements without the values of the measurements.

In this work a covariance function form is proposed and the coefficients of the covariance function are estimated using a real-time method. This adaptive covariance function allows the covariance function model to tune to changing spatial and temporal error characteristics.

The adaptive covariance between two observations was modelled as a function of the distance between the ionosphere pierce points for the ionosphere, and the distance between two receivers and the great circle angle between two observations for the troposphere. This is shown in the consecutive days for the MAGNET network in Turkey. This estimated parameters follow expected daily variations for an equatorial region network. The covariance function is validated by comparing the double difference variance as computed by the covariance function to the variance of the measurement errors. This shows that the covariance function can effectively model the double difference measurement errors.

Although the coefficients of the covariance function can be estimated in real-time to generate valid double difference variances, the absolute value of the parameters is weakly observable because the single observation parameters are estimated by double difference residuals. A test shows that although varying initial conditions changes the absolute estimate of the covariance function coefficients, all solutions provide valid double difference variances.

This was used in all of the single and multiple reference station solutions, which all provide a high level of position accuracy. There are apparent observability problems with this method, therefore it is only recommended for use with a reference station network, where many observations of the measurement errors are available. Although,

the measurement residuals would be successfully tracked with this method, the effect of blunders or estimation errors, especially in the roving position, could cause either more or less measurement errors to be represented in the covariance function than are actually present in the measurements.

8.1.2 Collocation-based multiple reference station approach

The next method described in this work is the development of a collocation-based multiple reference station approach. This method uses the state vector and variance-covariance matrix from the ambiguity estimation and resolution stage to predict the errors of the reference stations to the measurements of a rover receiver within or around the network. This produces a vector of single observation (undifferenced) corrections and the variance-covariance matrix of the corrections. A method for applying the corrections and the variance covariance matrix of the corrections is also shown. The estimated variance covariance of the float and fixed ambiguities and the estimated variance covariance of the estimated corrections were not used in previous work.

The collocation-based multiple reference station approach is an effective method of predicting the measurement residuals of the network to the rover measurements. The estimated corrections are effective in reducing the measurement errors at the rover and improving position accuracy. Once again, this is tested using three consecutive days from the MAGNET network.

The network corrections provide a significant level of improvement relative to the single reference station solution in the observation, and position domains. The L1 phase measurement errors are reduced by 16 percent on average, a majority of which is due to a reduction of the ionosphere components of the measurement errors.

The 3D position accuracy is improved by 24 percent on average, which is significant. There is only a significant increase in the percentage of rover ambiguities resolved for the first of the three days of data of 21 percent.

8.1.3 Tightly coupled multiple reference station approach

The third method introduced in this work is the tightly coupled approach to multiple reference station positioning. This approach includes the rover's measurements and estimated parameters into the network filter. No corrections are calculated and there is no prediction step in this approach. This method is also tested using three consecutive days from the MAGNET network.

The tightly coupled approach provides a high level of improvement relative to the single reference station approach in the position domain in most cases. On average for both rovers (TU and DU), the tightly coupled method reduces 3D position RMS errors by 44 percent.

This chapter also discusses the ability of estimating two rovers in the same filter to improve positioning accuracy. The estimation of two rovers can improve the position accuracy for some of the rovers, however, in general the estimation of multiple rovers decreases the position accuracy relative to estimating them independently. Both solutions provide extremely high position accuracies for these baseline lengths.

This approach has been shown to provide sufficient accuracy to be used for precise deformation monitoring (Pugliano et al., 2004).

It is interesting to note that for one data set the tightly coupled approach performed worse than the single reference station approach, however the multiple reference station approach performed better than the single reference station approach when estimating multiple rovers. Every test using multiple rovers perform better than

the single reference station approach, even though in general the position solutions are slightly worse when estimating multiple rovers. The difference between the two solutions may be a matter of reliability more than accuracy. Once again, further tests are suggested to expose these properties.

The relative position accuracy between the two rovers was also compared, unfortunately these tests are not able to conclusively show the effect of estimating multiple rovers on relative position accuracy.

8.1.4 Comparison of the collocation-based and tightly coupled multiple reference station approach

The collocation-based and tightly coupled approaches ultimately have the same objective: to accurately estimate the rover position. Chapter 7 compares the two approaches in terms of the use of information. The tightly coupled approach allows for a greater sharing of information than the collocation-based approach because the rover information is available to the reference station network. This is likely the reason for the differences in the solutions. These methods are compared using the SAN network.

Tests show that the there is an apparent stepwise progression in performance between the methods. The single reference station approach produced a 3D position accuracy of slightly less or better than 6 cm. This is improved by the collocation-based multiple reference station approach by 35 percent, which reduces the 3D position RMS to 3.9 cm. This is further improved by the tightly coupled approach, which gives a 3D position RMS of 3.4 cm (or 43 percent relative to the single reference station approach).

The difference in the methods is due to the sharing of available information and data. The single reference station approach using only a small subset of all the data

available. The collocation-based approach improves performance by using the data from all of the reference stations to predict the corrections for the rover's data. The tightly coupled approach further improves the position accuracy by including the rover data in combined network adjustment.

The above conclusions are valid for the data used herein. Given that many parameters affect performance, including the inter-station distance, the level of ionospheric activity and the geometry and number of satellites available, one has to be very careful in extending these findings to other cases. Alves and Lachapelle (2004) shows similar performance using the Southern Alberta Network over a wider variety of atmospheric activity.

8.2 Recommendations for future work

Multiple reference station positioning is a complex research topic that involves many layers of information, methods, and processing. Consequently, there is almost an endless amount of additional research that can be conducted in this field. This section describes a few potential extensions of this research.

8.2.1 Prediction for initialization of the ionosphere

The collocation-based prediction can be further utilized for both the collocation-based and tightly coupled approaches. Stochastic ionosphere modelling is used in both the collocation-based and tightly coupled methods. The network data can be used to predict the ionosphere for a new satellite. In this case the new satellite does not yet have residuals so there is no feedback loop of the residuals to the corrections. The predicted ionosphere for the new satellite can be estimated along with the estimated variance of the predicted ionosphere. The predicted value is likely much better than

initializing the ionosphere with a value of zero with an arbitrary variance.

In order for the network to predict the measurement errors of a new, low elevation satellite, the covariance function must be able to calculate the covariance between two satellites at the same station. Although the covariance function presented in this thesis is acceptable, covariance functions that are only a function of baseline length would not be acceptable.

8.2.2 Characterizing the effectiveness of the predictions

Further research could be conducted as to the parameters that affect the effectiveness of the multiple reference station predictions. This characterizing of the would involve processing multiple reference station data for a variety of baseline lengths, network configurations and environmental conditions. A detailed evaluation of the parameters affecting multiple reference station performance would be useful for design of reference station networks or integrity monitoring and notification.

8.2.3 Relative positioning of multiple rovers

The tightly coupled approach can be used to estimate the positions of multiple rovers at the same time. Tests from this work are inconclusive as to whether or not processing the rovers in the same filter affects the relative position accuracy of the rovers. Further tests may conclusively show wether or not the tightly coupled approach can affect relative position accuracy. This should be tested for rovers that are connected by a baseline and rovers that are only connected to the reference station network.

8.2.4 External filtering of network corrections

Fortes (2002) shows a method of applying a Kalman filter to the corrections to improve the accuracy of the corrections when a satellite is setting and the satellite is slowly observed by fewer and fewer baselines. With the addition of this research, the network corrections could be filtered using the variance-covariance estimate of the corrections. This could further improve the accuracy for setting satellites. An external filter approach would also help to reduce discontinuities in the corrections. These discontinuities may cause the rover receiver to perceive cycle slips using the phase rate method. This filtering would assist in reducing the discontinuities and the likelihood that the rover will detect a cycle slip.

References

Alves, P. and G. Lachapelle (2004) A Comparison of Single Reference Station, Correction-Based Multiple Reference Station and Tightly Coupled Methods using Stochastic Ionospheric Modelling. *CD-ROM Proceedings of the International Symposium on GPS/GNSS, (December 2004, Sydney, Australia)*, 16 pages.

Alves, P., G. Lachapelle, M. E. Cannon, J. Liu, and B. Townsend (2001) Evaluation of Multiple-Reference DGPS RTK Using a Large Scale Network. *Proceedings of the National Technical Meeting of the Institute of Navigation, ION NTM/2001 (January 2001, Long Beach, USA)*, 665 – 671. Institute of Navigation.

Brown, R. G. and P. Y. C. Hwang (1997) *Introduction to Random Signals and Applied Kalman Filtering*. John Wiley & Sons, Inc., third edition.

Cannon, M. E., G. Lachapelle, P. Alves, L. P. Fortes, and B. Townsend (2001a) GPS RTK Positioning Using a Regional Reference Network: Theory and Results. *Proceedings of the Global Navigation Satellite Systems Conference (May 2001, Seville, Spain)*. Global Navigation Satellite Systems.

Cannon, M. E., G. Lachapelle, L. P. Fortes, P. Alves, and B. Townsend (2001b) The Use of Multiple Reference Station VRS For Precise Kinematic Positioning. *Proceedings of the Japan Institute of Navigation, GPS Symoposium (November 2001, Tokyo, Japan)*, 29 – 37. Japan Institute of Navigation.

Chen, K. (1994) *Developement of a Fast Ambiguity Search Filtering (FASF) Method of GPS Carrier Phase Ambiguity Resolution*. Ph.D. thesis, University of Calgary. URL `http://www.geomatics.ucalgary.ca/`

Dai, L., S. Han, J. Wang, and C. Rizos (2004) Comparison of Interpolation Algorithms in Network-Based GPS Techniques. *Navigation*, 50(4), 277 – 293.

de Jonge, P. and C. Tiberius (1996) The LAMBDA method for integer ambiguity estimation: implementation aspects. *Publications of the Delft Geodetic Computing Centre*, (12).

Erickson, C. (1992) *Investigations of C/A Code and Carrier Measurements and Techniques for Rapid Static GPS Surveys*. Master's thesis, University of Calgary. URL `http://www.geomatics.ucalgary.ca/`

Euler, H. J., C. R. Keenan, B. E. Zebhauser, and G. Wübbena (2001) Study of a Simplified Approach in Utilizing Information from Permanent Reference Station Arrays. *Proceedings of the National Technical Meeting of the Satellite Division of the Institute of Navigation, ION GPS/2001 (January 2001, Salt Lake, USA)*, 379 – 391. Institute of Navigation.

Euler, H.-J., S. Seeger, and F. Takac (2004a) Influence of Diverse Biases on Network RTK. *Proceedings of the National Technical Meeting of the Satellite Division of the Institute of Navigation, ION GNSS/2004 (September 2004, Long Beach, USA)*. Institute of Navigation.

Euler, H. J., S. Seeger, O. Zelzer, T. Takac, and B. E. Zebhauser (2004b) Improvement of Positioning Performance Using Standardized Network RTK Messages. *Proceedings of the National Technical Meeting of the Satellite Division of the Institute of Navigation, ION GPS/2004 (January 2004, San Diego, USA)*, 453 – 461. Institute of Navigation.

Fortes, L. P., M. E. Cannon, and G. Lachapelle (2000a) Testing a Muilti-Reference GPS Station Network for OTF Positioning in Brazil. *Proceedings of the 13th International Technical Meeting of the Satellite Division of the Institute of Navigation, ION GPS/2000 (September 2000, Salt Lake City, USA)*, 1133 – 1143. Institute of Navigation.

Fortes, L. P., M. E. Cannon, S. Skone, and G. Lachapelle (2001) Improving a Multi-Reference GPS Station Network Method for OTF Positioning in the St. Lawrence Seaway. *Proceedings of the 14th International Technical Meeting of the Satellite Division of the Institute of Navigation, ION GPS/2001 (September 2001, Salt Lake City, USA)*, 404 – 414. Institute of Navigation.

Fortes, L. P., G. Lachapelle, M. E. Cannon, G. Marceau, S. Ryan, S. Wee, and J. Raquet (1999) Testing of a Multi-Reference GPS Station Network for Precise 3D Positioning in the St. Lawrence Seaway. *Proceedings of the National Technical Meeting of the Satellite Division of the Institute of Navigation, ION GPS/1999 (September 1999, Nashville, USA)*, 1259 – 1269. Institute of Navigation.

Fortes, L. P., G. Lachapelle, M. E. Cannon, S. Ryan, G. Marceau, S. Wee, and J. Raquet (2000b) Use of a Multi-Reference GPS Station Network For Precise 3D Positioning in Constricted Waterways. *International Hydrographic Review*, 1(1), 15 – 29.

Fortes, L. P. S. (2002) *Optimising the Use of GPS Multi-Reference Stations for Kinematic Positioning*. Ph.D. thesis, University of Calgary.
URL `http://www.geomatics.ucalgary.ca/`

Fotopoulos, G. (2000) *Parameterization of DGPS Carrier Phase Errors Over a Regional Network of Reference Stations*. Master's thesis, University of Calgary.
URL `http://www.geomatics.ucalgary.ca/`

Gelb, A. (1974) *Applied Optimal Estimation*. The M.I.T. Press, Massachusetts Institute of Technology, Cambrigde, Massachusetts. 16th Printing.

Gertler, J. J. (1998) *Fault Detection and Diagnosis in Engineering Systems*. Marcel Dekker, Inc.

Goad, C. C. and L. Goodman (1974) a Modified Hopfield Tropospheric Refraction Correction Model. *Proceedings of the Geophysical Union (December 1974, San Francisco, USA)*.

Grimmett, G. and D. Stirzaker (2001) *Probability and Random Processes*. Oxford University Press, third edition.

Joosten, P. and C. Tiberius (2000) Fixing the Ambiguities, Are You Sure They're Right? *GPS World*, 46 – 51.

Julien, O., M. E. Cannon, P. Alves, and G. Lachapelle (2004) Triple Frequency Ambiguity Resolution Using GPS/GALILEO. *European Journal of Navigation*, 2(2), 51 – 57.

Kennedy, S. L. (2002) *Acceleration Estimation from GPS Carrier Phases for Airborne Gravimetry*. Master's thesis, University of Calgary.
URL `http://www.geomatics.ucalgary.ca/`

Klobuchar, J. A. (1996) Ionospheric Effects on GPS. B. W. Parkinson and J. J. Spilker, Jr., eds., *Global Positioning System: Theory and Applications*, volume 1, chapter 12, 486 – 516. American Institute of Aeronautics and Astronautics, Inc., Washington D.C., USA.

Koch, K.-R. (2000) *Introduction to Bayesian Statistics*. Springer-Verlag Berlin Heidelberg. English translation.

Krakiwsky, E. J. (1990) The Method of Least Squares: A Synthesis of Advances. Technical report, UCGE Reports Number 10003, Department of Geomatics Engineering, University of Calgary.

Krakiwsky, E. J. and M. A. Abousalem (1995) Adjustment of Observations. Technical report, UCGE Reports Number 10015, Department of Geomatics Engineering, University of Calgary.

Lachapelle, G. and P. Alves (2002) Multiple Reference Station Approach: Overview and Current Research, Invited Contribution, Expert Forum. *Journal of Global Positioning Systems*, 1(2), 133 – 136.

Lachapelle, G., C. Liu, and G. Lu (1993) Quadruple Single Frequency Receiver System for Ambiguity Resolution on the Fly. *Proceedings of the International Technical Meeting of the Satellite Division of the Institute of Navigation, ION GPS/03 (September 1993, Salt Lake City, USA)*, 1167 – 1172.

Landau, H., U. Vollath, and X. Chen (2002) Virtual Reference Station Systems, Invited Contribution, Expert Forum. *Journal of Global Positioning Systems*, 1(2), 137 – 143.

Landau, H., U. Vollath, A. Deking, and C. Pagels (2001) Virtual Reference Station Networks - Recent Innovations by Trimble. *Proceedings of the Japan Institute of Navigation, GPS Symposium (November 2001, Tokyo, Japan)*, 39 – 52. Japan Institute of Navigation.

Li, Z. and Y. Gao (2000) Improving Ambiguity Resolution for a Regional Area DGPS System Using Multiple Days of Data. *Proceedings of the National Technical Meeting of the Satellite Division of the Institute of Navigation, ION GPS/1998 (September 1998, Nashville, USA)*, 389 – 399. Institute of Navigation.

Liu, G. and G. Lachapelle (2002) Ionosphere Weighted GPS Cycle Ambiguity Resolution. *Proceedings of the National Technical Meeting of the Institute of Navigation, ION NTM/2002 (January 2002, San Diego, USA)*, 889 – 899. Institute of Navigation.

Liu, G. C. (2001) *Ionosphere Weighted Global Position System Carrier Phase Ambiguity Resolution*. Master's thesis, University of Calgary.
URL `http://www.geomatics.ucalgary.ca/`

Liu, J. (2003) *Implementation and Analysis of GPS Ambiguity Resolution Strategies in Single and Multiple Reference Station Scenarios*. Master's thesis, University of Calgary.
URL `http://www.geomatics.ucalgary.ca/`

Luo, N. (2001) *Precise Relative Positioning of Multiple Moving Platforms Using GPS Carrier Phase Observables*. Ph.D. thesis, University of Calgary.
URL `http://www.geomatics.ucalgary.ca/`

Luo, N. and G. Lachapelle (2003) Relative Positioning of Multiple Moving Platforms using GPS. *IEEE Transactions on Aerospace and Electronic Systems*, 39(3), 936 – 948.

Moritz, H. (1980) *Advanced Physical Geodesy*. Herbert Wichmann Verlag, second edition.

Mutambara, A. (1998) *Decentralized Estimation and Control for Multisensor Systems*. CRC Press LLC.

Odijk, D. (1999) Sochastic Modelling of the Ionosphere for Fast GPS Ambiguity Resolution. *Proceedings of General Assembly of the International Association of Geodesy (July 1999, Birmingham, England)*, volume 121, 387 – 392. International Association of Geodesy, Springer-Verlag.

Odijk, D. (2000) Weighting Ionospheric Correction to Improve Fast GPS Positioning Over Medium Distances. *Proceedings of the National Technical Meeting of the Satellite Division of the Institute of Navigation, ION GPS/2000 (September 2000, Salt Lake, USA)*, 1113 – 1124. Institute of Navigation.

Odijk, D. (2002) *Fast precise GPS positioning in the presence of ionosphereic delays*. Optima Grafische Communicatie, the Netherlands.

Parkinson, B. W. (1996) GPS Error Analysis. B. W. Parkinson and J. J. Spilker, Jr., eds., *Global Positioning System: Theory and Applications*, volume 1, chapter 11, 469 – 485. American Institute of Aeronautics and Astronautics, Inc., Washington D.C., USA.

Petovello, M. (2003) *Real-Time Integration of a Tectical-Grade IMU and GPS for High-Accuracy Positioning and Navigation*. Ph.D. thesis, University of Calgary.
URL `http://www.geomatics.ucalgary.ca/`

Pugliano, G., F. Obrizza, F. Pingue, V. Sepe, P. Alves, and G. Lachapelle (2004) Monitoring the Neapolitan Volcanic Area Using an Advanced Multiple Reference Station RTK DGPS Technique. *Proceedings of the Institute of Navigation Satellite Division Technical Meeting, GPS 04 (September 2004, Long Beach, USA)*.

Radovanovic, R., N. El-Sheimy, and W. F. Teskey (2001) Rigorous Network Adjustment of GPS Carrier Phases for Airborne Positioning Via Tropospheric Error Variance-Covariance Modelling. *Proceedings of the third International Symposium on Mobile Mapping Technology (January 2001, Cairo, Egypt)*.

Radovanovic, R. S. (2002) *Adjustment of Satellite-Based Ranging Observations for Precise Positioning and Deformation Monitoring*. Ph.D. thesis, University of Calgary.
URL `http://www.geomatics.ucalgary.ca/`

Raquet, J. (1998) *Developement of a Method for Kinematic GPS Carrier-Phase Ambiguity Resolution Using Multiple Reference Receivers*. Ph.D. thesis, University of Calgary.
URL `http://www.geomatics.ucalgary.ca/`

Raquet, J., G. Lachapelle, and L. P. Fortes (2001) Use of a Covariance Analysis Technique for Predicting Preformance of Regional-Area Differential Code and Carrier-Phase Networks. *Navigation*, 48(1), 25 – 34.

Raquet, J., G. Lachapelle, and T. E. Melgård (1998) Test of a 400 km x 600 km Network of Reference Receivers for Precise Kinematic Carrier-Phase Positioning in Norway. *Proceedings of the National Technical Meeting of the Satellite Division of the Institute of Navigation, ION GPS/1998 (September 1998, Nashville, USA)*, 407 – 416. Institute of Navigation.

RTCM (1998) RTCM Recommended Standards for Differential GNSS Service, Version 2.2. Developed by RTCM Special Committee No. 104, January 15, 1998.

Salychev, O. (1998) *Inertial Systems in Navigation and Geophysics*. Bauman MSTU Press, Moscow.

Skone, S. (1998) *Wide Area Ionosphere Grid Modelling in the Auroral Region*. Ph.D. thesis, University of Calgary.

Spilker, J. J., Jr. (1996) Tropospheric Effects on GPS. B. W. Parkinson and J. J. Spilker, Jr., eds., *Global Positioning System: Theory and Applications*, volume 1, chapter 12, 517 – 546. American Institute of Aeronautics and Astronautics, Inc., Washington D.C., USA.

Teunissen, P. J. G. (1994) A New Method for Fast Carrier Phase Ambiguity Estimation. *Position Location and Navigation Symposium, IEEE PLANS/1994 (April 1994, Las Vegas, USA)*, 562 – 573. IEEE.

Teunissen, P. J. G. (1997) The Geometry-Free GPS Ambiguity Search Space With a Weighted Ionosphere. *Journal of Geodesy*, 71(6), 370 – 383.

Teunissen, P. J. G. (1999) An Optimatlity Property of the Integer Least-Squares Esimator. *Journal of Geodesy*, 73, 587 – 593.

Teunissen, P. J. G. (2000) The Success Rate and PRecision of GPS Ambiguities. *Journal of Geodesy*, 74, 321 – 326.

Townsend, B., K. V. Dierendonck, J. Neumann, I. Petrovski, S. Kawaguchi, and H. Torimoto (2000) A Proposal for Standardized Network RTK Messages. *Proceedings of the National Technical Meeting of the Satellite Division of the Institute of Navigation, ION GPS/2000 (September 2000, Salt Lake, USA)*, 1871 – 1778. Institute of Navigation.

Townsend, B., G. Lachapelle, L. P. Fortes, T. E. Melgård, T. Nørbech, and J. Raquet (1999) New Concepts for a Carrier Phase Based GPS Positioning Using a National Reference Station Network. *Proceedings of the National Technical Meeting of the Institute of Navigation, ION NTM/1999 (January 1999, San Diego, USA)*, 319 – 328. Institute of Navigation.

Vollath, U., A. Buecherl, and H. Landau (2000a) Long-Range RTK Positioning Using Virtual Reference Stations. *Proceedings of the National Technical Meeting of the Satellite Division of the Institute of Navigation, ION GPS/2000 (September 2000, Salt Lake, USA)*, 1143 – 1147. Institute of Navigation.

Vollath, U., A. Buecherl, H. Landau, C. Pagels, and B. Wagner (2000b) Multi-Base RTK Positioning Using Virtual Reference Stations. *Proceedings of the National Technical Meeting of the Satellite Division of the Institute of Navigation, ION GPS/2000 (September 2000, Salt Lake, USA)*, 123 – 131. Institute of Navigation.

Vollath, U., H. Landau, X. Chen, K. Doucet, and C. Pagels (2002) Network RTK Versys Single Base RTK - Understanding the Error Characteristics. *Proceedings of the National Technical Meeting of the Satellite Division of the Institute of Navigation, ION GPS/2002 (September 2002, Portland, USA)*, in press. Institute of Navigation.

Walpole, R. E. and R. H. Myers (1993) *Probability and Statistics for Engineers and Scientists*. Prentice-Hall, Inc., fifth edition.

Wanninger, L. (1999) The Performance of Virtual Reference Stations in Active Geodetic GPS-networks under Solar Maximum Conditions. *Proceedings of the National Technical Meeting of the Satellite Division of the Institute of Navigation, ION GPS/1999 (September 1999, Nashville, USA)*, 1419 – 1427. Institute of Navigation.

Wübbena, G., A. Bagge, and M. Schmitz (2001a) Network-Based Techniques for RTK Applications. *Proceedings of the Japan Institute of Navigation, GPS Symposium (November 2001, Tokyo, Japan)*, 53 – 65. Japan Institute of Navigation.

Wübbena, G., A. Bagge, and M. Schmitz (2001b) RTK Networks based on Geo++ GNSMART - Concepts, Implementation, Results. *Proceedings of the National Technical Meeting of the Satellite Division of the Institute of Navigation, ION GPS/2001 (September 2001, Salt Lake, USA)*, 368 – 378. Institute of Navigation.

Zhang, J. (1999) Precise Estimation of Residual Tropospheric Delays in a Spatial GPS Network. *Proceedings of the National Technical Meeting of the Satellite Division of the Institute of Navigation, ION GPS/1999 (September 1999, Nashville, USA)*, 1391 – 1401. Institute of Navigation.

Zhang, J. and G. Lachapelle (2001) Precise Estiamtion of Residual Tropospheric Delays Using a Regional GPS Network for RTK Applications. *Journal of Geodesy*, 75, 255 – 266.